Development of Pasture Growth Models for Grassland Fire Danger Risk Assessment

By

Helen Glanville Daily B. App. Sc. (Ag.) (Hons.)
(University of Adelaide)

Submitted in fulfillment of the requirements for the Degree of
Doctor of Philosophy

School of Agricultural Science
University of Tasmania

October 2012

Declaration

This thesis contains no material that has been accepted for a degree or diploma by the University of Tasmania or any other institution, except by way of background information and duly acknowledged in this thesis. To the best of my knowledge and belief this thesis contains no material previously published or written by another person except where due acknowledgement is made in the text of the thesis, nor does the thesis contain any material that infringes copyright.

Helen Glanville Daily

This thesis may be made available for loan and limited copying in accordance with the Copyright Act 1968.

Helen Glanville Daily

Abstract

Assessment of grassland curing (the proportion of dead to total material in a grassland fuel complex) is of great importance to fire authorities, which use it as an input into fire behaviour models and to calculate the Grassland Fire Danger Index. Grass curing assessments require improved accuracy to better define fire danger periods and improve management of resources, particularly around the use of prescribed burns.

This project investigated the suitability of existing plant growth models in three agricultural decision support tools (DST), namely, APSIM, GrassGro™ and the SGS Pasture Model, to estimate curing in a range of grass growth types. Simulations using appropriate DST were developed for phalaris (perennial introduced), annual ryegrass (annual introduced), or perennial native pastures, and for wheat (annual cereal) crops. The DST were not able to produce reliable curing estimates compared to the field assessments of curing, in part because the current state of knowledge on the senescence stage of leaf development has not been easy to incorporate into DST algorithms.

A Leaf Curing Model was developed for the same species grown under glasshouse conditions. The Leaf Curing Model was based on the proportion of cured leaf material over time but was not suitable for estimating curing in the field because it lacked responsiveness to plant leaf development and assumed irreversibility of curing.

This thesis provides a comprehensive study of leaf turnover rates determined from leaf measurements recorded on glasshouse-grown plants, over the entire lifecycle. The relationship between leaf appearance rate (LAR), leaf elongation

rate (LER), leaf life span (LLS), leaf length, and leaf senescence rate (LSR) with leaf position on the plants were determined.

The effect of terminal water stress imposed early, mid-way, or late in spring in glasshouse-grown plants was contrasted to LSR and leaf length of field-grown plants. In most conditions, water stress increased LSR but did not affect leaf length. The relationship between the leaf rates and leaf position was maintained under conditions of water stress.

Finally, a Bayesian model was developed from the full range of leaf turnover characteristics calculated from glasshouse-grown plants under optimal conditions. The Bayesian model predicted green leaf biomass and percentage of dead material (curing percentage) over thermal time. A derivative of the curing output of the Bayesian model was successfully validated against field methods, and would provide a higher level of accuracy of grass curing prediction than the pasture growth models currently incorporated into commonly-available DST.

Keywords: grassfire, grass curing, fire danger rating, plant growth modelling, Bayesian modelling

Acknowledgements

I would like to thank my supervisors for their support, encouragement and trust during this journey, particularly when the going got tough; in no particular order, Dr Peter Lane, Dr Shaun Lisson, Mr Stuart Anderson, Dr Kerry Bridle, and Dr Ross Corkrey. Each brought a different perspective and expertise to this work, which was of benefit to me personally, and increased the value of the work.

This work would not have been possible without the financial support of the University of Tasmania, and the Bushfire Cooperative Research Centre (CRC). Access to laboratory and glasshouse facilities at The University of Adelaide and South Australian Research and Development Institute campuses is greatly appreciated. Special thanks go to Phil Holmes (Landmark Clare), Warren and Sonia Baum (Farrell Flat), and Dr Nick Edwards and John Cooper (SARDI, Struan) for access to field sites. Darren Callaghan, Fire Prevention Officer for the Naracoorte Lucindale Council was kind enough to provide visual curing estimates for the region. Ross Corkrey deserves a big thank-you for his work on the Bayesian model, and his patience in training and guiding me through the statistical analyses.

Lastly, I want to thank my good friends for their support, and Tim, Rose and Bob (the four-legged friends) for maintaining my sanity.

I dedicate this work to all those farmers who fight fires, but especially to the memory of my uncle, Gilbert Michael O'Connell, AFSM.

Table of Contents

Abbreviations

APSIM	Agricultural Production Systems Simulator
BCRC	Bushfire Cooperative Research Centre
CFA	Country Fire Authority (Victoria)
CFS	Country Fire Service (South Australia)
DM	Dry matter
DST	Decision Support Tool(s)
FDI	Fire Danger Index/Indices
FMC	Fuel moisture content
FFDI	Forest Fire Danger Index
gdd	Growing degree days
GFDI	Grassland Fire Danger Index
GG	GrassGro™
LAR	Leaf appearance rate
LER	Leaf elongation rate
LL	Leaf length
LLS	Leaf life span
LSR	Leaf senescence rate
ME	Metabolisable energy
MJ	megajoules
ODW	Oven dried weight
ROS	Rate of spread
SARDI	South Australian Research and Development Institute
SGS	The SGS Pasture Model

Table of Figures

Table of Tables

1 Introduction

Grass is a major vegetation component of Australian landscapes, and an important source of fuel for grassfires. Curing is the term used to describe senescence and desiccation of grass material across the landscape, and is reported as the percentage of dead material in the sward (Anderson and Pearce 2003). Grass becomes increasingly flammable as the degree of curing increases. Fire management agencies require accurate and timely assessments of curing for planning activities such as prescribed burning, implementing fire prevention measures, and fire danger rating (Cheney and Sullivan 2008) for risk assessment purposes.

This thesis investigates the ability of pasture growth models currently incorporated into commonly available agricultural decision support tools (DST) to improve the assessment of grass curing. Further, the thesis tests if a detailed understanding of the relationships between leaf growth rates can be applied to improve the accuracy of grass curing assessment through development of stand-alone models.

This review describes the characteristics of grass-dominant landscapes in southern temperate regions of Australia, and the annual cycles of grass plant growth, senescence and death and their relevance to fire management. Fuel moisture content usually affects fire behaviour in predictable ways, and its assessment is integral to wildfire management. The size and arrangement of grasses classifies them as “fine fuels” and causes the fuel moisture content of grass to change more rapidly than other fuels such as trees in forests. Curing is used as a means of capturing the seasonal changes in flammability of grass-

dominated landscapes. An overview of the current methods of curing measurement is given and the potential of agricultural plant growth DST for the assessment of grass curing is considered.

1.1 Temperate grasslands

In this thesis, the term "grasslands" describes grass-dominated landscapes, including cereal crops (Carter *et al.* 2003), as commonly used by fire management agencies. It does not adhere to strict ecological definitions (e.g. Faber-Langendoen and Josse 2010). In Australian agricultural landscapes, grasslands comprise native and exotic grass and legume species with annual and perennial growth habits, along with a range of other herbs and forbs such as broad-leaf weeds.

1.1.1 Australian climatic zones

The Australian continent can be broadly classified into three climatic zones based on rainfall seasonality and amount (Munro *et al.* 2007) (Figure 1.1). Each zone differs in terms of the spatial and temporal distribution of fuel and fire occurrence. The temperate zones of southern Australia differ in terms of rainfall distribution. The southern parts of Western Australia and South Australia, western parts of Victoria and north-eastern parts of Tasmania receive winter-dominant rainfall, giving them a Mediterranean-like climate with a hot dry summer and a cool wet winter. The rainfall pattern in the eastern parts of Victoria, the east coast of Tasmania, and southern parts of New South Wales is uniformly distributed (Johnson 1997).

Figure 1.1. Climatic regions of Australia (Munro *et al.* 2007).

1.1.2 Extent of grasslands in Australia

According to the Australian Bureau of Agricultural and Resource Economics (2003), 52% of the Australian continent is covered by native grasslands or minimally modified pastures, with distribution of these grasslands differing markedly between the states (Table 1.1). Non-native grasslands comprise annual crops and both annual and perennial pastures and account for just 8% of the Australian land mass, and differ widely between the states (Table 1.1). The higher economic value of grasslands and their proximity to urban areas and other assets such as plantation forests give them high significance from a fire risk perspective.

Grasslands provide fine fuels to fires in the form of natural and improved (sown) pastures, and cereal and hay crops (Luke and McArthur 1978). Fire is used as a management tool in many grasslands, particularly those with high conservation value (Gill and Bradstock 1994; Marsden-Smedley and Catchpole

1995a; Prober *et al.* 2007; Leonard *et al.* 2010; Murphy and Russell-Smith 2010). To date, research on curing has focused on improved pastures (ryegrass/clover mixtures) and cereal crops (Garvey 1989; Barber 1990; Martin 2009), largely ignoring native and naturalised species.

Table 1.1. Land area ('000 sq km) of different Australian states and territories, and area ('000 sq km) occupied by different grassland types with percentage of respective state, territory or continent land area given in brackets. Adapted from Integrated Vegetation Cover (Australian Bureau of Agricultural Resource Economics and Sciences 2003).

	Total land area	Native grassland or minimally modified pastures	Annual crops and highly modified pastures
WA	2 327	1 599 (68.7)	186 (8.0)
SA	984	393 (39.9)	77 (7.8)
Vic	228	52 (23.0)	77 (33.7)
NSW	801	322 (40.2)	92 (11.5)
ACT	2	0.2 (8.0)	0.04 (1.5)
QLD	1 725	834 (48.4)	134 (7.8)
NT	1 348	698 (51.8)	2 (0.1)
TAS	68	4 (6.2)	12 (16.9)
Australia	7 483	3 903 (52.2)	579 (7.7)

1.1.3 Grassland types

Grasslands are categorized into different types describing the general arrangement of the grassland communities. Northern Australia is dominated by tropical grasslands, tussock grasslands and hummock grasslands, which were not included in this study. Temperate grasslands are generally comprised of native tussock grasslands, along with introduced pastures and cereal crops.

1.1.3.1 Native grasslands

The genera *Austrodanthonia* (H.P. Linder), *Austrostipa* (S.W.L. Jacobs & J. Everett), *Bothriochloa* (Kuntze), *Chloris* (Sw.), *Enteropogon* (Nees), *Lomandra* (Labill.), *Poa* (L.) and *Themeda* (Forssk.), all contain species which form tussocks (Carter *et al.* 2003). Tussock grasslands sometimes occur as mosaic patches

throughout many regions of south eastern Australia. In Victoria, these tussock grassland communities occur on the plains of the Wimmera, Western Basalt, central Gippsland, and Northern districts. The South Eastern Highlands grassland ecological community stretches from Melbourne in Victoria to Bathurst in NSW. Other tussock grassland communities occur on the Liverpool and Moree plains, and the Riverina plain of NSW. In South Australia, tussock grasslands stretch from the Flinders Ranges to the mouth of the Murray River, while in Tasmania, tussock grasslands occur in the Northern Midlands, Northern Slopes, South East, Ben Lomond and Flinders Island bioregions (Carter *et al.* 2003). These grasses accumulate dead material in tussocks of about 30 cm in height, and they can accumulate large quantities of fuel in the absence of grazing or fire. Growth of other annual and perennial species between the tussocks contributes to the continuity of the fuel bed (Cheney and Sullivan 2008).

1.1.3.2 Introduced pastures

Grasslands are often termed "improved" where native species have largely been replaced by a mixture of introduced annual and perennial grasses and legumes, in an effort to increase the carrying capacity for livestock grazing enterprises (Cheney and Sullivan 2008). Distribution of introduced pasture species is largely dependent on rainfall and altitude (Kemp and Dowling 1991). Management practices have influenced the distribution of plant types within introduced pastures (Lodge *et al.* 1998). Grazing management practices such as continuous grazing have been said to encourage the "annualisation" of pastures, where annual grasses invade perennial pastures (Morley *et al.* 1969; Kemp and Dowling 1991; Scott *et al.* 2000).

In southern Australia, many of the introduced species have become naturalised, such as *Phalaris aquatica* L. (phalaris), *Lolium rigidum* Gaud. (annual ryegrass), *Trifolium subterraneum* L. (subterranean clover) and *Medicago polymorpha* L. (burr medic). The annualisation of many sown pastures has been recognised in Victoria and New South Wales (Schroder *et al.* 1992; Kemp and Dowling 2000; Mason and Kay 2000; White *et al.* 2003; Friend *et al.* 2007; Mitchell 2008). In some cases, perennial native species have been able to exploit changes in soil fertility and grazing management (Virgona *et al.* 2002) and are increasingly being recognised as having a legitimate place in agriculture (Bellotti 2001; Dear *et al.* 2006; Islam *et al.* 2006; Mitchell 2008).

The fuel loads that result from pasture improvement are considered to be greater than those of native grasslands (Cheney and Sullivan 2008). Higher fuel loads and grass fires of greater intensity during summer are attributed to the shift from perennial to annual species, particularly cereals and weedy annual species across agricultural lands, and the suppression of fire as a land management tool (Chandler *et al.* 1983). This may be a reflection of management practices rather than biological composition. Improved pastures usually provide continuous fuel beds; however, these can be managed by grazing and mowing or slashing.

1.1.3.3 Crop lands

Broad acre cropping lands make up a small but highly valuable area of grass-dominated landscapes in Australia (3% of the land mass (Hutchinson 1992; Munro *et al.* 2007)). Wheat (*Triticum aestivum* L.) and barley (*Hordeum vulgare* L.) are the major cereal grains grown in southern Australia (Cheney and Sullivan 2008).

Accidental ignition of mature cereal crops by harvesting equipment is of concern to fire agencies (Miller 2008). Stubble remaining after harvest can also pose a fire risk and the increasing adoption of stubble retention practices will increase this risk. The presence of weeds or other grasses under the crop stubble can increase the fuel bed continuity (Cheney and Sullivan 2008).

1.2 Phenology of grasses

Growth and development of grasses are different, though related, concepts. Growth involves an expansion or enlargement of the plant structure, and in agriculture this translates to an increase in dry weight of leaf or grain matter. In contrast, development indicates a transition from one stage or phase to another, implying time units, but the interval between phases can also be measured in terms of temperature and photoperiod accumulation (Wilhelm and McMaster 1995; Campbell and Norman 1998). Plant growth occurs during development and may influence the final herbage or grain yield but the two processes should not be confused. Growth can cease under environmental stress but development will typically accelerate (Wilhelm and McMaster 1995). The study of plant development as it relates to climate is known as phenology (Perry *et al.* 1987).

1.2.1 Grass development phenostages

In agriculture, different phenological stages ("phenostages") are considered important in different industries. Livestock industries are concerned with pasture growth, usually maintaining sown pastures in the vegetative phenostage of development to maximise the green leaf material for consumption by grazing animals (Bircham and Hodgson 1983; Chapman *et al.* 1983). The focus in grain

industries is the reproductive phenostage and the associated production of seeds or grains.

Descriptions of grass plant development tend to focus on the development period of interest. Hence plant development guides for wheat (e.g. Figure 1.2) (Large 1954; Haun 1973; Zadoks *et al.* 1974) emphasise different phenostages to those for sown pasture grasses (Simon and Park 1983; Moore *et al.* 1991). However, none adequately describe senescence of leaf material during vegetative, reproductive or subsequent phenostages. These phenostages are of particular importance in grass fuel and fire management and are described in general detail for grasses in the following sections.

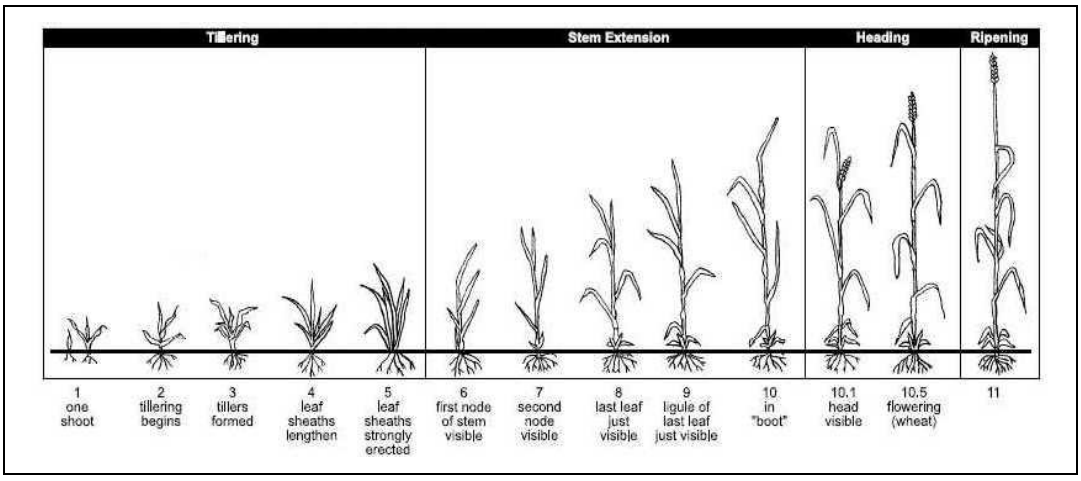

Figure 1.2. Feekes scale of wheat development (Large 1954).

1.2.1.1 Vegetative phenostage

Plant development begins with the germination and emergence phenostages (Langer 1979). The following vegetative phenostage is characterised by the appearance and elongation of leaves, and the differentiation (but not elongation) of stem nodes (Moore and Moser 1995).

Cell division takes place at the base of the new leaf, pushing the leaf up through the folded or rolled sheath of the previous leaf. The exposed leaf tissue

does not expand further, but does begin to photosynthesize. Leaf maturity is reached at the end of leaf cell division and sheath elongation and is signaled by the differentiation of the ligule. In general in sown pasture grass species, as the youngest leaf appears, the next oldest is rapidly growing, and the third oldest is reaching maturity (Langer 1979).

The vegetative phase may also involve tillering, where new shoots branch off from nodes or buds on the stem of the plant, and emerge through the lower leaf sheath. In grass species, tiller appearance usually begins after the first three leaves have appeared. Annual grasses produce tillers for a limited period, which may or may not flower (Langer 1979).

1.2.1.2 Reproductive phenostage

The transition from the vegetative to the reproductive phenostage can be triggered by a range of signals including temperature accumulation, photoperiod, vernalisation and leaf accumulation (McMaster and Wilhelm 1997). As temperature increases in spring, green herbage production typically peaks. Species and cultivars may respond to different signals, and different threshold values at which these signals operate (McMaster and Wilhelm 1997). When the reproductive phase begins, the stem elongates and no further leaf primordia are generated, capping the number of leaves, although they continue to appear until the leaf primordia are exhausted (Moore and Moser 1995). The bud primordia develop rapidly to form the inflorescence, which is enclosed in the sheath of the final or “flag” leaf, and is carried upwards by the elongating stem (Langer 1979).

Once the flower or “ear” has emerged from the flag leaf, opening of the floret or “anthesis” is soon followed by a number of brief pollination events. Seed fill takes place after fertilisation (Langer 1979).

Most grass species require a vegetative phase, when they are temporarily insensitive to the transitional signals such as photoperiod, before entering the reproductive phase. The vegetative phase may be quite short, as in the case of most annual grasses. Generally the reproductive phase is regarded as a point of no return, but some grasses can revert to vegetative proliferation if conditions, primarily photoperiod, are not conducive to completing seed set (Langer 1979).

1.2.1.3 Senescence phenostage in annual grasses

The lifecycle of grass growth and death in southern Australia follows the pattern of rainfall distribution. The annual and perennial grasses which use the C_3 photosynthetic pathway display a seasonal life cycle involving death or dormancy to avoid the seasonal drought during summer in southern Australian. This senescence which is most obviously seen as chlorophyll loss (Nooden 2004) is accompanied by desiccation, and is termed "curing" in fire management circles.

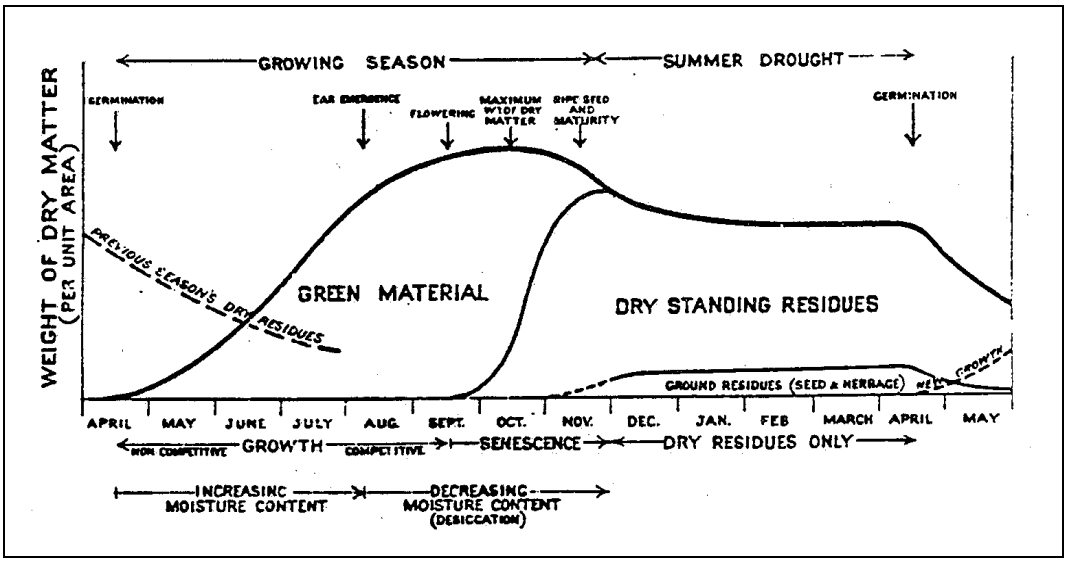

Figure 1.3. Generalized diagram of annual pasture life cycle in a Mediterranean environment (Parrott 1964).

Annual plants go through "whole plant senescence" (Nooden *et al.* 2004) and die, leaving the dry standing residues associated with grass fuel. In a crop, harvesting of the physiologically mature grain leaves behind stubble. In a pasture,

the dry plant material provides a standing "haystack" for livestock grazing. This general relationship is shown in Figure 1.3.

Senescence, which in grasses commences at the tip of the oldest leaf, is a development process which serves a number of purposes. It is an energy-demanding process (Thomas and Donnison 2000) in which accumulated and synthesised plant resources are actively mobilized (Buchanan-Wollaston and Morris 2000). In annual plants, senescence of vegetative tissue is the source of nitrogen and carbohydrate for the developing seed or grain (Frith and Dalling 1980). Once critical leaf area is reached, when the canopy intercepts 95% of incident light (Brougham 1960), older leaves begin to senesce and die (Moore and Moser 1995). Tillers die with the main stem. Ultimately, resources are salvaged by the plant to ensure ongoing survival through harsh environmental conditions in the form of seeds or dormant root stocks and crowns. Death is not always a consequence of senescence, and plants can die without senescing (Thomas and Donnison 2000).

1.2.1.4 Development variations of perennial grasses

The growth habit of perennial grasses differs in a number of respects to those of annual grasses. Perennial grasses can produce tillers over an extended period and may have vegetative and reproductive tissues growing at the same time (Moore and Moser 1995). Individual tillers have a finite lifespan, although vegetative tillers may live for quite long periods in the absence of environmental stress or flowering. Tillers in the reproductive phenostage have been shown to survive summer drought (Silsbury 1964; Hoen 1968). While tiller numbers may remain the same over time, some tillers will have died and been replaced by others (Langer 1979).

Once the reproductive phase is reached, differences exist between perennial species in their subsequent rates of senescence. Tillers of *Lolium perenne* L. (perennial ryegrass) and *Festuca arundinacea* Schreb. (tall fescue) tend to be more resistant to death with only around 30% death rates in tillers which have flowered. In contrast, 90% of flowering tillers of *Phleum pratense* L. (timothy) and *Bromus willdenowii* Kunth (prairie grass) will die (Valentine and Matthew 1999).

Perennial plants may grow for many years but herbaceous perennials exhibit annual growth followed by "top senescence" (Nooden 1988). This is a mechanism for escaping adverse weather conditions and in many parts of the world is demonstrated by plants becoming dormant over the winter. In temperate climates like Australia however, perennial C_3 grasses express a top senescence called "summer dormancy" to avoid harsh summer conditions. Nutrient reserves (primarily carbon and nitrogen) are translocated from the aerial portions of the plant to the crown of the plant (Watson and Lu 2004). The grass develops a "resting organ" such as swollen stems or tubers with dormant buds at the time of floral initiation followed by top senescence with which to escape summer drought (Hoen 1968).

1.2.2 Curing

Reproductive development, maturity and senescence of grasslands are of particular interest to fire agencies, as these development stages coincide with increasing desiccation of plant material and its escalation as a fire hazard. The transition from the reproductive phenostage to senescence in grass plants is employed by fire agencies to determine the onset of the fire danger season, and curing estimates are necessary to determine fire danger rating and potential rate of

fire spread in grasslands. The assessment of curing in grasslands is in fact an assessment of the phenology of those grasslands.

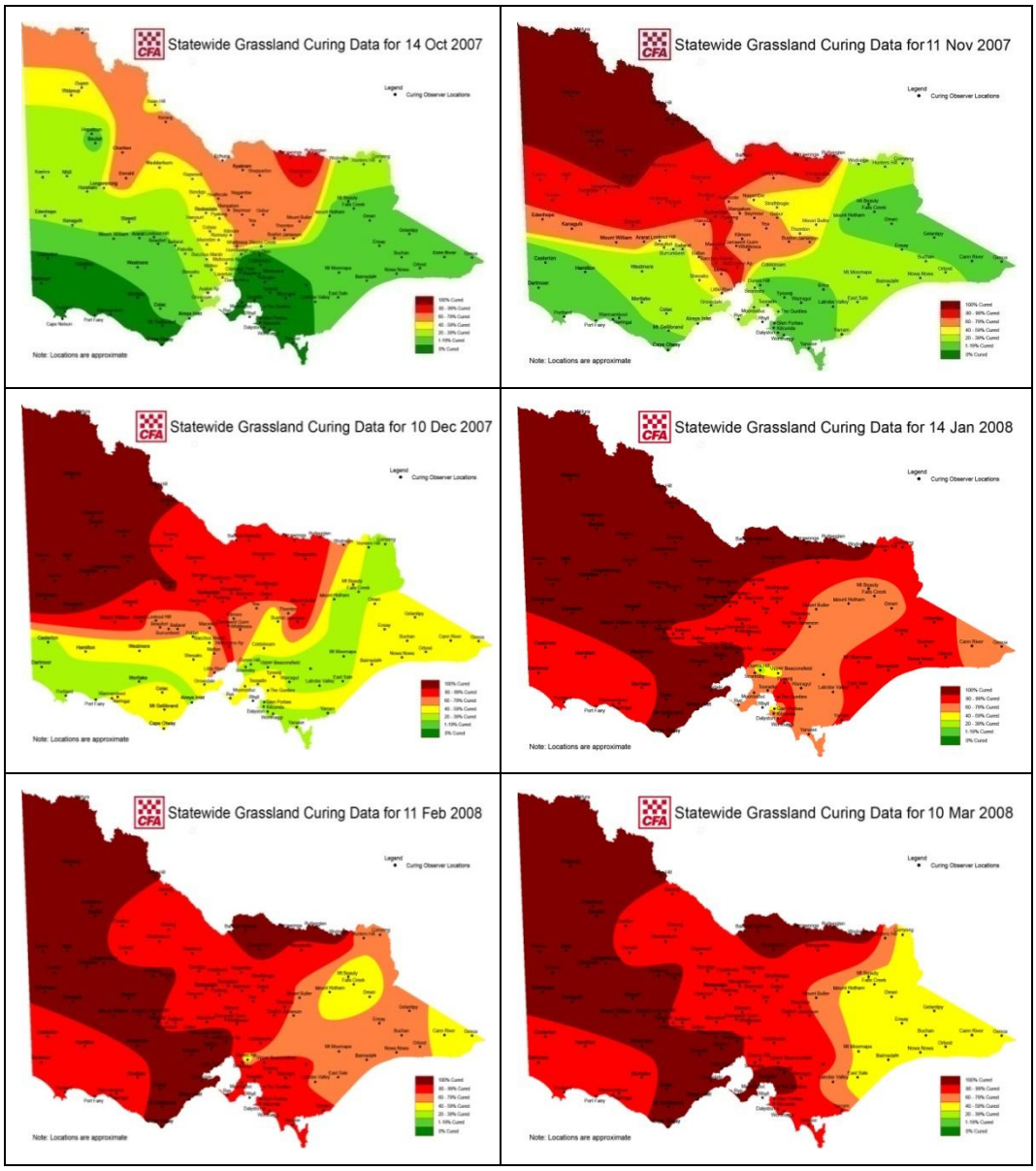

Figure 1.4. Curing progress across Victoria 2007/8 (source: Country Fire Authority, Victoria)

It has been generally accepted in southern Australia that grasses will become fully cured in about six weeks from the seed head maturity, in the absence of rain (Parrott 1964; McArthur 1966). Therefore the point at which 100% curing is reached should be easily predicted (McArthur 1966). However, it is also recognized that the curing season of C_3 grasses is both temporally and spatially variable across southern Australia (McArthur 1966).

This temporal and spatial variation is the result of variation in climate and species distribution. For instance, perennial plants tend to be distributed in higher rainfall areas which have longer growing seasons (Sanford *et al.* 2003) so that spring growth ends at different times between districts as illustrated by the curing map in Figure 1.4. Temporal variation in curing also occurs within districts. Perennials with extended growth period and later flowering time will display an extended curing pattern compared to the annual species growing in the same environment (Sanford *et al.* 2003).

Curing rates vary over time due to the phenological progression of the plants, but importantly, senescence of leaves occurs at a number of plant development stages, before the "senescence" phenostage. The first display of senescence is the regular "sequential" senescence of the oldest leaf upon its maturity. This occurs during vegetative growth and is necessary to allow replacement of old leaves with new (Peoples and Dalling 1988; Thomas and Sadras 2001). The second, more dramatic senescence coincides with reproduction, whereby lower leaves are sacrificed and their nutrients salvaged to fill the developing seed or grain. This corresponded with the progressive decline in moisture noted by Parrott and Donald (1970b) in the living plant, which started a few weeks before the attainment of maximum dry matter and ended afterwards. Once the moisture content fell to around 170% of dry weight, the rate at which the plants desiccated increased along with death rate. At this point moisture content was inversely linearly related to the curing percentage (or the percentage of dry herbage) of the pasture (Parrott and Donald 1970b). A third senescence phase which is triggered by environmental stresses is possible for perennial tillers which have survived the reproductive phase.

To fully estimate the curing rates of grass plants, senescence from all triggers, whether they are phenological or environmental, must be accounted for to capture the transition from live to dead state and the accompanying changes in fuel moisture.

1.2.3 Curing as a function of leaf growth processes

To determine curing in grass-dominated landscapes, knowledge of the change in proportion of the live and dead leaf pools in a sward over time is needed. The live pool is the culmination of leaf appearance and elongation to a fully expanded leaf length, for the duration of each leaf's life span, for all leaves in the sward. The dead leaf pool is determined by the onset and duration of senescence in each leaf in the sward.

Turnover of vegetative leaves in agriculturally-important perennial grasses and cereals has been well studied (e.g. Peacock 1976; Bircham and Hodgson 1983; Vine 1983; Chapman *et al.* 1984; Porter and Gawith 1999). However, often leaf rates have been reported on just a subset of leaves and cannot easily be extrapolated to other species, regions and seasons (Bircham and Hodgson 1983; Grant *et al.* 1983). Linear measures of leaf turnover are not frequently available, but would overcome the need to harvest, and hence interrupt, the growth of the plant in order to determine the proportion of live and dead leaf pools over time. It is possible to convert linear measures to mass measures if leaf weight per unit length is known (Mazzanti *et al.* 1994; Hepp *et al.* 1996).

Leaf characteristics such as leaf appearance rate, leaf elongation rate, leaf length and life span, and leaf senescence rate are genetically controlled and are also responsive to environmental factors (Lemaire and Agnusdei 2000),

particularly temperature, but also photoperiod, water, nitrogen, salinity, light, CO_2, soil and seed factors (McMaster and Wilhelm 1995).

1.2.3.1 Leaf appearance rate

Leaf turnover begins with the appearance of successive leaves. The time interval between leaves is described as "phyllochron". The reciprocal of phyllochron is leaf appearance rate (LAR) which is the proportion of the leaf which has appeared in each time unit. Phyllochron is often assumed to be constant (McMaster *et al.* 1991; Rickman and Klepper 1995), however, there is evidence that the rate at which leaves appear may vary with increasing leaf position, but not always in the same direction (Table 1.2). Phyllochron varied between wheat tillers (Evers *et al.* 2005) and between years in several grass species (Frank and Bauer 1995), but was not reported for individual leaves.

Table 1.2. The rate of leaf appearance relative to leaf position for different grass species, as reported in different studies.

Common name	Botanical name	Reference	Effect on LAR
Cocksfoot	*Dactylis glomerata* L.	Calviere and Duru (1995)	Increases then decreases
Cocksfoot	*Dactylis glomerata*	Duru and Ducrocq (2000a)	Decreases
Green panic (C_4)	*Panicum maximum* var. *trichoglume* Robyns	Wilson (1976)	Decreases
Phalaris	*Phalaris aquatica*	Kemp and Guobin (1992)	Constant
Wheat	*Triticum aestivum*	Streck *et al.* (2003)	Decreases
Wheat	*Triticum aestivum*	Baker *et al.* (1980), Kirby (1995), Kirby and Perry (1987), Slafer and Rawson (1997)	No consistent trend

1.2.3.2 Leaf elongation rate

Leaf elongation describes the period from the appearance of the leaf tip to the appearance of the ligule, and the rate at which it occurs is determined by the

length of leaf per unit of time or thermal time. Previous studies have reported the average leaf elongation rate (LER) of a number of leaves in kangaroo grass (*Themeda triandra* L.) (Wallace *et al.* 1985), or a subsample of leaves of perennial ryegrass and phalaris, expressed in terms of calendar time (Peacock 1975a; Kemp and Guobin 1992). However, the relationship between LER and leaf position differed not only between species, but also between years in the same species (Table 1.3).

Table 1.3. The rate of leaf elongation relative to leaf position for different grass species as reported in two studies.

Common name	Botanical name	Reference	Effect on LER
Green panic	*Panicum maximum* var. *trichoglume*	Wilson (1976)	Increases then decreases (non-linear)
Cocksfoot	*Dactylis glomerata*	Duru and Ducrocq (2000a)	Non-linear, linear and no response, varying between years

1.2.3.3 Leaf life span

Leaf life span (LLS) is usually defined as the period between leaf appearance and the onset of leaf senescence (Wilson 1976; Calviere and Duru 1995; Lemaire and Chapman 1996; Lemaire and Agnusdei 2000; Lemaire *et al.* 2009), but senescence has sometimes been included in LLS (Duru and Ducrocq 2000a; b). LLS has been documented as a single value for a range of species (Lemaire *et al.* 2009) implying that life span is constant for all leaves on a plant. However, LLS was found to increase linearly with leaf position in cocksfoot and green panic (Wilson 1976; Calviere and Duru 1995; Duru and Ducrocq 2000a; b). Leaf longevity of perennial grasses in the field varied with time of year, being a function of thermal time accumulation (Vine 1983; Chapman *et al.* 1984).

1.2.3.4 Leaf senescence rate

Senescent material is the dead portion of the leaf which is still in contact with the green component of the live leaf. Dead and senescent leaf material must be determined for curing to be modelled. Few studies have reported the proportion of dead material present in the sward. Wilman and Mares Martins (1977) captured the percentage of cured material every three days; however, their method of removing senescent leaf material directly from the green living material within the sward may have affected the subsequent senescence of the remaining leaf. Thomas and Norris (1977) estimated the proportion of dead material present along the leaf length at monthly intervals. Their results may have been confounded, however, by decomposition of senescent material in the intervening period (Tainton 1974). The rate of senescence cannot be determined from such studies if the length of the leaves is unknown. Some studies have reported the number of leaves (Calviere and Duru 1995), or the length of tiller senescing per unit of thermal time (Duru and Ducrocq 2000a; b), rather than the rate of linear senescence in individual leaves in thermal time. Leaf senescence rate (LSR), expressed as length per day, increased linearly with leaf position in green panic, although a non-linear function could have also fitted the data (Wilson 1976). LSR increased with thermal time in cocksfoot (Duru and Ducrocq 2000a; b) but could not be related to leaf position.

1.2.3.5 Leaf length

Many assumptions are made to simplify our understanding of leaf turnover rates (Rickman and Klepper 1995). Turnover rates are often reported as single values, implying that these rates remain constant across all leaves produced by the

plant (e.g. Lemaire and Agnusdei 2000). However, successive leaves do not necessarily develop in an identical fashion (Dale 1988), with leaf length being the characteristic to most obviously demonstrate differences between leaves. Leaf length increased with leaf position in perennial ryegrass, cocksfoot and green panic (Robson 1973; Wilson 1976; Duru and Ducrocq 2000a; b) and a small decrease in leaf length was observed in the penultimate or flag leaves of wheat and perennial grasses (Humphries and Wheeler 1963; Robson 1973; Hodgkinson and Quinn 1976; Wilson 1976; McMaster 1997; Evers *et al.* 2005).

Variation in leaf length might also explain variation in some leaf turnover rates. Evers *et al*. (2005) stated that there was little variation in the duration of elongation of leaves. If this is so, then shorter leaves at earlier leaf positions will have a slow LER and longer leaves at medium leaf positions will have a fast LER. It follows that the same might be true for appearance and senescence rates. If leaf length and other turnover characteristics vary between leaves, then it would make sense to present turnover rates in terms of leaf position, however this is not common.

1.2.3.6 Leaf numbers

Number of leaves produced by a plant is often reported for a limited amount of time rather than over the complete life cycle (e.g. Ong 1978; Sambo 1983). In wheat, leaf numbers produced by main tillers were constant within, but not between varieties (Kirby and Perry 1987), with each progressive daughter tiller growing fewer leaves (Evers *et al.* 2005). The number of leaves produced by wheat tillers increased with decreasing photoperiod, but was not affected by temperature (Slafer and Rawson 1995). The number of leaves present at any given

time could alternatively be determined from LAR and the period of time elapsed (Streck *et al.* 2003).

Duru and Ducrocq (2000b) found that cocksfoot leaf numbers increased with both defoliation and nitrogen application. This was in contrast to Ong (1978), who found that the number of live leaves produced per perennial ryegrass tiller remained relatively constant regardless of the level of nutrient treatment, but was reduced by shading. The number of live leaves could be used as a surrogate for LLS in determining the onset of senescence in each leaf, when old leaves were transferred into the dead pool (Vine 1983). The number of live leaves have been determined by multiplying LLS and LAR (Lemaire and Agnusdei 2000).

It is clear that leaf turnover is dependent on a number of genetic and environmental components. Aspects of leaf turnover in early leaves have received some attention; however, there is a lack of detailed information on leaf turnover for the entire life cycle. Certainly, the literature is scant on leaf turnover dynamics, particularly the rate of leaf senescence, for annual and native species common in southern Australian grass-dominated landscapes. Also, the lack of consistency with which leaf turnover rates have been reported makes it difficult to use the existing information to develop a model to estimate grass curing.

1.3 Fire

In the simplest terms, fire requires fuel, oxygen and heat for ignition (Pyne *et al.* 1996; Cheney and Sullivan 2008). Energy previously stored in cellulosic material during photosynthesis is released as heat, along with light (Pyne *et al.* 1996).

The burning process has three distinct stages. The pre-ignition phase involves endothermic reactions (Pyne *et al.* 1996). Heat applied to cellulosic material

evaporates any moisture present, and then begins to break down the material through pyrolysis (Cheney and Sullivan 2008). Ignition occurs at the transition point between endothermic and exothermic reactions, where fire can continue without a pilot heat source. Combustion is the third stage of burning, in which heat is released (Pyne *et al.* 1996). The products of thermal degradation include hydrocarbon gases which themselves can be ignited with sufficient temperature or an ignition source, to release heat. The additional heat can induce the process of drying, ignition and flaming in neighbouring material (Cheney and Sullivan 2008).

Flammability, or the ability or propensity for a fuel to burn, is the result of ignitability, sustainability, combustibility and consumability. Ignitability is defined as the time until ignition, after exposure to a heat source. Sustainability refers to the continuation of burning after the initial ignition or heat source is removed. Combustibility describes the rapidity or intensity of the burn (Anderson 1970; Dimitrakopoulos and Papaioannou 2001; White and Zipperer 2010). In addition, consumability is the proportion of the fuel consumed by combustion (White and Zipperer 2010). Of the four components of flammability, ignitability is the most important, for without it, the other components are irrelevant (White and Zipperer 2010).

1.3.1 Bushfire

Wildfires are unplanned events in which fuel characteristics, weather conditions, fire behaviour and interactions between these elements are not controlled (Fernandes and Botelho 2003). Wildfires in Australia (colloquially termed bushfires) occur in all climatic regions, in a range of vegetation types, such as forest, woodland, shrubland and grassland. The fuel type and amount, its continuity and structure, all determine whether fires will occur and spread

(Flannigan *et al.* 2009). "Fine fuels" with a diameter of less than 6 mm are required for fires to establish. Fine fuels such as grass, leaves and twigs, are more easily ignited and are usually wholly consumed by fire, depending on moisture content. Heavy fuels such as logs require fine fuels to sustain ignition along the surface of the fuel (Luke and McArthur 1978; Bresnehan and Pyrke 1998).

Fire behaviour encompasses the aspects of flammability such as ignition, growth and spread of the fire (or sustainability) and its intensity, and hence is an important characteristic for fire management. Fire behaviour is determined by the surrounding environment, including the interactions between fuel, weather conditions such as temperature and wind speed, and topography (Packham *et al.* 1995). The fire itself can also influence the fire environment, which further affects fire behaviour (Pyne *et al.* 1996).

Fire sustainability is achieved through access to more fuel and oxygen. The speed at which a fire travels, known as rate of spread, is determined largely by wind speed (Cheney *et al.* 1993), the continuity and arrangement of the fuel bed, dead fuel moisture content and curing percentage of the fuel (Coleman and Sullivan 1996; Cheney *et al.* 1998), and slope of the terrain (Cheney and Sullivan 2008). Fuel load and height do not influence rate of spread in grass fuels (Cheney *et al.* 1993), although both may influence the continuity of the fuel bed and flame height which impact on the difficulty of fire suppression. In grasslands, the continuity of the fuel bed is also influenced by the degree of disturbance through grazing or mowing.

Fire intensity is the heat released from the fuel during combustion. It is calculated at the fire perimeter and reported in kilowatts per metre. Fire intensity is an indication of control difficulty, and varies with position on the perimeter of

the fire, relative to the wind direction and speed (Cheney and Sullivan 2008). Fire intensity and subsequently the hazard posed through reduction in opportunities for fire control, increase with fuel load (Gill *et al.* 1987) and impact on the ability to safely conduct planned burns or suppress wildfires.

1.3.2 Grassfire

Much of the research into wildfires globally has targeted forest fires (e.g. Stocks *et al.* 1988; Daniel and Ferguson 1989). Less research activity has been conducted into grassfires. Fires in grasslands and savannas make up 80-86% of all burned area globally (Flannigan *et al.* 2009). In Australia 72% of all fire damage is the result of grassfires (Gill *et al.* 1989; Cheney and Sullivan 2008). Grassfires have the potential to cause significant and catastrophic impacts on livestock, property and human life, and can provide an ignition source for fire in neighbouring high-value forests (Marsden-Smedley and Catchpole 1995b) or peri-urban residential areas.

The flammability of grasses is derived from a number of characteristics. Grass swards have a high biomass of fine leaves, arranged so as to be highly aerated (Murphy and Russell-Smith 2010) which improves the access of oxygen and heat to the combustion process. Furthermore, grass swards often have a high proportion of cured leaves and the moisture content of cured grass can change rapidly (Dimitrakopoulos *et al.* 2010).

1.4 Fuel moisture content

The moisture content of fuel affects fire behaviour characteristics such as likelihood and time of ignition, rate of spread, the amount of fuel available to the fire, flame height (and spotting potential in eucalypt forests). Fuel moisture

content is used to determine the fire danger rating index which describes the degree to which fires will start, spread, cause damage and be difficult to suppress (Luke and McArthur 1978). Most fire danger rating systems use empirically determined relationships to ascertain fuel moisture content (Viney 1991).

The moisture content of fuels can be gravimetrically determined by weighing fresh, "wet" samples of the fuel in the field, then drying to a constant weight in an oven (usually 105°C for 24 hours), and reweighing to calculate moisture content (Barber 1990; Anderson *et al.* 2011). Moisture content is expressed as a percentage of the oven-dry weight (ODW) of the fuel (Viney 1991; Aguado *et al.* 2007).

Grass fuel moisture content is affected by plant development and death. As pasture grasses mature, senesce and die or become dormant, moisture content falls rapidly from around 175% ODW (or 1.75 times ODW) at flowering and seed formation towards around 2% ODW (McArthur 1966; Parrott and Donald 1970b). Grasses are considered saturated at about 35% ODW, which is sufficient to allow self-extinguishment in many fuels (Cheney 1981).

1.4.1 Dead fuel moisture content

Live and dead plant materials differ in respect to moisture content. As a fuel type, dead plant material will respond to atmospheric moisture changes. Grass fuels, along with other cellulosic material, absorb and desorb moisture from the environment (Wilson 1958; Anderson 1990) due to the hygroscopic nature of the plant cell walls (McArthur 1966; Luke and McArthur 1978; Tunstall 1988; Anderson *et al.* 2005). Atmospheric moisture moves by precipitation (rainfall or snow), or water vapour state change (e.g. condensation (dew) and evaporation from leaves). Changes in state depend on temperature, relative humidity and latent

heat exchange (Hatton and Viney 1988) and both temperature and relative humidity usually demonstrate clear diurnal fluctuations (Wilson 1958). Dead fuel moisture content can vary with aspect, altitude and shade, across a landscape (Catchpole 2002).

Typically, peaks of relative humidity and dead fuel moisture content coincide around dawn (Pook and Gill 1993). As temperature increases and relative humidity decreases through the course of the day, the moisture content of dead grass moves towards equilibrium with relative humidity (McArthur 1966) but exhibits a lag in the gain and loss of water vapour, called hysteresis (Catchpole *et al.* 2001; Cheney and Sullivan 2008). The lag is variously reported as between one and four hours for grass fuels (Anderson 1990; Catchpole *et al.* 2001). For fine fuels, most of the variation in dead fuel moisture content occurs during the day (Hatton and Viney 1988). Relative humidity has been found to affect dead fuel moisture content in grasses more so than temperature (McArthur 1966), and Viney (1991) described the relationship as non-linear.

The moisture content of dead grass fuels can be quickly and reliably ascertained from the atmospheric conditions at the time and these are included in fire danger rating systems (McArthur 1966) as well as models of fire behaviour (Cheney *et al.* 1998). However, Pook and Gill (1993) cautioned that models describing dead fine fuel moisture content of pine forest surface litter in terms of atmospheric variables such as temperature and humidity were not accurate enough at the very low moisture values to be used with confidence. The relationship between moisture content and very low humidity in grasses may be similarly inaccurate.

1.4.2 Live fuel moisture content

The moisture content of growing plants is termed live fuel moisture content. Temperature and relative humidity influence live fuel moisture content through transpiration rates. Water is transpired from the leaves and replenished from soil water reserves (Tunstall 1988). Other environmental factors, particularly those that affect soil moisture content (rainfall, drought, and soil texture), also alter live plant moisture content through water availability.

Live fuel moisture content varies with plant part and the stage of growth (Hoen 1968; Luke and McArthur 1978). In lush, actively growing vegetation, the moisture content may be as high as several hundred percent of the dry weight of the plant (Parrott and Donald 1970a; Luke and McArthur 1978; Frame 1992). The senescence phenostage is associated with moisture loss, and at plant death, the moisture content reflects only the ambient moisture content of the environment. The live fuel moisture content of annual plants in mid-summer is influenced more by phenological stage than by environmental factors such as soil water availability (Dimitrakopoulos and Bemmerzouk 2003). Live fuel moisture responds more slowly than dead fuel moisture to environmental and atmospheric conditions and tends to remain higher than dead fuel moisture during spring and summer (Catchpole 2002). It is a necessarily complex interaction between physical and biological processes, and as such, has received much less attention than dead fuel moisture content (Viegas *et al.* 2001).

1.4.3 The effect of fuel moisture content on grassfire behaviour

Fuel moisture impacts on grassfire behaviour in a number of ways. The probability of ignition is inversely related to fuel moisture content (Aguado *et al.*

2007). Parrott and Donald (1970b) reported that fuel moisture content had a far greater effect on ignitability of annual pastures than did temperature and humidity. The drier the grass fuel, the easier it is to ignite (Catchpole *et al.* 2001; Catchpole 2002), and conversely, fuel with high moisture content is difficult to light without a sustained ignition source to drive the moisture out of the fuel (Dimitrakopoulos and Papaioannou 2001; Cheney and Sullivan 2008).

In comparison to dead fuel moisture, live moisture content has a marginal role in ignition (Chuvieco *et al.* 2004). Parrott and Donald (1970b) found that ignition could be achieved at least 40% of the time in grasses with 100% moisture content, and the success of ignition being sustained rose quickly after moisture content fell below 100% but varied between different annual grass species. Although the fuel moisture of the live and dead components of the sward were not reported separately, with around 40% dry herbage in these grass fuel complexes (Parrott and Donald 1970b), it must be the relatively lower moisture content of the dead fuel component that enables ignition.

Once ignited, combustion is more likely to be sustained by dry fuels (Catchpole *et al.* 2001; Catchpole 2002). When present, water vapour released by evaporation will tend to smother the fire by preventing oxygen from reaching the base of the fire. Water vapour also acts to reduce radiant heat, reducing the drying effect on fuel ahead of the firefront, and reducing fire intensity (Pompe and Vines 1966). Moisture contents of 18% to 35% have been found to be sufficient to extinguish ignition sources or prevent the continuation of the fire once alight (Catchpole 2002).

Grasslands are often a mixture of live and dead fuels therefore the rate of spread of fire cannot be determined from the effect of atmospheric conditions on

the dead fuel alone. Live moisture content must be taken into account because of the damping effect it has on the fire (Catchpole 2002), and therefore is also necessary in fire modelling (Chuvieco *et al.* 2004). Curing is used as an alternative to live fuel moisture, to reflect the damping effect of live fuels on fire behaviour.

1.4.4 Uses of fuel moisture content in bushfire management

Fuel moisture content is a critical input to both the modelling of fire behaviour which is used by fire managers to plan controlled burns and fire suppression efforts, and in prediction of the fire danger rating used on a regional basis for community warning, preparedness and safety measures. Fire behaviour models and fire danger ratings have been developed for specific vegetation types (Cheney 1981; Packham *et al.* 1995).

1.4.4.1 Rate of fire spread

Fuel moisture and grass curing vary temporally and spatially, and this affects the rate of fire spread, the difficulty of suppression and the fire danger rating. The CSIRO Grassland Fire Spread Meter combines environmental variables with grassland variables of curing and condition (natural, grazed or "eaten out") to estimate rate of fire spread across a continuous grassland. This gives an index of the difficulty of fire suppression in a "standard" 4 t/ha southern Australian pasture (Anonymous 2008a; Cheney and Sullivan 2008).

In a model proposed by Cheney *et al.* (1998), curing percentage had a greater effect than dead fuel moisture content on rate of spread when grasslands were between 70 and 90% cured. However, work on the rate of spread was conducted in grasslands which were almost fully cured with low fuel moisture content

(Cheney *et al.* 1993; Cheney and Gould 1995a). The model may therefore not have captured the full effect of curing. Lower rates of spread than would be predicted for fully cured pastures would be expected where there is spatial variability in curing (Cheney and Gould 1995b). The increase in rate of spread as fuel moisture decreases is very sensitive to changes at very low moisture values (Cheney *et al.* 1998). Therefore, any inaccuracy in defining moisture content, particularly low dead fuel moisture content, will have a marked effect on the accuracy of rate of spread models (Trevitt 1988).

1.4.4.2 Fire danger ratings

The terms “hazard”, “risk” and “danger” are often used interchangeably, but have specific meanings in fire management. Hazard refers to fuel factors such as quantity, arrangement, and flammability as well as the difficulty of fire suppression if the fuel is ignited (McArthur 1958; Luke and McArthur 1978). Fire risk combines the risk of ignition and the risk of fire spread as shown in Figure 1.5. Risk defines the probability of a fire starting, but must be considered in conjunction with fuel hazard, because there is no fire risk if fuel is not present (Luke and McArthur 1978). Fire danger occurs when there is potential for ignition, spread and damage (McArthur 1958; Luke and McArthur 1978; Cheney and Gould 1995b).

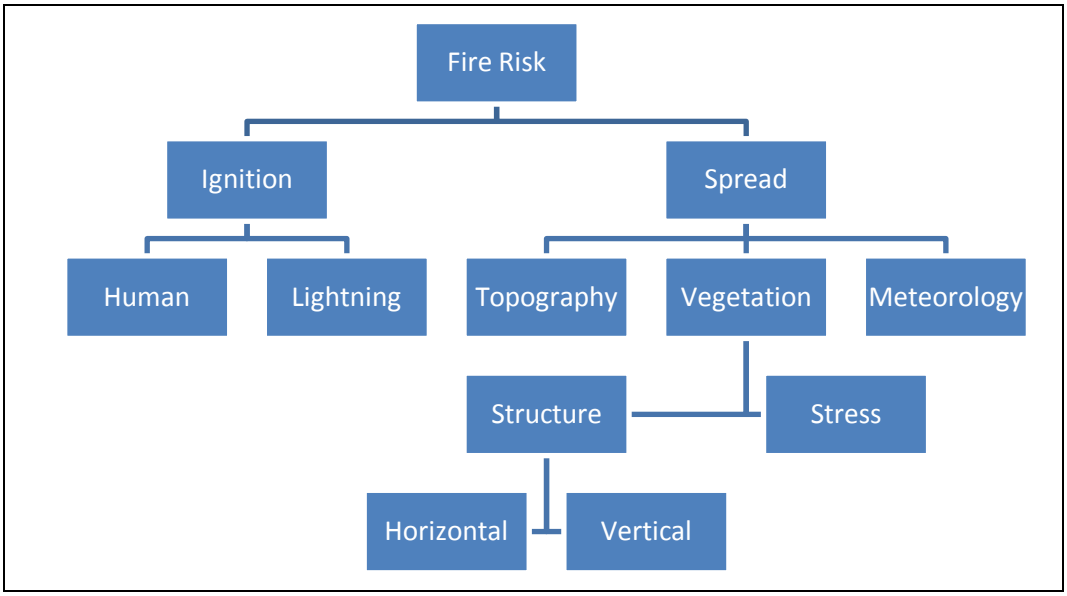

Figure 1.5. Components of fire risk (after Perestrello de Vasconcelos 1995).

Ratings of fire danger encapsulate the variables that represent severe fire weather and fuel flammability (Cheney and Gould 1995b). The fire danger ratings used in Australia use numerical indices and qualitative terms to represent the chance of a fire starting and spreading, its intensity and difficulty of suppression (McArthur 1966) (see Table 1.4). They are used by fire authorities to allocate resources for fire preparation, detection and suppression, and to provide public warnings to ensure safety and reduce the chance of ignition from land management or recreation activities (Cheney and Gould 1995b).

Table 1.4. Grassland Fire Danger Classes, index, rate of spread and difficulty of suppression (after McArthur 1966) (Cheney and Gould 1995b).

Fire Danger Class	Fire danger index (FDI)	Rate of spread at maximum FDI in class (km/hr)	Difficulty of suppression
Low	0 – 2.5	0.3	Low: headfire stopped by roads and tracks
Moderate	3 – 7.5	1.0	Moderate: headfire easily attacked with water
High	8 – 20	2.6	High: head attack generally successful with water
Very high	20.5 – 50	6.4	Very high: head attack may fail except under favourable circumstances and back burning close to the head may be necessary
Extreme	50.5 – 100	12.8	Direct attack will generally fail – backburns difficult to hold because of blown embers. Flanks must be held at all costs.

Alan McArthur developed empirical models in the 1960s to represent fire danger for forest and grassland fuels which have been widely used in Australia, with occasional modifications. The Forest Fire Danger Index (FFDI) was developed from data drawn from 800 experimental fires in forests with 12 t/ha fuel loads (McArthur 1967). Weather variables were used to predict fine dead fuel moisture content using the McArthur FFDI (McArthur 1967). Moisture content was used to predict rate of fire spread, which in turn was assigned a relative fire danger rating (Cheney and Gould 1995b).

The McArthur Grassland Fire Danger Rating Index (McArthur 1966) and its successor, the Grassland Fire Danger Meter (Anonymous 2008c) used degree of curing between 70 and 100% as a surrogate for live fuel moisture content in establishing fire danger ratings for grasslands (Table 1.4). Degree of curing is also used in the Canadian Forest Fire Danger Rating System, to describe fire danger and spread in grasslands in Canada and New Zealand (Stocks *et al.* 1989; Anderson *et al.* 2011). Fire danger according to the Grassland Fire Danger Meter increases exponentially between 70% and 100% cured, indicating the increased fire suppression difficulty experienced as grasslands lose moisture (Cheney and Gould 1995b). In contrast, a sigmoidal relationship between rate of spread and curing percentages between 50 and 100 was described by Cheney and Gould (1995b) (Figure 1.6). This showed that fires could spread faster than indicated in the original fire danger ratings (Table 1.4). However, declarations of fire danger based on the McArthur Grassland Fire Danger Meter have widespread acceptance and understanding, at least in rural populations. Cheney and Gould (1995b) argued that because variables such as curing influenced rate of spread and fire danger rating in different ways then the two should be separated. This allowed the

McArthur Grassland Fire Danger Meter to predict fire danger at the regional level, and the rate of spread functions to be used at the site specific level (Cheney and Gould 1995b).

Fuel load influences the risk of fire occurring and the subsequent need for suppression. Fuel load was included in the fire danger rating in terms of grassland disturbance (heavily grazed through to undisturbed), to describe fuel bed continuity, even though it did not affect rate of spread. For instance, if a grassland is kept relatively short through grazing, there is little chance of a fire spreading, hence the fire danger is low (Cheney and Gould 1995b; Leonard *et al.* 2010).

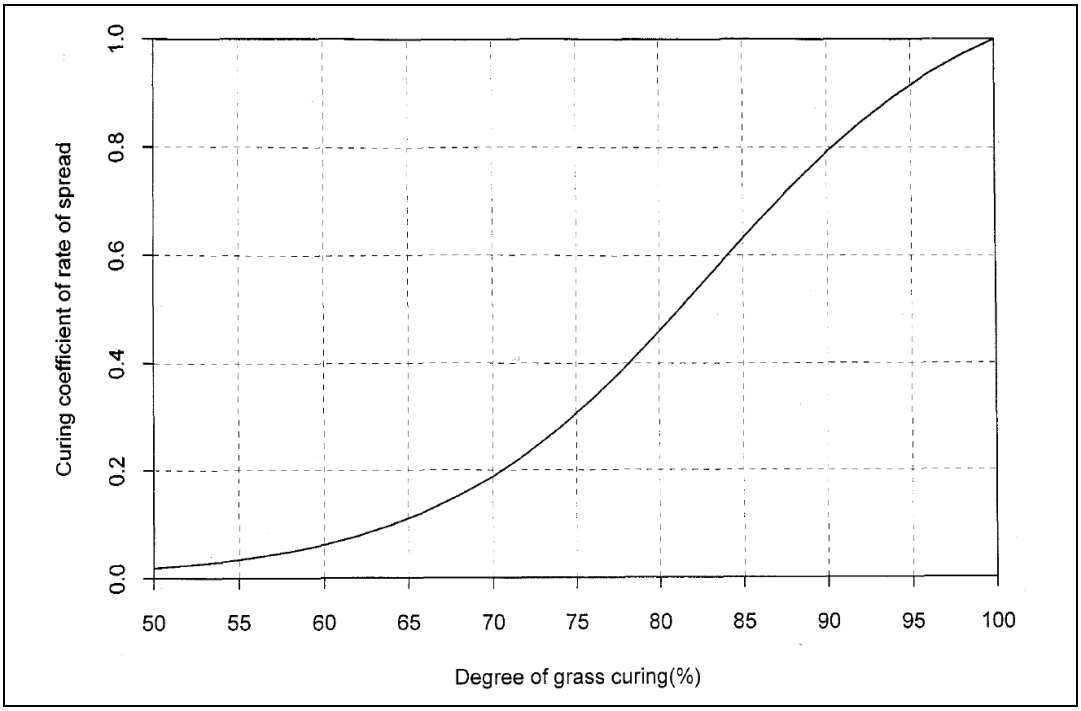

Figure 1.6. The effect of degree of curing on the rate of fire spread (Cheney *et al.* 1998).

Fuel height is not included in either rate of spread equations, or the fire danger meter, but may have a small effect on the rate of spread. When taller, tussock-like grasses were grazed, the proportion of dead material remaining in the sward increased, as did the likelihood of sustainable burning (Leonard *et al.* 2010). Fuel height may also influence fire intensity and therefore the difficulty of suppression. Tall fuels may emit greater radiant heat and be difficult to extinguish

in the short term, while low dense fuels may be more easily approached, but be difficult to fully extinguish if allowed to smoulder (Cheney and Gould 1995b).

1.4.4.3 Planned fires

The use of planned fire is known variously as fuel reduction, controlled or prescribed burning, but the objectives of such burning may go well beyond fuel reduction. Planned burning is conducted in conditions that allow a fire to spread but to be controlled or self-extinguish (King *et al.* 2006; Higgins *et al.* 2011). As a fuel reduction strategy, planned burning reduces the amount and continuity of fine fuel, to reduce the number and intensity of subsequent unplanned fires, as well as the area burned. Fire suppression success in the landscape generally, and at the peri-urban interface, should subsequently increase (Bradstock *et al.* 1998; Fernandes and Botelho 2003; King *et al.* 2006; Cary *et al.* 2009; Higgins *et al.* 2011; Price and Bradstock 2011). Planned fire is also used to manipulate and maintain biodiversity in both forested and grassland ecosystems (Robertson 1985; Gill and Bradstock 1994; Marsden-Smedley and Catchpole 1995a; King *et al.* 2006).

Severe fire weather conditions including high wind speed and temperature, and low relative humidity, reduces fuel moisture content, which has a greater impact on fire behaviour than do other fuel characteristics (Fernandes and Botelho 2003; King *et al.* 2006). Planned burns attempt to reduce uncertainty regarding suitable burn conditions (Higgins *et al.* 2011). Fuel moisture content must be suitable to allow ignition and spread of a planned fire, and subsequent self-extinguishment. Due to the complex and dynamic nature of fuel moisture content in grasslands, accurate assessment of curing over time is vital in determining the

behaviour of grassfires and the potential use of planned fire as a management tool in grasslands.

1.5 Curing as a surrogate for fuel moisture content in grasses

The measurement of fuel moisture content is time consuming and labour intensive. Direct measures are often not readily available to fire agencies and operations in timeframes suitable for planned burns or in fighting wildfires. However, it is possible to use indirect measures if they are closely related to fuel moisture content and it makes sense to do so if these surrogates are accurate, timely, inexpensive and relatively easy to obtain (Purvis 1995).

In the case of grasslands, fuel moisture content is dependent on the simultaneous moisture contents of both live and dead material within the sward. A relationship between fuel moisture content and curing values in grasslands has been developed (Parrott and Donald 1970b; Luke and McArthur 1978). Low curing percentage is associated with high fuel moisture while high curing percentage is associated with very low fuel moisture content (Figure 1.7).

Curing percentages less than 100 are a surrogate indicator for the moisture content of live fuel (Catchpole 2002). Accurate curing assessments are required for grassfire danger ratings to ensure the readiness of the general public and appropriate suppression forces when extreme fire weather is anticipated, and to calculate the rate of spread of fire in grasslands.

Curing percentages between 70 and 90% have the greatest influence on rate of spread of fire and are incorporated into the rate of spread models for grassfires using a curing coefficient (Figure 1.6) (Cheney and Gould 1995b; Cheney *et al.*

1998). Curing values in the 50 – 75% range provide an opportunity to use fire for planned burning of grasslands (Anderson 2007), as in suitable weather conditions such fires should have a reduced rate of spread and be more easily extinguishable. Importantly, these curing conditions occur earlier in the spring and summer fire season in southern Australia, coinciding with milder weather conditions, which also mediate the fire behaviour and increase the likelihood of suppression (McCarthy 1989).

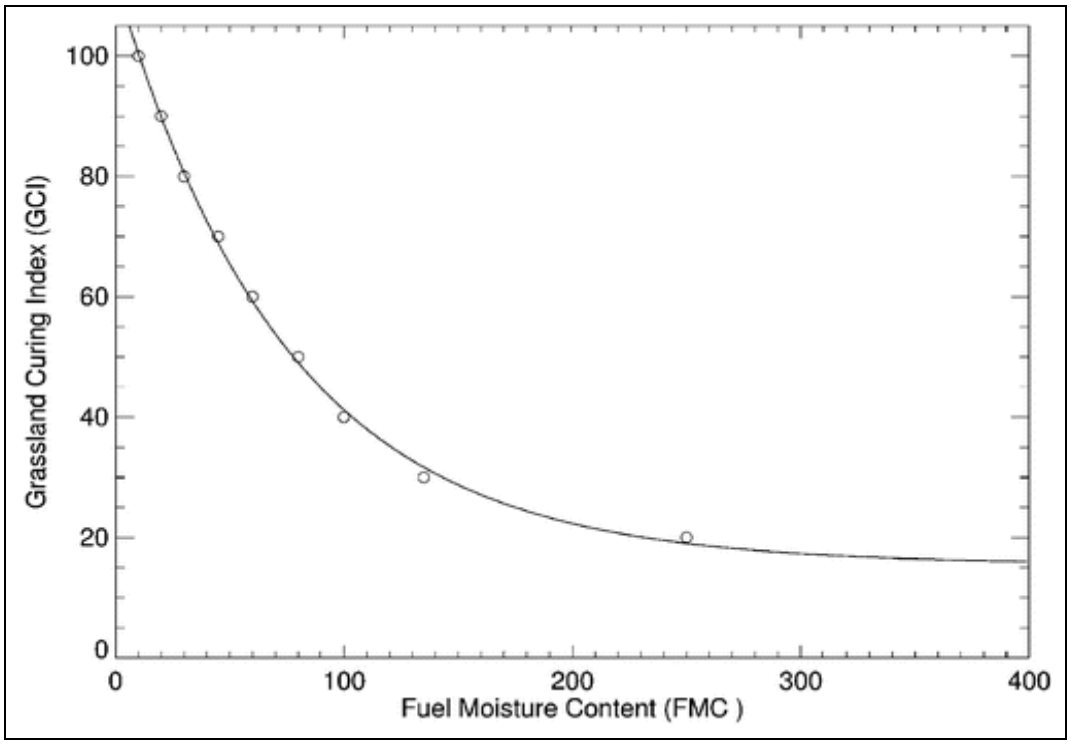

Figure 1.7. Relationship between percentage of dead grass (grass curing index) and fuel moisture content (after Barber 1990) (Dilley *et al.* 2004).

Curing values greater than 90% indicate there is insufficient fuel moisture to dampen ignition or sustainability of fire. Grasslands with high proportions of dead fuel will become flammable as residual moisture is driven off by low humidity and high temperature associated with fire weather conditions.

Grasslands with curing values below 50% are generally considered unable to sustain fire (Cheney *et al.* 1998; Cheney and Sullivan 2008). However, Parrott and Donald (1970b) found that ignition rates for two annual grasses, *Hordeum*

leporinum Link (barley grass) and *Lolium rigidum* Gaudich. (Wimmera annual ryegrass), approached 100% when curing was only around 40%. In contrast, when 80% cured, another annual grass (*Bromus mollis* L., or soft brome grass), could sustain ignition only 50% of the time. The potential of fire to spread at curing values below 50% has been reflected in revisions to the Canadian grass fire spread models (Anderson *et al.* 2011).

1.5.1 Current curing measurements and their limitations

Oven drying is used as a benchmark for determination of fuel moisture content in grass samples (Matthews 2010). Although it is a simple method, variation in drying temperature can affect the fuel moisture content (Matthews 2010) and the 24-hour drying cycle render the technique too time-consuming to provide fuel moisture content values in real-time for fire agency use. The method cannot account for spatial variability in fuel moisture content unless samples are collected over the entire landscape which may not always be practical. Hence, alternatives to oven drying are required.

Obtaining timely and accurate measures of curing across the landscape has proved problematic. Destructively-harvested and oven-dried grass samples can be physically separated into live (green) and dead (dry) fractions and this is the most accurate method for determining a curing percentage (Anderson *et al.* 2011). This separation is both labour and time-intensive, compounding the disadvantages of the oven drying technique (Anderson *et al.* 2011). Capturing variability across landscapes remains a limitation.

Visual guides to estimate grass curing have been developed to allow field operators to align grass colour (from green to bleached straw) and physiological stage, with a curing percentage (Garvey and Millie 1999; Flavelle 2002; Anderson

et al. 2011). Fire agencies in most Australian states use field observers to visually assess curing percentages and relay this to a central point, where state-wide information is collated and hand-drawn maps are generated to display the rate of curing at a given time. Figure 1.4 shows the progress of curing across Victoria at monthly intervals in summer 2007/8 established from visual curing estimates.

Visual estimation has been the cornerstone of grass curing assessment in much grassfire research but there has been concern about variation between operators in conducting this task (Cheney *et al.* 1998). Visual estimates are often poorly correlated with the destructive sampling technique (Millie 1999; Anderson *et al.* 2011; Newnham *et al.* 2011) and the low frequency and partial coverage of observations is a constraint (Newnham *et al.* 2011).

Comparison of field assessment techniques for curing has shown that a modified Levy Rod technique (Levy and Madden 1933) whereby curing percentage calculated from counts of live and dead leaves touching a metal rod placed vertically into the sward (Anderson *et al.* 2011), yielded comparable results to the destructive sampling benchmarks (Anderson *et al.* 2011; Newnham *et al.* 2011). It was quick and easy to carry out, and overcame the subjectivity of the visual observation technique (Anderson *et al.* 2011). The accuracy of the Levy Rod method in tall grasslands under windy conditions has been questioned (Carter and Cochrane 1992), however Anderson *et al.* (2011) found that windy conditions did not influence their observations. The Levy Rod technique remains labour-intensive and does not overcome the challenges of capturing landscape variability. While it was recently recommended for field assessment (Anderson *et al.* 2011) it has not yet widely replaced visual assessment (e.g. Callaghan 2010; Anderson *et al.* 2011).

Remote sensing is also used to estimate curing (Barber 1990; Chladil and Nunez 1995; Dilley *et al.* 2004; Anderson and Botha 2007; Martin *et al.* 2007). Vegetation characteristics are assessed using Advanced Very High Resolution Radiometer (AVHRR) and Moderate Resolution Imaging Spectroradiometer (MODIS) sensors orbiting the Earth daily on satellites operated by the US National Oceanic and Atmospheric Administration. Red and near-infrared reflectance bands are used to calculate the Normalised Difference Vegetation Index (NDVI) which has been related to curing through visual assessments and fuel moisture content. Maps of curing changes have been produced by the Bureau of Meteorology for Victoria and south-eastern Australia using these technologies since the 2002-3 fire season (Newnham *et al.* 2010). Remotely sensed imaging operates at a coarse spatial scale and is subject to distortion or disruption by cloud, smoke or haze, tree presence, bare ground, etc. (Anderson and Pearce 2003). Development of a Relative Greenness Index may overcome particular problems with NVDI such as bare ground caused by landscape change, and tree presence (Newnham *et al.* 2011). Recent research funded by the Bushfire Cooperative Research Centre aims to enhance the utility of satellite products (Martin *et al.* 2007).

1.6 Plant growth models

Tunstall (1988) recognised that it would be simpler to measure live fuel moisture directly than to derive it from the complex inter-relationships between soil, plant and atmosphere. However, he did identify the potential for using models of plant photosynthetic production to predict growth phases and leaf carbohydrate changes, which influence live plant moisture content. Plant growth models incorporated in decision support tools (DST) such as GrassGro™ (Moore

et al. 1997), APSIM (Keating *et al.* 2003) and the SGS Pasture Model (Johnson *et al.* 2003) are sophisticated mathematical representations of components of temperate grassland ecosystems that have been used for a variety of purposes. Computer simulations allow models of biophysical relationships to be explored over long periods of time and in a range of locations, which would be prohibitively costly and time-consuming if conducted via field work. Investigating variability due to weather effects through modelling may identify environmental outcomes that only emerge in the long term (Johnson 2011).

The potential of pasture modelling has been explored as a means of generating curing estimates (Gill *et al.* 1989; Gill 1999; Anderson and Pearce 2003; Gill *et al.* 2010). If a wide range of grass species parameters are available then these might be applied to a number of environments (specifically climate, soil, and management factors) in almost limitless combinations. This could provide better spatial coverage of curing across the landscape for the assessment of fire danger rating and the imposition of fire bans. Use of plant growth models contained in DST could complement other sources such as remote sensing, by providing spatially specific estimates of curing where other sources are not available.

The predictive functions within some DST could be used to provide seasonal outlooks of curing, to better identify windows of opportunity for prescribed burning activities. The potential to predict curing with weather forecasts is not available in other systems and would be extremely valuable for fire management.

DST could provide a platform to quantify the effect of grassland management practices such as mowing, grazing and burning on fire hazard. DST could then be used as a planning tool to assist fire agencies in allocating prescribed burn and

suppression resources and, potentially, in manipulating curing rates to optimize resource allocation.

1.6.1 Previous attempts to use models for curing assessment

A prototype version of GrassGro™ (Moore *et al.* 1997) was used to estimate daily curing rates from green and dead biomass for a phalaris pasture at Canberra (Gill *et al.* 1989). These values were used in the Grassland Fire Danger Index to predict the rate of spread and intensity of grass fire given historical weather patterns, in order to ascertain the time to reach the 'extreme' fire danger category.

Water deficit outputs from a wheat yield model called CEREAL (Hignett 1975) were incorporated with Soil Dryness and Grass Curing Indices to create a grassland curing model for 30 sites across South Australia. The resultant model was used to better define fire danger districts and the beginning and length of fire danger periods within each district (Dawson *et al.* 1991).

In the Palmerston North region of New Zealand, a local pasture model was used to determine the rate of curing for a narrow range of pasture species, soil types and reproductive plant development (Anderson and Pearce 2003). Initial work suggested that the onset and rate of curing predicted by the model were similar to that measured in the field (Baxter and Woodward 1999).

More recently, Gill *et al.* (2010) explored the potential to produce Grassland Fire Danger Index (GFDI) values and potential fire intensities using simulated curing estimates derived from the GRAZPLAN model. Simulations of ungrazed exotic and native perennial pastures, and exotic annual pastures, were run over historical time frames and resultant curing rates were used to calculate GFDI. The different pasture species produced seasonal and yearly differences in curing rates and GFDI. However, no archived records of GFDI observations exist to allow

comparison with the modeled GFDI (Gill *et al.* 2010). Gill (2008) considered that the Ausfarm suite of decision support tools, including GrassGro™ (Moore *et al.* 1997), could be widely applied to estimate curing across temperate Australian grasslands, providing adequate coverage of regional areas and accounting for a range of pasture management treatments such as mowing. However, he noted that differences in curing status and moisture content between native and introduced grasses with different fertility status, as well as differences between standing dead and leaf litter were not addressed in Ausfarm (Gill 2008).

1.6.2 The ability of current models to assess curing

A comprehensive review of the ability of commonly available DST to provide timely and accurate grass curing data for fire management purposes has not been undertaken. Here, three such DST are reviewed: 1) the Agricultural Production Systems Simulator (APSIM) (version 7.2, build date 20/8/2010) (Keating *et al.* 2003); 2) GrassGro™ (version 3.2.3, build date June 2010) (Moore *et al.* 1997) and; 3) the SGS Pasture Model (version 4.8.3, release date 26/2/2009) (Johnson *et al.* 2003). APSIM is the most commonly used cropping model in Australia for agronomic research and management (Robertson and Carberry 2010). GrassGro™ is used as both a research and management DST for grazing industries, incorporating the Australian Ruminant Feeding Standards, and a number of flexible animal management options (Moore *et al.* 1997). The SGS Pasture Model was developed as a research tool for analyzing individual sites and generic pasture systems during the Sustainable Grazing Systems National Experiment (Johnson *et al.* 2003).

1.6.2.1 Modelling of senescence and death

APSIM, GrassGro™ and the SGS Pasture Model use various strategies for modeling grass senescence as summarized in Table 1.5 which make it difficult to monitor senescence, or represent leaf senescence in all stages of plant growth. In the wheat module of APSIM, any leaf senescence prior to flowering is caused by water stress, light competition or frost, rather than being an integral part of plant growth. Constant leaf death algorithms underlying the GrassGro™ model restricts the ability to provide accurate and dynamic curing outputs which adjust to changing seasonal conditions. Rate of leaf senescence in the SGS Pasture Model responds to temperature and water stress but not to developmental progression.

Table 1.5. DST strategies for modelling components of leaf senescence.

Components of leaf senescence	APSIM	GrassGro™	SGS Pasture Model
Progressive senescence of leaf tissue in vegetative stages	Modelled through light competition, water stress, frost, and nitrogen and high temperature in some species	Modelled through change in dry matter digestibility in living leaves; constant death rate once senescence of leaf tip is evident	Modelled through leaf flux in response to temperature and water stress
Triggers between phenological stages	Thermal time and photoperiod	Thermal time or day length	Number of days
Post-reproductive phase	Death due to age (#leaves per day) occurs only after flowering	Constant death rate (in terms of thermal time) applied to whole plant	Modelled through leaf flux in response to temperature and water stress
Achievement of "senescent" phenostage	May be interrupted by harvest	At the end of the reproductive phenostage	Not modelled
Extent of environmental influences on senescence	Not calibrated	None (constant death rate)	Not calibrated

1.6.2.2 APSIM

APSIM calculates plant and leaf characteristics such as leaf and node appearance, development stages, leaf area development, and plant component biomass on a daily basis in response to climate and management inputs. APSIM

uses the relationships between temperature and leaf initiation rate, leaf appearance rate and plant leaf area to simulate leaf area production and senescence (Keating *et al.* 2003). Phenological progression between sowing and floral initiation is determined by a combination of thermal time accumulation, sowing depth, soil water availability, and vernalisation and photoperiod requirements. APSIM crop stages after floral initiation are determined by fixed thermal time values (Anonymous 2011a).

Senescence due to plant age is applied after flowering to the oldest leaf, with a fraction of the leaf dying each day at a given rate of leaves per day. The senesced leaf area due to age is multiplied by the greatest limiting factor from light competition, water stress, and frost, to obtain the total amount of leaf area senescing that day. The wheat and barley modules, which represent two grass species modelled by APSIM, refine the triggers for senescence by including nitrogen stress and high temperature stress. Separate factors, which range in magnitude from 0 (no effect) to 1 (complete effect) are determined each day to capture the extent of nitrogen, water and temperature stress experienced by the crop. The maximum of these factors is multiplied by the 'potential' rate of leaf senescence (based on age) to derive the 'actual' daily senescence rate (Anonymous 2011a).

1.6.2.3 GrassGro™

A number of phenological stages for annual and perennial plants are defined within GrassGro™. The reproductive phenostage is followed by the "senescence" phenostage in annuals and the "summer dormancy" phenostage in perennials. Plants entering senescence or summer dormancy are treated as if they are alive, but experience an accelerated death rate (Moore *et al.* 1997). The senescence

phenostage output accumulates in daily units until the resumption of growth, and does not distinguish between senescent and dead plant material.

Grass leaves are not modelled individually in GrassGro™, but are rather classified into various tissue pools within the sward (Figure 1.8). The live tissue pool is made up of seedlings and established plants. Tissue in the live pool may be in one of two digestibility stages, depending on its age. The first is equivalent to leaf elongation, where the live tissue maintains a constant digestibility, and does not die. A second stage representing post-elongation growth is triggered by thermal time, whereby digestibility declines, but death rate continues to be zero. Live tissue enters the senescing pool at a further thermal time signal, and continues to decline in digestibility and begins to die at a constant death rate (Anonymous 2011c). This allows dead herbage to gradually accumulate during the vegetative and reproductive phases of the plant's life (Moore 2010).

When the reproductive phase finishes in both annuals and perennials, all remaining live biomass is transferred into the senescent biomass pool and a further constant death rate is applied, until all herbage is dead. So, at the onset of the senescence phenostage, the biomass in the senescent tissue pool is both green and at its maximum level, and decreases over time as it transfers to the dead pool (Moore 2010).

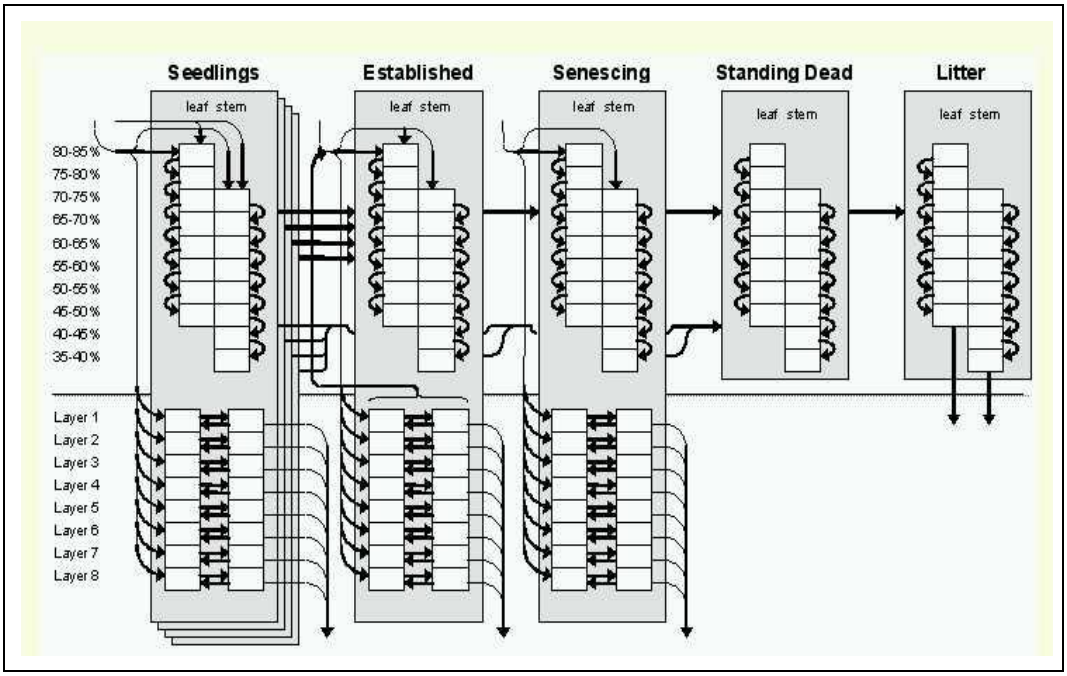

Figure 1.8. Turnover between sward components (horizontal axis) and digestibility classes (percentage dry matter digestibility on vertical axis) and soil layers in GrassGro™ (Anonymous 2010).

With the exception of frost (ΔF), death (Δ_{cpd}) of above ground (p), green sward components (c), of any pasture species (j), can only take place from the 50 to 70% digestibility classes (d=2…4, where 2 = 70%, 3 = 60% and 4 = 50 %), and occurs at a constant rate (K_{D1cpj}). Death is faster from the senescing pool (c=*senc*) than the live pool (c=*live*, d=1, where 1= 80%) (Equation 1.1) (Moore *et al.* 1997).

(1.1)

$$\Delta_{cpd} = \begin{cases} \Delta F & d=1 \\ K_{D1cpj} + \Delta F & d=2...4 \end{cases} \forall c = live, senc$$

While GrassGro™ allows for an increase in death rate, this occurs only after the reproductive phase has been completed.

1.6.2.4 The SGS Pasture Model

In the SGS Pasture Model, the photosynthetic assimilate available to plant growth is partitioned between the shoot and root portions of the plant, and cycles through the aerial and underground components until returned to litter or soil organic matter respectively (Johnson 2008). Shoot turnover is illustrated in Figure

1.9. Initially, leaves, sheath and stem are actively growing, before moving through two non-specified live stages. It is convenient to think of the first live stage as maturity (i.e. the leaf is fully elongated and the ligule developed) and the second as the onset and progress of senescence before entering the standing dead phase.

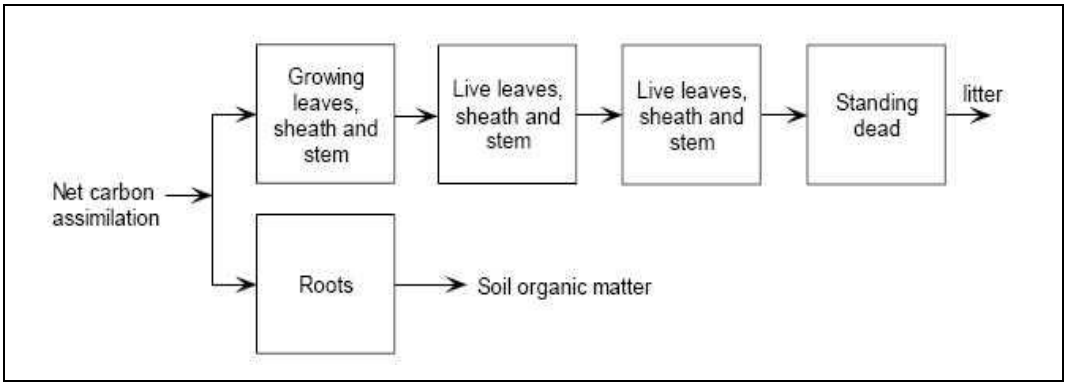

Figure 1.9. Schematic representation of tissue turnover in SGS Pasture Model (Johnson 2008).

The movement of tissue weight (W) between these compartments of live tissue (*live*, numbered 1, 2 and 3 for growing, mature and senescing respectively) is controlled by flux parameters (γ) from one to the next. The curing process is represented by the flux from the senescing leaves (compartment 3) to the dead leaf pool (*dead*) (Equation 1.2).

$$Flux(3 \rightarrow dead) = \gamma W_{live,3} \quad \textbf{(1.2)}$$

Flux (γ) between tissue classes occurs at a reference rate (γ_{ref}), with additional responses to temperature ($f_{\gamma,T}$) and water stress ($f_{\gamma,W}$) also possible (Equation 1.3).

$$\gamma = f_{\gamma,T} f_{\gamma,W} \gamma_{ref} \quad \textbf{(1.3)}$$

Leaf appearance rate declines with water stress in all species and with high temperatures in C_3 species. The response of leaf flux to temperature (T) (Equation 1.4), and to water stress (GLF_{water}) (Equation 1.5) results in an increase in leaf

turnover with increasing temperature and water stress as fewer leaves appear and are removed more quickly by senescence.

(1.4)

$$f_{\gamma,T} = \begin{cases} 0, & T \le T_{mn;} \\ \dfrac{(T - T_{mn})}{(T_{opt} - T_{mn})}, & T_{mn} \le T \le T_{opt} \\ 1, & T > T_{opt}; \end{cases}$$

(1.5)

$$f_{\gamma,W} = \begin{cases} (f_{\gamma,W0} - 1)\left(\dfrac{GLF_{water,opt} - GLF_{water}}{GLF_{water,opt}}\right) + 1, & GLF_{water} \le GLF_{water,opt} \\ 1, & GLF_{water,opt} \le GLF_{water} \end{cases}$$

Senescence rate increases with water stress and high temperatures. The SGS Pasture Model uses default values for minimum temperature (T_{mn}=5°C), optimal temperature (T_{opt}=20°C), response to water stress ($f_{\gamma,W0}$=2) and growth limitation at optimum water ($GLF_{water,opt}$=0.5). Without specific knowledge of the parameters for individual species, it is likely that the SGS Pasture Model would produce similar rates for curing outputs across species, or at least, that the onset of curing would be similar across species, through these temperature and water stress triggers.

1.6.2.5 Other aspects of DST scope and functionality

The scope and functionality of each DST varies in its ease of use and suitability for curing assessment. The number of grass species able to be simulated is limited in each DST (Table 1.6).

Common modeling protocols have been used to link the soil moisture and crop modeling capabilities of APSIM with the pasture and animal modeling used in GrassGro™ (Moore *et al.* 2007) in a research tool called Ausfarm. Common modeling protocols have also allowed pasture species used in GrassGro™ to be

incorporated into APSIM (Table 1.6), which has the widest range of parameters for cereals. However, use of these pasture models in APSIM requires additional licensing of the Ausfarm DST (Anonymous 2009). The SGS Pasture Model provides parameters for generic native grasses with both the C_3 and C_4 photosynthetic pathways. No single DST can currently simulate each of the four common species used in the experiments reported in this thesis; however if grazing oats were substituted for wheat on the basis of phenotypic similarity (Lopez-Castaneda and Richards 1994), then the SGS Pasture Model would be best suited to the task.

Table 1.6. Grass species incorporated into common DST, listed by annual or perennial growth type. These are divided into use of the C_3 or C_4 photosynthetic pathway, with cereals further separated. Species included in the following experiments are highlighted by bold font.

Grass growth type	Photosynthetic pathway	APSIM (7.2)	GrassGro™ (3.2.3)	SGS Pasture Model (4.8.3)
Annual	C_3	Available via Ausfarm: **Annual ryegrass** Annual grass - early	**Annual ryegrass** Annual grass - early	**Annual ryegrass**
Annual Cereal	C_3	Barley, maize, oats, rice, **wheat**		Grazing oats
Perennial	C_3	Available via Ausfarm: Perennial ryegrass **Phalaris** Cocksfoot	Perennial ryegrass **Phalaris** Cocksfoot	**Native** **Phalaris** Perennial ryegrass Tall fescue
	C_4	Sugar cane		Native Kikuyu Rhodes grass Paspalum

The growth and development processes captured in the models in DST are driven or influenced by key climate variables such as temperature, rainfall and radiation, as well as soil factors such as water holding capacity and nutrition, and a raft of management (e.g. cultivar, irrigation, fertilizer) factors. Each DST requires these variables as inputs, although the format of inputs may differ. Each DST supplies a number of default variables. For instance, GrassGro™ has

weather files for a number of standard locations throughout southern temperate Australia. Additional weather data files can be downloaded from SILO (Bureau of Meteorology 2009). SILO weather files need to be downloaded and processed slightly differently in the other DST; however, the ability to access and use such data ensures the currency of simulations developed and increases the geographical range of simulations.

Reliable simulation of the pasture base with DST requires a definition of realistic management regimes; however the options available in the DST are less comprehensive and responsive than those which occur in reality. Management rules within DST are often set out on a yearly plan, with some DST being better able to respond to current conditions than others, with greater flexibility in sowing decisions, stock movements or supplementary feeding. For example, rules in APSIM allow crop sowing to be triggered by a mix of calendar and weather events such as rainfall, and physical conditions such as soil moisture levels, whereas in GrassGro™, the option to re-sow a pasture can be triggered only if the seedbank of annual species or root mass of perennial species falls below a threshold level. GrassGro™ and the SGS Pasture Model both provide a range of stock movement options, but the supplementary feeding options in GrassGro™ are more sophisticated than those in the SGS Pasture Model.

Other points of difference between the DST include the scale at which input variables are expressed. For instance, the SGS Pasture Model and APSIM describe bulk density in terms of g/cm^3, and GrassGro™ lists this measure in the glossary but refers to mg/m^3 in the input section. Field capacity and wilting point are expressed as m^3/m^3 in GrassGro™, while SGS Pasture Model uses percent volume. Although the values are equivalent, it is necessary to convert the units in

which many variables are expressed, to simulate the same species growing in the same location, using different DST.

No single output describes the onset or the rate of progress of curing and consequently curing percentage is not specifically represented in any of the three DST. However, curing percentage could be manually calculated from APSIM and the SGS Pasture Model using outputs of green and dead herbage mass. A report-building function within GrassGro™ enables curing percentage to be calculated from appropriate outputs to automatically generate customised graph or table outputs.

Each DST differs in terms of the supplied inputs and case studies, provision of training and assistance and cost and license conditions. This complexity may discourage fire agencies to invest time and effort in incorporating DST into the suite of resources used to assess curing.

1.7 Thesis aims and structure

The review of the literature has shown that existing knowledge of leaf growth and turnover has not been gathered with an emphasis on leaf death, and hence it cannot be applied directly to the process of curing in grasses. Much of this knowledge is incorporated into current DST. Although these DST provide a potential platform to predict curing rates in grasslands, a number of limitations in these tools have been identified.

The indirect measurement of live fuel moisture content in grasses through curing assessment is vital for fire management in grass-dominated landscapes. **This thesis tests the hypothesis that in order to improve the assessment of grass curing, stand-alone models developed with a detailed understanding of the relationships between leaf growth rates will provide a higher level of**

accuracy of grass curing than the pasture growth models currently incorporated into commonly-available DST.

The suitability of commonly-available process-based crop and pasture dynamic models to estimate curing rates for fire managers remains to be thoroughly tested. The focus of current agricultural DST is mainly on generative plant growth, rather than the senescence and death of plants. It may be beyond the scope of a single current DST to assess curing across the full range of species with varying growth habits found in temperate grasslands in southern Australia. In **Chapter 3**, the curing outputs of APSIM, GrassGro™ and the SGS Pasture Model are compared to curing estimates derived from field methods traditionally used by fire agencies to assess curing, namely Levy Rod, visual and destructive harvesting techniques.

In its simplest form, leaf curing can be determined from the length of green and dead leaf components. Knowledge of these characteristics, along with leaf length, allows the calculation of the proportion of live and dead material within the leaf before death is complete. Calculated across all leaves present on a tiller, plant or sward, this allows curing percentage to be measured over time. In **Chapter 4**, new species-specific models of leaf curing percentage are developed and tested to determine if they might provide a valid alternative to other methodologies for measuring curing in the field and estimates derived from DST.

The initial work describes curing in terms of thermal time, which assumes a known starting point for thermal time accumulation. However, curing can also be described in terms of leaf turnover. The curing process begins with the onset of leaf senescence, and the rate of leaf senescence determines the duration of curing in each leaf. Therefore, to model the progress of curing in a process-based manner,

knowledge is required about leaf life span and leaf senescence rate. However, differences in leaf turnover characteristics may be responsible for the differing growth habits exhibited within the Poaceae family. **Chapter 5** reports the models of leaf turnover characteristics to allow conclusions to be drawn about the transferability of such models between grass species with differing growth habits.

Variable environmental conditions can make it difficult to collect sufficient field data to calibrate and validate models in an ideal way. Controlled environment trials are appropriate to develop an understanding of processes, but the suitability of models based on glasshouse observations to predict curing in the field may be problematic (Turner and Begg 1978). A range of limitations to growth are experienced by plants under field conditions, the most significant of which is water stress. Water stress has been shown to increase leaf senescence rate (Fischer and Hagan 1965; Fischer and Kohn 1966; Hall 2001; Munne-Bosch and Alegre 2004) and decrease leaf length (Murty and Ramakrishnaya 1982). **Chapter 6** reports on separate glasshouse and field studies to explore the effect of water stress on leaf characteristics and specifically, whether the timing and severity of water stress produce different effects on leaf turnover, and if the relationship between leaf position and these leaf turnover characteristics remains consistent regardless of soil moisture status.

Leaf turnover algorithms do not, when used separately, predict leaf accumulation or curing in a tiller, plant or sward. Bayesian modelling may provide an approach to capture the relationships between the component leaf processes in order to most accurately predict leaf curing. A Bayesian model of leaf turnover is described in **Chapter 7,** to test if such an approach is superior over other methods in predicting curing in the field. The relevance of the findings

to the field of curing assessment for grassfire management and the potential modelling of leaf production and curing in grasses are discussed in **Chapter 8**.

2 General materials and methods

2.1 Introduction

This chapter sets out the rationale for species and site selection, and experimental and statistical techniques common to a number of the following experimental chapters. Where methods are specific to a particular chapter, then these methods or variations are given in the relevant chapter.

2.2 Species selection

The species included in this study were all common grasses in southern Australian landscapes which shared the C_3 photosynthetic pathway. They each differed in growth habit and phenology, and included examples of both native and annual species for which little leaf turnover information is currently available. The species chosen were wheat, annual ryegrass, phalaris, and wallaby grass (*Austrodanthonia duttoniana* (Cashmore) H.P. Linder) (Table 2.1), and these were used in glasshouse work reported in Chapters 4 to 7. The same species were used where possible in field work, reported in Chapters 3, 4, 6 and 7.

Table 2.1. Identity and growth habit details for target species used in the study.

Botanical Name	Common Name	Growth habit
Triticum aestivum L.	Wheat	Introduced cereal, synchronized annual phenology
Lolium rigidum Gaud.	Annual ryegrass	Introduced pasture, asynchronous annual phenology
Phalaris aquatica L.	Phalaris	Introduced naturalised perennial pasture
Austrodanthonia duttoniana (Cashmore) H.P. Linder	Wallaby grass	Native perennial pasture

2.2.1 Annual cereal crop

Fire prevention in cereal crops is important to fire agencies because of the high ignition potential at harvest time and the high asset values of crops and

associated machinery (Miller 2008; Anonymous 2012a; b). Cereals are annual grasses that are genetically selected to display synchrony of phenology and uniformity of leaf and tiller production, and grain yield. Wheat was chosen in this study because of its geographical spread across Australia (85% of the total cereal grain production in temperate Australia (Lopez-Castaneda and Richards 1994)) and the fact that it is a well-researched grass crop. The research cultivar "Bob White" was used in glasshouse trials. Field work took advantage of existing plantings of commercial varieties of wheat or barley, depending on their presence at selected field sites.

2.2.2 Annual introduced pasture grass

Other annual grasses display less synchrony and uniformity within the population than wheat. Many high rainfall pastures have become annualised over the past decades with the ingress of annual "weedy" species (Anonymous 2008b). For example, annual ryegrass, the most common ryegrass in Australia, is an important naturalized weed in the Australian wheatbelt (Kloot 1983; Owen *et al.* 2007). Previous work on moisture content and ignitability of annual pastures also used annual ryegrass (Parrott 1964). The "Wimmera" cultivar was used in glasshouse plantings, while the commercial cultivars available at field sites are shown in Table 2.3.

2.2.3 Perennial introduced pasture grass

Perennial grasses may show reproductive phenological stages and leaf senescence and death as a result of deteriorating environmental conditions, culminating in the dormancy of the plant crowns to allow later growth resumption. Phalaris is an introduced but naturalised perennial grass, common in pastures in

southern Australia regardless of level of management inputs (Virgona and Hildebrand 2007), with weed-like properties on unmanaged roadsides in southern Australia (Miller 2008). It was included in this study as an example of a non-native perennial species. "Holdfast" was the cultivar used in glasshouse plantings, while the commercial cultivars used at field sites are given in Table 2.3.

2.2.4 Perennial native grass

Common wallaby grass (*Austrodanthonia caespitosa* (Gaud.) H.P.Linder) is a perennial native grass that grows widely in the southern states of Australia (Council of Heads of Australasian Herbaria Inc 2011). Plants grown in the glasshouse trials, from seed purchased as *Austrodanthonia caespitosa*, were subsequently identified by the South Australian State Herbarium to be *Austrodanthonia duttoniana*, also known as brown-back wallaby grass (Robertson 1985). It has been widely collected throughout South Australia, Victoria and New South Wales (Council of Heads of Australasian Herbaria Inc 2011).

Positive identification of wallaby grass in the field prior to flowering proved difficult. In 2008, native grass plants selected in the field were identified after flowering as spear grass (*Austrostipa* S.W.L. Jacobs & J. Everett spp.), another native perennial grass which uses the C_3 photosynthetic pathway (Table 2.3). The distribution of common spear grass species, such as rough spear grass (*Austrostipa scabra* ((Lindl.) S.W.L. Jacobs & J. Everett), is widespread over temperate Australia (Council of Heads of Australasian Herbaria Inc 2011).

2.3 Glasshouse experiments

The experiments that provided data for Chapters 4 to 7 were conducted in a glasshouse at the South Australian Research and Development Institute's (SARDI)

Plant Research Centre at Waite Campus, Adelaide, South Australia (34.97°S, 138.63°E). Glasshouse temperature was maintained between 16 and 22°C; however there was no control for relative humidity. Additional morning and evening lighting during the winter and spring months maintained the photoperiod at a constant 15 hours per day.

Approximately 12 seeds were planted in each pot on the 16th July 2008. To remove any possible influence due to varying water and nutrient stress on treatment responses, pots of 30 cm diameter were filled with a SARDI-produced pre-fertilised "coco-peat" potting mix (Appendix A, Table A-1) to ensure adequate plant nutrition, and saturated with tap water at seeding. Thereafter pots were lightly watered with a handheld spray each weekday and once on weekends. Pots were monitored for signs of topsoil dryness as biomass increased, and watered to field capacity when necessary, except when allocated to water stress treatments, as discussed in section 2.3.2.

2.3.1 Leaf growth under optimal growth conditions

In the first experiment, plants were grown under optimal glasshouse conditions for the duration of their lifecycle, and leaf turnover observations were recorded (Chapters 4, 5, and 7). A completely randomized design was used with four species as treatments, making 16 pots in total, laid out as illustrated in Table 2.2. Each treatment was represented by 4 replicates, each consisting of two plants per pot. The balance of the plants in each pot was allocated to sequential destructive sampling. Random effects were used in statistical analysis to account for pseudo-replication corresponding to plants within pots.

Table 2.2. Pot layout across glasshouse bench where A, D, P and W indicate annual ryegrass, wallaby grass, phalaris and wheat respectively.

1: D	2: A	3: W	4: A
5: D	6: A	7: P	8: W
9: W	10: P	11: A	12: D
13: D	14: W	15: P	16: P

2.3.2 Leaf growth under conditions of water stress

Additional plants were established in order to test the effects of terminal water stress on leaf growth rates (Chapter 6). Plants were subjected to terminal water stress at one of three different times, coinciding with early, mid- and late spring. A split plot design was used in which the imposition of the water stress treatment was applied to main plots. Within each treatment plot, species were represented by 8 randomly arranged pots, each containing two plants (Table 6.2). At the 3-leaf stage, plants were thinned to four uniform plants per pot. A single plant in each pot was randomly selected for measurement.

2.4 Field trials

This study incorporated the use of field sites for two reasons. Firstly, because the suitability of models based on glasshouse observations to predict field phenomena has sometimes been questioned (Turner and Begg 1978), it was important to know how leaf turnover characteristics in the field behaved compared to those observed in the glasshouse, under both optimal conditions (Chapter 5), or conditions of terminal water stress (Chapter 6). Secondly, the field data was used to validate the glasshouse-derived models in Chapters 4 and 7.

2.4.1 Site selection

Selection of field sites took into account a number of criteria including: 1) an inventory of recent and current grassland research sites in southern Australia

(Appendix A, Table A-2); 2) a list of essential and desirable criteria for potential field sites to validate finalised models (Appendix A, Table A-3); 3) input from fire authorities on characteristics of grasslands they deemed to be important; 4) occurrence of uniform stands of the four target grass types listed in Table 2.1.

Contacts from the inventory, as well as private agronomists, were approached to identify sites with the necessary grass types in a range of environments. Sites were established around Clare in the mid-north of South Australia, and Naracoorte in the south-east of South Australia during August 2008 (Figure2.1). The "Mid North" sites included two pasture demonstration trials with individual plots of different crop and pasture species, and a paddock of native grasses. The "South East" sites were paddocks of sown introduced crop and pastures, and remnant native pastures, all under the management of the SARDI Struan Research Centre. The species measured at each site are listed in Table 2.3.

Table 2.3. Grass species measured at each field site.

Region	Site	Species	Common Name	Cultivar
Clare, Mid North SA	Penwortham and Black Springs	*Hordeum vulgare*	Barley	'Dictator'
		Lolium rigidum	Annual ryegrass	'Tetrone'
		Phalaris aquatica	Phalaris	'Atlas'
	Farrell Flat	*Austrostipa* spp.	Spear grass	
Naracoorte, South East SA	Bool Lagoon 2008	*Triticum aestivum*	Wheat	
	Bool Lagoon 2010	*Hordeum vulgare*	Barley	
	Struan Paddock 1	*Lolium rigidum*	Annual ryegrass	'Winter Star'
	Struan Paddock 2	*Phalaris aquatica*	Phalaris	'Australian'
	Kybybolite 2008	*Austrostipa* spp.	Spear grass	

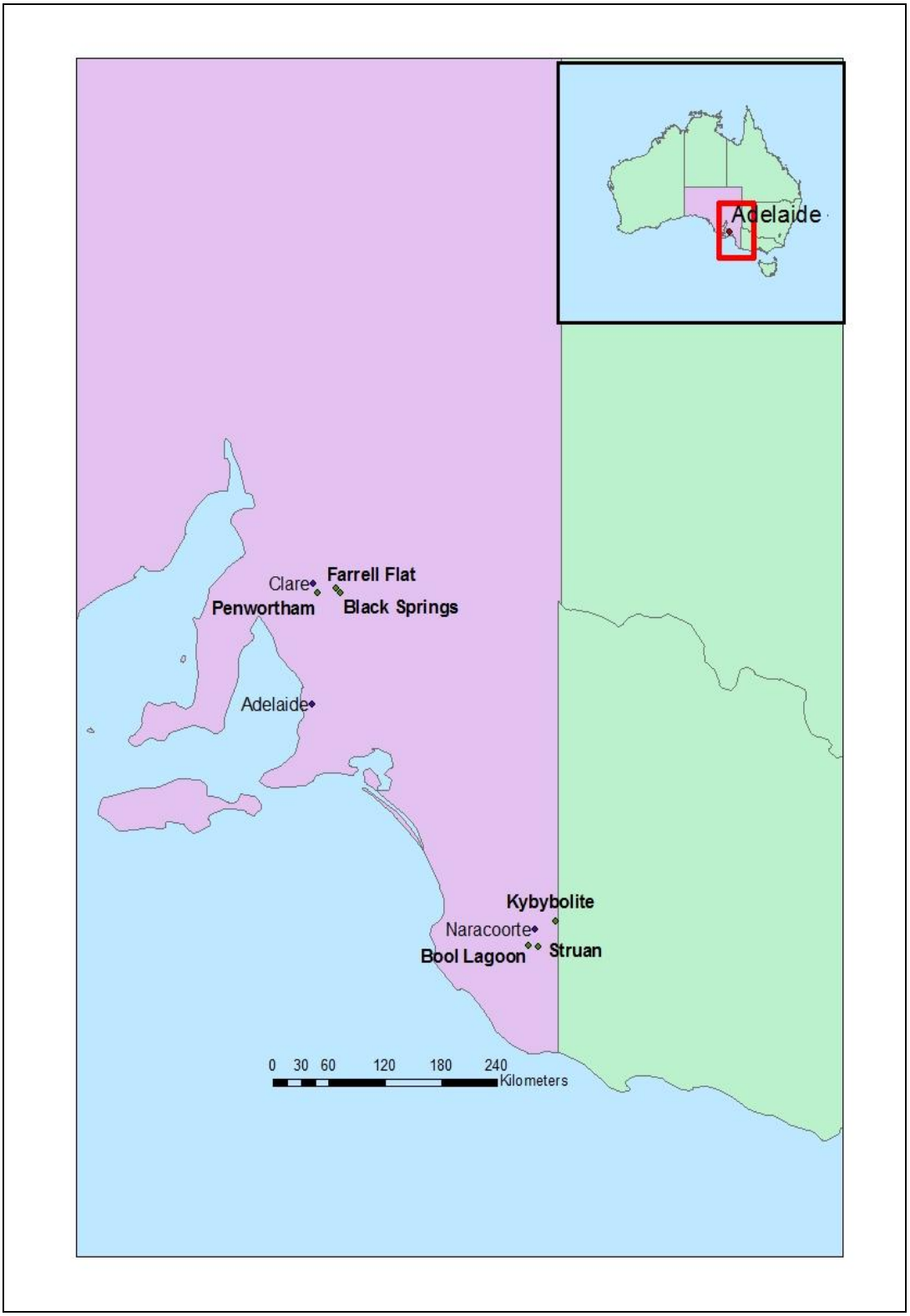

Figure 2.1. Partial map of South Australia with location of field sites.

2.4.2 Plant selection

Plant selection was not entirely random due to individual site constraints, such as the nature of the demonstration plot layout, impending silage harvesting, avoiding spray rig travel paths, and water logging. Outside of these constraints however, systematic sampling was used to select plants to attempt to cover the geographic spread of the sward. Each plant was identified with a coloured cable tie placed loosely around its base and its location was recorded with the use of a GPS handheld unit. Plants were protected by pasture cages at Struan, Bool Lagoon, Kybybolite (2008-9 only) and Farrell Flat, where there was the possibility of grazing by domestic or native animals.

2.5 Thermal time

2.5.1 Calculation

Previous studies expressed leaf turnover rates in calendar time, which limited the transferability of results to other sites and seasons (McMaster 2005; Otto *et al.* 2007). Thermal time is more universally applicable than calendar time, as it is independent of the temperature profile over time, and is accepted by most researchers as an excellent indicator of plant development rates (Davidson and Campbell 1983). In both the field and glasshouse studies reported in this thesis, rates were expressed in thermal time (growing degree days, or gdd) (Equation 2.1) at the level of the individual leaf.

$$T_{\mu} = [(T_{\max} + T_{\min})/2] - T_{base} \quad \textbf{(2.1)}$$

where if $[(T_{\max} + T_{\min})/2] < T_{base}$, then $T_{\mu} = T_{base}$. T_{μ} is thermal time, $T_{\min}$ and $T_{\max}$ are the minimum and maximum daily temperatures respectively and T_{base} is the base temperature below which growth ceases.

2.5.2 Base temperature

Base temperatures are thought to vary between species, cultivars, and phenological stage (McMaster and Wilhelm 1997; Lemaire and Agnusdei 2000). However, a base temperature of 0°C has been commonly used for wheat (Gallagher 1979; Baker *et al.* 1986; Kirby and Perry 1987; McMaster *et al.* 2003) and other pasture grasses (Kemp and Guobin 1992; Frank and Bauer 1995; Frank *et al.* 1995; Duru and Ducrocq 2000a). Otto *et al*. (2007) used a base temperature of 5°C across a number of species and phenological stages for simplicity. Lemaire and Agnusdei (2000) suggested base temperatures of 4°C and 8.5°C be used for calculating phyllochron in C_3 and C_4 plants respectively, but used a base temperature of 0°C for calculation of other rates and to allow comparison across different treatments in the same species.

In the absence of consensus in calculating base temperature (Ansquer *et al.* 2009) and in the interests of simplicity, thermal time was calculated from sowing date in the glasshouse, and from the commencement of observations in the field, and assumed a common base temperature of 0°C, across all species.

2.5.3 Temperature measurement in the glasshouse

Accumulated thermal time, calculated from temperature data logged with a Digitech data logger placed in the glasshouse, was used in Chapters 4 to 7. Initially the data logger was placed on the metal window-sill of the south-facing external wall behind the pots, and the data showed both high temperatures and large variations in temperature. It was relocated onto a wooden stake within the plant canopy next to a Hobie data logger supplied by the University of Adelaide for comparison for a week. The temperature readings from the two data loggers

were equivalent (paired t_{101}=1.2, P=0.23) (PROC TTEST (SAS Institute Inc. 2002-3)) which indicated that the canopy position gave equivalent temperatures, representative of canopy conditions. A linear regression (r^2=0.54) was performed in Microsoft Excel between the glasshouse temperatures recorded after repositioning of the Digitech datalogger in mid-October 2008 and outdoor temperatures from the SILO website (Bureau of Meteorology 2009). This regression (Equation 2.2) was used to correct the glasshouse temperatures for the initial period before the repositioning of the datalogger.

$$T_{corrected} = (0.2954 \times T_{SILO}) + 19.309 \quad \textbf{(2.2)}$$

The adjusted indoor temperature points are visually aligned with those from the relocated datalogger and smooth out the more extreme high and low temperatures found in the original data (Figure 2.2).

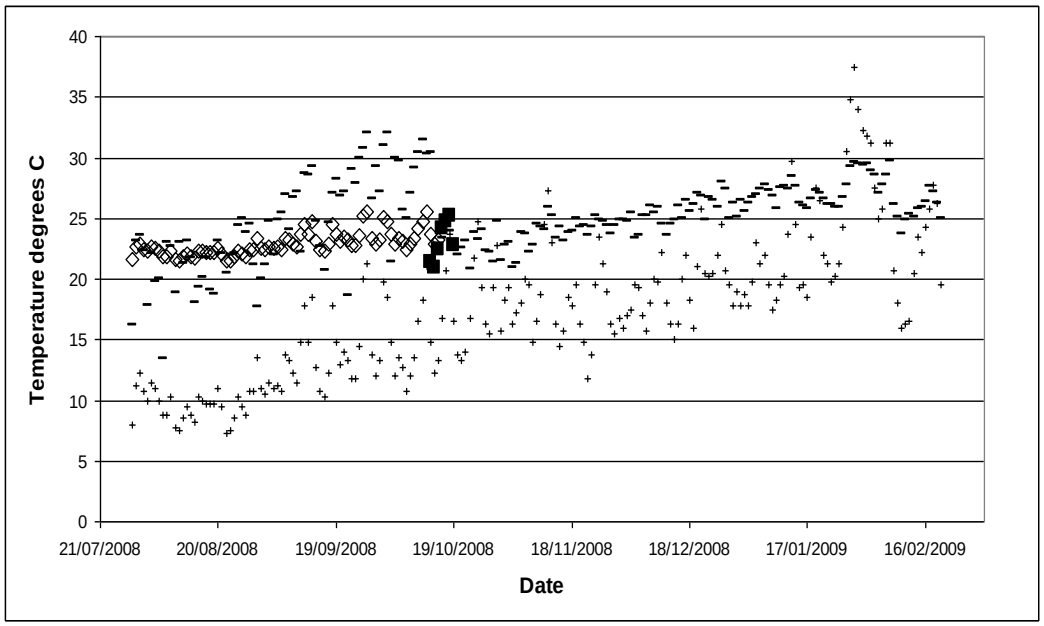

Figure 2.2. Temperatures inside and outside Glasshouse 22 at Waite campus during the period of the glasshouse experiment: where cross represents daily SILO temperatures for Waite (Bureau of Meteorology 2009), dash is glasshouse temperature recorded by Digitech datalogger, filled square is glasshouse temperature recorded by Hobie datalogger, and open diamond is adjusted glasshouse temperature.

2.5.4 Thermal time calculation in the field

Chapters 4, 6 and 7 required thermal time to be calculated in field locations. Temperature records from a number of sites were used to calculate thermal time for field locations, based on the proximity of the weather station to the field site (Table 2.4). Thermal time was calculated in the same manner as in the glasshouse, using Equation 2.1.

Table 2.4. Location of field sites relative to nearest available SILO weather station (Bureau of Meteorology 2009).

Region	Field site	Lat/Long	SILO site	Lat/Long
Clare, Mid-North, SA	Penwortham	33.55.100S 138.38.970E	Watervale	33.57.636S 138.38.676E
	Black Springs	33.55.158S 138.52.611E	Manoora	34.00.30S 138.48.852E
	Farrell Flat	33.52.490S 138.50.068E	Farrell Flat	33.49.890S 138.47.502E
Naracoorte, South East, SA	Bool Lagoon	37.05.837S 140.41.235E	Struan	37.05.706S 140.47.466E
	Struan	37.06.572S 140.46.833E	Struan	37.05.706S 140.47.466E
	Kybybolite	36.52.652S 140.56.412E	Kybybolite Research Centre	36.52.818S 140.55.716E
Canberra, ACT	Majura	35.27S 149.19E	Canberra Airport	35.18.294S 149.12.084E
	Tidbinbilla	35.43S 148.94E	Tidbinbilla Nature Reserve	35.26.448S 148.56.532E

2.6 Leaf measurements

2.6.1 Glasshouse experiments

Plants were checked twice-weekly, or daily when possible, to carry out leaf measurements and identify development stages. Leaves on the main stem were numbered acropetally, with the first leaf identified as leaf 1 (after Klepper *et al.* 1982).

Observations and measurements collected for the basis of Chapters 4 to 7, commenced at appearance of the third leaf, which was marked with a permanent pen. These measurements began on 3/8/2008, 6/8/2008, 9/8/2008 and 14/8/2008

for wheat, annual ryegrass, phalaris, and wallaby grass respectively. Leaves were counted and designated as live, mature or dead (see Table 2.5). Leaf length and the length of green and senesced leaf tissue was measured (Thomas 1980; Lemaire and Agnusdei 2000) and phenological stage noted (Simon and Park 1983). Due to prolific tillering in some species and time constraints, tiller counting ceased when the tiller population reached 100 per plant. Measurements ceased on February 20th 2009. A full list of the observations recorded is given in Table 2.5.

Table 2.5. Observations and measurements recorded and leaf turnover rates.

Measurement or Rate	**Features used to identify leaf turnover rates**	**Reference for techniques**
Number leaves – total plant	Count over time, and assign leaf position numbers	Klepper *et al*. (1982)
- Live plant leaves	Green without ligule	Thomas (1980), Parsons *et al*. (1991), Carrere *et al.* (1997)
- Mature plant leaves	Green with ligule	
- Dying plant leaves	Only partly green, some yellowing from the tip end	
- Dead plant leaves	Completely yellow or brown	
Number tillers	Count over time	Thomas (1980)
Leaf length		
- Green leaf length (mm)	Length of leaves, tip to base or ligule	Wallace *et al.* (1985)
- Senescent leaf length (mm)	Length of yellow or brown tissue from tip	Thomas (1980)
- Final leaf length (mm)	Length of leaf from tip to ligule	Lemaire and Agnusdei (2000)
Phenological state noted		
- Vegetative	Green leafy growth with no sign of reproductive development	Simon and Park (1983)
- Stem elongation	Stem extending and nodes palpable	
- Boot	Swollen in flag leaf	
- Head	Visible	
- Anthesis	Pollen shedding	
- Maturity	Head no longer green	
Leaf appearance rate	leaves/day or leaves/gdd	Thomas (1980), Lemaire and Agnusdei (2000)
Leaf appearance interval	days/leaf or gdd/leaf	Thomas (1980), Lemaire and Agnusdei (2000)
Leaf elongation rate	mm/day or mm/gdd	Thomas (1980), Wallace *et al.* (1985), Lemaire and Agnusdei (2000)
Leaf senescence rate	mm/day or mm/gdd	Thomas (1980)

2.6.2 Leaf turnover measurements at field sites

The main tiller, or a suitable tiller with green leaves, was identified with a coloured plastic cable tie on each plant. Leaves were numbered acropetally from the lowest recognisable leaf (leaf number 1) on the observation tiller (after Klepper *et al.* 1982) regardless of whether the leaves were live, senescing or dead.

Leaf measurements were conducted approximately fortnightly from August 2008 through to February 2009, until all the leaves on the observation tiller were dead. Leaves were counted and classified as live, mature or dead (Thomas 1980). Leaf length and length of green and senesced leaf tissue was measured (Thomas 1980; Lemaire and Agnusdei 2000) and phenological stage noted (Simon and Park 1983). Rates of leaf elongation (LER) and senescence (LSR) were calculated for each leaf position (Thomas 1980; Lemaire and Agnusdei 2000) as a single thermal time value (gdd) with a base temperature of 0°C (Baker *et al.* 1986; Kirby and Perry 1987; McMaster *et al.* 2003) used for each species.

2.7 Calculation of leaf rates

Rates of leaf appearance, elongation and senescence were calculated (Thomas 1980; Lemaire and Agnusdei 2000) as a single thermal time value for each leaf. Life span was determined from leaf appearance to the beginning of senescence. In this study, senescence refers to the process of curing or leaf yellowing from the tip to the base. A leaf was deemed to be senescing from the first observance of yellowing at the leaf tip and death was deemed to occur when the leaf was fully yellow or brown. While this differs from the plant physiologist's standpoint, where senescence refers to cellular processes beginning once leaf elongation is complete, the terminology used here allowed the period of visible leaf senescence

to be aligned with the curing process for fire management purposes. The stages in the life of a theoretical grass leaf are shown in Figure 2.3. Leaf position on the plant has been previously used to explain variation in leaf development rates (Wilson 1976; Duru and Ducrocq 2000a) and was used here to test the common assumption that leaf development rates are constant with leaf position (e.g. Peacock (1976), Calviere and Duru (1995), and Agnusdei *et al.* (2007)).

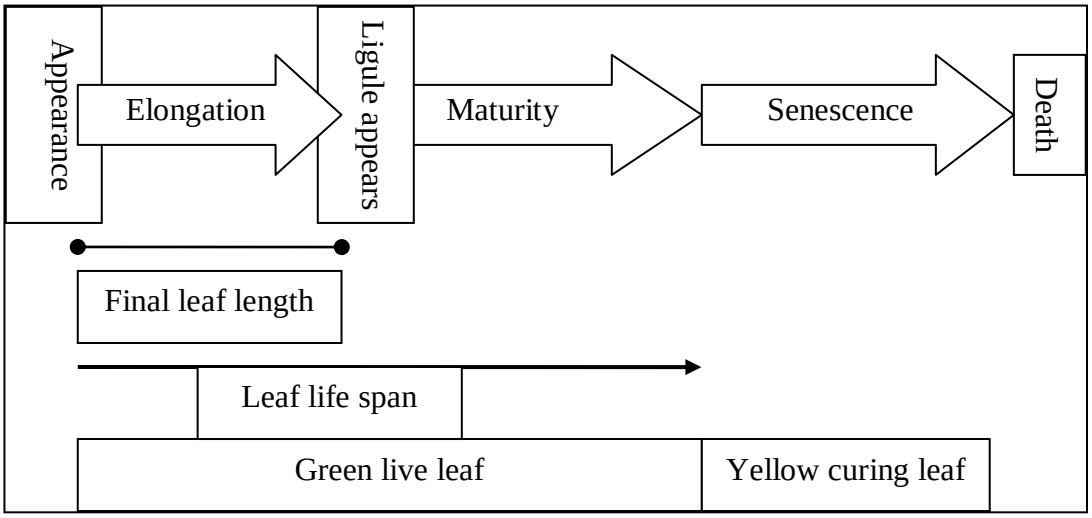

Figure 2.3. Leaf growth processes and visible characteristics expressed during the life of a grass leaf.

Measurements were carried out on each leaf until it had fully senesced. Leaf appearance rate (LAR) (leaf /gdd) was the proportion of the leaf which appeared past the sheath of the previous leaf per unit of thermal time (Equation 2.3).

(2.3)

$$LAR_l = \frac{1}{TA_l - TA_{l-1}}$$

where l is the leaf index, TA_l is thermal time of leaf appearance and TA_{l-1} is thermal time of appearance of previous leaf.

Leaf elongation rate (LER) (mm/gdd) was calculated by dividing leaf length by the thermal time from appearance of the leaf tip to the leaf ligule, or when length was constant (Equation 2.4). Progressive LER was calculated for the few leaves which had not finished growing at the cessation of measurement.

(2.4)

$$LER_l = \frac{LL_l}{TLL_l - TA_l}$$

where LL_l is the maximum leaf length, TLL_l is the time that maximum leaf length is achieved and TA_l is thermal time of leaf appearance.

Maximum leaf length (mm) (LL) was determined when the ligule had emerged and/or leaf length appeared to be constant (Equation 2.5). Where leaf breakages were suffered due to repeated handling, the maximum leaf length previously recorded was used.

(2.5)

$$LL = \begin{cases} L_{lig} & \text{if ligule emerged} \\ L_{con} & \text{if leaf broken} \end{cases}$$

where L_{lig} is length when ligule has emerged, or L_{con} is constant length if ligule has not emerged.

Leaf senescence rate (LSR) (mm/gdd) was calculated by dividing the leaf length by the thermal time from the first appearance of senescence on the leaf tip to the death of the entire leaf (Equation 2.6). Progressive LSR was calculated for those leaves which had not completed senescence by cessation of measurement.

(2.6)

$$LSR_l = \frac{LL_l}{TSb_l - TSa_l}$$

where TSb_l is thermal time at the end of leaf senescence (leaf is completely dead), and TSa_l is thermal time at the beginning of leaf senescence at the leaf tip.

The thermal time period between leaf appearance and the onset of senescence of the leaf was the leaf life span (LLS) (gdd) (Equation 2.7).

(2.7)

$$LLS_l = TSa_l - TA_l$$

Where TSa_l is thermal time at the beginning of leaf senescence at the leaf tip, and TA_l is thermal time of leaf appearance.

2.8 Traditional curing assessments

Assessments of curing were conducted on each of the species at each field site. Due to time constraints, assessments were undertaken following operational procedures (Anderson *et al.* 2011), rather than the more detailed research procedures. Details of the sampling frequency are given in Appendix A, Table A-4.

2.8.1 Visual assessment

At each visit, a visual estimate of the percentage of cured vegetation was made over the general area of the sward by visually comparing the colour of the sward to photographic standards (Garvey and Millie 1999).

2.8.2 Modified Levy Rod

The modified Levy Rod technique uses a 1.3 m metal rod with a diameter of 5 mm (Anderson *et al.* 2011). The assessment procedure involves the operator pacing 4 m intervals along a transect, then fully extending the arm (with Levy Rod) out from the body, and striking the rod vertically into the earth. Working from the top of the rod, vegetation touching the rod is classified as live or dead, at the point where it makes contact with the rod, depending on colour (green for live, and yellow, brown or bleached for dead). Dense thatch vegetation at the bottom of the rod is counted as far down as practically possible. Live and dead counts are tallied separately and recorded, to allow calculation of grass curing (Equation 2.8) (Anderson *et al.* 2005).

(2.8)

$$Curing(\%) = \frac{K_d}{K_{total}} \times 100$$

where K_d is the number of dead touches and K_{total} is total number of touches.

A 20 m transect was established in a uniform area of sward at each site to assess curing using the modified Levy Rod method. Five assessments were made at 4 m intervals along the transect, with a further five assessments made along a 20 m transect at right angles to the first to account for spatial variability across the sample area and to ensure a representative estimate was obtained for each sample area. The transects were rotated 30° clockwise at each visit to assess a new section of the sward.

At Penwortham and Black Springs, the 30 m-long agronomic demonstration plots were used as the transects. Ten assessments were made at 4 m intervals along the outside of each plot to avoid trampling. Where plots had been mown by the demonstrators, half of the assessments were conducted on mown sward, and half on unmown sward.

2.8.3 Destructive sampling

When possible, three samples of "combined" (live and dead) sward were harvested for later sorting into green and dead fractions to determine curing. A quadrat (0.25 m^2) was placed at intervals along the same transect used to obtain the Levy Rod assessments, and all vegetation was cut to ground level with secateurs and sealed in a pre-weighed and identified ziplock plastic bag. These samples were transported in an insulated container to Adelaide and stored in domestic freezers until dried in paper bags in drying ovens at 105°C for 24 hours (Anderson *et al.* 2011), at either Waite Campus, Roseworthy Campus or Struan Research Centre.

Due to time constraints, dried samples were stored until being later sorted into live (green) and dead (yellow, brown or bleached material) fractions, and weighed, in contrast to the method of Anderson *et al.* (2011), who sorted prior to

drying. The percentage of dead material or degree of curing was calculated from the sorted fractions (Equation 2.9).

$$Curing\% \equiv Dead\% = (Wt_{dead} / Wt_{total}) \times 100 \quad \textbf{(2.9)}$$

where *Dead%* is percentage of dead material in the harvested sample, Wt_{dead} is net sample dead weight and Wt_{total} is the total sample weight.

Due to ongoing agronomic demonstrations, it was not possible to collect samples from the Penwortham and Black Springs sites. At other sites, destructive sampling was undertaken if time permitted after collection of leaf growth measurements, and if weather permitted. It was planned to ascertain fuel moisture content from destructively-harvested samples. However, destructive sampling was not conducted when rain was present, because of the error this would have introduced to fuel moisture calculations. Subsequently, there were insufficient samples to analyse fuel moisture content.

2.9 Computer simulations of field sites

Two predominantly native grasslands measured by the Bushfire CRC (BCRC) in the ACT, and the four grassland types (wheat crop, annual ryegrass pasture, phalaris pasture, and native pasture) under the management of the Struan Research Centre, around Naracoorte in South East, SA were simulated using commercial agricultural DST (APSIM, GrassGro™ and the SGS Pasture Model) which contained the appropriate species parameters for each field site. The Struan Research Centre farm manager reviewed system outputs in the acceptability testing phase. Data from these simulations are presented in Chapter 3 and 4. Input details specific to each simulation are detailed in Chapter 3.

2.9.1 Soil inputs

In general, the latitude and longitude coordinates of each location were used to find the Landscape Unit in the Soil Atlas (Bureau of Rural Sciences (after CSIRO) 1991) contained in GrassGro™ and a suitable principal profile form was selected from those available for that Landscape Unit. The soil depth, water holding capacity and bulk density values for the principal profile form were used as starting values for the soil physical properties in the SGS Pasture Model soil water module. Because the soil layers are defined differently in GrassGro™ and the SGS Pasture Model, a surface layer of 2 cm was assumed in the SGS Pasture Model and the topsoil depth from GrassGro™ became the depth of the A horizon in the SGS Pasture Model. The subsoil depth from GrassGro™ was used for the B2 horizon in the SGS Pasture Model. Similarly, soil values from the GrassGro™ soil atlas were used to adjust the soil values from the APSRU soil data base supplied in APSIM. Where no specific information was available, default values were used for saturated water content, and air dry water content values were set to just below wilting point. Site-specific input values are given in Chapter 3.

2.9.2 Weather inputs

Weather data downloaded as Patched Point Datasets (PPD) from the SILO website (Bureau of Meteorology 2009) were obtained for weather stations nearby the field sites (Table 2.4) in formats to suit the three DST.

2.9.3 GrassGro™

GrassGro™ (Moore *et al.* 1997) version 3.2.3 (build date June 2010) was used to simulate phalaris and annual ryegrass pastures at Struan, SA, to evaluate its performance in providing curing information against traditional methods

(Chapter 3) and against a model developed to represent leaf curing (Chapter 4). Curing percentage was included in the customised Pasture Curing Report in GrassGro™ as the percentage of total dry herbage mass divided by total herbage mass.

2.9.4 APSIM

APSIM (Keating *et al.* 2003) version 7.2 (build date August 2010) was used to simulate a wheat crop rotation at Bool Lagoon, SA, and curing percentage was determined in a Microsoft Excel spreadsheet from the outputs of senesced leaf and green leaf dry matter. Curing percentage generated by APSIM was compared against traditional methods of curing assessment in Chapter 3 and against a leaf curing model in Chapter 4.

2.9.5 The SGS Pasture Model

The SGS Pasture Model (Johnson *et al.* 2003) (version 4.8.3, release date 26/2/2009) was used to simulate annual ryegrass and phalaris pastures at Struan, SA, and native-dominant pastures at Kybybolite, SA, and Tidbinbilla and Majura, ACT. Curing percentage was calculated from outputs provided in the export of data. The mass of dead shoots was divided by the total mass of dead and live shoot and multiplied by 100. SGS-derived curing percentages were compared against traditional methods of curing assessment in Chapter 3 and against a leaf curing model in Chapter 4.

2.10 Statistical analyses

Data were analysed using SAS 9.1.3 and SAS 9.2 (SAS Institute Inc. 2002-3). Analyses that made use of calendar time rates were found to produce less

significant models than when thermal time rates were used. For this reason all the following analyses used thermal time.

Exploratory analysis indicated that some variables were not linearly related to the predictors and in these cases quadratic polynomial models of the general form shown in Equation 2.10 were found to provide a reasonable fit. These were used in Chapters 5 and 6. Elsewhere, non-linear models are used. These are defined as models in which the parameters appear non-linearly (Ratkowsky 1990). In Chapter 6, models of the general form shown in Equation 2.11 were needed to fit the non-linear relationships.

(2.10)

$$y = \frac{1}{a + bx + cx^2}$$

where y is the modelled variable, x is leaf position and a, b and c are constants to be estimated.

(2.11)

$$y = e^{\left(a+bx+cx^2\right)}$$

where y is the modelled variable, x is leaf position and a, b and c are constants to be estimated.

A variation in the logistic model of the form shown in Equation 2.12 was required when fitted to thermal time data (Chapter 4). In Chapter 7, s-shaped logistic curves of the general form shown in Equation 2.13 were fitted.

(2.12)

$$y = a/\left(b + e^{(-cx)}\right)$$

where y is the modelled variable, x is thermal time and a, b and c are constants to be estimated.

(2.13)

$$y = 100/\left(1 + e^{(-a(x-b))}\right)$$

where y is the modelled variable, x is thermal time and a and b are constants to be estimated.

The data were analysed by introducing random effects at the pot and plant level for glasshouse data (Chapters 4, 5, 6) or at the site and/or plant level for field

data (Chapters 4 and 6) (Onofri *et al.* 2010). Linear models used the Kenward-Rogers adjustment for the degrees of freedom (Kenward and Roger 1997) as recommended by Littell *et al*. (2006) when dealing with correlated data. Full details of models fitted are given in individual chapters.

Outlier observations subject to interval censorship (Quinn and Keough 2002) were removed. Plots of residuals were checked for normality, and predicted values were plotted against observed values to ensure visual goodness-of-fit of the models. Goodness-of-fit statistics between the model predictions and observations of leaf curing was established using a number of methods. Linear regression of predicted against observed values were used to generate adjusted r^2 values ($\overline{R}^2$) for non-linear models. Chi-square (χ^2) statistics (Equation 2.14) were calculated to determine the probability of the models. Reduced Chi-squared (χ^2_{red}) statistics (Equation 2.15) indicated under- or over-fitting of the models. Large values of χ^2_{red} (greater than one) indicated a poor model fit or that the error variance had been under-estimated, while χ^2_{red} values less than one indicated the model was over-fitted, or the error variance was over-estimated. When χ^2_{red} equalled one, the fit of the model was in agreement with the error variance. The Nash-Sutcliffe Model Efficiency coefficient (E) (Nash and Sutcliffe 1970) (Equation 2.16) was calculated to indicate the degree of fit of the model to the observed data. When E equals one the fit was perfect. Values between 0 and 1 indicated a less-than-perfect fit. When E was zero, the model was as accurate as the observed data, while values less than zero indicated that the mean of observations were a better fit than the model. Finally, the root mean square deviation (RMSD) (Equation

2.17) quantified the degree of fit by indicating the variation of the model from the observed data, in the same units as the observed data.

(2.14)

$$\chi^2 = \sum \frac{(O-P)^2}{\sigma^2}$$

where O is an observation and P is a value predicted by the model, and σ^2 is observation variance.

(2.15)

$$\chi^2_{red} = \frac{X^2}{\nu} = \frac{1}{\nu}\sum \frac{(O-P)^2}{\sigma^2}$$

where O is an observation, P is a value predicted by the model, and σ^2 is observation variance, and ν is the number of degrees of freedom.

(2.16)

$$E = 1 - \frac{\sum (O-P)^2}{\sum (O-\overline{O})^2}$$

where O is an observation, P is a value predicted by the model, and $\overline{O}$ is the mean of observations.

(2.17)

$$RMSD = \sqrt{\sum (O-P)^2}$$

where O is an observation and P is a value predicted by the model.

Where variables were not normally or symmetrically distributed, root mean square deviation (RMSD) was used to quantify the degree of fit by indicating the variation of the model from the observed data, in the same units as the observed data. Acceptability of $\overline{R}^2$ values were considered in conjunction with the significance of the model being fitted. Effects were considered significant at the 5% level.

Observations and models are not presented for leaf positions where data were either not collected or subject to interval censorship. Modelled results are presented up to the maximum observed leaf position for each species. Observed data are presented in box-and-whisker (boxplot) plots, where the upper, internal and lower bounds of each box correspond to the 75th, 50th and 25th percentiles,

respectively. Upper and lower whiskers represent the nominal data range, which extends the upper and lower quartiles by 1.5 times the interquartile range. Open circles indicate samples which lie outside the nominal data range, and are considered outliers. Use of the interquartile range provides a more robust approach to detection of outliers than does use of standard deviation (Anonymous 2011d; Pearson 2011).

3 Evaluation of agricultural DST for curing estimation

3.1 Introduction

The potential of agricultural decision support tools (DST) to provide grass curing data for fire management has been previously reported (Gill *et al.* 1989; Dawson *et al.* 1991; Baxter and Woodward 1999; Anderson and Pearce 2003; Gill *et al.* 2010), but a comprehensive analysis is yet to be conducted. This chapter analyses the potential of three such DST to provide curing predictions, namely: 1) the Agricultural Production Systems Simulator (APSIM) (version 7.2, build date August 2010) (Keating *et al.* 2003); 2) GrassGro™ (version 3.2.3, build date June 2010) (Moore *et al.* 1997) and; 3) the SGS Pasture Model (version 4.8.3, release date 26/2/2009) (Johnson *et al.* 2003). The relevant attributes of these three DST are described in detail in Chapter 1.

In this chapter each DST is used to simulate curing for a range of annual and perennial crops and pastures, and the results are compared against estimates from traditional curing assessments. Modifications to these DST to make them more suitable for this application are suggested.

3.2 Materials and methods

Three DST were evaluated for their ability to represent curing over time in a crops and pastures comprising grasses of different growth types at two locations, around Naracoorte in South East, South Australia (Figure 2.1), and in the Australian Capital Territory. Curing estimates from the DST were compared to field-based curing assessments, the procedures for which are given in Chapter 2.

An overview of each of the DST and soil and weather inputs is described in Chapter 2. The default soil atlas within GrassGro™ was used to identify soil variables for Struan and Bool Lagoon, SA, and Tidbinbilla and Majura, ACT, sites. Soil input data for Kybybolite was supplied by GrassGro™. Three pastures and a wheat crop were simulated using the appropriate DST, as indicated in Table 1.6. APSIM could not be used to model the annual ryegrass, phalaris or native grass pastures, due to lack of access to the Ausfarm DST which are required to model pastures in APSIM. The SGS Pasture Model and GrassGro™ do not contain models to allow simulation of wheat crops. The version of GrassGro™ used in this experiment did not contain models to allow simulation of native grass species. The pastures at Struan Research Centre were dominated by phalaris and annual ryegrass respectively. The pastures at Kybybolite Research Centre, SA, and Tidbinbilla and Majura, ACT, consisted of native grass species. A wheat crop was grown at Bool Lagoon, SA. The pastures were all subject to different levels of grazing pressure, as described below.

3.2.1 Simulation of South Australian field sites

3.2.1.1 Overview of management

Descriptions of the management of the pastures at Struan and Kybybolite were supplied by the farm manager and are summarised in Table 3.1. The wheat crop at Bool Lagoon was sown in yearly rotation following canola and barley, between late May and mid-June. This time-frame ensured at least 25 mm rainfall was received to provide adequate soil moisture for weed germination, and avoid risk of frost at flowering. Seed was sown to a depth of 5-7.5 cm to a plant density of 100 plants/m^2, with 80 kg/ha monoammonium phosphate (MAP) fertiliser and

trifluralin herbicide. The crop was later top-dressed with 100 kg/ha urea in late July and harvested in mid December.

Table 3.1. General description and management of South East SA pasture paddocks.

Location	**Struan**	**Struan**	**Kybybolite**
Grass type	**Phalaris**	**Annual Ryegrass**	**Native**
Composition	Phalaris dominant, but 20-25% clover	Sown annually to "Winterstar"	*Austrostipa* spp., *Themeda* spp., *Austrodanthonia* spp., phalaris, annual grasses, and broadleaf weeds
Paddock size (ha)	42	29	1.5
Enterprise	Lamb production	Lamb production and Silage	Merino wool
Livestock	First cross ewes	First cross ewes	Merino wethers
Stocking rate – dry sheep equivalents (DSE)	12-13	12-13	2
Body weight (kg)	55	55	50
Condition score - autumn	3	3	3
Micron (µm)	28	28	19
GFW (kg)	3.0	3.0	5.0
Yield (%)	70	70	70
Shearing date	November	November	Mid October
Lambing date	1st week June	1st week June	n/a
Marking rate (%)	120	120	n/a
Lamb sale weight (kg)	45	45	n/a
First lamb sale	October	October	n/a
Weaning date	November	November	n/a
Cast for age (CFA) (years)	7	7	7
CFA (date)	January	January	January
Supplementary feeding	Late January to late April (or longer)	Late January to late April (or longer)	n/a
Supplement (kg/hd/day)	Barley 0.3	Barley 0.3	n/a
Livestock rotation	Set stocked spring to lambing, then rotated around sub-paddocks July to spring	Set stocked from late June to late August, then late November to mid April (break)	Set stocked from mid April to late December, then destocked
Silage cut	n/a	Early November 5 tDM/ha	n/a

3.2.1.2 Phalaris model configuration at Struan

The phalaris pasture was simulated using GrassGro™ and the SGS Pasture Model. APSIM could not be used to model the phalaris pasture, due to lack of

access to the Ausfarm DST. The soil input values from the soil atlas (Bureau of Rural Sciences (after CSIRO) 1991) within GrassGro™ were entered into the SGS Pasture Model (Table 3.3). Other input variables for pasture, livestock and management of the simulations are described in Table 3.2. If not specifically stated, then DST default values were used.

Table 3.2. Pasture, livestock and management starting parameters used for the phalaris pasture at Struan, SA in GrassGro™ and the SGS Pasture Model. Parameters are given in the scale required by the different DST.

Input parameter	GrassGro™	SGS
Length of run	1/1/1983 - 22/1/2011	1/1/1983 – 31/12/2010
Weather data location	Struan	Struan
Paddock size (ha)	420	420
Species 1	Phalaris at 1/1/1983 - summer dormant, 1500 kg/ha live, 2998 kg/ha standing dead, 747 kg/ha litter, 5000 kg/ha roots, 1200 mm rooting depth	Phalaris - 1.5 t/ha shoots, 30% green, 2 t/ha roots, 150 cm rooting depth
Species 2	Annual grass (early flowering) at 1/1/1983 – senescent, 0 kg/ha biomass, 2 kg/ha seed, 45 mm rooting depth	Annual ryegrass – 0 t/ha shoots, 20 cm rooting depth, earliest emergence March 15th, anthesis September 1st, 45 days from anthesis to maturity
Species 3	Seaton Park Sub Clover at 1/1/1983 – senescent, 0 kg/ha biomass, 4 kg/ha seed, 55 mm rooting depth	Sub clover – 0 t/ha shoots, 25 cm rooting depth, earliest emergence March 1st, anthesis September 1st, 30 days from anthesis to maturity
Livestock breed /sex	First cross ewes mated to Dorset rams	Ewes
Stocking rate	Set stocked at 6.5 head/ha	Set stocked at 6.43 head/ha
Livestock details	Purchased January 1st at 18 months, 55 kg body weight, condition score 3 in autumn, sold at 7 years on January 1st	55 kg body weight, minimum condition score 4
Wool production details	28 µm, 3.0 kg greasy fleece weight, 70% yield, shorn November 15th	3.0 kg greasy fleece weight, shorn September 1st
Lambing details	Conceive 75% singles, 25% twins to lamb on June 4th, marked, and weaned and sold October 15th	Average 1.2 lambs per ewe, lambing on June 4th, sold at 100 days
Supplementary feeding	Fed 0.3 kg/head/day barley when condition score falls below 2.5 or total DM falls below 400 kg/ha	Fed maximum of 0.3kg/head/day concentrate (13.7 ME MJ/kg) when ME falls below 90% of requirement or body weight falls below 50 kg

Table 3.3. Soil water module inputs for phalaris pasture at Struan, SA were derived from Principal Profile Form Ug5.11 from the Soil Atlas (Bureau of Rural Sciences (after CSIRO) 1991) in GrassGro™ (GG). These were used in the SGS Pasture Model, and extrapolated to the surface and B1 soil profiles which are not differentiated in GrassGro™. Parameters are given in the scale required by the different DST.

Soil Layer	**Surface**	**A horizon / topsoil**		**B1 horizon /subsoil**	**B2 horizon /subsoil**	
DST input	**SGS**	**GG**	**SGS**	**SGS**	**GG**	**SGS**
Depth	2 cm	200 mm	20 cm	110 cm	1200 mm	120 cm
Field capacity	46 %vol	0.46 m^3/m^3	46 %vol	46 %vol	0.46 m^3/m^3	46 %vol
Wilting point	31 %vol	0.31 m^3/m^3	31 %vol	31 %vol	0.31 m^3/m^3	31 %vol
Bulk density	1.2 g/cm^3	1.2 mg/m^3	1.2 g/cm^3	1.2 g/cm^3	1.2 mg/m^3	1.2 g/cm^3
Saturated conductivity	2.4 cm/day	1.0 mm/hr	2.4 cm/day	0.72 cm/day	0.3 mm/hr	0.72 cm/day
Saturated water content	48 %vol	n/a	48 %vol	48 %vol	n/a	48 %vol
Air dry water content	13 %vol	n/a	13 %vol	13 %vol	n/a	13 %vol

3.2.1.3 Annual ryegrass model configuration at Struan

The annual ryegrass pasture was grazed by first-cross ewes in winter, before being locked up in late August to be cut for silage in early November. Traditional field curing assessments coincided with the destocked and silage cutting phases. GrassGro™ and the SGS Pasture Model each required different initial herbage values to simulate the pastures correctly (Table 3.4). The GrassGro™ simulation was started on 1/1/1983 and run until 31/12/2006. This was necessary to ensure the simulation was not unduly affected by the drought conditions experienced in 2006, in order to initialise the subsequent period which was run from 31/12/2006 to 31/12/2010.

Table 3.4. Pasture, livestock and management starting parameters used for the annual ryegrass pasture at Struan, SA in GrassGro™ and the SGS Pasture Model. Parameters are given in the scale required by the different DST.

Input parameter	GrassGro™	SGS
Length of run	31/12/2006-31/12/2010	1/1/1983-31/12/2010
Weather data location	Struan	Struan
Paddock size (ha)	2x290ha	2x290ha
Species 1	Annual ryegrass at 31/12/2006 – senescent, 3316 kg/ha standing dead, 790 kg/ha litter, 169 kg/ha seed, 700 mm rooting depth	Annual ryegrass – 4.5 t/ha shoots, 40 cm rooting depth, earliest emergence April 1st, anthesis November 15th, 60 days from anthesis to maturity
Livestock breed / sex	First cross ewes mated to Dorset rams	Ewes
Stocking rate	3.3head/ha equivalent to stocking density of 6.6 head/paddock	3.27 head/ha equivalent to stocking density of 6.55 head/paddock
Livestock details	Purchased January 1st at 18 months, 55 kg body weight, condition score 3 in autumn, sold at 7 years on January 1st	55 kg body weight, minimum condition score 4
Wool production details	28 µm, 3.0 kg greasy fleece weight, 70% yield, shorn November 15th	3.0 kg greasy fleece weight, shorn September 1st
Lambing details	Conceive 75% singles, 25% twins to lamb on June 4th, marked, and weaned and sold October 15th	Average 1.2 lambs per ewe, lambing on June 4th, sold at 100 days
Supplementary feeding	Fed 0.3 kg/head/day barley when condition score falls below 2.5 or total DM falls below 400 kg/ha Fed 0.33kg/hd in feedlot from November 15th to April 24th	Fed maximum of 0.3kg/head/day concentrate (13.7 ME MJ/kg) when ME falls below 90% of requirement or body weight falls below 50 kg
Livestock rotation	Paddock 1 grazed November 15th – April 24th, July 1st – August 24th. In alternative periods stock graze Paddock 2	Grazed on a feed budget rotations starting November 15th to April 24th; if insufficient feed, stock move to second paddock. From April 25th to June 30th stock stay put, regardless of feed. From July 1st to August 31st, if insufficient feed, stock move to second paddock. From September 1st to November 14th stock stay put, regardless of feed.
Silage	Not available in livestock enterprise.	Cut between October 15th and November 1st if herbage mass reaches 3.5t/ha

The grazing and silage harvesting management practices needed to be captured by the DST to assess curing in spring (Table 3.4). Multiple paddocks were configured in the simulations, to allow for movement of animals during pasture rest phases. In GrassGro™, grazing of animals cannot be incorporated into silage harvesting simulations. However, fixed-time grazing rotations were used in the GrassGro™ simulation to represent curing prior to silage cutting. Grazing and

silage harvesting was possible in the SGS Pasture Model but feed availability over-ruled fixed time rotations, with the paddock with the greatest pasture availability always being grazed first. This resulted in pasture set aside for silage being grazed in some years, making it difficult to adequately capture both stock movements and cutting over a long time frame. However, the years 2006-2010 of the SGS Pasture Model simulation had both correct stock movements and silage cuts.

The Principal Profile Form Ug5.11 (Bureau of Rural Sciences (after CSIRO) 1991) provided suitable soil inputs for GrassGro™, but in the SGS Pasture Model, these inputs did not generate correct pasture availability. Instead, default values for a clay-loam soil (Table 3.5) were used, as these did simulate pasture availability and silage yields correctly for this site.

Table 3.5. Soil water module inputs for Struan, Naracoorte annual ryegrass pasture were derived from Principal Profile Form Ug5.11 from the Soil Atlas (Bureau of Rural Sciences (after CSIRO) 1991) in GrassGro™ (GG) and default clay-loam in the SGS Pasture Model. Note that the surface and B1 soil profiles are not differentiated in GrassGro™. Parameters are given in the scale required by the different DST.

Soil Layer	**Surface**	**A horizon / topsoil**		**B1 horizon /subsoil**	**B2 horizon /subsoil**	
DST input	**SGS**	**GG**	**SGS**	**SGS**	**GG**	**SGS**
Depth	2 cm	200 mm	50 cm	100 cm	1200 mm	200 cm
Field capacity	40 %vol	0.46 m^3/m^3	40 %vol	40 %vol	0.46 m^3/m^3	40 %vol
Wilting point	19 %vol	0.31 m^3/m^3	19 %vol	19 %vol	0.31 m^3/m^3	19 %vol
Bulk density	1.3 g/cm^3	1.2 mg/m^3	1.3 g/cm^3	1.3 g/cm^3	1.2 mg/m^3	1.3 g/cm^3
Saturated conductivity	6.7 cm/day	1.0 mm/hr	6.7 cm/day	6.7 cm/day	0.3 mm/hr	6.7 cm/day
Saturated water content	48 %vol	n/a	48 %vol	48 %vol	n/a	48 %vol
Air dry water content	13 %vol	n/a	13 %vol	13 %vol	n/a	13 %vol

3.2.1.4 Native grass model configuration at Kybybolite

The SGS Pasture Model was the only DST able to simulate the native pasture at Kybybolite, SA. The soil atlas and soil library in GrassGro™ indicated that the soil at the Kybybolite Research Centre was Principal Profile Form Dy5.43 (Bureau of Rural Sciences (after CSIRO) 1991). Values from GrassGro™ were converted to those required for the SGS Pasture Model, as shown in Table 3.6. Other starting values for inputs into the SGS Pasture Model are described in Table 3.7.

Table 3.6. Soil water module inputs from the Kybybolite Research Centre, SA, derived from Principal Profile Form Dy5.43 from the Soil Atlas (Bureau of Rural Sciences (after CSIRO) 1991) in GrassGro™ (GG) were used for soil water values in the SGS Pasture Model. Parameters are given in the scale required by the different DST.

Soil Layer	**Surface**	**A horizon / topsoil**		**B1 horizon /subsoil**	**B2 horizon /subsoil**	
DST input	**SGS**	**GG**	**SGS**	**SGS**	**GG**	**SGS**
Depth	2 cm	200 mm	20 cm	100 cm	1200 mm	120 cm
Field capacity	25 %vol	0.25 m^3/m^3	25 %vol	27 %vol	0.27 m^3/m^3	27 %vol
Wilting point	10 %vol	0.10 m^3/m^3	10 %vol	18 %vol	0.18 m^3/m^3	18 %vol
Bulk density	1.4 g/cm^3	1.4 mg/m^3	1.4 g/cm^3	1.8 g/cm^3	1.8 mg/m^3	1.8 g/cm^3
Saturated conductivity	72 cm/day	30 mm/hr	72 cm/day	0.24 cm/day	0.10 mm/hr	0.24 cm/day
Saturated water content	30 %vol	n/a	30 %vol	35 %vol	n/a	35 %vol
Air dry water content	7 %vol	n/a	7 %vol	7 %vol	n/a	7 %vol

Table 3.7. Pasture, livestock and management starting parameters used for the native pasture at Kybybolite, SA, in the SGS Pasture Model.

Length of run	1/1/1983-31/12/2010
Weather data location	Kybybolite
Paddock size (ha)	2x150ha
Species 1	C_3 perennial native – 4.5 t/ha shoots, 30% green, 100 cm rooting depth
Livestock breed /sex	Merino wethers
Stocking rate	1 head/ha equivalent to stocking density of 2 head/paddock
Livestock details	50 kg body weight, minimum condition score 4
Wool production details	5.5 kg greasy fleece weight, shorn September 1st
Supplementary feeding	Fed maximum of 0.3kg/head/day concentrate (13.7 ME MJ/kg) when ME falls below 60 % of requirement
Livestock rotation	Grazed on a feed budget with rotations starting December 25th to April 24th where stock stay put, regardless of feed. From April 25th to December 24th, if insufficient feed, stock move to second paddock.

3.2.1.5 Wheat model configuration at Bool Lagoon

APSIM was the only DST with suitable parameters to simulate a crop rotation including wheat at Bool Lagoon, SA. Details of the crop rotation inputs used to initialise APSIM are given in Table 3.8. Soil values for the Jessie district from the APSRU soil data base supplied in APSIM, were adjusted to reflect the principal profile form Ug5.11 soils of Bool Lagoon from the soil atlas (Bureau of Rural Sciences (after CSIRO) 1991) in GrassGro™ (Table 3.9).

Table 3.8. Cropping management starting parameters used for the cropping rotation at Bool Lagoon, SA, in APSIM.

Length of run	1/1/1983-31/12/2010		
Weather data location	Struan		
Crop rotation	Canola	Wheat	Barley
Variety	Hyola 42	Yitpi	Sloop SA
Sowing rules	Sow between May 25th and June 15th on 100 mm minimum available soil water, otherwise sow dry on June 15th		
Physical sowing specifications	100 plants/m^2, 25 mm depth, 180 mm row spacing	100 plants/m^2, 40 mm depth, 180 mm row spacing	100 plants/m^2, 30 mm depth, 180 mm row spacing
Sowing fertiliser	80 kg/ha N as NH_4		
Initial surface organic matter	1000 kg/ha wheat residue, 80 C:N		
Top-dressed fertiliser	100 kg/ha urea on July 31st if N in top two soil layers is less than 1000 kg/ha		

Table 3.9. Soil water module inputs for Bool Lagoon crop rotation derived from Principal Profile Form Ug5.11 from the Soil Atlas (Bureau of Rural Sciences (after CSIRO) 1991) in GrassGro™ (GG) were used to amend the sandy loam over brown clay soil from the Jessie district, SA, used in APSIM. Parameters are given in the scale required by the different DST.

Soil Layer	topsoil			subsoil				
DST input	**GG**	**APSIM**		**APSIM**			**GG**	**APSIM**
Soil depth	200 mm	0-12 cm	12-22 cm	22-40 cm	40-55 cm	55-86 cm	1200 mm	86-120 cm
Field capacity	0.46 m^3/m^3	0.46 mm/mm	0.46 mm/mm	0.46 mm/mm	0.46 mm/mm	0.46 mm/mm	0.46 m^3/m^3	0.46 mm/mm
Wilting point	0.31 m^3/m^3	0.31 mm/mm	0.31 mm/mm	0.31 mm/mm	0.31 mm/mm	0.31 mm/mm	0.31 m^3/m^3	0.31 mm/mm
Bulk density	1.2 mg/m^3	1.2 g/cc	1.2 g/cc	1.2 g/cc	1.2 g/cc	1.2 g/cc	1.2 mg/m^3	1.2 g/cc
Saturated conductivity	1.0 mm/hr	n/a	n/a	n/a	n/a	n/a	0.3 mm/hr	n/a
Saturated water content	n/a	0.5 mm/mm	0.5 mm/mm	0.5 mm/mm	0.5 mm/mm	0.5 mm/mm	n/a	0.5 mm/mm
Air dry water content	n/a	0.4 mm/mm	0.6 mm/mm	0.8 mm/mm	0.8 mm/mm	0.8 mm/mm	n/a	0.8 mm/mm

3.2.1.6 Acceptability testing of SA simulations

Regular monitoring of pasture and livestock production had not been routinely recorded for the paddocks used in this study. However, pasture and livestock production outputs from GrassGro™ and the SGS Pasture Model for phalaris and annual ryegrass pastures, and the SGS Pasture Model for native pasture, and wheat yields from APSIM were checked by the Struan farm manager in the acceptability testing phase, to ensure they agreed with key productivity indicators for those enterprises (Table 3.10). In addition, pasture production outputs were checked to ensure that the timing, amount and composition of pasture growth at the break of the season, and in spring, met the manager's expectations over the long term, including in severe drought years. For livestock production, this included matching ewe live weights and condition score over autumn, as well as the timing and amount of supplementary feeding offered over

the long term. Correct timing of livestock rotations and silage harvesting within the DST simulation was considered more important to the realistic simulation of curing than if DST outputs varied from the manager's estimates.

Table 3.10. Key productivity indicators nominated for three pastures and one crop by the Struan Farm Manager, and associated DST outputs. n/a indicates not applicable, because the DST did not produce that variable, or could not simulate that species.

Variable	Farm Manager	GrassGro	SGS Pasture Model	APSIM
Phalaris				
Ewe greasy fleece weight	3.0 kg	3.4 kg	n/a	n/a
Ewe condition score over summer / autumn	3	2	n/a	n/a
Lamb live weight at sale	45 kg	37.2 kg male 34.1 kg female	21.5 kg	n/a
Clover contribution to pasture	20-25%	17%	10%	n/a
Time of break	Late April – early May	April 5th	May 11th	n/a
Annual Ryegrass				
Ewe greasy fleece weight	3.0 kg	2.9 kg	n/a	n/a
Ewe condition score over summer / autumn	3	4	n/a	n/a
Lamb live weight at sale	45 kg	36.4 kg male 33.4 kg female	20.6 kg	n/a
Average silage cut	5 t DM/ha	7798 kg/ha (total available herbage at November 14th)	4.12 t/ha	n/a
Time of break	Late April – early May	April 28th	May 31st	n/a
Native Grass				
Wether live weight	50 kg	n/a	43.5kg	n/a
Wheat				
Average wheat yield	3 t/ha	n/a	n/a	2.5 t/ha
Barley yield in rotation	3 – 4 t/ha	n/a	n/a	3.3 t/ha
Canola yield in rotation	1.5 – 2 t/ha	n/a	n/a	1.9 t/ha

3.2.2 Simulation of the Australian Capital Territory field sites

A database of curing measurements from a number of different field techniques was available for a wide range of Australian and New Zealand sites (Newnham *et al.* 2010). Basic details of grass type and species, height, fuel condition, and growth stage were recorded. At Majura in the Australian Capital Territory (ACT), database records indicated that the native perennial, spear grass (*Austrostipa bigeniculata*), was the dominant species along with other less

abundant species including the native perennial, common wheat grass (*Elymus scaber*), and introduced species such as an annual, vulpia (*Vulpia muralis*) and a perennial, tall fescue. At another site in the ACT, Tidbinbilla, the perennial native, weeping grass (*Microlaena stipoides*) was recorded, along with introduced perennials, tall fescue and phalaris, and an introduced annual, vulpia (*Vulpia ciliata*). No other indication of the relative proportion of each species was recorded. In June 2008, the Majura and Tidbinbilla field sites were inspected to collect details that could be used as starting inputs for DST simulation. Soil colour and texture were assessed to a depth of around 10 cm and dominant pasture species identified. At the time of this visit, the Majura site was heavily grazed by kangaroos, and not actively managed for livestock production, and the Tidbinbilla site had a pasture comprised of phalaris, native perennial grasses and broad-leaf weeds, with Angus cattle grazing at low intensity. The SGS Pasture Model was used to simulate historical curing estimates as it was the only model to include parameters for the native perennial species present at those sites at the time of inspection.

The Majura site was described as Landscape Unit Mu4 in the Bushfire CRC database, and the Northcote classification Gn2.15 from the soil atlas in GrassGro™ (Bureau of Rural Sciences (after CSIRO) 1991) best described the red clay-loam soil observed at the site. Full details of the soil water module input variables are shown in Table 3.11.

The Tidbinbilla site was described as Landscape Unit Pb8 in the Bushfire CRC database, and the Northcote classification Dy3.41 best described the yellow-grey duplex soil observed at the site. Soil water module input variables are shown in Table 3.12.

Table 3.11. SGS Pasture Model soil water module inputs for Majura, ACT were derived from Principal Profile Form Gn2.15 from the Soil Atlas (Bureau of Rural Sciences (after CSIRO) 1991) in GrassGro™ (GG).

Soil Layer	Surface	A horizon / topsoil		B1 horizon /subsoil	B2 horizon /subsoil	
DST input	**SGS**	**GG**	**SGS**	**SGS**	**GG**	**SGS**
Depth	2 cm	150 mm	15 cm	100 cm	1000 mm	100 cm
Field capacity	27 %vol	0.27 m^3/m^3	27 %vol	29 %vol	0.29 m^3/m^3	29 %vol
Wilting point	13 %vol	0.13 m^3/m^3	13 %vol	17 %vol	0.17 m^3/m^3	17 %vol
Bulk density	1.4 g/cm^3	1.4 mg/m^3	1.4 g/cm^3	1.5 g/cm^3	1.5 mg/m^3	1.5 g/cm^3
Saturated conductivity	240 cm/day	100 mm/hr	240 cm/day	240 cm/day	100 mm/hr	240 cm/day
Saturated water content	48 %vol	n/a	48 %vol	48 %vol	n/a	48 %vol
Air dry water content	10 %vol	n/a	10 %vol	13 %vol	n/a	13 %vol

Table 3.12. SGS Pasture Model soil water module inputs for Tidbinbilla, ACT, were derived from Principal Profile Form Dy3.41 from the Soil Atlas (Bureau of Rural Sciences (after CSIRO) 1991) in GrassGro™ (GG).

Soil Layer	Surface	A horizon / topsoil		B1 horizon /subsoil	B2 horizon /subsoil	
DST input	**SGS**	**GG**	**SGS**	**SGS**	**GG**	**SGS**
Depth	2 cm	300mm	30 cm	100 cm	1200 mm	120 cm
Field capacity	24 %vol	0.24 m^3/m^3	24 %vol	31 %vol	0.31 m^3/m^3	31 %vol
Wilting point	14 %vol	0.13 m^3/m^3	14 %vol	22 %vol	0.22 m^3/m^3	22 %vol
Bulk density	1.6 g/cm^3	1.6 mg/m^3	1.6 g/cm^3	1.7 g/cm^3	1.7 mg/m^3	1.7 g/cm^3
Saturated conductivity	72 cm/day	30mm/hr	72 cm/day	7.2 cm/day	3mm/hr	7.2 cm/day
Saturated water content	48 %vol	n/a	48 %vol	48 %vol	n/a	48 %vol
Air dry water content	13 %vol	n/a	13 %vol	13 %vol	n/a	13 %vol

Little information on livestock and management practices was available because these aspects were outside the scope of the original Bushfire CRC research. As a result, some starting inputs required to simulate these grazing systems had to be estimated. The main variables for the two simulations are described in Table 3.13.

Table 3.13. Weather, soil, pasture and animal variables used in the SGS Pasture Model to simulate the Majura and Tidbinbilla, ACT sites.

Location	Majura	Tidbinbilla
Simulation length	1/1/1960-31/12/2010	
SILO weather location	Canberra Airport	Tidbinbilla
Northcote Soil classification	Gn2.15	Dy3.41
Grass type	Native	
Composition and proportion of the pasture at the start of simulation	Native C_3 perennial (40%), tall fescue (20%), annual ryegrass (40%)	Native C_3 perennial (33%), tall fescue (33%), phalaris (33%)
Paddock size (ha)	100	
Livestock	Wethers in lieu of kangaroos	Wethers in lieu of cattle
Stocking rate (DSE)	10	5
Body weight (kg)	50	
Minimum weight allowed (kg)	30	
Supplementary feeding	Forage - in response to ME requirements, to replicate ability of kangaroos to access feed out of this paddock	Concentrate - in response to ME requirements
Livestock rotation	Set stocked	
Shearing date	September 1st	
Greasy fleece weight (kg)	5.5	

In the absence of actual stocking rate data regarding the kangaroos at Majura, and cattle at Tidbinbilla, grazing pressure was simulated using sheep. The simulations were designed to contrast the pasture production of the two sites, rather than be representative of all facets of the whole system. Therefore, the Majura site had the better soil, was heavily grazed and still dominated by native pasture species, whereas the Tidbinbilla site had a poorer soil, and lower carrying capacity. Where specific inputs for the simulations were not known, either default values supplied by the DST, or estimates based on observations from the field visits, were used. The pasture growth module within the SGS Pasture Model was initialised with 2.5 t/ha dry matter (DM) at Majura and 3 t/ha (DM) at Tidbinbilla, allocated between the species as indicated in Table 3.13. Initial soil nutrient status was based on default values in the SGS Pasture Model and no fertiliser or irrigation was added. In some instances, substitutions were made. The only annual grass species available in the SGS Pasture Model was annual ryegrass and this was substituted for the annual vulpia in the Majura simulation.

Evaluation of the simulation outputs was based on the relative distribution of grass species over simulation runs of 50 years, to ensure that the native species remained dominant. The length of the runs lessened the influence of the starting values on the pasture outputs by 2005 which coincided with the curing measurements available in the Bushfire CRC database. Pasture composition was checked over the length of the run to ensure that each species remained present in the simulation in correct relative amounts, and that the pasture availability responded appropriately to the effects of droughts and good seasons. No more specific information was available on the sites with which to validate the simulations more robustly.

3.2.3 Statistical analyses

Curing values were calculated from outputs or extracted from outputs from the different DST (as detailed in Chapter 1, section 1.6.2.5). DST-generated curing percentages were plotted against curing assessments from the Levy Rod technique (Levy and Madden 1933; Anderson *et al.* 2011) and destructive sampling either collected at the South East field sites in South Australia, or recorded in the Bushfire CRC database. As field measurements were fewer than those generated by simulation, DST-generated values of curing were averaged over the 2.5 week interval surrounding the date of field measurements in South Australia, to produce a similar number of samples for comparison. Distance to field sites and limited resources constrained attempts to collect destructive samples, particularly when inclement weather conditions compromised the value of these samples. Destructive sampling was unable to be conducted frequently enough in South Australia to warrant further analysis and the Levy Rod method was used to assess the accuracy of DST curing estimates. Due to the non-normal

distributions of the curing estimates generated by the DST and Levy Rod curing estimates collected in the field, non-parametric Friedman tests were used to test for differences in curing estimates over time, using PROC FREQ (SAS Institute Inc. 2002-3).

3.3 Results

3.3.1 Simulation of South Australian field sites

3.3.1.1 Phalaris at Struan

For phalaris at Struan, curing estimates were derived from separate GrassGro™ and SGS Pasture Model simulations, and plotted against observed results derived from field techniques for the 2008-9 fire season (Figure 3.1). Field curing estimates varied with the technique used, as has been identified previously (Anderson *et al.* 2011).

There was no significant difference between the curing estimates derived from either Levy Rod assessment, GrassGro™ or the SGS Pasture Model, according to the Friedman test ($\chi^2(1)=1.14$, $P=0.5647$). Similarly, there was no significant difference between curing estimates from the Levy Rod method, and GrassGro™ ($\chi^2(1)=1.29$, $P=0.2568$) or the SGS Pasture Model ($\chi^2(1)=1.29$, $P=0.2568$), or between the DST themselves (($\chi^2(1)=0.1429$, $P=0.7055$). Hence both DST provide curing estimates comparable to those of the Levy Rod technique.

The short plateau and decrease in the GrassGro™ estimates were in response to rain events over a three-week period (8 mm on 21-22/11/2008, 17 mm on 4/12/2008, and 55 mm on 12/12/2008). A similar response was evident in the SGS

Pasture Model. The Levy Rod curing assessments identified this "greening-up" event, albeit with a considerable lag, which is likely to be an artefact of the measurement interval.

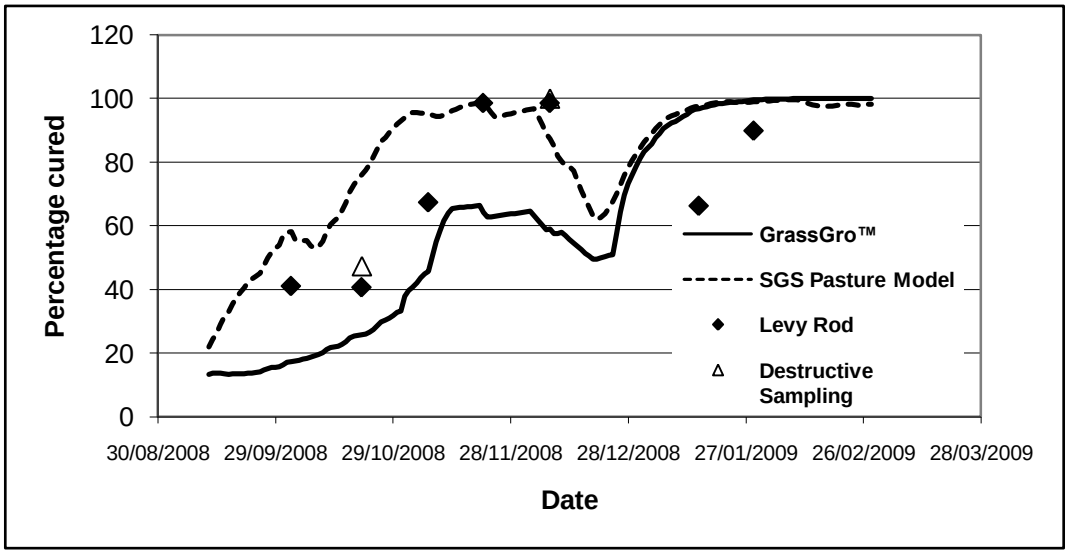

Figure 3.1. Comparison of field curing assessments with estimates of curing from GrassGro™ and the SGS Pasture Model for phalaris at Struan, SA, during the 2008-2009 fire season.

3.3.1.2 Annual ryegrass at Struan

Field assessments of curing were plotted against GrassGro™ and SGS Pasture Model estimates for annual ryegrass grown at Struan during the 2008-2009 fire season (Figure 3.2). The apparent differences in the increase in curing in the 20-80% range between the DST for annual ryegrass were not supported by the Friedman test which suggested that there was no significant difference between the curing estimates generated by either the Levy Rod technique, GrassGro™, or the SGS Pasture Model ($\chi^2(1)=0.4$, $P=0.8187$). There were no significant differences between the distributions of the Levy Rod-assessed curing and those produced by GrassGro™ ($\chi^2(1)=0.2$, $P=0.6547$) or the SGS Pasture Model ($\chi^2(1)=0.2$, $P=0.6547$), nor were there differences between the curing estimates of GrassGro™ and the SGS Pasture Model themselves ($\chi^2(1)=0.2$, $P=0.6547$). This

suggests that the curing estimates produced by either DST are not incomparable to that of the Levy Rod technique.

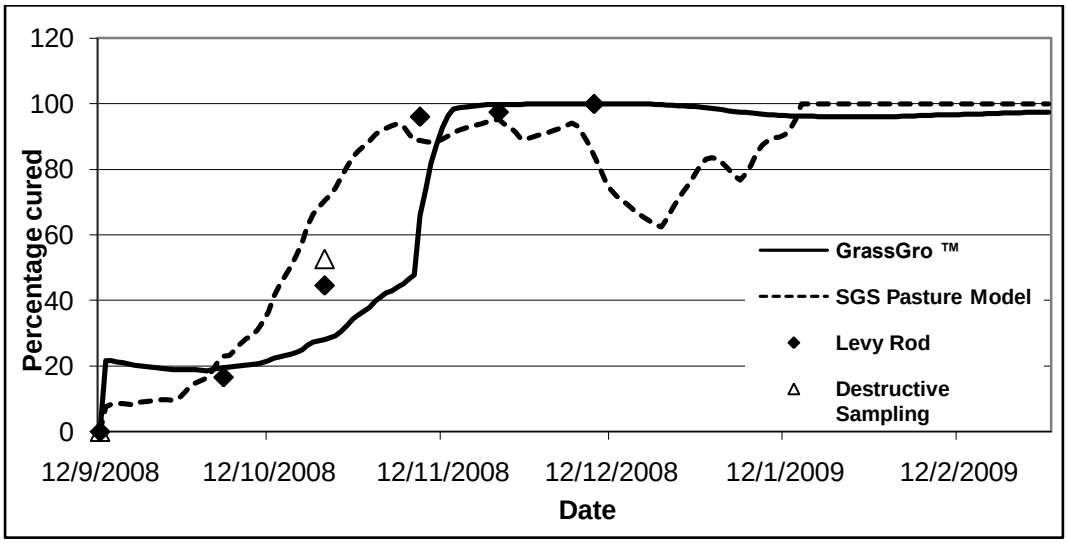

Figure 3.2. Comparison of field curing assessments with estimates of curing from GrassGro™ and the SGS Pasture Model for annual ryegrass cut for silage at Struan, SA, during the 2008-2009 fire season.

3.3.1.3 Wheat at Bool Lagoon

Figure 3.3 compares APSIM curing estimates for wheat at Bool Lagoon with those derived from field techniques. A Friedman test could not detect significant differences between the curing estimates produced by APSIM or the Levy Rod technique ($\chi^2(1)=2.0$, $P=0.1573$).

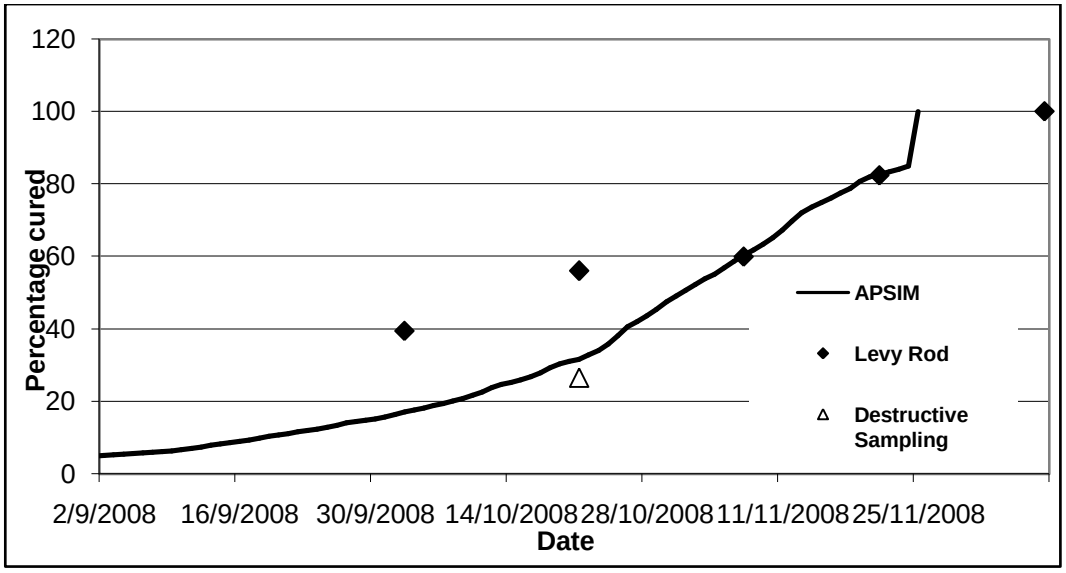

Figure 3.3. Comparison of field curing assessments with estimates of curing from APSIM for wheat at Bool Lagoon, SA, during the 2008-2009 fire season. The APSIM line ceased when the crop was assumed to be ready for harvest in the simulation, while the field assessments continued until 100% curing was achieved.

3.3.1.4 Native grass at Kybybolite

The SGS Pasture Model was the only DST suitable to provide a simulation for the native pasture at Kybybolite. The simulation based on a generic C_3 native grass appeared to underestimate curing particularly when plotted against Levy Rod curing estimates for the 2008-9 fire season (Figure 3.4). This was supported by a Friedman test which showed that the estimates of curing percentage from the SGS Pasture Model were significantly different to those from the Levy Rod technique ($\chi^2(1)=7.0$, $P=0.0082$).

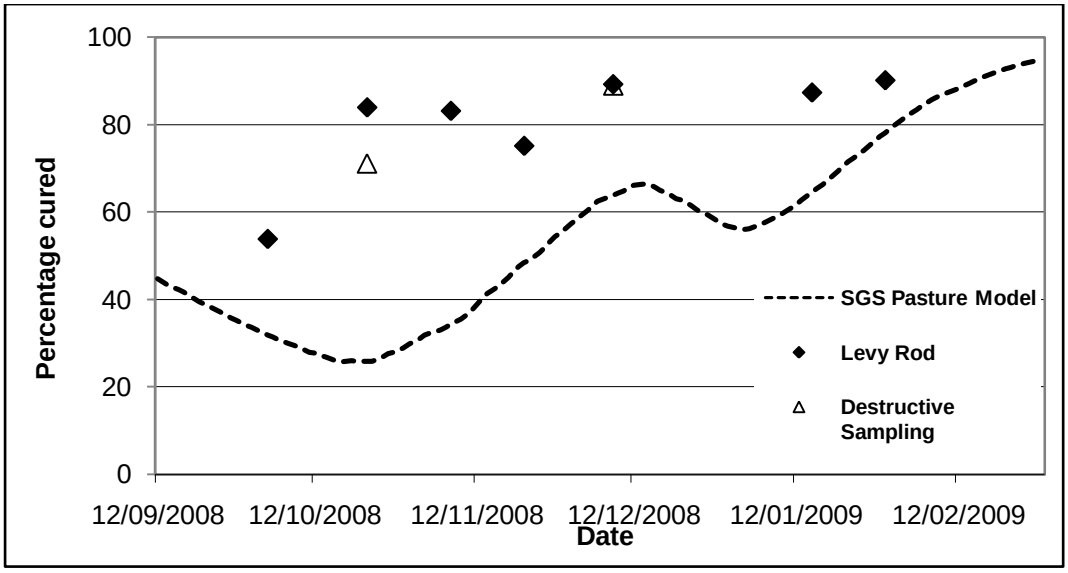

Figure 3.4. Comparison of field curing assessments with estimates of curing from SGS Pasture Model for native pasture at Kybybolite, SA, during the 2008-2009 fire season.

3.3.2 Simulation of ACT field sites

Some variation was evident between the traditional methods of field curing assessment at both the Majura (Figure 3.5) and Tidbinbilla (Figure 3.6) sites over time. A Friedman test indicated that at Majura, the difference between the curing estimates from the SGS Pasture Model (based on the generic C_3 native grass parameters) and the Levy Rod technique were significant ($\chi^2(1)=5.00$, $P=0.0253$), as they were with curing estimates from destructively harvested samples ($\chi^2(1)=7.00$, $P=0.0082$).

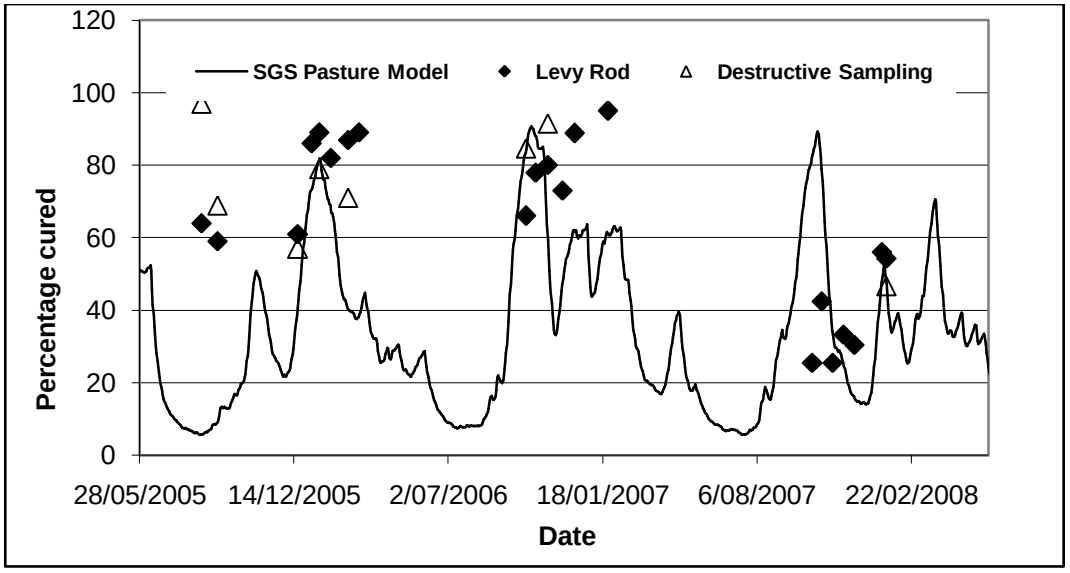

Figure 3.5. Comparison of field curing assessments with estimates of curing from SGS Pasture Model for native pasture at Majura, ACT, during the fire seasons from 2005 to 2008.

At Tidbinbilla, significant differences between the curing estimates from the SGS Pasture Model and the Levy Rod technique ($\chi^2(1)=4.26$, $P=0.0389$) and destructive sampling ($\chi^2(1)=4.00$, $P=0.0455$) were detected.

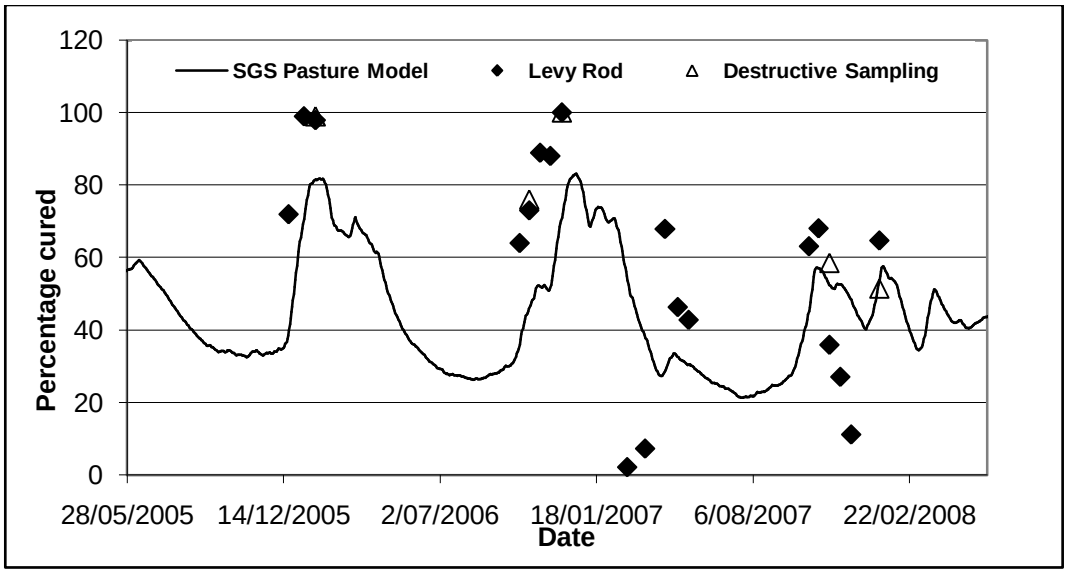

Figure 3.6. Comparison of field curing assessments with estimates of curing from SGS Pasture Model for native pasture at Tidbinbilla, ACT, during the fire seasons from 2005 to 2008.

3.4 Discussion

The DST all appeared to produce curing estimates similar to those of the Levy Rod assessments, with the exception of the SGS Pasture Model in native pastures. However, small sample size would have resulted in low statistical power to detect differences. Any differences between the curing estimates from the SGS Pasture Model native pasture simulation and the Levy Rod method may be due in part to error in the Levy Rod assessments as Anderson *et al.* (2011) found the latter method least reliable in native grasslands. However, the Levy Rod assessments of the native grasslands at Majura and Tidbinbilla, ACT, were conducted by experienced assessors The SGS Pasture Model simulation was based on generic C_3 native grass parameters which may not be a suitable representation of the mix of species found at the SA or ACT field sites. The SGS Pasture Model produced similar curing estimates to the Levy Rod in introduced pastures, and the ACT simulations included a proportion of improved pasture species. The Levy Rod assessments can be regarded as reliable at the ACT sites, so this suggests that the SGS Pasture Model may not be adequately simulating curing in pastures dominated by native species.

This study appears to be the first to test the ability of a number of DST to predict curing. Whereas previous studies have used default input values (Gill *et al.* 1989) or have been unable to test outputs thoroughly because of a lack of historical data (Gill *et al.* 2010), this study has attempted to produce credible simulations for the pastures and crop. The simulation of South Australian field sites was largely successful due to a reliable source of input data, and the ability to robustly validate the outcomes. The Friedman tests conducted here showed that, with appropriate and detailed knowledge of the field sites, it may be possible to

use DST to generate valid curing estimates in some grass species at least. However, not all DST produced the same results at the same site. In spite of similar levels of production over the whole of the phalaris simulation runs, in 2008 the SGS Pasture Model produced lower green herbage mass relative to dead material (data not shown), compared to GrassGro™ and this contributed to the considerable variation in the curing estimates derived from both DST, particularly earlier in the fire season.

The comparison of these DST would no doubt have been simpler without the inclusion of grazing; however, the pastures available to this study were grazed and grasslands more generally do have some grazing pressure. The difference between DST-generated curing estimates for the annual ryegrass pasture at Struan may have been due to lack of management flexibility within the DST. However, Gill *et al.* (1989) found no effect of grazing on curing outputs from a GrassGro™ prototype. Until the senescence algorithms in DST are calibrated for management practices which alter growth and curing patterns, this may remain the case. Livestock and silage (or hay) harvesting cannot be both included in the same GrassGro™ simulation. The attempt to mimic the silage cut by destocking the pasture between late August and mid-November was not successful in terms of generating curing estimates. The simulation predicted a sharp rise in curing in the excess pasture in early November which illustrated the complete switch from the reproductive phenostage to the senescent phenostage in GrassGro™, which accelerated the death rate of living tissue (Equation 1.1). In GrassGro™, generating simulation starting values for a second management practice, as a result of the previous management on the same paddock, uses a technique referred to as “spinning up”. For instance, grazed conditions would be “spun up” until a

date prior to the usual time of silage harvesting, allowing all the soil and pasture outputs under grazing management to be captured as starting values. If the first simulation is realistic, this technique should provide more accurate starting values than simple guesses, and these values would then be transferred to a new simulation with a silage harvesting enterprise. Therefore, calculation of curing over each whole fire season where livestock grazing and fodder conservation are practiced would require the consideration of two simulations. As yet, it is not possible to use simulation outputs such as dry matter herbage production or phenological stage to terminate the spinning up procedure in GrassGro™. In this case, it would be an advantage to be able to capture soil and pasture starting values based on the phenology of the grass component. If the senescent phenostage occurs before the arbitrary date used for the capture of starting values, then the sharp rise in curing will be repeated. In practice, pasture management is more flexible than the rigid calendar-based rules used in DST.

The SGS Pasture Model, on the other hand, allowed both practices, but moved animals on the basis of dry matter availability, and hence animals sometimes stayed on the paddock that had been nominated for silage harvesting. In this simulation, however, with the use of the clay-loam soil, pasture production was sufficient to mimic the real management practice, ensuring stock were moved to an alternative paddock to allow silage to be harvested each year from 2007-2010. However, in the simulation, stock did not return until the following winter. Curing appeared to increase rapidly after silage cutting on October 15th 2008, due to the removal of bulk green leaf material relative to dead material present. High temperature and water stress may have also triggered senescence, and as the level of these stressors are common to all species in the SGS Pasture Model (Chapter 1,

section 1.6.2.4), this timing could not be attributed to the annual ryegrass species *per se*. This is borne out by the fact that the curing outputs generated by the SGS Pasture Model were virtually identical through the 60-100% curing range for both the annual ryegrass and phalaris simulations (Figure 3.7), while those of the native pasture differed due to soil and weather differences as well.

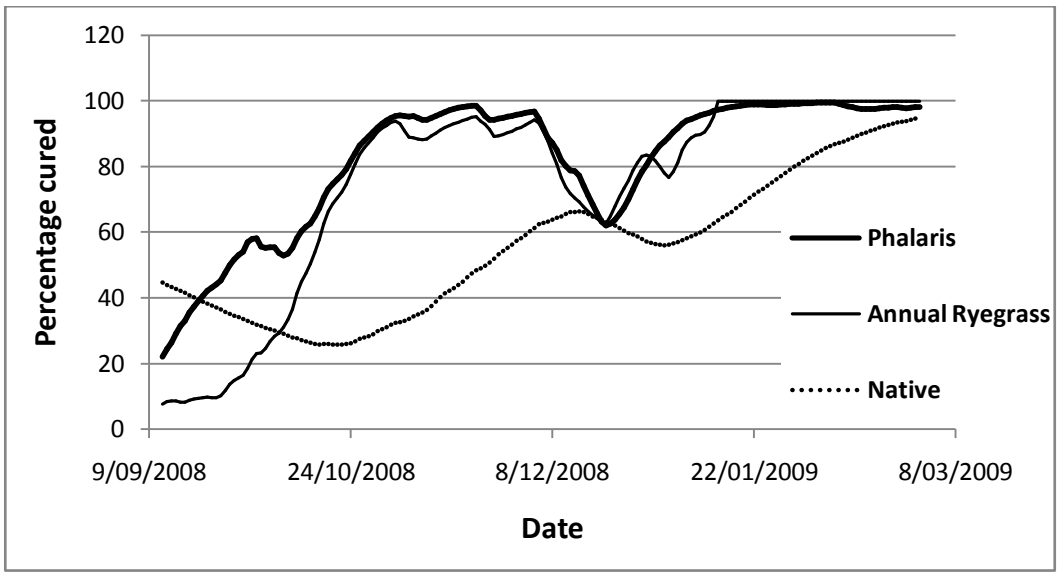

Figure 3.7. Comparison of the SGS Pasture Model curing outputs for phalaris pasture, annual ryegrass silage and native pasture simulations at South Australian sites during the 2008-2009 fire season.

Data from the Australian Capital Territory field sites were much more difficult to simulate. This is not surprising since the Bushfire CRC database was built with a specific purpose in mind, and did not contain model-ready information to either set up or evaluate pasture simulations. Therefore, we can have far less confidence in the outcomes of the simulations at those sites. Also, retrospective production of curing estimates will have limited value to fire management. Rather, this study highlights the need for extensive consultation with land holders to ascertain values for system inputs and outputs, to accurately simulate field sites to predict curing estimates. Fire management personnel using these DST will always need to have the knowledge, whether learned formally or through field experience, to provide inputs and evaluate the outputs of DST.

Previous workers have noted difficulties with data format and meaning (e.g. Dawson *et al.* 1991; Gill 2008) and this study highlighted inconsistencies and limitations between the DST that are currently available. From a practical perspective, no single DST was able to simulate the range of grass types evident in Australian temperate zones. GrassGro™ is best suited to simulations of improved pastures, APSIM is designed for cereal crops, and the SGS Pasture Model is able to simulate native grasslands, although the generic native grass parameters may not be representative of all native grasslands. It is likely that users would need training in more than one DST. Under grazing, the management options in GrassGro™ appear to provide greater flexibility than the SGS Pasture Model. None of the DST interfaces currently provide curing percentages as a direct output, but this could be overcome through negotiation with the DST developers. Herbage production estimates generated by DST, however, may prove useful indicators of fuel loads for fire management.

The promise of the application of DST to curing previously shown (Baxter and Woodward 1999) has been supported by findings here , but the suggested development and adoption of such technology (Anderson and Pearce 2003) seems to be problematic. Funding issues have restricted past attempts to use DST (e.g. Dawson *et al.* 1991) and this should be addressed to ensure that adequate DST access and training is available for fire management personnel, along with resources to provide inputs and validate simulations. Development of curing responses within plant models is also required.

The senescence and death phase of plant growth is not the major impetus for the development of the currently-available agricultural DST and there are inherent differences in the way these DST approach the task. Fundamentally, there is little

differentiation between annual and perennial species in the way leaf turnover is handled in these DST. However, if grass species with different growth habits exhibit different leaf turnover parameters, then development of specific parameters is required in order to better simulate curing in grasses. Improved parameterisation of senescence in a range of grass species will not only enable the development of stand-alone curing models, but also provide an opportunity to enhance the ability of the current DST to simulate senescence.

4 Development of a Leaf Curing Model

4.1 Introduction

The ability of commercially-available decision support tools (DST) to estimate curing in grass swards varied with species and DST (Chapter 3). Leaf senescence has been described in terms of length of dead material on the leaf over various measures of time (Mazzanti and Lemaire 1994; Agnusdei *et al.* 2007) and also as the proportion of dead leaf material (Wilson 1976). It follows that curing of grass plants can be directly established from the proportion of green and dead leaf by length, independently of any other input variables required to run a DST simulation. Here, a curing model was developed based on the proportion of green and dead leaf by length. The same approach could be applied in the field. This might allow leaf curing models to be developed quickly and directly for species and regions of interest. This work set out to test if models based on the proportion of leaf curing could provide a simpler alternative to other methodology for measuring curing in the glasshouse and field, specifically the Levy Rod method (Anderson *et al.* 2011) and estimates derived from DST.

4.2 Materials and methods

4.2.1 Glasshouse measurement of plant growth

Four grass species were grown under ideal conditions in a glasshouse, as outlined in Chapter 2. All leaves on the main tiller of each plant were measured regularly to determine the length of green, and subsequently dead, leaf material present.

4.2.2 Calculation of leaf curing percentage

Leaf curing percentage in this study is defined as the total length of dead leaf material divided by the total length of leaves being measured on the tiller at each thermal time point, multiplied by 100.

4.2.3 Statistical analysis and development of Leaf Curing Models

Data were analysed individually for each species, with curing percentage fitted against thermal time. Exploratory data analysis indicated that the relationships were non-linear in shape, and logistic functions were used for annual ryegrass, phalaris and wheat, in which covariance matrices for the random effect parameters for pots were parameterised using Cholesky decomposition (Pinheiro and Bates 1995) in PROC NLMIXED (SAS Institute Inc. 2002-3). A quadratic function was used for wallaby grass, with pot and plant fitted as random variables using PROC MIXED (SAS Institute Inc. 2002-3). These became the Leaf Curing Models. The visual fit of the models was not improved when Gompertz functions were tested as an alternative to the logistic or quadratic functions (data not shown). Goodness-of-fit statistics were generated as discussed in Chapter 2.

4.2.4 Performance of the Leaf Curing Model against other sources

The Leaf Curing Models for each species were validated against observations of leaf curing, determined by leaf measurement, collected at the South Australian field sites in 2008-9 and 2010-11 fire seasons. Northern sites were situated in the Clare district in the mid-north of South Australia. Struan, Bool Lagoon and

Kybybolite, all located around Naracoorte in south-eastern South Australia, comprised the Southern sites (Figure 2.1).

For each species, the Leaf Curing Model was plotted against field observations of leaf curing over thermal time. However, the accrual of thermal time began at different points in the glasshouse-based model (sowing) and the field data (first observation). This meant that an adjustment was needed in the validation to alter the starting point. When the model parameters were fitted to the field leaf curing data using PROC NLMIXED (SAS Institute Inc. 2002-3), an adjustment was made to the thermal time parameter in each function (Equation 4.1), to allow the model to move horizontally along the thermal time axis, to fit the model to the range of the field data. The glasshouse models were fitted to the field data and the only parameter then estimated by SAS was "R" (Appendix B, Table B-3), the other parameters being held fixed at values obtained from Appendix B, Table B-1 and Table B-2. This adjustment was subsequently used to plot the curing values from Levy Rod and DST sources because these data were collected or simulated for the same time range as the field leaf curing observations.

$$gdd_{adj} = gdd + R \quad \textbf{(4.1)}$$

where *gdd* is thermal time and R is a constant to be estimated.

4.2.4.1 Field observations of leaf curing

The Leaf Curing Model was fitted to field observations of leaf curing for each species, using PROC NLMIXED (SAS Institute Inc. 2002-3) to adjust thermal time to the range of the field data. Goodness-of-fit between the model predictions and the field data was assessed using the range of statistics indicated above (section 4.2.3).

4.2.4.2 Levy Rod curing assessments

Levy Rod assessments of curing collected in the field were plotted against the curing predictions of the Leaf Curing Models for all species, regions and years. Goodness-of-fit between the model predictions and the field data was assessed using the range of statistics indicated above (section 4.2.3).

4.2.4.3 DST-generated curing estimates

Finally, the Leaf Curing Models were plotted against estimates of curing generated from DST simulations of the South East South Australia field sites, as described in Chapter 3. Briefly, both GrassGro™ and the SGS Pasture Model were used to simulate annual ryegrass and phalaris; wheat was simulated with APSIM, and the native pasture with the SGS Pasture Model. Individual leaf curing observations, for plants at each site in the 2008-9 fire season, are also plotted. Goodness-of-fit between the Leaf Curing Model predictions and the field data was assessed using the range of statistics indicated above (section 4.2.3).

4.3 Results

4.3.1 Leaf Curing Models

The logistic Leaf Curing Models for annual ryegrass, phalaris and wheat all had good visual fit with the glasshouse data from which they were derived (Figure 4.1). Parameters for the logistic models are given in Appendix B, Table B-1. A quadratic function was used to fit the wallaby grass Leaf Curing Model (Appendix B, Table B-2).

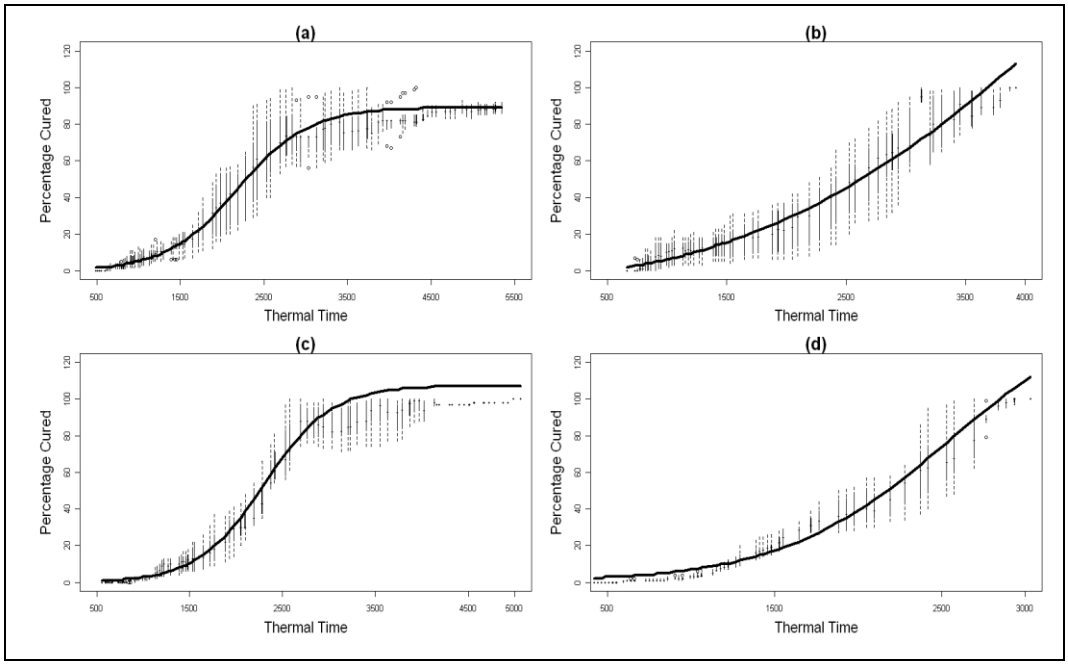

Figure 4.1. Observations (box plot) and model (line) of Leaf Curing with thermal time (gdd (T_{base}=0°C) for species grown in the glasshouse: a) annual ryegrass; b) wallaby grass; c) phalaris; d) wheat. The upper and lower bounds of the solid lines correspond to 75th and 25th percentiles respectively. Dotted lines forming upper and lower whiskers extend the upper and lower quartiles by 1.5 times the interquartile distance, to identify outliers beyond the whiskers, which are indicated by open circles.

The Nash-Sutcliffe Model Efficiency coefficients confirmed that the models predicted the observations on which they were based very closely in all species (Table 4.1). The root mean square deviations (RMSD) suggested that curing percentages predicted by the Leaf Curing Models would be within 10% of the observations.

Table 4.1. Chi square statistics and probability, RMSD and Nash-Sutcliffe Model Efficiency Coefficient (E) for each species from curing values from Leaf Curing Model fitted to leaf curing observations on which the model is based.

Species	χ^2 statistic	χ^2_{red} statistic	prob	RMSD (%)	n	E
Annual ryegrass	χ^2 (617)=40.95	χ^2_{red} (617)=0.07	1.00	9.08	619	0.93
Wallaby grass	χ^2 (456)=53.50	χ^2_{red} (456)=0.12	1.00	10.53	458	0.88
Phalaris	χ^2 (500)=24.92	χ^2_{red} (500)=0.05	1.00	8.32	502	0.95
Wheat	χ^2 (452)=30.23	χ^2_{red} (452)=0.07	1.00	7.13	454	0.93

4.3.2 Validation of Leaf Curing Model against field data

4.3.2.1 Field observations of leaf curing

The variables used to adjust the Leaf Curing Models to the thermal time frame of the field data are given in Appendix B, Table B-3. The Leaf Curing Models all fitted the field data to some extent (Figure 4.2) regardless of region.

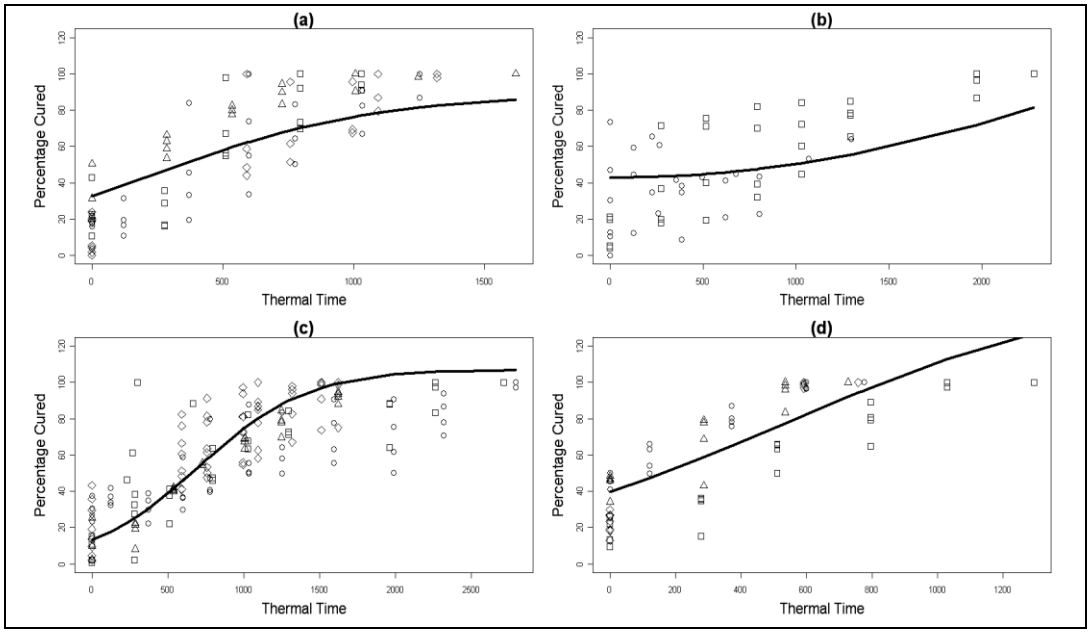

Figure 4.2. Leaf Curing Model (line) over thermal time (gdd (T_{base}=0°C): a) annual ryegrass; b) wallaby grass; c) phalaris; d) wheat. Field observations of leaf curing percentage (points): ○) northern site 1; △) northern site 2; □) southern site (2008); ◇) southern site (2010).

The RMSD of the Leaf Curing Models deviated from field observations by around 20% in all species (Table 4.2), but the Nash-Sutcliffe Model Efficiency coefficient suggested the models were as accurate as the field data (Table 4.2).

Table 4.2. Chi square statistics and probability, RMSD and Nash-Sutcliffe Model Efficiency Coefficient (E) for each species from curing values from Leaf Curing Model fitted to field leaf curing observations.

Species	χ^2 statistic	χ^2_{red} statistic	prob	RMSD (%)	n	E
Annual ryegrass	χ^2 (88)=34.05	χ^2_{red} (88)=0.39	1.00	20.57	90	0.62
Wallaby grass	χ^2 (53)=33.32	χ^2_{red} (53)=0.63	0.98	22.23	55	0.38
Phalaris	χ^2 (155)=64.49	χ^2_{red} (155)=0.42	1.00	17.86	157	0.59
Wheat	χ^2 (72)=22.42	χ^2_{red} (72)=0.31	1.00	17.01	74	0.69

4.3.2.2 Levy Rod curing assessments

The annual ryegrass and phalaris Leaf Curing Models visually fitted the Levy Rod observations of curing for field-grown annual ryegrass and phalaris (Figure 4.3), while the wheat Leaf Curing Model tended to over-estimate curing compared to Levy Rod curing observations which had been obtained in both wheat and barley crops. However, the shape of wallaby grass Leaf Curing Model did not match the Levy Rod curing observations obtained for pastures comprising other native species, and this was reflected in the goodness-of-fit measures in Table 4.3.

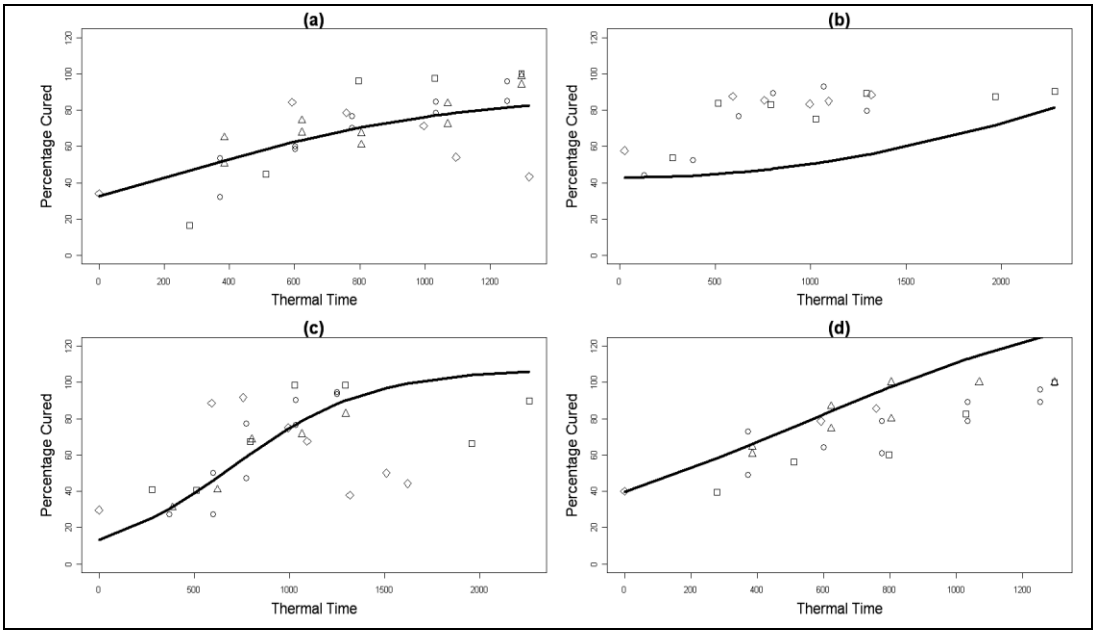

Figure 4.3. Leaf Curing Model (line) over thermal time (gdd (T_{base}=0°C): a) annual ryegrass; b) wallaby grass; c) phalaris; d) wheat. Levy Rod curing percentage (points): ○circle) northern site (2008); □) southern site (2008); ◇) southern site (2010). Levy Rod assessments were not conducted on the same cultivars, or species necessarily. In b) and d), assessments were conducted in mixed native grasses, and wheat and barley cereal crops, respectively.

Table 4.3. Chi square statistics, RMSD and Nash-Sutcliffe Model Efficiency Coefficient (E) for each species from curing values from Leaf Curing Model fitted to Levy Rod assessments.

Species	χ^2 statistic	χ^2_{red} statistic	prob	RMSD (%)	N	E
Annual ryegrass	χ^2 (29)=15.11	χ^2_{red} (29)=0.52	0.98	14.91	31	0.50
Wallaby grass	χ^2 (17)=77.49	χ^2_{red} (17)=4.56	0.09	29.76	19	-3.30
Phalaris	χ^2 (28)=25.65	χ^2_{red} (28)=0.92	0.59	22.67	30	0.12
Wheat	χ^2 (26)=35.84	χ^2_{red} (26)=1.38	0.00	21.07	28	-0.33

4.3.2.3 DST-generated curing estimates

Annual ryegrass and phalaris were simulated with both GrassGro™ and the SGS Pasture Model. Overall, the Leaf Curing Models for these grasses both provided curing estimates at least as accurate as curing estimates generated by both DST combined (Table 4.4), which in turn have been shown to be as accurate as curing determined by the Levy Rod method (Chapter 3, sections 3.3.1.1 and 3.3.1.2).

Table 4.4. Chi square statistics, RMSD and Nash-Sutcliffe Model Efficiency Coefficient (E) for each species from curing values from Leaf Curing Model fitted to DST-generated curing estimates.

Species	χ^2 statistic	χ^2_{red} statistic	prob	RMSD (%)	n	E
Annual ryegrass	χ^2 (174)=68.12	χ^2_{red} (174)=0.39	1.00	21.80	176	0.61
Phalaris	χ^2 (278)=171.13	χ^2_{red} (278)=0.62	1.00	22.12	280	0.39

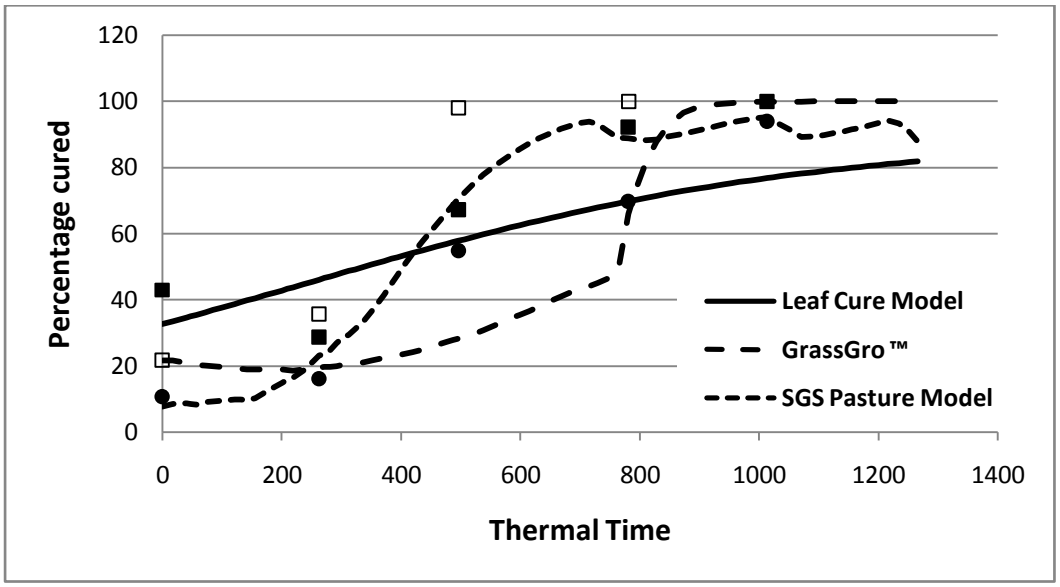

Figure 4.4. Leaf Curing Model plotted against curing estimates generated by GrassGro™ and the SGS Pasture Model for annual ryegrass over thermal time (gdd (T_{base}=0°C). Field observations of leaf curing percentage from individual annual ryegrass plants grown at Struan in 2008 are shown by individual symbols.

For annual ryegrass, the Nash-Sutcliffe Model Efficiencies suggest the Leaf Curing Model provided equivalent estimates to each of the DST (Table 4.5). The Leaf Curing Model over- and under-estimated curing, early and later in the observation period, respectively, compared to the DST estimates (Figure 4.4).

Curing estimates from the Leaf Curing Model are predicted to have slightly less variation around those generated by the SGS Pasture Model (20.15%) than GrassGro™ (23.34%) (Table 4.5).

Table 4.5. Chi square statistics, RMSD and Nash-Sutcliffe Model Efficiency Coefficient (E) for annual ryegrass from curing values from Leaf Curing Model fitted to DST-generated curing estimates.

DST	χ^2 statistic	χ^2_{red} statistic	prob	RMSD (%)	n	E
GrassGro™	χ^2 (86)=38.8	χ^2_{red} (86)=0.45	1.00	23.34	88	0.55
SGS	χ^2 (86)=29.95	χ^2_{red} (86)=0.35	1.00	20.15	88	0.66

The Leaf Curing Model generally fell within the range of curing estimates generated by GrassGro™ and the SGS Pasture Model for phalaris grown at Struan in 2008 (Figure 4.5), however, there were significant differences between the estimates from Leaf Curing Model and the two DST (Table 4.6). The Leaf Curing Model gave statistically similar curing estimates to those of GrassGro™ but not the SGS Pasture Model.

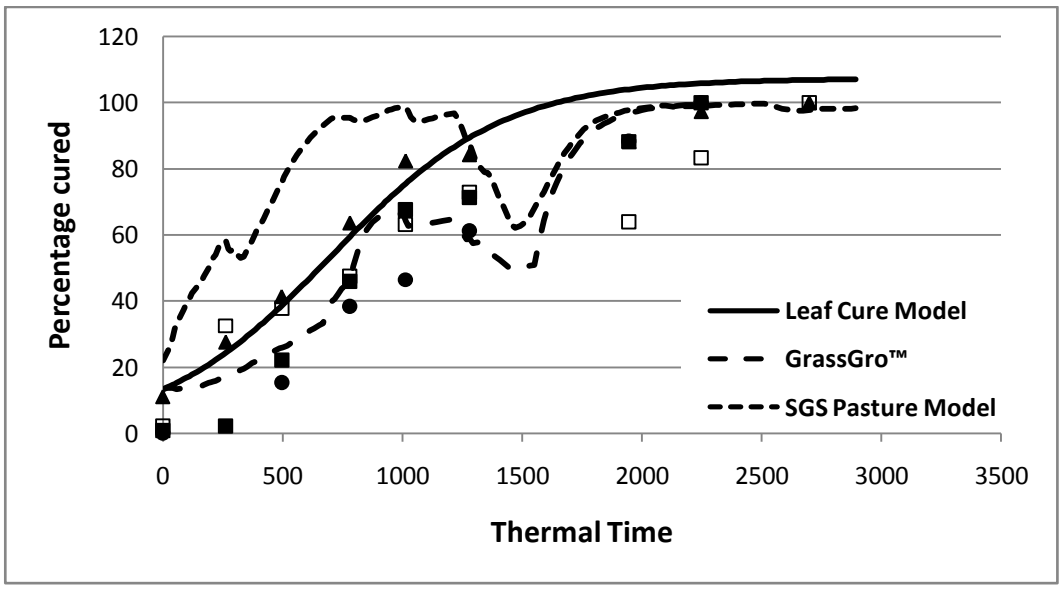

Figure 4.5. Leaf Curing Model plotted against curing estimates generated by GrassGro™ and the SGS Pasture Model for phalaris over thermal time (gdd (T_{base}=0°C). Field observations of leaf curing percentage from individual phalaris plants grown at Struan in 2008 are shown by individual symbols.

Table 4.6. Chi square statistics, RMSD and Nash-Sutcliffe Model Efficiency Coefficient (E) for phalaris from curing values from Leaf Curing Model fitted to DST-generated curing estimates.

DST	χ^2 statistic	χ^2_{red} statistic	prob	RMSD (%)	n	E
GrassGro™	χ^2 (138)=60.32	χ^2_{red} (138)=0.44	1.00	18.85	140	0.57
SGS	χ^2 (138)=198.32	χ^2_{red} (138)=1.44	0.00	25.00	140	-0.43

The wallaby grass Leaf Curing Model generally matched the curing rates of the SGS Pasture Model in a native pasture at Kybybolite in 2008-9 (Figure 4.6) and proved to be an efficient model which provided curing estimates within 10% of those of the DST (Table 4.7).

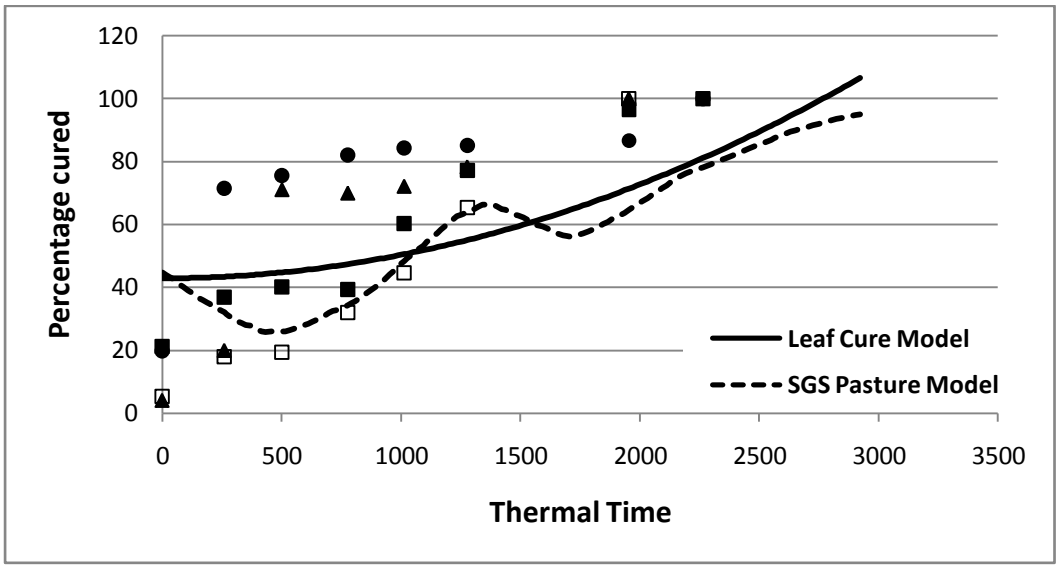

Figure 4.6. Leaf Curing Model plotted against curing estimates generated by the SGS Pasture Model for wallaby grass over thermal time (gdd (T_{base}=0°C). Field observations of leaf curing percentage from individual spear grass plants grown at Kybybolite in 2008 are shown by individual symbols.

Table 4.7. Chi square statistics, RMSD and Nash-Sutcliffe Model Efficiency Coefficient (E) for wallaby grass from curing values from Leaf Curing Model fitted to the SGS Pasture Model curing estimates.

Species	χ^2 statistic	χ^2_{red} statistic	prob	RMSD (%)	n	E
Wallaby grass	χ^2 (168)=34.52	χ^2_{red} (168)=0.21	1.00	9.46	170	0.80

The wheat Leaf Curing Model performed worse than the mean of the APSIM curing estimates (Table 4.8). The model overestimated curing compared to APSIM (Figure 4.7), which was quantified by the RMSD value (Table 4.8).

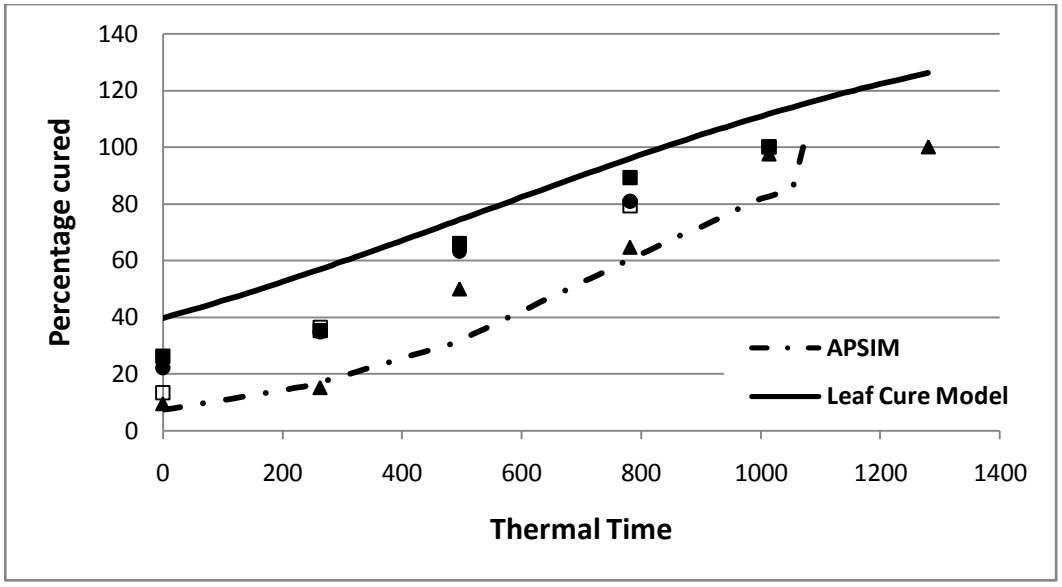

Figure 4.7. Leaf Curing Model plotted against curing estimates generated by APSIM for wheat over thermal time (gdd (T_{base}=0°C). Field observations of leaf curing percentage from individual wheat plants grown at Bool Lagoon in 2008 are shown by individual symbols.

Table 4.8. Chi square statistics, RMSD and Nash-Sutcliffe Model Efficiency Coefficient (E) for wheat from curing values from Leaf Curing Model fitted to APSIM curing estimates.

Species	χ^2 statistic	χ^2_{red} statistic	prob	RMSD (%)	n	E
Wheat	χ^2 (73)=152.19	χ^2_{red} (73)=2.08	0.00	36.91	75	-1.06

4.4 Discussion

Leaf Curing Models were successfully developed from data collected from glasshouse-grown plants for each species. The models for annual ryegrass and phalaris may have been superior to those of wheat and wallaby grass, because the former were naturally constrained to near the biological limit of curing (100%). The inability to constrain the Leaf Curing Model to the biological curing limit for wallaby grass and wheat resulted in a less elegant solution in these species. Attempts to constrain the models to less than 100% curing resulted in loss of fit (data not shown). Alternative functions may improve the fit, but the logistic and quadratic functions were considered reasonable within the limits of the observed data. Extrapolation outside this data range would be invalid.

The validation of the Leaf Curing Models against leaf curing field data was successful for annual ryegrass, phalaris and wheat (Table 4.2), even though field data were collected from different cultivars than those used to produce the Leaf Curing Model. Although there was some variation in the field data for the pasture grasses, the constraint of these models to the biological curing limit assisted in the fit of the models to the field data. Also, the field observations were not generally affected by the "greening-up" that occurred in some species, unless new leaves occurred on the same tillers already being measured.

The goodness-of-fit measures indicated that the wallaby grass model applied to native grass field observations, performed worse than the other species (E=0.38), explaining less variation in the field data and being more variable and less accurate than the other models (Table 4.2). This was in part due to the difficulty in identifying wallaby grass plants in the field in the vegetative state. The Leaf Curing Model was fitted to leaf curing observations for another perennial native with the C_3 photosynthetic pathway, with modest success. When grown in the same conditions, this suggests that it might be possible to fit models to other species with similar growth habits to those which produced the model.

The Levy Rod method has been recommended as the standard method for field collection of curing data (Anderson *et al.* 2011). The higher Nash-Sutcliffe Model Efficiency coefficients (E=0.50) and lower RMSD values (14.91%) (Table 4.3) clearly showed that annual ryegrass Leaf Curing Model had greater accuracy and would give predictions with lower variability around the Levy Rod estimates, than other species models. The Leaf Curing Model for phalaris could be considered as accurate as Levy Rod estimates (E=0.12), but had higher variability around those estimates than the annual ryegrass model. The Leaf Curing Model

failed to represent curing after significant rainfall caused greening-up of pastures such as in annual ryegrass and phalaris in 2010 (Figure 4.3). The decrease in Levy Rod curing values through greening up was more evident in phalaris. Being perennial, phalaris could respond to rainfall events even when curing was well progressed. Some reduction in Levy Rod curing estimates after rainfall in annual ryegrass pastures was due to new germination events, which were short-lived compared to phalaris. The Leaf Curing Model was based on glasshouse-grown plants which did not experience equivalent conditions of soil drying then wetting, and hence curing is portrayed as a continual irreversible process. The inability to respond to greening-up events reduced the fit of Leaf Curing Model to Levy Rod predictions of curing in phalaris, and is a serious limitation of the Leaf Curing Model. In environments with uniform rainfall distribution, this shortcoming of the Leaf Curing Model would be particularly evident.

The negative E values for both wallaby grass and wheat (Table 4.3) suggested that the Leaf Curing Models for these species did not represent curing in cereal crops or native pastures as determined by the Levy Rod technique. The wheat Leaf Curing Model tended to overestimate curing compared to Levy Rod assessment (Figure 4.3). In the case of the native pasture, this may be due to the apparent shortcomings of the Levy Rod technique in assessing curing in these grasslands (Anderson *et al.* 2011), rather than solely a fault of the Leaf Curing Model. In contrast to the phalaris and annual ryegrass examples, the Levy Rod assessments for wheat and wallaby grass were not conducted in single species swards. This may also have contributed to the poorer fit of the Leaf Curing Models to the Levy Rod assessments.

Overall, the Leaf Curing Model appeared to be able to produce similar curing values to those of the GrassGro™ DST in phalaris and annual ryegrass pastures. The Leaf Curing Model produced similar curing values to the SGS Pasture Model in annual ryegrass and native pastures, but not in phalaris. The Leaf Curing Model was not representative of the curing values produced by APSIM in wheat. There was, however, a large variation between the wallaby grass Leaf Curing Model determined in the glasshouse, and the observations of curing using the leaf measurement technique conducted on spear grass plants in this native pasture. This suggests that the wallaby grass Leaf Curing Model may not be representative of other C_3 native species. It was previously shown that curing estimates from the Levy Rod in native pastures were not similar to either the curing estimates from the SGS Pasture Model (Chapter 3, section 3.3.1.4), or the wallaby grass Leaf Cure Model (section 4.3.2.2). Although wallaby grass Leaf Cure Model matched curing estimates from the SGS Pasture Model, neither are representative of Levy Rod curing estimates in native pastures. The species on which the SGS Pasture Model simulation and the wallaby grass Leaf Cure Model are based are not necessarily representative of the native pasture at Kybybolite as a whole. Although some doubt exists over the accuracy of the Levy Rod method for native grasslands (Anderson *et al.* 2011) it cannot be assumed that the Leaf Curing Model is more accurate than the Levy Rod method simply because it provides different estimates.

The Leaf Curing Model generated curing values within 10% of the glasshouse data from which it was based and generated relatively similar RMSD values regardless of the field data against which it was tested. Generally the Leaf Curing Model would produce curing values around 20% of the curing values

generated by the Levy Rod technique or DST simulation with a couple of exceptions. The Leaf Curing Model produced curing values much closer to the DST estimates for native pastures (RMSD = 9.5), and with greater variability for wheat (RMSD = 37.0). However, a 20% variation between actual and predicted curing values is of practical importance. Overestimation of curing by 20% might allow prescribed burns to be scheduled that are subsequently not successful, or lead to the unnecessary declaration of fire bans before prescribed burns are carried out. Underestimation of curing by 20% could lead to prescribed burns being conducted when it is no longer safe to do so. Declaration of fire bans based on underestimation of curing may not be sufficiently cautious to protect the community.

Finally, the level of agreement between the Leaf Curing Model and other field and DST sources of curing estimates suggests that as a means of predicting curing from thermal time, the Leaf Curing Model is no more or less reliable than other methods currently available (Table 4.9).

Table 4.9. Agreement in curing percentage between different assessment and estimation methods. The Nash-Sutcliffe Model Efficiency Coefficient is used to determine the agreement between the Leaf Curing Model and alternative methods.

Species	Levy Rod and DST (from Chapter 3)	Levy Rod and Leaf Curing Model	DST and Leaf Curing Model
Annual ryegrass	Yes	Yes	Yes
Wallaby grass	No	No	Yes
Phalaris	Yes	Yes	Variable
Wheat	Yes	No	No

The leaf curing percentage technique provided a quick and simple method of calculating curing that could be undertaken frequently over the life of the plant that has been previously recognised (Wilson 1976) but not applied to curing assessments for fire management. The Leaf Curing Model provided a relatively simple representation of curing in a limited number of grass species. It was prudent to test this new approach, as other novel methods have been tested before

(e.g. Gill *et al.* 1989; Dawson *et al.* 1991; Baxter and Woodward 1999) to determine if a simple method had merit and should be pursued. The Leaf Curing Model derived from glasshouse grown plants could only be fitted to field data after an adjustment was made to thermal time, but showed promise in capturing leaf curing rates calculated in the same fashion, when applied to the same species (Figure 4.2). However where species variation occurs, as in native or unmanaged grasslands, it may not be sufficient to apply the Leaf Curing Model from one species to another.

The Leaf Curing Model provided a means of predicting curing from thermal time, but with no greater skill than more conventional methods such as the Levy Rod technique or DST simulation. In its present form it is suitable only predict curing for grasses with linear shaped leaves and not other pasture components such as legumes or broadleaf species. The Leaf Curing Model is a simplified representation of curing that assumes that curing is an irreversible process, not affected by rainfall events, and it describes nothing of the component leaf processes that are occurring simultaneously. Curing may also be described in terms of the onset and duration of senescence in the leaf, which requires knowledge of individual leaf turnover characteristics, such as leaf appearance, elongation, longevity and senescence. The data captured in this glasshouse trial, however, is suitable for the exploration of these component processes of leaf turnover, which are addressed in Chapter 5.

5 Characterisation of leaf growth rates in four grass species

5.1 Introduction

The Leaf Curing Model (Chapter 4) predicted curing with thermal time, but with a number of limitations. Curing across the sward is the result of a number of leaf turnover processes occurring simultaneously in a number of leaves. DST captured much of this leaf turnover but simplifications in the modelling and parameterization of senescence were evident in Chapter 3. Understanding the individual leaf turnover processes such as leaf appearance, elongation, longevity and senescence should allow the onset and duration of senescence to be identified within the individual leaf. Understanding the coordination of leaf turnover between leaves should allow the curing process to be monitored across an individual plant.

It is difficult to use previously published leaf growth information to characterize leaf turnover rates for the purpose of developing a model to estimate grass curing. These studies (e.g. Peacock 1976; Bircham and Hodgson 1983; Mazzanti *et al.* 1994; Hepp *et al.* 1996; Carrere *et al.* 1997; Marriott *et al.* 1999; Agnusdei *et al.* 2007) have often overlooked senescent phenostages and there is a lack of consistency in the reporting of leaf turnover rates. Furthermore, there is little information available on the leaf turnover characteristics in the annual and native species common in southern Australian grass-dominated landscapes.

Some attempts have been made to model leaf turnover on a linear basis. LER and LSR were determined as linear measures over thermal time in the SHOOTGRO 1.0 model, however the two rates were assumed to be equal, and

that elongation and senescence occurred on only one leaf at a time (McMaster *et al.* 1991). These truncations and simplifications make this model unsuitable to predict curing, because of the assumption that senescence is constant and irreversible.

Characterisation of plant development to create models of plant growth, or in this specific case, leaf curing, requires knowledge of the number of leaves on the plant and the thermal time required to develop the leaves (Frank and Bauer 1995). To deduce curing across a whole tiller, integration of the life cycle of all the leaves produced by the tiller (leaves per tiller) is needed. Finally, to assess curing on a landscape scale, curing must be extrapolated across both the plant and the sward, which requires knowledge of both tiller numbers (tillers per plant) and plant densities.

This chapter describes the results of a glasshouse study in which the component processes of leaf growth were quantified to test whether models in which leaf characteristics are expressed as functions of leaf position are of similar shape for grasses with differing growth habits. Data described here was also used in the development of a Bayesian model (Chapter 7).

5.2 Materials and methods

Species were selected and grown as outlined in Chapter 2.

The observation study was conducted as a completely randomized design with four species treatments. Each species was represented by two plants in each of four pots, i.e. eight plants per species, and 16 pots in total (refer Table 2.3).

Two plants were randomly selected for the observations of leaf turnover, with a further five plants progressively harvested throughout the study. The final plant in each pot was kept as a replacement in case of plant death. Plants allocated to

observation or harvest studies were identified by a different coloured plastic ring placed around the main stem of each plant.

Leaf measurements and calculation of turnover rates in thermal time are discussed in Chapter 2.

5.2.1 Statistical analysis

Statistical methods common across all chapters are detailed in Chapter 2. Specific analyses in this experiment were conducted using SAS for Windows, Version 9.1 and 9.2 (SAS Institute Inc. 2002-3). Analysis of variance was computed on numbers of leaves and tillers using a mixed model approach (PROC MIXED) and multiple comparisons of differences between species in leaf number and tillers were tested using a Tukey (HSD) test. Mixed models (PROC MIXED) were also used to analyse LAR and LLS. Non-linear mixed models (PROC NLMIXED), in which pot and plant were included as nested random effects using the first order method which approximates the integral of the likelihood over the random effects (Beal and Sheiner 1982; 1988) to assist with parameter estimation, were used to analyse LER and LSR. A CONTRAST statement was used to test the significance of variables in the LER model. Leaf length (LL) data could not be analysed with non-linear mixed models. Instead, non-linear models (PROC NLIN) were used, with bootstrap sampling of randomly-allocated plants within pots included to rule out random effects of pot and plant. The leaf position at which the maximum leaf rate for each species occurred was found visually for linear and cubic functions, and by solving $l = -b/2c$ (where b is the slope and c is the curve) for quadratic functions. Goodness-of-fit was tested using the procedures outlined in Chapter 2.

5.3 Results

5.3.1 Leaf senescence rate

Inverse polynomial models fitted to individual species allowed greater explanation of variation in the LSR data (Figure 5.1) than did a similar model fitted to all species combined. Model equations for each species are given in Appendix C, Table C-1. The models were all significant and explained similar amounts of the variation in observations for wheat ($F_{1,77}$=128.98, P<0.001), wallaby grass ($F_{1,76}$=135.33, P<0.001), phalaris ($F_{1,117}$=140.52, P<0.001) and annual ryegrass ($F_{1,160}$=31.24, P<0.001), regardless of whether measured in terms of $\overline{R}^2$ or the Nash-Sutcliffe Efficiency coefficient (E) (Table 5.1). The RMSD values suggest that the size of the variation around the models was very low compared to the LSR for wheat, wallaby grass and phalaris, but was much higher for annual ryegrass. The outliers shown in Figure 5.1 were responsible for the low explanatory power of the model for annual ryegrass in particular; however there was no clear justification to remove these points. Maximum LSR occurred at leaf 5.2 for wheat, 8.0 for wallaby grass, 11.2 for annual ryegrass and 11.9 for phalaris.

Table 5.1. Chi square statistics and probability, RMSD and Nash-Sutcliffe Model Efficiency Coefficient (E) and $\overline{R}^2$ derived from linear regression between LSR models fitted to LSR observations on which the models are based for each species.

Species	χ^2 statistic	χ^2_{red} statistic	prob	RMSD (mm/gdd)	n	E	$\overline{R}^2$ (%)
Annual ryegrass	χ^2 (159)=133.73	χ^2_{red} (159)=0.84	0.93	0.13	161	0.16	15.9
Wallaby grass	χ^2 (75)=28.51	χ^2_{red} (75)=0.38	1.00	0.05	77	0.62	63.9
Phalaris	χ^2 (116)=53.54	χ^2_{red} (116)=0.46	1.00	0.11	118	0.54	54.4
Wheat	χ^2 (76)=28.73	χ^2_{red} (76)=0.38	1.00	0.03	78	0.63	62.4

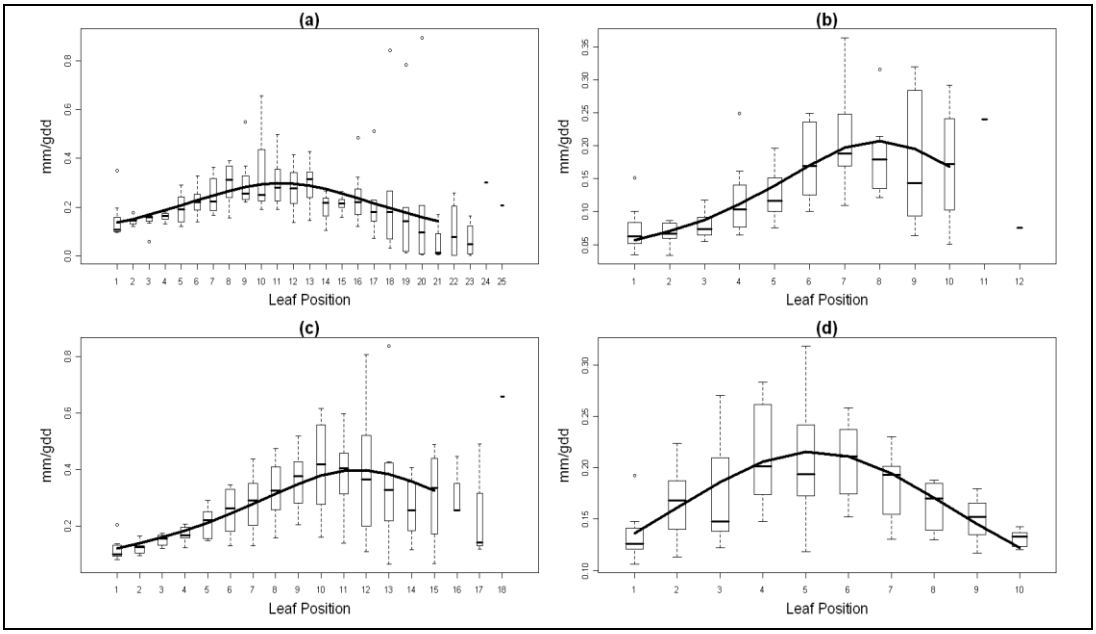

Figure 5.1. Observed (boxplot) and modelled (line) LSR (mm/gdd (T_{base} = 0°C)) with leaf position: a) annual ryegrass; b) wallaby grass; c) phalaris; d) wheat. Upper, internal and lower bounds of each box correspond to 75th, 50th and 25th percentiles respectively. Upper and lower whiskers extend the upper and lower quartiles by 1.5 times the interquartile distance, to identify outliers beyond the whiskers, which are indicated by open circles. Width of boxes is proportional to the square-roots of the number of observations in the groups. Modelled results are presented up to the maximum observed leaf position for each species.

5.3.2 Leaf length

A single inverse polynomial model fitted to leaf length across all species was significant ($F_{12,438}$=340.5, P<0.001). A further bootstrap sampling of plants within each pot was conducted to estimate the parameters for the model shown in Figure 5.2. Goodness-of-fit statistics are given in Table 5.2. The model for wheat fitted the leaf length observations better than other species, according to both the Nash-Sutcliffe Model Efficiency coefficient and $\overline{R}^2$ (Table 5.2) and this appeared to be due to the limited variation in leaf length in wheat. Model fit was reduced in other species which reflected the wider variation in leaf length at some leaf positions. The RMSD also suggested that the wheat model was the most accurate, predicting leaf length to within 28 mm of the true length. The equations for each species

model are given in Appendix C, Table C-2. Maximum length was achieved at leaf 5.7 for wheat, 7.0 for wallaby grass, 9.5 for phalaris and 11.1 for annual ryegrass.

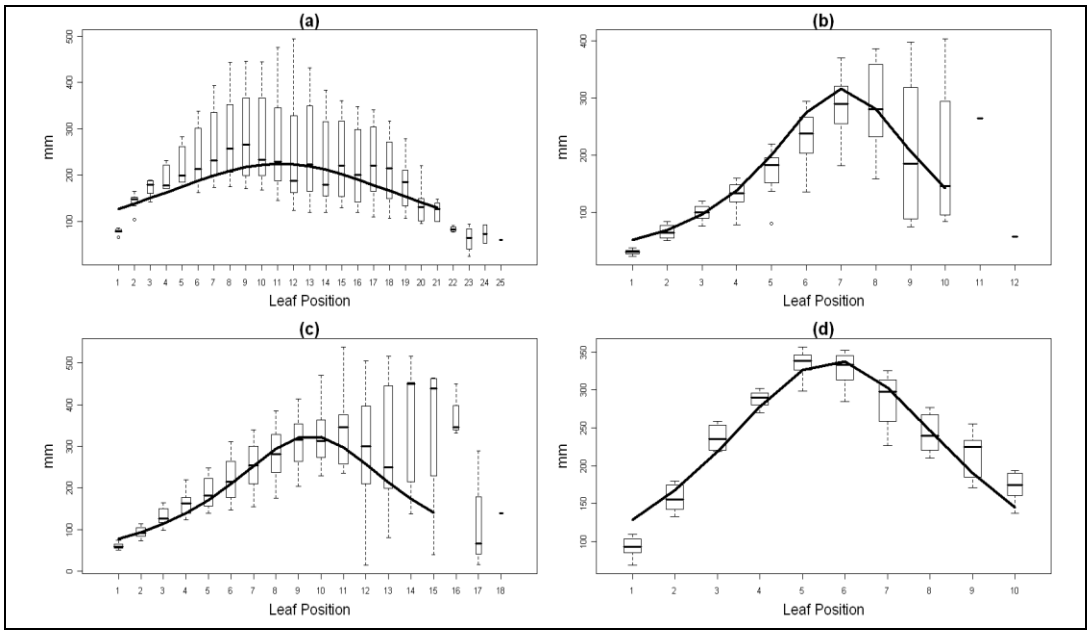

Figure 5.2. Observed (boxplot) and modelled (line) leaf lengths (mm) with leaf position: a) annual ryegrass; b) wallaby grass; c) phalaris; d) wheat. The structure of the boxplots is described in the caption of Figure 5.1.

Table 5.2. Chi square statistics and probability, RMSD and Nash-Sutcliffe Model Efficiency Coefficient (E) and $\overline{R}^2$ derived from linear regression between leaf length models fitted to leaf length observations on which the models are based for each species.

Species	χ^2 statistic	χ^2_{red} statistic	prob	RMSD (mm)	n	E	$\overline{R}^2$ (%)
Annual ryegrass	χ^2 (162)=123.19	χ^2_{red} (162)=0.76	0.99	85.32	164	0.24	38.8
Wallaby grass	χ^2 (76)=31.84	χ^2_{red} (76)=0.42	1.00	67.03	78	0.57	59.5
Phalaris	χ^2 (117)=92.57	χ^2_{red} (117)=0.79	0.95	112.70	119	0.22	29.7
Wheat	χ^2 (76)=10.44	χ^2_{red} (76)=0.14	1.00	28.43	78	0.86	86.3

5.3.3 Leaf elongation rate

The inverse polynomial relationship which existed between LER and leaf position for all species also included significant phenological variables (Figure 5.3). Significant variables in the model included species ($F_{3,13}$=26.5, P<0.001), leaf position ($F_{3,13}$=32.0, P<0.001), the quadratic of leaf position ($F_{3,13}$=32.0, P<0.001), reproductive status of the tiller at elongation of the leaf ($F_{2,13}$=11.5,

P<0.01) and phenological change in the tiller during elongation of the leaf ($F_{2,13}$=8.6, P<0.01). The equations for each species are given in Appendix C, Table C-3. The overall model accounted for 79.6% of the variation in the observed data of all species. The goodness-of-fit statistics (Table 5.3) indicated that the model explained slightly less variation in LER when fitted to individual species, but would predict LER within 0.15 to 0.3 mm/gdd of the true value. The leaf position at which maximum LER was reached was statistically significantly similar for wheat and wallaby grass, but lower than that for annual ryegrass and phalaris (Table 5.4).

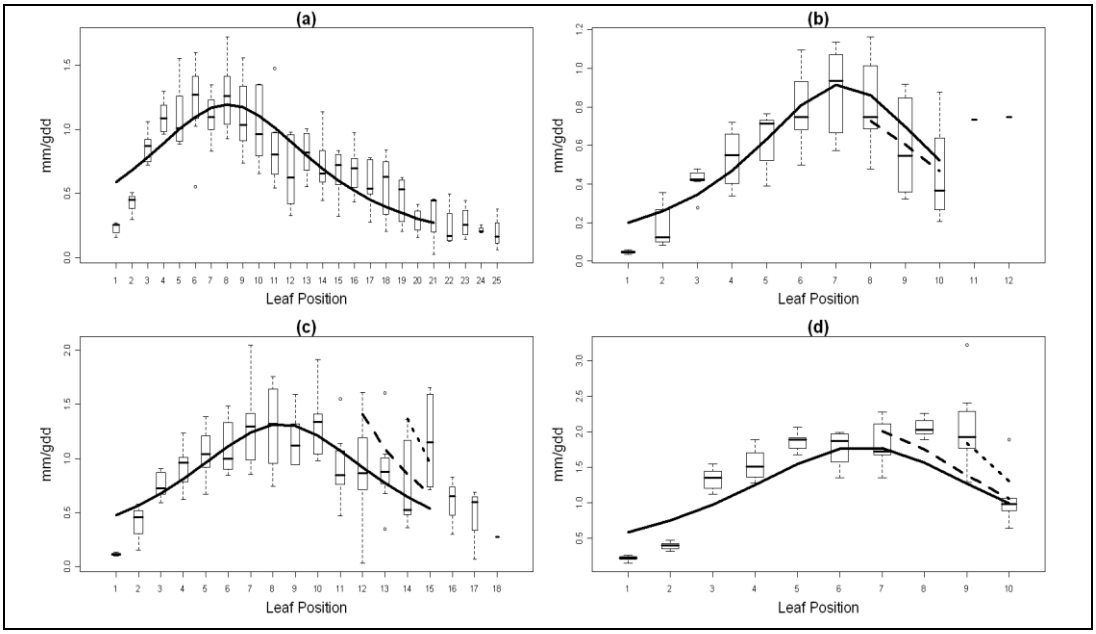

Figure 5.3. Observed (boxplot) and modelled (line) LER (mm/gdd (T_{base} = 0ºC)) with leaf position: a) annual ryegrass; b) wallaby grass; c) phalaris; d) wheat. Solid line represents vegetative model where tillers were vegetative throughout leaf elongation; dotted line represents reproductive model where tillers were reproductive at leaf appearance but did not progress towards maturity during leaf elongation; dashed line represents maturity model where tillers were reproductive at leaf appearance and progressed towards maturity. Models are presented only for leaf positions where data was collected. The structure of the boxplots is described in the caption of Figure 5.1.

Table 5.3. Chi square statistics and probability, RMSD and Nash-Sutcliffe Model Efficiency Coefficient (E) and $\overline{R}^2$ derived from linear regression between LER models fitted to LER observations on which the models are based for each species.

Species	χ^2 statistic	χ^2_{red} statistic	prob	RMSD (mm/gdd)	n	E	$\overline{R}^2$ (%)
Annual ryegrass	χ^2 (165)=48.14	χ^2_{red} (165)=0.29	1.00	0.21	167	0.71	71.0
Wallaby grass	χ^2 (76)=20.13	χ^2_{red} (76)=0.26	1.00	0.16	78	0.74	74.5
Phalaris	χ^2 (116)=39.12	χ^2_{red} (116)=0.34	1.00	0.25	118	0.67	66.7
Wheat	χ^2 (75)=18.35	χ^2_{red} (75)=0.24	1.00	0.32	77	0.76	76.8

Table 5.4. Leaf at which maximum LER occurs in each species. Standard errors and significance values refer to the comparisons between means and are given in brackets. Significant differences are indicated by different superscripts.

Species	Leaf at which maximum LER occurs
Annual ryegrass	8.1^b (s.e.=0.20, t_{13}=41.59, P<0.0001)
Wallaby grass	7.2^a (s.e.=0.28, t_{13}=25.42, P<0.0001)
Phalaris	8.4^b (s.e.=0.24, t_{13}=34.09, P<0.0001)
Wheat	6.5^a (s.e.=0.17, t_{13}=38.81, P<0.0001)

5.3.4 Leaf life span

Leaf life span displayed a curvilinear relationship with leaf position, with variation increasing around the mean as leaf position increased (Figure 5.4). A cubic model best explained LLS for annual ryegrass, phalaris and wheat, in which the interaction between species and leaf position was significant ($F_{2,280}$=8.1, P<0.001), along with the quadratic ($F_{2,280}$=5.9, P<0.01) and the cubic ($F_{2,280}$=4.5, P<0.05) of leaf position. However this model accounted for only 25.5% of the variation in the observed data for these three species. A quadratic function improved the explanatory power of the model for wallaby grass (56.0%), in which both leaf position ($F_{1,55.8}$=24.7, P<0.001) and its quadratic ($F_{1,55.9}$=16.8, P=0.001) were significant. Goodness-of-fit statistics for individual species support the fit of the quadratic model to the wallaby grass LLS observations (Table 5.5). The Nash-Sutcliffe Model Efficiency coefficients for the cubic models indicate that these models are as accurate as the observations on which they are based, and the χ^2_{red}

all approach one, suggesting that the models are fitted in accordance with the variances. Equations providing the best model of LLS for each species are given in Appendix C, Table C-4.

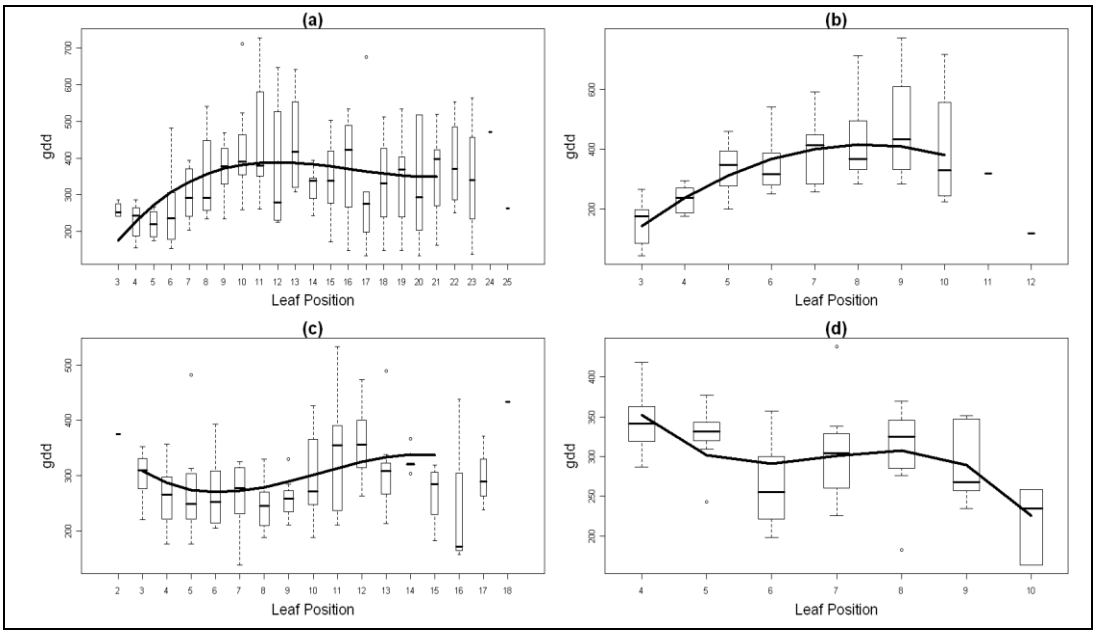

Figure 5.4. Observed (boxplot) and modelled (line) LLS (gdd (T_{base} = 0°C)) with leaf position: a) annual ryegrass; b) wallaby grass; c) phalaris; d) wheat. The structure of the boxplots is described in the caption of Figure 5.1.

Table 5.5. Chi square statistics and probability, RMSD and Nash-Sutcliffe Model Efficiency Coefficient (E) and $\overline{R}^2$ derived from linear regression between LLS models fitted to LLS observations on which the models are based for each species.

Species	χ^2 statistic	χ^2_{red} statistic	prob	RMSD (gdd)	n	E	$\overline{R}^2$ (%)
Annual ryegrass	χ^2 (140)=107.95	χ^2_{red} (140)=0.77	0.98	113.79	142	0.23	23.1
Wallaby grass	χ^2 (58)=25.59	χ^2_{red} (58)=0.44	0.99	98.82	60	0.57	56.0
Phalaris	χ^2 (101)=89.92	χ^2_{red} (101)=0.89	0.78	72.11	103	0.12	11.1
Wheat	χ^2 (52)=33.10	χ^2_{red} (52)=0.64	0.98	47.78	54	0.38	36.5

5.3.5 Leaf appearance rate

Unlike other leaf rates, LAR displayed a linear relationship with leaf position. A significant interaction between species and leaf position ($F_{3,311}$=12.9, P<0.001) was demonstrated with wheat increasing linearly with leaf position in contrast to the other species which decreased (Figure 5.1). Observations of LAR varied

widely both within and between leaf positions for the same species. This may have contributed to the modest explanatory power ($\overline{R}^2$ = 45%) of the linear model when regressed against the observations of all species. This trend was echoed in the goodness-of-fit statistics (Table 5.6) for the individual species; however, the Nash-Sutcliffe Model Efficiency coefficients suggested that the models were at least as accurate as the observed data. The species equations are shown in Appendix C, Table C-5.

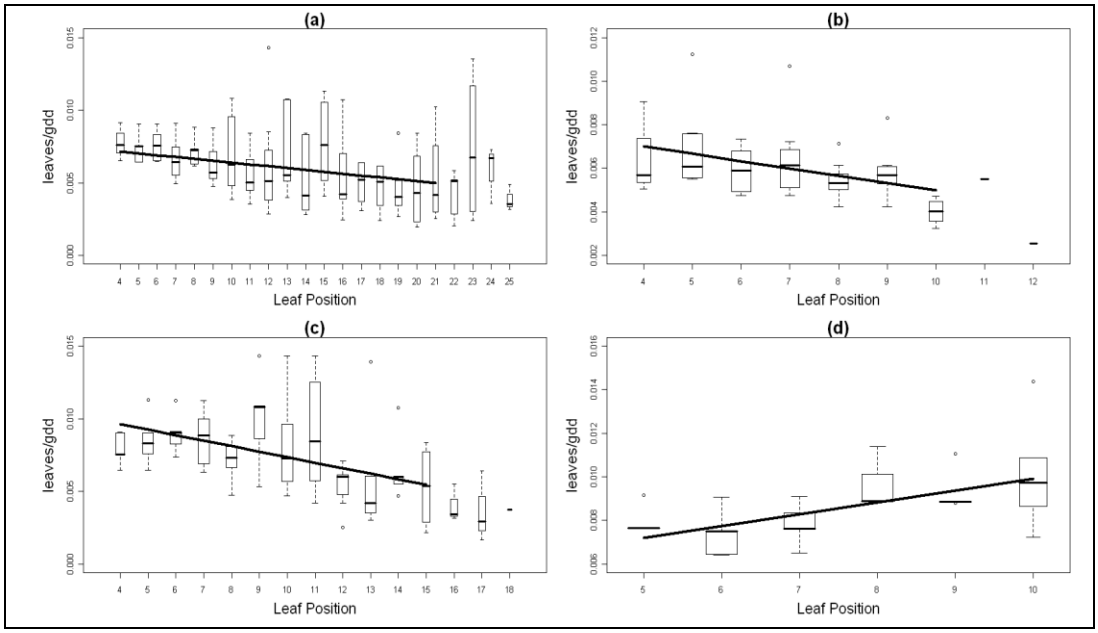

Figure 5.5. Observed (boxplot) and modelled (line) LAR (leaves/gdd (T_{base} = 0°C)): a) annual ryegrass; b) wallaby grass; c) phalaris; d) wheat. The structure of the boxplots is described in the caption of Figure 5.1.

Table 5.6. Chi square statistics and probability, RMSD and Nash-Sutcliffe Model Efficiency Coefficient (E) and $\overline{R}^2$ derived from linear regression between LAR models fitted to LAR observations on which the models are based for each species.

Species	χ^2 statistic	χ^2_{red} statistic	prob	RMSD (leaves/gdd)	n	E	$\overline{R}^2$ (%)
Annual ryegrass	χ^2 (138)=88.49	χ^2_{red} (138)=0.64	0.99	0.001856	140	0.36	36.1
Wallaby grass	χ^2 (48)=38.34	χ^2_{red} (48)=0.81	0.82	0.001409	50	0.21	19.1
Phalaris	χ^2 (88)=55.37	χ^2_{red} (88)=0.63	0.99	0.002086	90	0.38	37.2
Wheat	χ^2 (44)=25.84	χ^2_{red} (44)=0.59	0.99	0.001350	46	0.43	41.4

5.3.6 Leaf and tiller number

Numbers of leaves ($F_{3,12}$=37.8, P<0.001) and tillers ($F_{3,12}$=19.9, P<0.001) varied significantly with species with no differences evident due to perenniality of growth habit (Table 5.7). As counting ceased when tiller numbers exceeded 100, this variable may be underestimated for annual ryegrass.

Table 5.7. Mean numbers of leaves and tillers. Standard errors and significance values refer to the comparisons between means and are given in brackets. Significant differences are indicated by different superscripts.

Species	Leaves mean	Tiller mean
Annual ryegrass	20.9[a] (s.e.=0.86, t_{12}=24.15, P<0.0001)	79.9[a] (s.e.=6.32, t_{12}=12.64, P<0.0001)
Wallaby grass	9.8[c] (s.e.=0.86, t_{12}=11.28, P<0.0001)	41.3[b] (s.e.=6.32, t_{12}=6.53, P<0.0001)
Phalaris	14.4[b] (s.e.=0.86, t_{12}=17.06, P<0.0001)	25.1[b] (s.e.=6.32, t_{12}=3.98, P=0.0018)
Wheat	9.6[c] (s.e.=0.86, t_{12}=11.13, P<0.0001)	16.1[b] (s.e.=6.32, t_{12}=2.55, P=0.0254)

5.4 Discussion

A summary of the shapes of the models and the leaf positions at which maxima and minima values for the models occur for the different leaf growth rates is shown in Table 5.8. These results agree with some previous studies for leaf appearance rate (Table 1.2) and leaf elongation rate (Table 1.3), and vary from previous reports for LLS (Wilson 1976; Calviere and Duru 1995; Duru and Ducrocq 2000a; b) and LSR (Wilson 1976).

Model fit is unlikely to ever be perfect in biological systems and in this experiment it ranged from 80% in LER for all species combined, to 16% for LSR in annual ryegrass. In the latter case, the fit of the model was reduced by the presence of outliers which appeared to demonstrate atypical accelerated leaf senescence. Greater numbers of outliers than expected may be due to errors in the model or incorrect assumptions of normality in the distribution of the data. However, the extended growth of several of the annual ryegrass plants under optimal glasshouse conditions might also be considered not typical of field

situations, in all except the most favourable (e.g. irrigated) environments. The favourable glasshouse conditions may have allowed the expression of these outlier data, hence the model fit may improve in "normal" situations where these outlying samples are less likely to be generated.

Table 5.8. Summary of the shapes of models (stylised) for different leaf growth rates for four species, along with the leaf position at which rate maxima and minima occur. Note that for some rates, maximum and minimum values occur at multiple leaf positions, depending on the shape of the model.

Variable	Wheat	ARG	Wallaby grass	Phalaris
Number of leaves	10	21	10	14
LAR (model shape)				
LER (model shape)				
LER maximum	Leaf 7	Leaf 8	Leaf 7	Leaf 8
LL (model shape)				
LL maximum	Leaf 6	Leaf 11	Leaf 7	Leaf 10
LLS (model shape)				
LLS maximum	Leaf 4	Leaf 11-16	Leaf 8	Leaf 3, 14
LLS minimum	Leaf 10	Leaf 3	Leaf 3	Leaf 8
LSR (model shape)				
LSR maximum	Leaf 5	Leaf 11	Leaf 8	Leaf 12
LSR minimum	Leaf 1, 10	Leaf 1, 21	Leaf 1	Leaf 1

Generally, the approach to fit one model to all species combined worked well. This allows for individual parameterization, but variances and random effects were common between each species. Where a model was fitted to individual species, individual parameters, variances and random effects could be fitted to individual species, and this may account for improvement in fit when individual species models were used.

5.4.1 Leaf senescence rate

In this study, LSR increased with leaf position before an obvious decline occurred in all species. This agrees with Wilson (1976) who found that LSR increased up to the seventh leaf in green panic, before a decrease was noted. However, leaf length was only reported for a subset of leaves in the latter study, meaning that calculation of senescence on the basis of length of leaf per unit of thermal time was not possible for the full cohort of leaves.

The fastest LSR coincided with the longest leaves with greatest life span (Table 5.8). In these pasture grasses, leaves with greatest length and longevity remain in an elevated leaf position for an extended period which, under grazing, increases the risk of defoliation (Lemaire and Agnusdei 2000). These leaves have relatively greater photosynthetic resources stored in them for longer than other leaves. Fast senescence in these leaves may be a genetic response to recycle these resources before defoliation occurs, to allow production of further leaves.

The measurement technique and frequency adopted here enabled accurate measurement of the accumulation of dead material over time. Previous leaf death studies have included senescent material in the live leaf pool (Chapman *et al.* 1983; 1984) or have not captured the progression of curing in individual leaves at the frequency adopted here.

In this experiment, plants were grown under optimal conditions not typical of field situations. However, this allowed the genetic potential of leaf growth to be expressed, measured and modelled, without the influence of confounding environmental factors or limitations. One criticism of pot experiments is that the root microclimate is different to that in the field. Abnormal shoot senescence was reported when root temperatures reached 35°C in wheat (Kuroyanagi and Paulsen

1988). Senescence rates produced here were expected to be normal given that glasshouse temperatures reported in Chapter 2 indicated that it was unlikely that root temperatures were sufficiently high to induce abnormal shoot senescence.

In this experiment growth rates were not disturbed by defoliation. Other studies have demonstrated that leaves on ungrazed or lightly defoliated plants had greater opportunity to senesce than those on heavily defoliated plants (Wade 1979; Bircham and Hodgson 1983; Agnusdei *et al.* 2007), without describing the relative rate of senescence between leaves. In the present study, the top-most leaves showed a decline in senescence rate which could reflect the lack of shading in that part of the canopy. Grazing or cutting might mask the decline of senescence rate with increasing leaf number that was demonstrated here. In addition, reduction in LSR at a given leaf position threshold might be a genetic response aimed at suppressing production of new leaves due to reduced retranslocation of nutrients, and extending photosynthetic capacity to allow seed fill.

5.4.2 Leaf length

The increase in leaf length with leaf position shown in the current study has been previously reported for a number of perennial grasses; however these previous studies (Robson 1973; Wilson 1976; Duru and Ducrocq 2000a; b) used a limited number of leaves or time, and so did not investigate a full complement of leaves.

The shape of the models used here to describe leaf length not only portrayed the observed length of leaves in this experiment adequately, but also accounted for the small decrease in leaf length previously described in the penultimate or flag leaves of other wallaby grasses (Hodgkinson and Quinn 1976), the tropical

grass green panic (Wilson 1976) and most annual crops (Humphries and Wheeler 1963; McMaster 1997). However, leaf length reduction in the two annual species occurred mid-way through the leaf cohort, in contrast to other reports of wheat (Baker *et al.* 1986; Evers *et al.* 2005). The upper leaves of annual ryegrass and wheat decreased to be of similar length to the earliest leaves.

Leaf lengths predicted by the model (Figure 5.2) were similar to previous reports for phalaris (Sambo 1983) and wheat (Baker *et al.* 1986; Evers *et al.* 2005), while penultimate leaf length for wallaby grass was about twice that reported by Waters (2007) for five wallaby grass species grown in outdoor plots. This may reflect both genetic and environmental differences. No previous records of annual ryegrass leaf length were found. Greater uniformity of length with leaf position was evident in wheat, compared to the pasture grass species. Annual ryegrass leaf length was markedly variable at most leaf positions, whereas wallaby grass and phalaris leaves became more variable with higher position on the tiller.

Both soil temperature and time of year have been found to increase leaf length in perennial grasses (Robson 1972; Thomas and Norris 1977; Chapman *et al.* 1983). The decline in leaf length in both perennial and annual species here, however, would indicate that these environmental effects did not affect leaf length, because although this trial was conducted from mid-winter through to late summer, photoperiod, air and soil temperatures were held relatively stable.

5.4.3 Leaf elongation rate

This study appeared to be the first in which LER was recorded in thermal time for these species over an entire cohort of leaves. The non-linear relationship between LER with leaf position which was previously demonstrated in some perennial species (Wilson 1976; Duru and Ducrocq 2000a) was evident for all

species (Figure 5.3). Here, LER fell within the range reported for other perennial pasture grasses (Robson 1972; Duru and Ducrocq 2000a; b); however no records of wheat LER appear to have been published. This may be due to the importance of leaf appearance rather than elongation, on subsequent tiller production of wheat for grain production.

Maximum LER occurred at roughly the same leaf position regardless of leaf production potential; leaf 7 for wallaby grass and wheat, and leaf 8 for phalaris and annual ryegrass (Table 5.8). Maximum LER and length coincided in the same leaf in wallaby grass, but maximum LER occurred in leaves which preceded those of maximum length in phalaris and annual ryegrass. This may reflect the selection pressure in commercial pasture grasses to increase leaf production. In wheat, the leaf with maximum LER was produced slightly later than the longest leaf. This continued production of shorter leaves would spare some nutrients for grain fill, while also maintaining a photosynthetic capacity to aid grain fill.

The observation that LER was faster for leaves on reproducing tillers (Peacock 1976) was supported by wheat and phalaris here, while wallaby grass growth contradicted this trend. However, few leaves elongated on reproductive tillers in any species.

5.4.4 Leaf life span

In this experiment, LLS encompassed both the period of leaf elongation and maturity (Figure 2.3). The relationship between LLS and leaf position was not as straightforward as for other leaf characteristics. Here, LLS was either relatively stable, or quite variable with leaf position and species (Figure 5.4). Similar variation in LLS in early leaves was evident in cocksfoot in different years (Calviere and Duru 1995; Duru and Ducrocq 2000a), while LLS of green panic

generally increased with leaf position (Wilson 1976). While a cubic function fitted most species, LLS remained relatively static especially for many of the later leaves of annual ryegrass and phalaris, when LER was also slowing. This may indicate that the period after ligule development may vary between leaves with the overall effect of maintaining relatively constant LLS. Regardless, identification of the end of the life span of each leaf is important because it signals the onset of curing in that leaf.

In all species, the longest LLS generally corresponded with the leaves which had the fastest LSR (Table 5.8). The exception to this was the longevity shown by early phalaris leaves which had low LSR.

Thermal time measures of LLS recorded in this study were rather less than those found in the literature because the measurement period used in this study was specific to leaf life rather than death. Other approaches used inconsistent measurement intervals and included periods of senescence (when the leaf has begun to yellow and die) in LLS (Vine 1983; Calviere and Duru 1995; Duru and Ducrocq 2000a; Duru *et al.* 2002).

5.4.5 Leaf appearance rate

It has been suggested that non-linear models may provide better prediction of LAR than linear models, especially under normal growth conditions (Xue *et al.* 2004). However, the results from this study provided little support for this theory. LAR demonstrated a linear relationship with leaf position in this study, and also with thermal time (data not shown), in agreement with other studies (Baker *et al.* 1980; Longnecker *et al.* 1993; Kirby 1995).

Temperature and photoperiod were held relatively constant during the current experiment so it is unlikely that changes in LAR were due to these factors (Cao

and Moss 1989; Kirby 1995), but rather due to leaf position. The relationship between leaf position and LAR varied widely between species in previous studies (Table 1.2). Streck *et al.*(2003) found that LAR changed with leaf position in wheat, and reasoned that it was faster in early leaves due to seed reserves, and slower in later leaves because of the increased distance which the leaves must extend before appearance. The pasture grasses in this study appeared to support this theory with LAR decreasing with leaf position (Figure 5.5). This was similar to previous results for green panic and cocksfoot (Wilson 1976; Duru and Ducrocq 2000a), but not phalaris which was reported to have constant LAR with leaf position (Kemp and Guobin 1992). LAR in pasture grasses might be slowed in later leaves as a result of a feedback mechanism from earlier leaves. The high vegetative production in phalaris and annual ryegrass, compared to wheat and wallaby grass, might increase the importance of retranslocation of nutrients, compared to the recruitment of nutrients from the environment. LAR might be limited by the rate of retranslocation of nutrients through senescence.

In this study, LAR increased with leaf position in wheat (Figure 5.5.d), which disagreed with the results of Streck *et al.* (2003). Since the number of leaf primordia available for appearance are fixed at the time of reproductive development (Kemp and Culvenor 1994), it may be that genetic selection for grain yield in the wheat has led to increased LAR in order to maximise the duration of photosynthetic area to maximise grain fill, but why this should be the case in this cultivar, and not in other wheat cultivars or species is not clear.

Although observations of LAR varied widely both within and between leaf positions for each species (Figure 5.5), similar rates of LAR in wheat (Baker *et al.* 1980; Kirby and Perry 1987; Longnecker *et al.* 1993; Rawson and Zajac 1993),

phalaris (Kemp and Guobin 1992), and other perennial grasses (Robson 1972; Calviere and Duru 1995; Frank and Bauer 1995) have been reported. No difference between phenological stages in rate of leaf appearance was apparent, in contrast to the findings of Chapman *et al*. (1983) who showed that LAR decreased sharply at the onset of the reproductive phase.

5.4.6 Leaf and tiller number

Leaf numbers observed here agreed with previous reports for wheat (Baker *et al.* 1986; Kirby and Perry 1987; Longnecker *et al.* 1993; Rawson and Zajac 1993), common wallaby grass (*Austrodanthonia caespitosa*) (Hodgkinson and Quinn 1976) and phalaris (Sambo 1983). Annual ryegrass grew significantly more leaves than the other species, but no clear distinction between annual and perennial growth types was apparent. The species used in this study can be ranked in terms of leaf numbers, even though absolute leaf numbers may decrease under field conditions with later sowings (Kirby *et al.* 1985).

Leaf measurements in this study were carried out on the main stem; however tillers also contribute leaf material to the sward. Few records of tiller number are available for these species, because tillering is often measured in terms of numbers per unit area. The Holdfast phalaris cultivar used here produced half to one-third of the tillers compared with other phalaris varieties (Culvenor 1993) and slightly fewer tillers than perennial ryegrass (Robson 1973). Wallaby grass produced more tillers in this study than recorded for another species, *A. caespitosa*, in which wide variation in tiller number has been noted (Hodgkinson and Quinn 1976). These values provide an indication of the number of tillers able to be produced by these species in the absence of field pressures. They also point to the relative biomass produced by each species, albeit approximately, as daughter

tillers produce progressively fewer leaves (Evers *et al.* 2005), but were not directly measured in this study.

5.4.7 Phenological effects

Phenological state of the tiller was not sufficiently varied to be a significant effect in the models for most of the leaf rates. Greater sample size may be required to detect effects of phenological change on leaf rates. The exception was leaf elongation rate, in which phenology of the tiller on which the leaf was located sometimes changed during elongation of the leaf. Four combinations of vegetative or reproductive phenostage and evidence of phenological advancement were tested in the model and three contributed to the explanation of variation in LER for wheat, phalaris and wallaby grass (Figure 5.3). Most commonly, tillers were vegetative at leaf appearance, and remained so throughout the elongation of the leaf (vegetative model). This was the only combination of phenostage and phenological progress in which leaf elongation was observed in annual ryegrass. No instances were recorded of tillers which were vegetative at leaf appearance, but subsequently entered stem elongation during leaf elongation. Tillers that were reproductive at appearance of the leaf but did not progress towards maturity during leaf elongation (reproductive model) were not common and coincided only with later produced leaves, usually penultimate or flag leaves. Finally, some leaves elongated on tillers that were reproductive and progressed towards maturity (maturity model). An additional phenological variable (whether the tiller eventually flowered) was tested but found not to be significant for any species.

The common consideration of senescence as a process occurring only after reproductive or environmental triggers ignores the sequential leaf death process which has been quantified throughout plant growth in this study, and is vital for

the purposes of estimating curing. Woodward (1998) reported that leaf material accounted for 90% of the total senescent material in the vegetative sward, with the remainder contributed by stem parts. Phenological effects did not significantly impact on leaf senescence rate in this experiment; however, wheat was the only species in which all observed tillers completed the life cycle over the duration of the experiment. In other species, the main tillers under observation did not necessarily reach reproductive or maturation phenostages. Variability in resistance to reproductive development has been reported previously (Valentine and Matthew 1999). Reproductive development has been found to have little effect on senescence of perennial ryegrass (Vine 1983), but flag leaf senescence was delayed in wheat (Feller 1979; Patterson and Brun 1980), hastened in barley (Mandahar and Garg 1975) and both delayed or accelerated in maize (Thomas and Smart 1993) when the ear was removed. Feller and Fischer (1994) suggested that source-sink relationships within the plant that may regulate leaf senescence, might also exist between the tillers and not be limited to the presence or absence of reproductive structures.

This work has provided a baseline study of the leaf turnover characteristics of four common and important agricultural grasses of differing growth habits. This work has enhanced knowledge on leaf turnover rates for a complete cohort of these leaves, albeit for plants grown under optimal ungrazed glasshouse conditions. However, growth rates established under non-grazed experimental conditions have been considered sufficient to estimate growth rates under grazed conditions (Carrere *et al.* 1997). From this starting point a number of further investigations can be carried out. Firstly, it is necessary to determine how common growth restrictions, such as soil moisture limitation, alter LSR displayed

in field situations (Chapter 6). Then, a more complex integration of leaf rates will be attempted using a Bayesian modeling approach (Chapter 7).

6 Effect of water stress on leaf length and senescence

6.1 Introduction

Chapter 5 described a number of measures of leaf turnover rates including senescence, for four common grass species grown under optimal glasshouse conditions. However, Turner and Begg (1978) cautioned that models based on glasshouse observations alone could not necessarily be relied upon in the field. Field environments impose limitations on plant growth, and hence leaf turnover, which vary in the nature of the limitation, its temporal and spatial occurrence, as well as the interactions between limitations. Low rainfall conditions in southern temperate Australia often lead to conditions of restricted soil moisture that coincide with the beginning of the spring fire season, that may accelerate the rate of curing. A rapid change in curing, from low to high flammability, places pressure on fire management agencies and has serious implications for conduct of prescribed burns, readiness planning, risk mitigation, etc. It is important to be able to predict curing under field conditions, and hence knowledge of the effect of water stress on leaf turnover rates is needed.

Under conditions of water stress, transpiration slows or stops and photosynthesis and growth is restricted. The reduction in canopy leaf area is a drought adaptation strategy designed to limit water loss (Schulze *et al.* 1987). The main cause of reduced leaf area is reduced rate of leaf expansion, or LER in the case of grasses (Fischer and Hagan 1965; Turner and Begg 1978; Jones *et al.* 1980a; Dale 1982; Hsiao 1982). Water stress has also been found to affect final

leaf size and length, tiller production and death, and LSR (Turner and Begg 1978; Jones *et al.* 1980a; Dale 1982; Turner 1982).

Leaf senescence is less sensitive than leaf expansion to water stress (Turner 1982), and is sometimes even considered insensitive to water stress (Woodward 1998). Water stress caused leaf senescence to begin earlier and proceed faster in grasses (Fischer and Hagan 1965; Fischer and Kohn 1966), which resulted in reduced leaf area and water loss (Begg 1980). Accelerated LSR enabled retranslocation of nutrients from older leaves to younger ones to limit transpiration losses in vegetative plants, and it allowed completion of reproduction to ensure species survival, if not survival of individual plants (Munne-Bosch and Alegre 2004).

The effects of water stress varied depending on the severity and timing of the stress. Mild water stress caused a reduction in LER (Jones *et al.* 1980a) even before stomatal closure was triggered (Begg 1980). The reduction in LER varied between species (Turner and Begg 1978). Under severe water stress, leaf number was reduced, also restricting canopy development, although this result was dependent on temperature, and the effect increased as temperature increased (Cutforth *et al.* 1992).

In terms of phenological stage, water stress during the vegetative phenostage and tillering in rainfed dryland rice reduced plant height and leaf length and increased the length of the vegetative stage (Murty and Ramakrishnaya 1982). Water stress at anthesis in cereals had a severe effect on senescence (Sinha 1987), presumably because stress imposed late in the growing season accelerated LSR (Hall 2001). During the reproductive and senescent phenostages, moderate water stress increased LSR (Hsiao 1982). LSR increased with sink size in cereals (Sinha

1987), supporting the hypothesis that the effects of water stress may increase with phenological development.

Development of water stress in the field is a gradual process, often interspersed with overnight recovery periods. Plants grown in the field demonstrated greater resilience to water stress conditions than glasshouse-grown plants, due to potential for osmotic adjustment and access to a larger soil water volumes through increased root development (Turner and Begg 1978). The ability of the canopy to recover after the relief of water stress and to attain pre-stress levels of biomass accumulation, appeared to diminish the later that water stress was imposed during canopy development (Hsiao 1982). This is presumably because of a compounding effect over time of reduced LER, rather than the effect of increased LSR alone.

In southern Australia, the chance of plants encountering a water stress event which is not relieved before plant death becomes more likely as the spring season progresses. Terminal water stress, in which water is withheld until plant death, is the extreme application of such a water stress treatment in the glasshouse. It can be imposed at different stages throughout spring to ascertain if timing of water stress has any effect. It should be possible to quantify the changes to leaf growth rates caused by water stress, by growing plants under controlled water stress conditions in the glasshouse. Underlying mechanisms for these changes may also be elucidated when growth conditions are controlled in such a way, which would be difficult under variable field conditions. Verification of models developed from such controlled environment studies in field situations is a secondary, but necessary, part of sound model development.

To better inform the development of the LSR and leaf length models, measurements were conducted on, and models developed for, water-stressed plants in the glasshouse and field-grown plants. It was expected that leaf senescence rate should increase and leaf length decrease under conditions of water stress. However, it was hoped that the relationship between leaf position and these leaf turnover characteristics would remain consistent regardless of soil moisture status.

6.2 Materials and methods

6.2.1 Field monitoring

Field sites were selected as outlined in Chapter 2.4.1.

Four plants were selected at random from each species sward at each site for leaf measurements to determine leaf turnover rates as described in Chapter 0. Although this number is not sufficient to represent each site, site was not used in the analysis except for random effects for plants within sites. This enabled all the data to be combined into a single analysis to provide a comparison to the glasshouse data. It also ensured that all measurements and travel to or from the field site could be completed in one day. This minimized the need for overnight accommodation, and maximized the time available for the glasshouse based experiments being conducted concurrently. Nevertheless, conclusions from the field data should be treated with caution.

At Black Springs, one seedling selected amongst the barley sward was subsequently identified as an annual ryegrass plant and included in the annual ryegrass analysis. After the accidental grazing of phalaris plants at Black Springs, replacement plants were selected, in keeping with the practice of other workers

such as Jones *et al*. (1980a). Distribution of samples across the field sites in 2008-9 and total sample numbers for each species are shown in Table 6.1.

Table 6.1. Number of samples of each species measured at field sites in the 2008-9 fire season.

	Annual Ryegrass	Phalaris	Cereal	Native
Penwortham	4	4	4	-
Black Springs	5	4	3	-
Farrell Flat	-	-	-	4
Naracoorte	4	4	4	4
Total	13	12	11	8

6.2.2 Glasshouse water stress experiment

A split plot design was used to randomly allocate three water stress treatments to plots within each of two blocks. Two replicates of each of four species were randomly allocated to eight pots within each treatment plot (Table 6.2), giving four pots for each combination of species and treatment. Approximately twelve seeds were planted in each pot on 16th July 2008. At the 3-leaf stage, plants were thinned to four uniform plants per pot. This provided a similar plant density to that used in the experiment described in Chapter 5, and allowed for both the random selection of a study plant, and for any plant death prior to the commencement of treatments.

Table 6.2. Pot layout across glasshouse bench with timing of treatments indicated. A, D, P and W indicate annual ryegrass, wallaby grass, phalaris and wheat respectively.

Block 1						Block 2					
Late Spring		Mid-Spring		Early Spring		Mid-Spring		Early Spring		Late Spring	
1 D	5 D	9 D	13 W	17 P	21 A	25 D	29 A	33 D	37 P	41 A	45 P
2 P	6 W	10 W	14 P	18 D	22 W	26 W	30 P	34 P	38 A	42 W	46 W
3 A	7 A	11 A	15 P	19 D	23 A	27 P	31 W	35 A	39 W	43 D	47 A
4 P	8 W	12 D	16 A	20 P	24 W	28 D	32 A	36 D	40 W	44 D	48 P

Water stress treatments were imposed on 26/9/2008 (early spring), 25/10/2008 (mid-spring), and 25/11/2008 (late spring), at which time watering of those pots ceased. Because the imposition of water stress late in spring coincided with the general maturity of the wheat plants, wheat was excluded from the

analysis. At the commencement of each treatment, one plant within each pot was randomly selected for measurement. The main tiller, or a suitable tiller with green leaves, was identified with a coloured plastic cable tie. Leaves were numbered consecutively from the lowest recognisable leaf on the observation stem, being identified as leaf 1 (as per Klepper *et al.* 1982) regardless of whether the leaves were dead, senescing or live. Leaf measurements, as outlined in Chapter 2, commenced at the imposition of water stress and continued at least twice-weekly until all the leaves on the selected tiller were dead. Pots were weighed at each measurement until pot weights were stable, which indicated that no further water was able to be taken up by the plants.

6.2.3 Statistical analysis

6.2.3.1 Field monitoring

Details of statistical methods common to all chapters are given in Chapter 2. Initial attempts to fit inverse polynomials using PROC NLMIXED (SAS Institute Inc. 2002-3), following the successful analysis of other parts of the experiment, experienced convergence problems, so the use of log functions allowed polynomials to be fitted using linear models. A log function (Equation 2.11) fitted to LSR and leaf length for each species using PROC MIXED (SAS Institute Inc. 2002-3) allowed slope and intercept to be fitted as random effects with respect to plant. Leaf position was used as the explanatory variable in all models. Goodness-of-fit statistics were calculated as described in Chapter 2.10. Linear regression of observed against predicted values was used to generate adjusted r^2 ($\overline{R}^2$) values for models.

6.2.3.2 Glasshouse water stress experiment

Correct identification of leaf position was checked during the analysis of LSR by fitting a random term to the leaf position term in each model. This allowed the fitted curve to move horizontally along the leaf position axis, with the intention of obtaining a better fit. However, inclusion of the random term did not improve the fit of the models as determined by the Akaike Information Criterion (Akaike 1974), and thereafter, identification of leaf position was assumed to be correct.

An inverse polynomial function with leaf position as the explanatory variable was fitted to LSR and leaf length using PROC NLIN and PROC NLMIXED (SAS Institute Inc. 2002-3) separately for each combination of species and water stress treatment. As there was only a single experimental unit (plant) per pot, no random effects were fitted. The leaf length models were scaled using a numerator of 10.

A cross validation technique which used macros within SAS (SAS Institute Inc. 2002-3) to partition the data to allow analysis on a training (or calibration) set, and validate the analysis on the balance of the data (a testing set). Use of a cross validation technique overcame the lack of independent data to provide an estimate of how well the model predicted the data (Anonymous 2011b). Four rounds of cross-validation were performed using each pot as a different partition, with validation results averaged over the rounds to reduce variability. The cross validation provided $\overline{R}^2$ values for the models. Goodness-of-fit statistics were calculated as described in Chapter 2, section 2.10.

6.3 Results

6.3.1 Leaf senescence rate response to water stress

The log function fitted the relationship between LSR and leaf position for the field-grown species, but the direction of the curve in native species was opposite to that of the non-native species (Figure 6.1). Spear grass (*Austrostipa spp.*) was the native species measured in the field, rather than wallaby grass (*Austrodanthonia duttoniana*) used in the glasshouse; however, both use the C_3 photosynthetic pathway. Interactions between species and leaf position ($F_{3,237}$=13.45, P<0.0001) and its quadratic ($F_{3,206}$=10.74, P<0.0001) were significant, and the interaction explained 79.3% of the variation in data. Nash-Sutcliffe Model Efficiency coefficients (Table 6.3) for the phalaris and spear grass models were closer to one than the cereal or annual ryegrass models, which suggested that the models fitted at least as well as the mean of observed data. The RMSD values are a gauge of the fit of the log of LSR, rather than LSR itself. The RMSD values are on par with the higher values of log of LSR (data not shown). This suggested that the models may give predictions which vary somewhat from the true value. Model equations for each species are given in Appendix D, Table D-1.

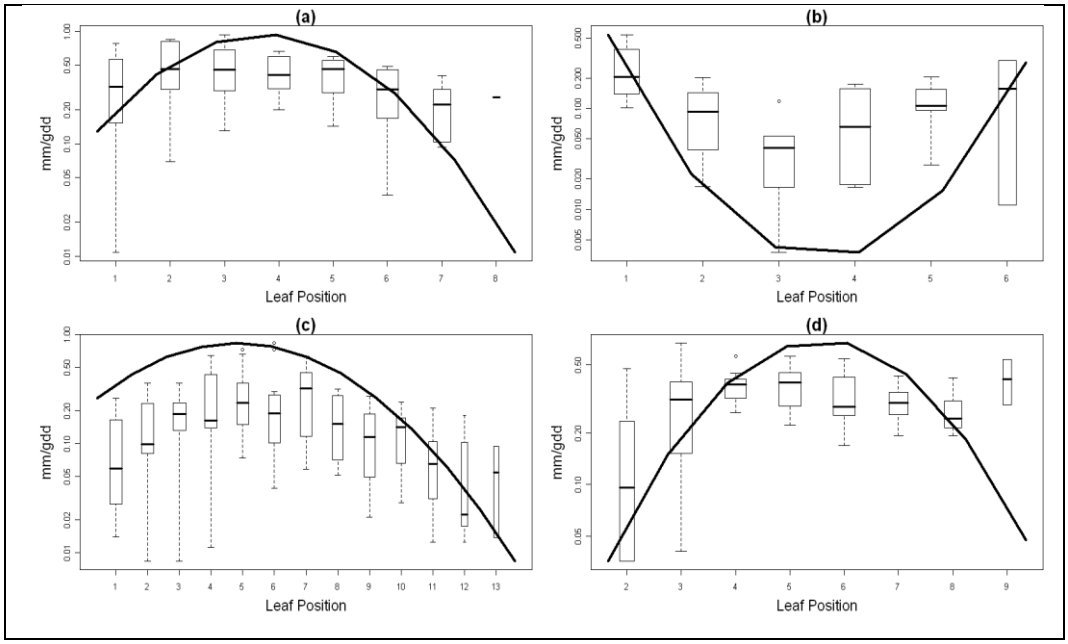

Figure 6.1. Field observations (box plot) and modelled (line) LSR (mm/gdd (T_{base} = 0°C)) plotted on a logarithmic scale with leaf position for four species: a) annual ryegrass; b) spear grass; c) phalaris; d) cereal. Upper, internal and lower bounds of each box correspond to 75th, 50th and 25th percentiles respectively. Upper and lower whiskers extend the upper and lower quartiles by 1.5 times the interquartile distance, to identify outliers beyond the whiskers, which are indicated by open circles. Width of boxes is proportional to the square-roots of the number of observations in the individual groups.

Table 6.3. Chi square statistics and probability, RMSD and Nash-Sutcliffe Model Efficiency Coefficient (E) and $\overline{R}^2$ derived from linear regression between LSR models fitted to LSR observations on field-grown plants on which the models are based for each species.

Species	χ^2 statistic	χ^2_{red} statistic	prob	RMSD log (mm/gdd)	n	E	$\overline{R}^2$ (%)
Annual ryegrass	χ^2 (60)=28.16	χ^2_{red} (60)=0.47	0.99	0.54	62	0.54	55.7
Spear grass	χ^2 (28)=6.48	χ^2_{red} (28)=0.23	0.99	0.53	30	0.78	77.7
Phalaris	χ^2 (126)=23.48	χ^2_{red} (126)=0.19	1.00	0.43	128	0.82	82.0
Cereal	χ^2 (76)=41.70	χ^2_{red} (76)=0.55	0.99	0.45	78	0.46	46.0

Under glasshouse conditions, when a terminal water stress treatment was applied in early spring, the inverse polynomial relationship between LSR and leaf position ($F_{3,34}$=209.58, P<0.0001), was of the same shape in wallaby grass (Figure 6.2) as it had been under well-watered conditions (Chapter 5). Amongst the non-native species, the inverse polynomial relationship remained significant, but explained less of the variation evident in LSR. The Nash-Sutcliffe Model Efficiency Coefficients (Table 6.4) suggested that the model for wheat

($F_{3,32}$=83.82, P<0.0001) was the best of the three non-native species. The models for phalaris ($F_{3,36}$=77.74, P<0.0001) and annual ryegrass ($F_{3,27}$=66.64, P<0.0001) remain valid although they had E values closer to zero. The RMSD values for all models were low in comparison to the range of LSR expressed in all species. Equations for each species are given in Appendix D, Table D-2.

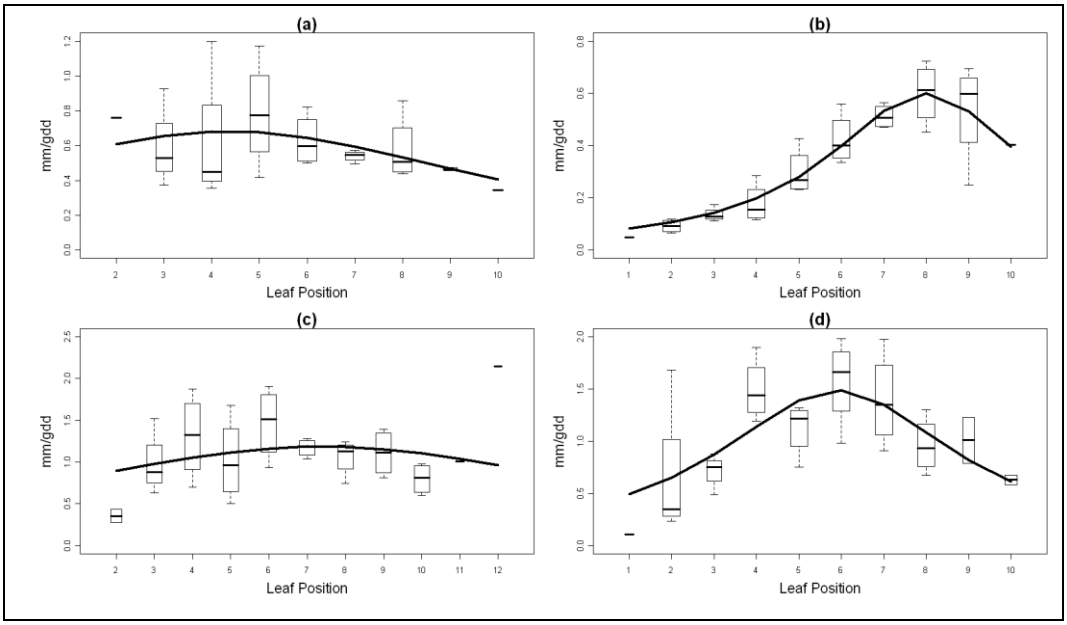

Figure 6.2. Glasshouse observations (box plot) and modelled (line) LSR (mm/gdd (T_{base} = 0ºC)) with leaf position for species subjected to water stress in early spring: a) annual ryegrass; b) wallaby grass; c) phalaris; d) wheat. The structure of the boxplots is described in the caption of Figure 6.1.

Table 6.4. Chi square statistics and probability, RMSD and Nash-Sutcliffe Model Efficiency Coefficient (E) and $\overline{R}^2$ derived from cross validation techniques between the LSR models fitted to the LSR observations on which the models are based for each species when subjected to water stress in early spring.

Species	χ^2 statistic	χ^2_{red} statistic	prob	RMSD (mm/gdd)	n	E	$\overline{R}^2$ (%)
Annual ryegrass	χ^2 (25)=22.92	χ^2_{red} (25)=0.47	0.58	0.21	27	0.12	5.3
Wallaby grass	χ^2 (32)=5.81	χ^2_{red} (32)=0.18	1.00	0.09	34	0.82	81.2
Phalaris	χ^2 (34)=33.40	χ^2_{red} (34)=0.98	0.50	0.41	36	0.05	1.3
Wheat	χ^2 (30)=17.76	χ^2_{red} (30)=0.59	0.96	0.38	32	0.43	39.9

LSR maintained a visually strong polynomial relationship with leaf position in wallaby grass ($F_{3,27}$=69.18, P<0.0001) when water stress was imposed on the plants in the middle of the spring growth period. However, the response appeared

more linear for the annual species (Figure 6.3). Inverse polynomial models were significant for the non-native species; annual ryegrass ($F_{3,22}$=42.87, P<0.0001), phalaris ($F_{3,31}$=57.92, P<0.0001) and wheat ($F_{3,17}$=55.18, P<0.0001). The fit of the models for mid-spring imposition of water stress improved compared to those for early spring stress for annual ryegrass and phalaris, but declined for wallaby grass and remained similar for wheat, according to the Nash-Sutcliffe Model Efficiency Coefficients (Table 6.5). The RMSD values remained low in each species compared to the observations of LSR. Equations for each species are given in Appendix D, Table D-3.

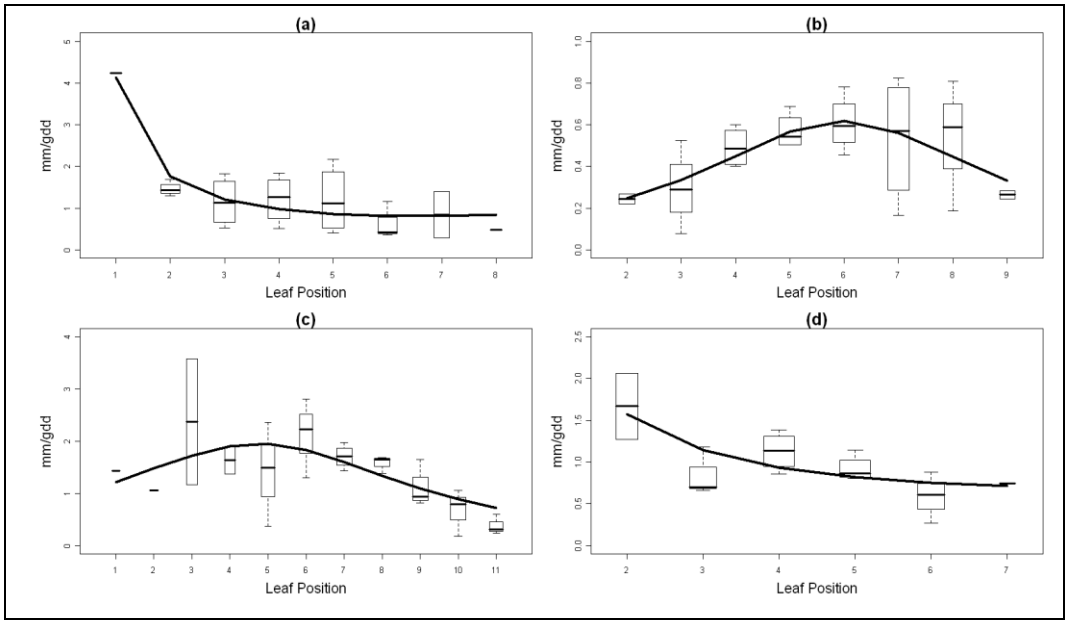

Figure 6.3. Glasshouse observations (box plot) and modelled (line) LSR (mm/gdd (T_{base} = 0ºC)) with leaf position for species subjected to water stress in mid-spring: a) annual ryegrass; b) wallaby grass; c) phalaris; d) wheat. The structure of the boxplots is described in the caption of Figure 6.1.

Table 6.5. Chi square statistics and probability, RMSD and Nash-Sutcliffe Model Efficiency Coefficient (E) and $\overline{R}^2$ derived from cross validation techniques between the LSR models fitted to the LSR observations on which the models are based for each species when subjected to water stress in mid-spring.

Species	χ^2 statistic	χ^2_{red} statistic	prob	RMSD (mm/gdd)	n	E	$\overline{R}^2$ (%)
Annual ryegrass	χ^2 (20)=8.23	χ^2_{red} (20)=0.41	0.99	0.54	22	0.61	37.6
Wallaby grass	χ^2 (25)=16.73	χ^2_{red} (25)=0.67	0.89	0.16	27	0.36	32.0
Phalaris	χ^2 (29)=18.50	χ^2_{red} (29)=0.64	0.93	0.58	31	0.38	31.5
Wheat	χ^2 (15)=9.21	χ^2_{red} (15)=0.61	0.87	0.29	17	0.42	33.6

The non-linear relationship between LSR and leaf position was less obvious when water stress was imposed in late spring (Figure 6.4). However, it was appropriate to test this model given its suitability in the previous cases. The inverse polynomial models were significant, although they accounted for only a small proportion of the variation seen in each species: annual ryegrass ($F_{3,19}$=40.22, P<0.0001), wallaby grass ($F_{3,20}$=14.34, P<0.0001), and phalaris ($F_{3,32}$=52.41, P<0.0001). The Nash-Sutcliffe Model Efficiency Coefficients suggested the models were valid while the RMSD values were generally large compared to the LSR observations recorded in the late spring water stress treatment (Table 6.6). Equations for each species are given in Appendix D, Table D-4.

Table 6.6. Chi square statistics and probability, RMSD and Nash-Sutcliffe Model Efficiency Coefficient (E) and $\overline{R}^2$ derived from cross validation techniques between the LSR models fitted to the LSR observations on which the models are based for each species when subjected to water stress in late spring.

Species	χ^2 statistic	χ^2_{red} statistic	prob	RMSD (mm/gdd)	n	E	$\overline{R}^2$ (%)
Annual ryegrass	χ^2 (17)=10.87	χ^2_{red} (17)=0.64	0.86	0.33	19	0.40	35.6
Wallaby grass	χ^2 (18)=15.48	χ^2_{red} (18)=0.86	0.63	0.57	20	0.19	11.0
Phalaris	χ^2 (30)=21.62	χ^2_{red} (30)=0.72	0.87	0.54	21	0.30	19.3

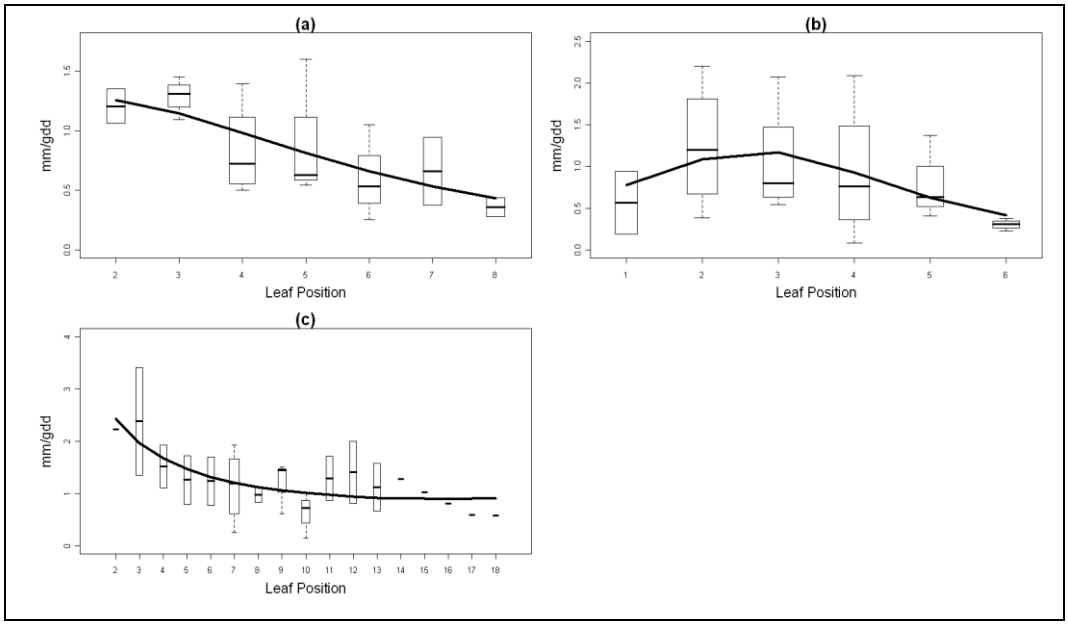

Figure 6.4. Glasshouse observations (box plot) and modelled (line) LSR (mm/gdd (T_{base} = 0°C)) with leaf position for species subjected to water stress in late spring: a) annual ryegrass; b) wallaby grass; c) phalaris. The structure of the boxplots is described in the caption of Figure 6.1.

6.3.2 Leaf length response to water stress

The shape of the relationships between leaf length and leaf position for non-native species in the field (Figure 6.5) was similar to that found in well-watered conditions in the glasshouse (Chapter 5). Models incorporated a log function in which interactions between species and leaf position ($F_{2,209}$=6.64, P=0.0016) and the square of leaf position ($F_{2,103}$=5.70, P=0.0045) were both significant and accounted for 80% of the variation in observed leaf length in the non-native species. No clear trend between leaf length and leaf position was evident for spear grass. The Nash-Sutcliffe Model Efficiency coefficients and $\overline{R}^2$ were high for all models, while the low RMSD values suggested that each model predicted the log of leaf length well (Table 6.7). Model equations for each species are given in Appendix D, Table D-5.

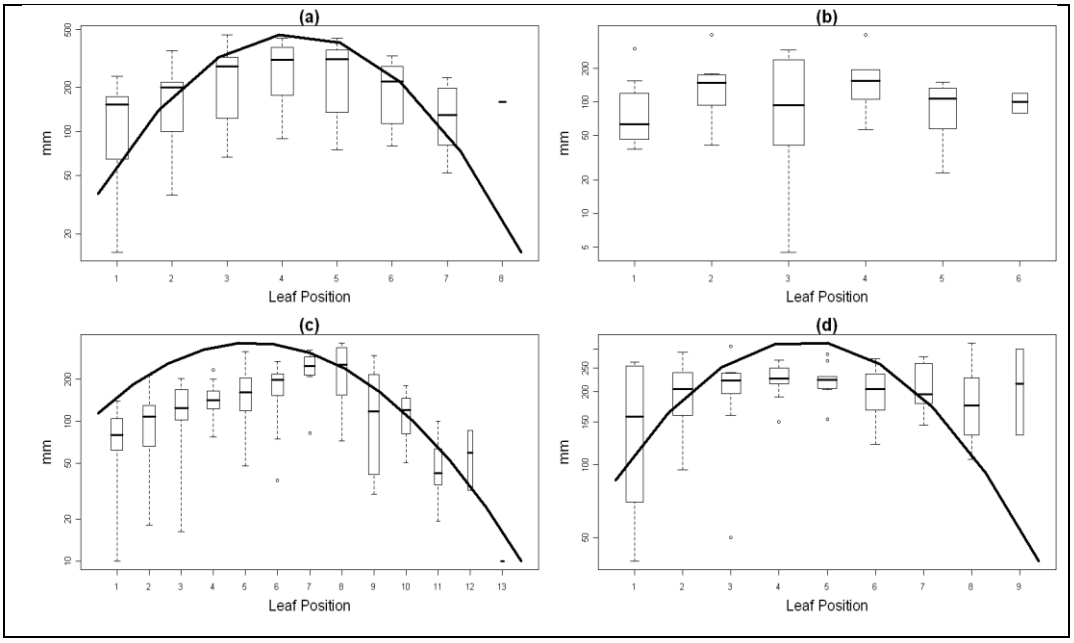

Figure 6.5. Field observations (box plot) and modelled (line) leaf length (mm) plotted on a logarithmic scale with leaf position for four species: a) annual ryegrass; b) spear grass (no solution evident); c) phalaris; d) cereal. The structure of the boxplots is described in the caption of Figure 6.1.

Table 6.7. Chi square statistics and probability, RMSD and Nash-Sutcliffe Model Efficiency Coefficient (E) and $\overline{R}^2$ derived from linear regression between leaf length models fitted to leaf length observations on field-grown plants on which the models are based for each species.

Species	χ^2 statistic	χ^2_{red} statistic	prob	RMSD log(mm)	n	E	$\overline{R}^2$ (%)
Annual ryegrass	χ^2 (72)=7.80	χ^2_{red} (72)=0.11	1.00	0.24	74	0.89	90.0
Phalaris	χ^2 (142)=38.29	χ^2_{red} (142)=0.27	1.00	0.37	144	0.71	73.9
Cereal	χ^2 (93)=26.26	χ^2_{red} (93)=0.28	1.00	0.20	95	0.72	71.1

Leaf length of all species grown in the glasshouse under ideal conditions showed an inverse polynomial relationship with leaf position (Chapter 5), and this relationship remained when plants were subjected to water stress early (Figure 6.6) or mid-way (Figure 6.7) through spring. Models were significant and explained considerable variation in the observed leaf lengths for phalaris ($F_{3,42}$=458.34, P<0.0001), wallaby grass ($F_{3,37}$=191.74, P<0.0001), wheat ($F_{3,36}$=495.18, P<0.0001), and annual ryegrass ($F_{3,34}$=125.16, P<0.0001,) under early water stress conditions. Goodness-of-fit statistics (Table 6.8) suggested that

the phalaris model was the best-fitting (E=0.86), while the wheat model would predict leaf lengths closest to the true value of the leaf length (RMSD=40mm). Equations for the models are given in Appendix D, Table D-6.

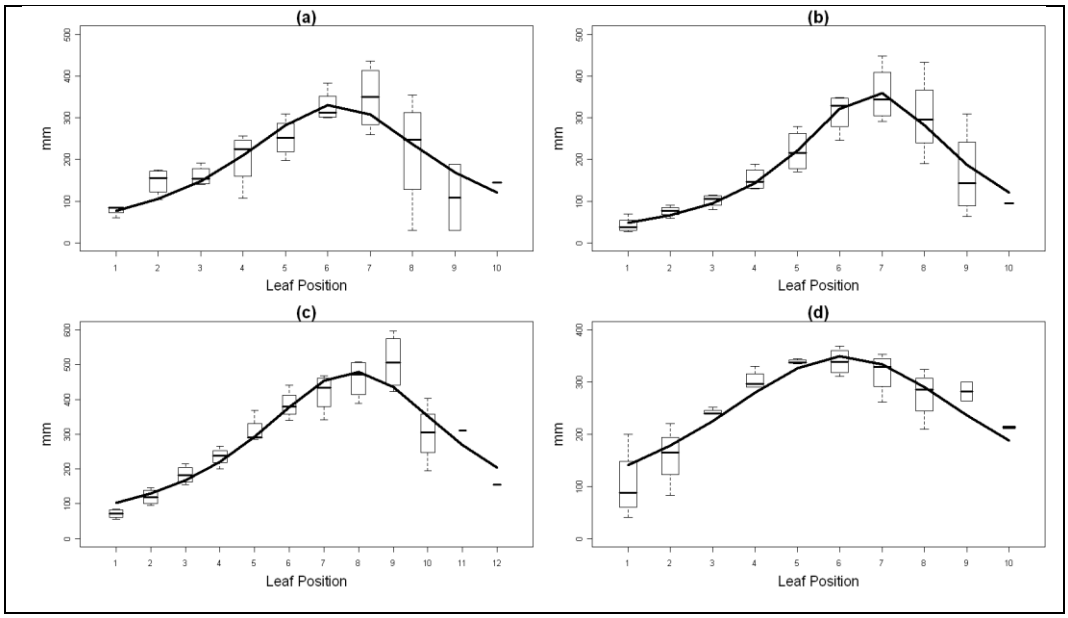

Figure 6.6. Glasshouse observations (box plot) and modelled (line) leaf length (mm) with leaf position for species subjected to water stress in <u>early spring</u>: a) annual ryegrass; b) wallaby grass; c) phalaris; d) wheat. The structure of the boxplots is described in the caption of Figure 6.1.

Table 6.8. Chi square statistics and probability, RMSD and Nash-Sutcliffe Model Efficiency Coefficient (E) and $\overline{R}^2$ derived from cross validation techniques between the leaf length models fitted to the leaf length observations on which the models are based for each species when subjected to water stress in <u>early spring</u>.

Species	χ^2 statistic	χ^2_{red} statistic	prob	RMSD (mm)	n	E	$\overline{R}^2$ (%)
Annual ryegrass	χ^2 (32)=13.25	χ^2_{red} (32)=0.41	0.99	65.24	34	0.60	58.4
Wallaby grass	χ^2 (35)=7.25	χ^2_{red} (35)=0.21	1.00	52.77	37	0.80	78.3
Phalaris	χ^2 (40)=5.93	χ^2_{red} (40)=0.15	1.00	54.67	42	0.86	85.1
Wheat	χ^2 (34)=7.90	χ^2_{red} (34)=0.23	1.00	40.10	36	0.77	76.4

For plants subjected to water stress mid-way through spring (Figure 6.7), models of leaf length remained significant and explained much of the variation in the observed leaf lengths for wallaby grass ($F_{3,32}$=304.16, P<0.0001), and phalaris ($F_{3,43}$=312.79, P<0.0001) (Table 6.9). Increased leaf length variation in annual ryegrass ($F_{3,26}$=83.19, P<0.0001) and wheat ($F_{3,24}$=113.47, P<0.0001,) was

responsible for lower explanatory power of these models. The RMSD values suggested that the models would predict leaf length in wallaby grass and wheat plants experiencing water stress mid-way through spring nearer to the true result than the phalaris and annual ryegrass models (Table 6.9). Equations for the models are given in Appendix D, Table D-7.

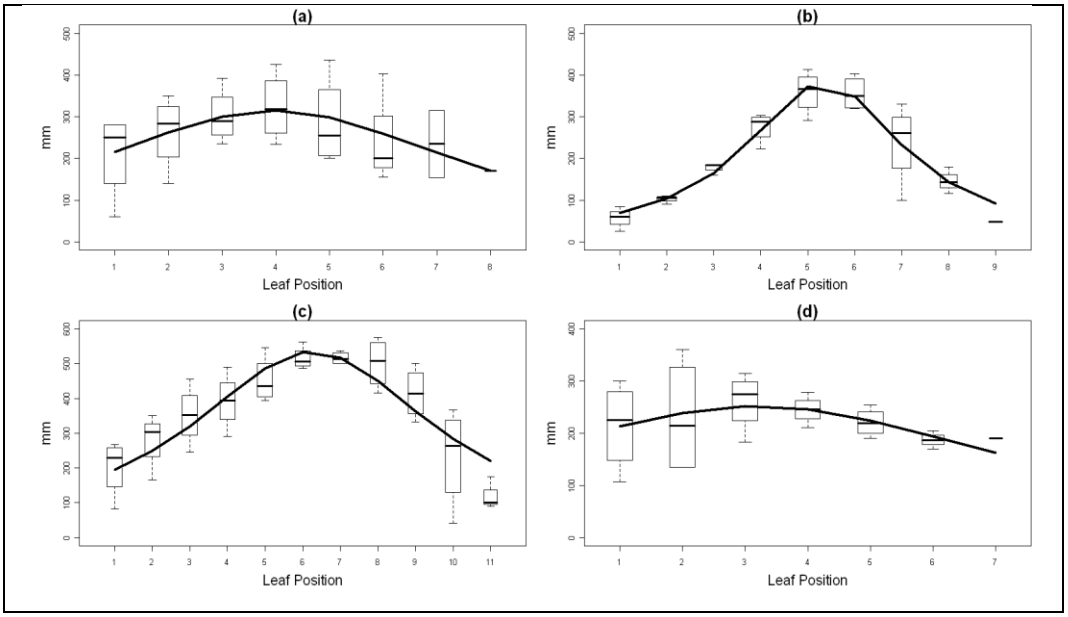

Figure 6.7. Glasshouse observations (box plot) and modelled (line) leaf length (mm) with leaf position for species subjected to water stress in mid-spring: a) annual ryegrass; b) wallaby grass; c) phalaris; d) wheat. The structure of the boxplots is described in the caption of Figure 6.1.

Table 6.9. Chi square statistics and probability, RMSD and Nash-Sutcliffe Model Efficiency Coefficient (E) and $\overline{R}^2$ derived from cross validation techniques between the leaf length models fitted to the leaf length observations on which the models are based for each species when subjected to water stress in mid-spring.

Species	χ^2 statistic	χ^2_{red} statistic	prob	RMSD (mm)	n	E	$\overline{R}^2$ (%)
Annual ryegrass	χ^2 (24)=20.14	χ^2_{red} (24)=0.84	0.69	81.97	26	0.19	15.0
Wallaby grass	χ^2 (30)=3.86	χ^2_{red} (30)=0.13	1.00	41.88	32	0.88	86.8
Phalaris	χ^2 (41)=13.05	χ^2_{red} (41)=0.32	0.99	79.76	43	0.69	67.2
Wheat	χ^2 (22)=20.00	χ^2_{red} (22)=0.91	0.58	56.55	24	0.13	7.4

Non-linear models remained significant in describing the relationship between leaf length and leaf position when plants were subjected to water stress late in spring (Figure 6.8). The models explained much of the variation for wheat

($F_{3,17}$=898.54, P<0.0001), but less for annual ryegrass ($F_{3,26}$=65.86, P<0.0001), wallaby grass ($F_{3,22}$=36.32, P<0.0001), and phalaris ($F_{3,48}$=102.98, P<0.0001) (Table 6.10). Large variation in leaf length at different leaf positions for annual ryegrass, wallaby grass and phalaris was reflected in large RMSD values (Table 6.10). Equations for the models are given in Appendix D, Table D-8.

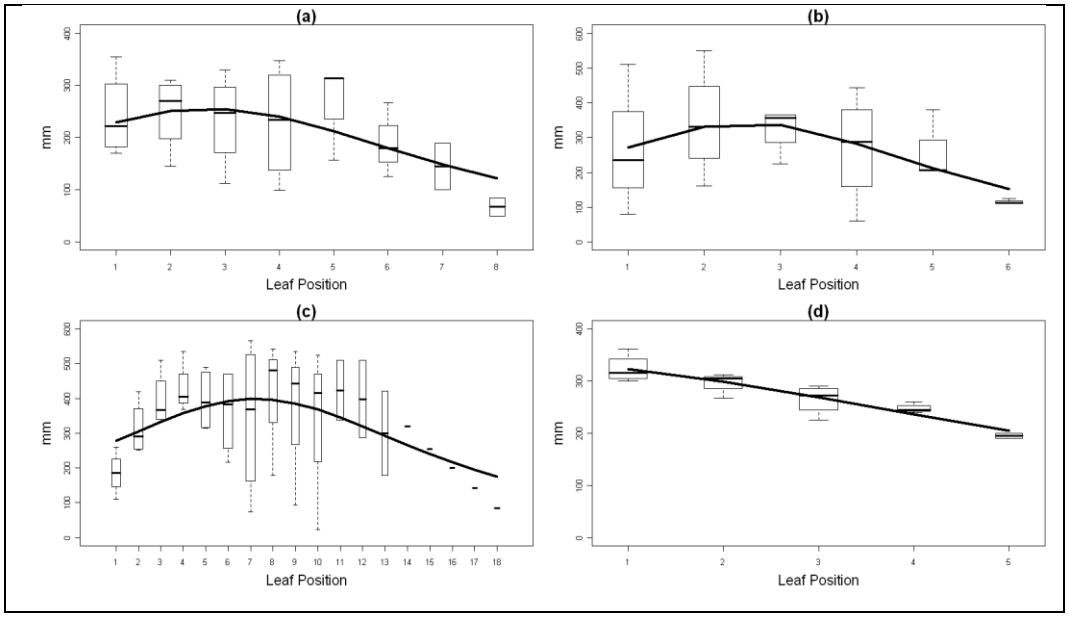

Figure 6.8. Glasshouse observations (box plot) and modelled (line) leaf length (mm) with leaf position for species subjected to water stress in late spring: a) annual ryegrass; b) wallaby grass; c) phalaris; d) wheat. The structure of the boxplots is described in the caption of Figure 6.1.

Table 6.10. Chi square statistics and probability, RMSD and Nash-Sutcliffe Model Efficiency Coefficient (E) and $\overline{R}^2$ derived from cross validation techniques between the leaf length models fitted to the leaf length observations on which the models are based for each species when subjected to water stress in late spring.

Species	χ^2 statistic	χ^2_{red} statistic	prob	RMSD (mm)	n	E	$\overline{R}^2$ (%)
Annual ryegrass	χ^2 (24)=18.20	χ^2_{red} (24)=0.76	0.79	75.14	26	0.27	20.0
Wallaby grass	χ^2 (20)=16.06	χ^2_{red} (22)=0.80	0.71	116.30	22	0.24	15.6
Phalaris	χ^2 (46)=38.22	χ^2_{red} (46)=0.83	0.79	130.79	48	0.17	14.3
Wheat	χ^2 (15)=3.33	χ^2_{red} (15)=0.22	0.99	20.03	17	0.79	77.6

6.4 Discussion

The disparity between previous reports on the response of LSR to water stress may depend on the timing and severity of the stress. The water stresses applied in this experiment resulted in different levels of responses in LSR.

In the field, soil water availability at Struan over all days in the spring and summer of 2008-9 was lower than the long term average (paired t_{211}=-2.435, P<0.0001) (data from GrassGro™ not shown). LSR was similar under these field conditions to that of well-watered conditions (Figure 6.9), supporting previous suggestions that LSR is relatively insensitive to water stress (Cayley *et al.* 1980; Woodward 1998), at least under some field conditions. This may reflect the adaptive response of plants to water stress in the field (Turner and Begg 1978) but also suggests that the field conditions were more similar to the well-watered glasshouse conditions than to the terminal water stress treatments. However, different field conditions may yield different results, and studies involving a wider range of soils and soil moisture availabilities may improve understanding.

LSR increased under terminal water stress conditions when imposed in early, mid or late spring (Figure 6.9), in agreement with some previous work (Fischer and Hagan 1965; Turner 1982; Hsiao *et al.* 1984; Van Herwaarden *et al.* 1998). This increase was seen in all leaves, but particularly the oldest leaves under later water stress. This result could point to three possibilities. Firstly, older leaves had already begun senescing, but still had the potential to accelerate the recycling of cell components. Secondly, slower senescence in younger leaves might have reflected the reduction in sink activity of new leaves and reproductive organs and an inability to utilise retranslocated nutrients in the event of severe water shortage. Finally, both factors may have been evident. Previous work suggesting that

senescence is slower (Ludlow 1975) or faster (Turner *et al.* 1986) in younger leaves relative to older ones, was conducted on only a subset of leaves and not under conditions of terminal water stress.

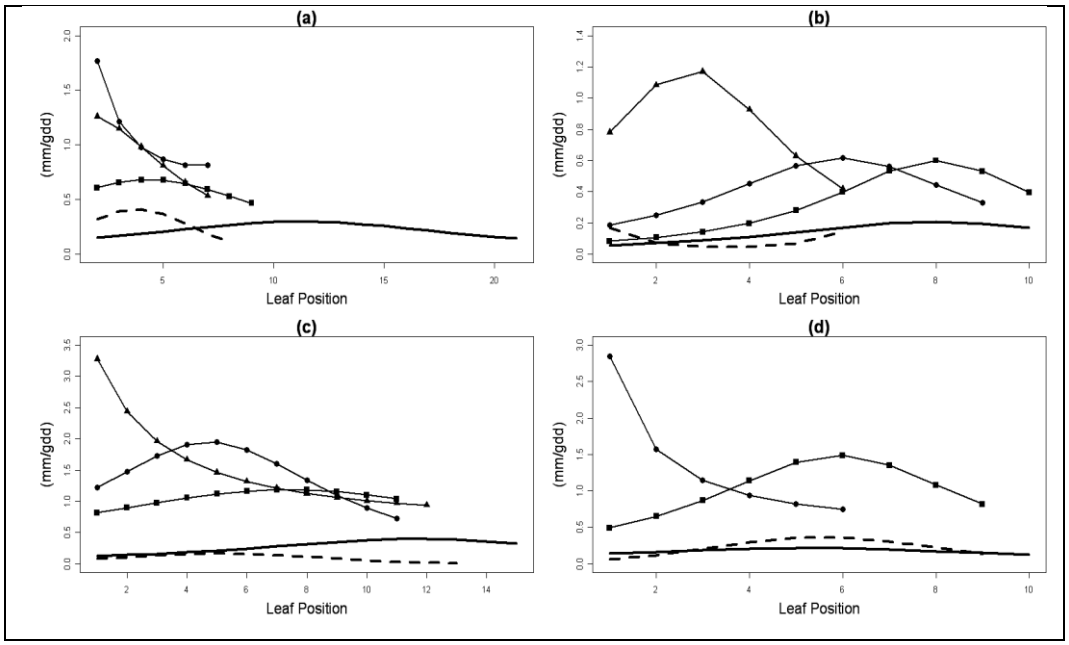

Figure 6.9. Models describing LSR of grasses: a) annual ryegrass; b) native grasses; c) phalaris; d) cereals; where solid line represents well watered growth conditions, lines with square, circle and triangle markers represent water stress conditions imposed in early, mid- and late spring respectively and dashed line represents field growth conditions.

The later that a water stress event occurs in the spring season, the more likely it is to be terminal for the plant and therefore, greater the urgency for recycling of leaf resources. Munne-Bosch *et al*. (2004) presented evidence that leaf senescence may be the result of genetic and/or hormonal changes associated with plant age and/or reproductive development. The increase in LSR with the late onset of water stress in this experiment would ensure that recycling was maximized, providing an opportunity to successfully reproduce and complete the life cycle (Munne-Bosch and Alegre 2004) or initiate summer dormancy (Hoen 1968). Generally, LSR increased with later imposition of the water stress treatment, in agreement with Langer and Ampong (1970). Being adapted to temperate climates, these species may be genetically programmed to respond differently to the timing

of the water stress in terms of LSR, as suggested by Hsiao (1982). The native wallaby grass senesced at about half the rate of the non-native species until the last imposition of water stress, which may demonstrate an adaptation to drier climates, and also reflect the lack of selection pressure on these species for vegetative growth.

The relationship between LSR and leaf position tended to break down when terminal water stress was applied in all species, except for native wallaby grass under early water stress. Wallaby grass maintained a more orderly leaf growth and death pattern for a longer period of time, possibly allowing for relief of drought conditions. Although wallaby grass shares perenniality with phalaris, its evolution in the harsh Australian climate may render it more resilient to water stress than species evolved in other parts of the world.

The relationship between leaf length and leaf position appeared to be consistently non-linear for all species when water stress was encountered early or mid-way through spring, or for non-native species grown in the field through spring and early summer (Figure 6.10). The non-linear model remained appropriate to leaf length under the imposition of water stress in late spring, even though the relationships appeared to be more linear (Figure 6.8). This may have been due to fewer data available in the late spring treatment. Differences between the field and glasshouse models for leaf length may simply represent cultivar differences in the case of annual ryegrass and phalaris, or species differences in the case of cereals and native grasses. Comparison of the models of leaf length revealed similarities in length in glasshouse-grown wallaby grass, regardless of watering regime, and between well-watered wheat plants and those that were stressed early in spring. Reduction in leaf length through reduced LER has been

noted in plants exposed to prolonged water stress (Jones *et al.* 1980a; b; Dale 1982). Too few elongating leaves were available for statistical analysis in this study; however, it is unlikely that the period of water stress was sufficient to elicit an effect on leaf length through a LER response. Variation between the glasshouse models may reflect the natural variation in the cohort of leaves chosen to construct the model. Leaves measured as part of treatments imposed later may have been on daughter tillers, particularly on the annual ryegrass and phalaris plants, which tillered prolifically. It may be inferred then, that leaf length on daughter tillers has a similar non-linear relationship with leaf position, but that the peak leaf length may be longer and occur at a lower position on the tiller, due to fewer leaves being produced relative to main tillers.

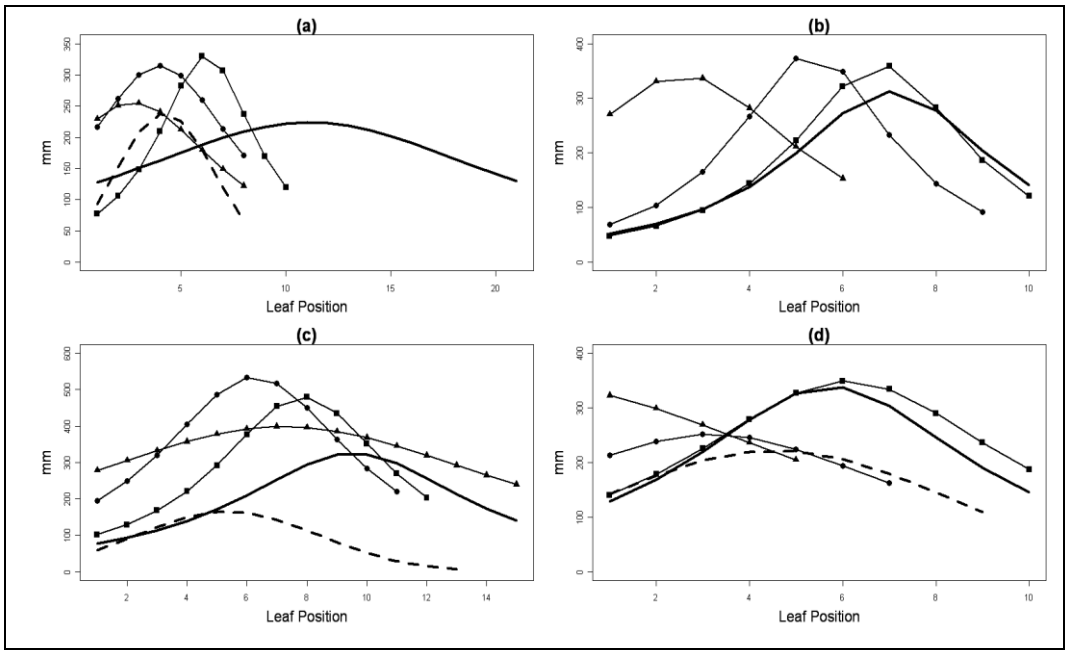

Figure 6.10. Models describing leaf length of grasses: a) annual ryegrass; b) native grasses; c) phalaris; d) cereals; where solid line represents well watered growth conditions, lines with square, circle and triangle markers represent water stress conditions imposed in early, mid and late spring respectively and dashed line represents field growth conditions.

The relationship between both LSR and leaf length with leaf position remained strong for plants grown in the field. This is encouraging, since the non-natives species and cultivars differed between the glasshouse and field work. It

may be that models established in ideal glasshouse conditions are of the right shape to represent LSR and leaf length in the field for cereal and grass pasture species. However, the shapes of these relationships in the native spear grass were different to that of wallaby grass, being reversed for LSR and not evident for leaf length. Genetic diversity between native species may be sufficiently large to not allow these species to be grouped together on the basis of similarities such as photosynthetic pathway and perennial growth habit.

The models described here fit the LSR and leaf length curves in some of these species better than others. Furthermore, the models are of a similar structure to those evident under non-limiting growth (Figure 6.9, Figure 6.10). Senescence may have already been completed in some of the early leaves at the imposition of the water stress treatments, leaving fewer leaves available on which to collect senescence measurements than were recorded for the tillers.

The similarities and differences in models between plants grown in the field and those subjected to water stress treatment in the glasshouse are not surprising, given that the development of water stress between plants grown in pots situated indoors or outdoors, and in the field, will differ in speed of onset and potential for recovery (Turner and Begg 1978; Hsiao 1982). Plants grown in the field may encounter other stressors besides water limitation, and field growth is not always water stressed. In this particular year of growth, although soil moisture availability was lower than average, it increased as a result of around 60 mm rainfall received in mid-December. Water stress may have been relieved by these events, for those species still able to take advantage of it. To mimic conditions possibly experienced by plants in the field it would be necessary to test a vast range of water stress and recovery regimes under controlled glasshouse

conditions. Terminal water stress imposed under glasshouse conditions is just one extreme set of moisture-limiting conditions.

The response of these species to intermittent water stress events, where re-wetting of the soil may reduce or halt leaf senescence remains another area of interest. Changes in soil moisture content may well affect moisture content of plants before senescence processes commence, uncoupling the relationship between visual curing percentage and moisture content relied upon in fire hazard determination. Nevertheless, this work provides insights into the senescence responses under conditions of terminal water stress for key grass species. This may provide a ceiling of response that might be encountered in the field, under extreme water stress conditions.

In summary, LSR increased under conditions of terminal water stress but not necessarily under field conditions, whereas leaf length appeared not to be greatly affected by water stress. It was encouraging that the relationship between leaf position and both LSR and leaf length appeared to be consistent under water stress conditions. This should aid in extrapolation of glasshouse-based models to field situations.

7 A Bayesian approach to modelling curing

7.1 Introduction

Models derived by statistical fitting procedures are variously referred to as statistical or empirical modelling approaches (Weber 1991; Pastor *et al.* 2003; Higgins *et al.* 2008). Models which use the underlying physical or biological mechanisms to describe natural phenomena are referred to as physical, mechanistic or theoretical models (Weber 1991; Pastor *et al.* 2003; Higgins *et al.* 2008). Models which use experimentation and/or statistical procedures to provide parameters for the underlying physical principles lie between these extremes. These are variously known as empirical or semi-empirical models (Weber 1991; Pastor *et al.* 2003; Higgins *et al.* 2008). Any errors in all or some of the functions, parameters or variables underlying models may cause them to not perform adequately, and it may be difficult to use them with confidence outside the range of environments in which they were developed (Weber 1991; Pastor *et al.* 2003; Higgins *et al.* 2008).

The semi-empirical approach has the benefit of providing values for variables that may be unobserved, or are difficult or impractical to measure, which then can be used with confidence in other applications of the model in which the same physical processes exist (Higgins *et al.* 2008). Bayesian data analysis uses probability distributions to quantify unknown or unobserved parameters and specify their uncertainty. It uses the probability distributions from which the observed data are assumed to come, which can be included to make models more biologically sound and can be used to solve complex problems with multiple parameters (Gelman *et al.* 2004). It assumes that all parameters follow probability

distributions while data are fixed, unlike classical methods that assume parameters are constants and data are unknown.

This chapter tests whether a Bayesian modelling approach would allow prediction of curing percentage from the full range of leaf turnover characteristics already collected from the glasshouse studies (Chapter 5). Green leaf accumulation (Figure 7.1), and subsequent cured leaf accumulation (Figure 7.2) over time was conceptualised diagrammatically in conjunction with a statistician, who developed the Bayesian model using data collected in Chapter 5. This chapter assesses whether the Bayesian model is superior to other methods to predict curing in the field.

7.2 Materials and methods

7.2.1 Development of a Bayesian model

Gelman *et al.* (2004) summarised three steps to construct a Bayesian model. First, a full probability model is constructed, which describes the relationship between each of the measured and unknown parameters. This model should reflect both the data collection process and the underlying knowledge of the science.

In the second step, prior distributions of the known parameters are used to calculate posterior distributions for the unknown parameters. Prior distributions represent what was thought to be true of those parameters before the model was run and the posterior distributions represent updated knowledge. Lastly, the model is evaluated to ensure the fit is reasonable and the conclusions sensible. The sensitivity of the results to the chosen model should also be addressed (Gelman *et al.* 2004).

Following the above process a Bayesian framework was developed whereby the percentage of dead material at any given time could be predicted. In order to find this value, the green biomass present at any given time must also be known. Due to the linear nature of grass leaf growth, the linear measures previously collected and reported in Chapter 4 to calculate the Leaf Curing Model were used. Although the term "biomass" usually associated with mass rather than length, it is used here to describe the length of leaf material. Hence biomass in this context has dimensions of length, rather than mass. The increase in green biomass for a single leaf is assumed to be linear with thermal time and is shown in Figure 7.1. Green biomass decreases during leaf senescence until there is none left at the point of leaf death.

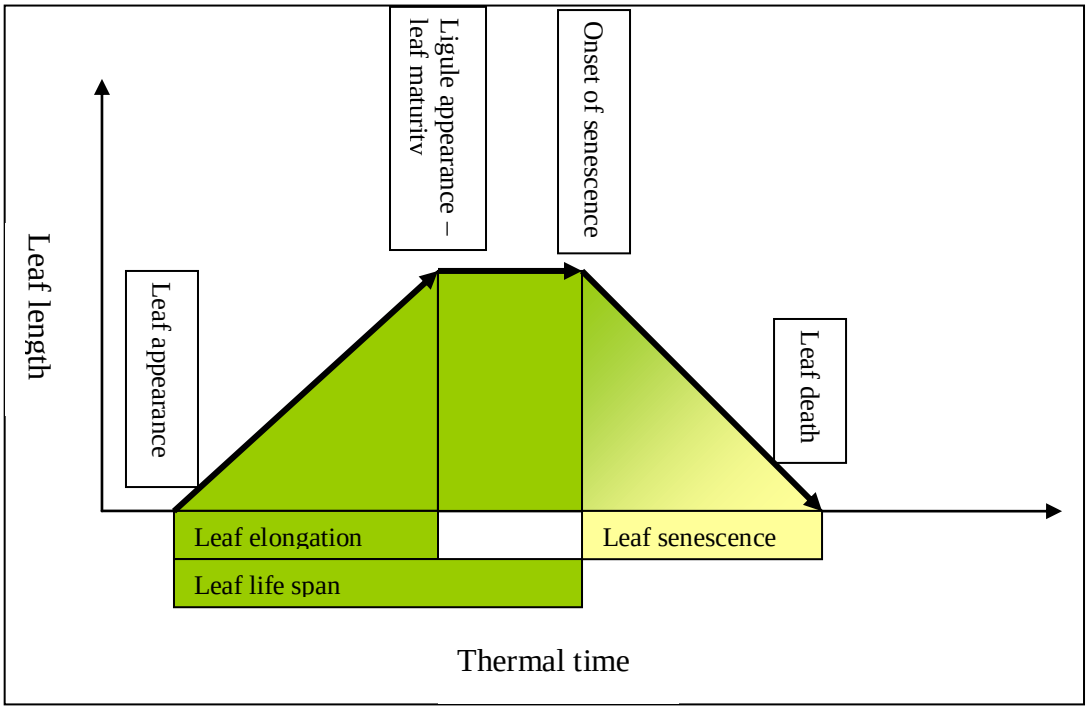

Figure 7.1. Diagrammatic representation of the increase in green biomass in a single leaf over time.

The transition from green to dead biomass occurs during leaf senescence, beginning with no dead biomass, and increasing until all the leaf is dead as shown in Figure 7.2. In effect, this is exactly the complement of biomass accumulation.

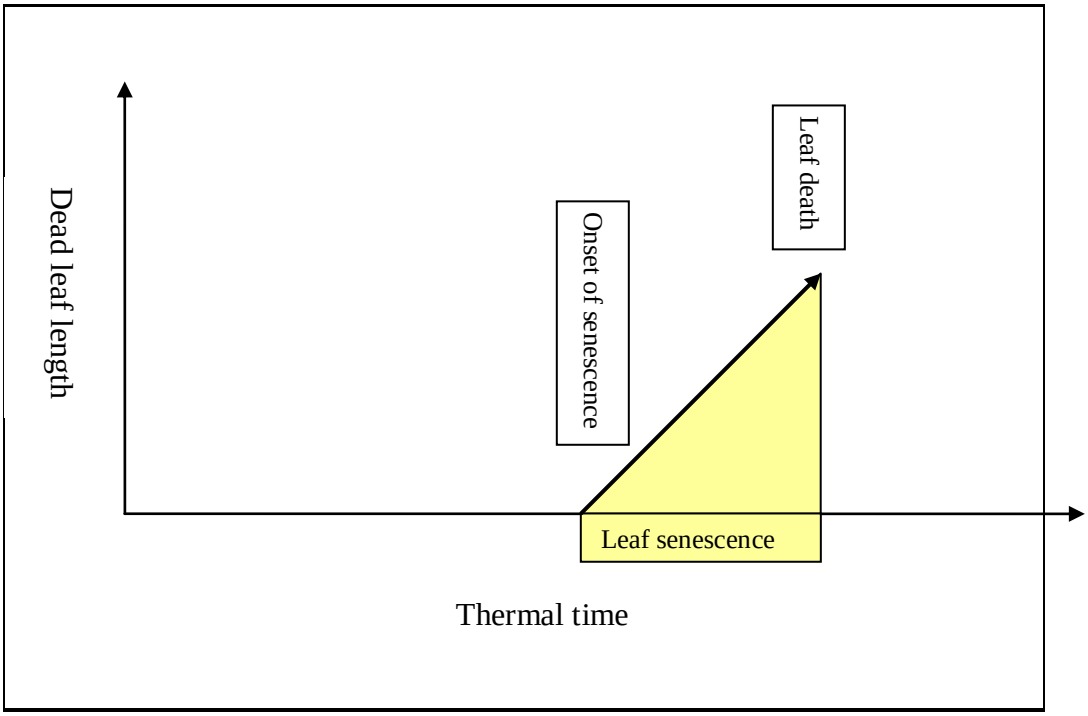

Figure 7.2. Diagrammatic representation of the increase in dead biomass in a single leaf over time.

A Bayesian model was constructed (Appendix G) to allow all the leaves of all plants of each species to be modelled simultaneously. Briefly, the model attempts to find leaf length, *m*, at a given thermal time, *t*. Leaf turnover characteristics were converted to parameters to explicitly represent lengths, times and rates at which events controlling the accumulation of green leaf and its subsequent transition to dead leaf occurred. New models describing each of the leaf turnover parameters (*D*, *E*, *L*, *P* and *X*) were adopted based on an exponential function (Equation 7.1) rather than the original inverse polynomial functions used in Chapter 5. The exponential function achieved a similar model shape as the polynomial, but kept the majority of the parameters positive, and proved to be a more stable function. A negative α value is required in the model for *X*. The symbols used to describe variables in the models are listed in Table 7.1.

$$y(l) = \alpha l \exp(-\beta l) \quad \textbf{(7.1)}$$

where α controls the upward slope of the curve and the peak of the curve is reached when the position of the leaf, $l = 1/\beta$, as per Figure 1 in Appendix G.

Table 7.1. Parameters used in the model.

Symbol	Meaning
D	Thermal time at which a leaf appears (gdd)
E	Elongation rate (m/gdd)
L	Length at which a leaf stops growing (m)
S	Length of dead leaf (m)
P	Thermal time spent at mature leaf length (gdd)
X	Senescence rate (m/gdd)
l	Leaf position from first (lowest) leaf numbered acropetally
m	Leaf length (m)
t	Thermal time (gdd)
n	Final number of leaves on each plant
j	Species
k	ID code for a plant
r	ID code for a pot
B	Green biomass
Y	Percentage dead
a	Thermal time at which a leaf starts to grow
f	Thermal time at which a leaf stops growing
w	Thermal time at which a leaf starts to die
z	Thermal time at which the leaf has zero length

The change in length of green biomass in a single leaf from appearance to death is shown in Figure 7.3. Each of the points labelled in Figure 7.3 represent a green leaf length (*m*), and the thermal time (*t*) taken to reach these points can be explained in terms of the leaf turnover parameters previously mentioned (Equation 7.2).

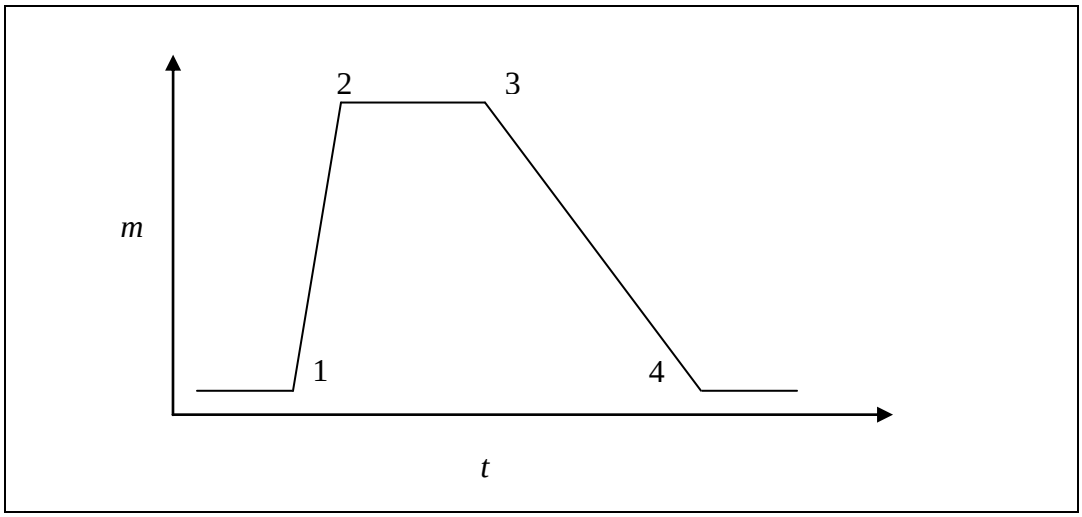

Figure 7.3. Plot of change in green leaf length over time (*t*), where leaf length (*m*) increases from zero at point 1 at elongation rate *E*, reaching final length *L* at point 2. This length is maintained until it begins to senesce at point 3, at the rate of senescence *X*, until it reaches zero again at point 4. At point 1, *t=D;* point 2, *t=(L/E)+D;* point 3, *t=P+D+L/E;* and point 4, *t=-[L-X*(P+D+L/E)]/X.*

(7.2)

$$m_t = \begin{cases} Et & 0 \le t < f \\ L & f \le t < P \\ L - X(t-P) & P \le t < (L+XP)/X \\ 0 & (L+XP)/X \le t \end{cases}$$

Using estimates of the time to appearance (D) of subsequent leaves, a model can be built up of multiple leaves (Equation 7.3).

(7.3)

$$m_{l,t} = \begin{cases} 0 & t < D \\ E(t-D) & D \le t < D+f \\ L & D+f \le t < D+P \\ L - X(t-D-P) & D+P \le (L+X(D+P))/X < t \\ 0 & (L+X(D+P))/X \le t \end{cases}$$

where f= L/E.

In all, five submodels were created, one for each term (L, P, X, D, E) in the overarching model, each of which contained two parameters, α and β. The relationship between the α and β parameters required to establish the individual leaf turnover models, thermal time and leaf length, in order to model the length of leaf present for a given species at a given time is shown in the Directed Acyclic Diagram in Figure 7.4.

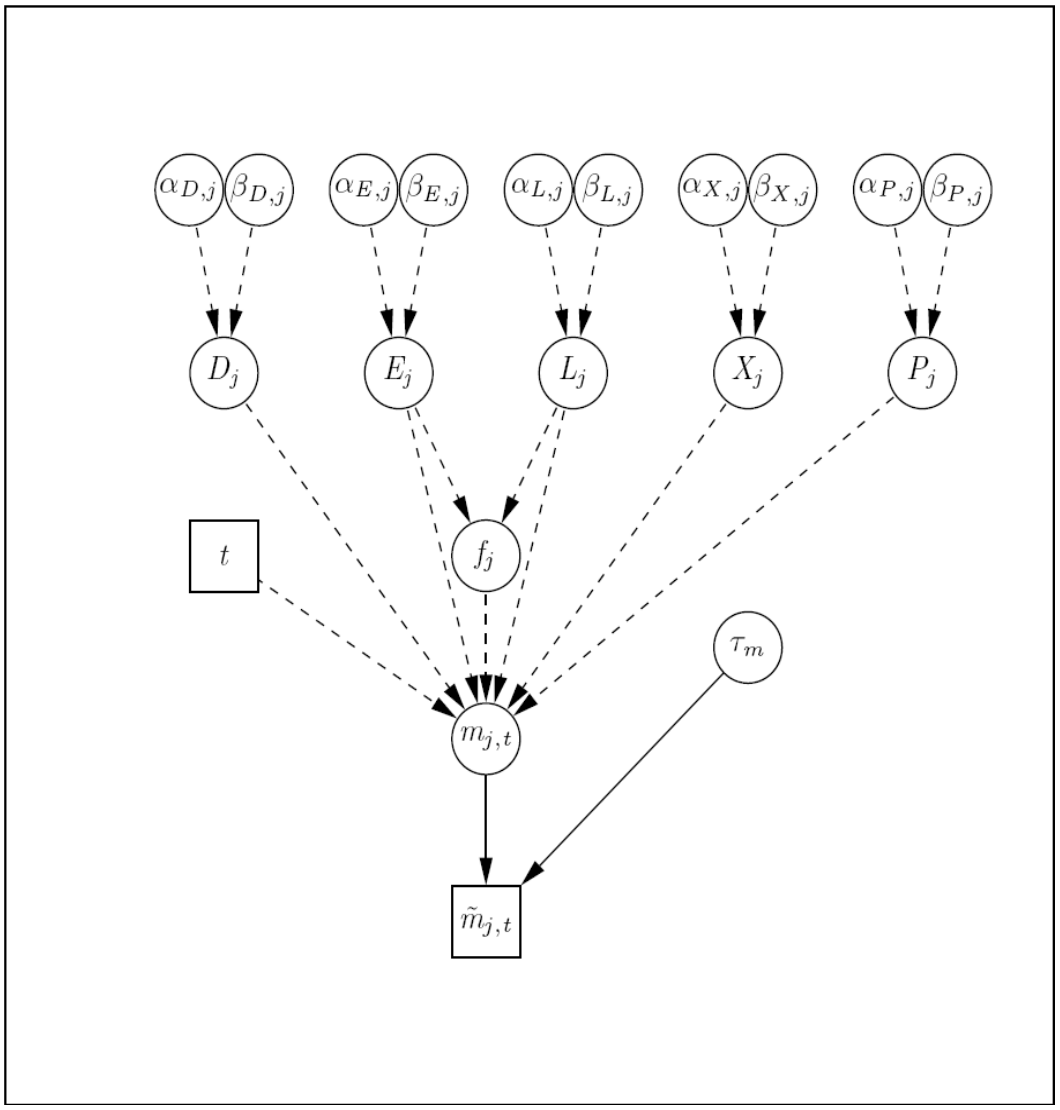

Figure 7.4. Directed acyclic diagram for history for species *j* and time *t*. Stochastic relationships are indicated by solid edges, deterministic relationships by dotted lines, observed data by square symbols, and unobserved parameters by round symbols.

Prior probability distributions were assigned to each of the 10 α and β parameters for each of annual ryegrass, wallaby grass, phalaris and wheat, using a normal distribution characterised by a mean and a reciprocal variance. The prior means are listed in Appendix G. Gamma distributions were assigned to the variances and their parameters selected to give non-informative prior distributions, so that the parameter priors could assume any value without affecting the outcome greatly, and allow the data to drive the model. This meant that the model conclusions were dependent on the data rather than on the priors assumed,

overcoming the possible drawback of selecting priors that produced a desired conclusion. Lastly, the observed length was assumed to have a Gaussian distribution with mean given by $m_{l,t}$ and a reciprocal variance specified by a non-informative prior was used.

The full joint distribution is the product of the likelihood and the prior distributions. Markov Chain Monte Carlo (MCMC) simulation was used to generate posterior means and variances, shown in Appendix G. The fit of the model was visually checked against observed length of green leaf for each leaf included in the model, and presented for each leaf, plant and species (Appendix G). The relationship of the shape of green leaf length with leaf position was analysed using general linear models (PROC GLM in SAS Institute Inc. 2002-3).

The model for each species was then used to obtain a curve for the length of green leaf biomass accumulated over thermal time and leaves (Equation 7.4). The percentage of dead material present is shown by a curve of the accumulation of dead material over thermal time and leaves, divided by green biomass (Equation 7.5).

(7.4)

$$B_j = \sum_{\ell=1}^{\ell=n_j} \int_{t=a_{j,t}}^{t=P_{j,t}} L_{t,\ell}$$

(7.5)

$$Y_j = \frac{1}{B_j} \sum_{\ell=1}^{\ell=n_j} \int_{t=a_{j,\ell}}^{t=P_{j,t}} S_{j,t,\ell}$$

7.2.2 Performance of the Bayesian model

7.2.2.1 Curing observations collected in the glasshouse

The predicted curing values from the Bayesian model were compared with observations of leaf curing measured on the same plants grown in the glasshouse

(Chapter 4). Goodness-of-fit was tested by calculating Chi-square statistics (χ^2 and χ^2_{red}), root mean square deviation (RMSD) and Nash-Sutcliffe Model Efficiency coefficients (E) for each species.

7.2.2.2 Fitting a logistic curve to represent the Bayesian model

The Bayesian model values could not be tested directly against the field observations of curing, because accounting for thermal time accumulation began later in plant growth and development in the field compared to the glasshouse plants which were the basis of the Bayesian model. However, the Bayesian model produced a fitted curve with a similar shape to that of a logistic function. Hence a two-step procedure was applied, in which a logistic curve (Equation 7.6) was fitted to the mean posterior predictions of the Bayesian model using PROC NLIN (SAS Institute Inc. 2002-3). The logistic curve with the *c* parameter was then held fixed (see Appendix E, Table E-2) and re-fitted to the field data, which resulted in the *b* parameter being estimated. This allowed the logistic curve to move sideways without changing shape so as to fit different starting times within the thermal time range of field data.

$$y = 100/\left(1 + e^{(-c(gdd-b))}\right) \quad \textbf{(7.6)}$$

Chi-square statistics (χ^2 and χ^2_{red}), root mean square deviation (RMSD) and Nash-Sutcliffe Model Efficiency coefficients (E) were calculated for each species to test the goodness-of-fit.

7.2.2.3 Field observations of leaf curing and Levy Rod curing assessments

The logistic curve was used as a proxy to validate the Bayesian model (as described in the previous section) against leaf curing observations (based on the proportion of dead leaf material on each tiller; refer Chapter 4, section 4.2.2) and Levy Rod assessments conducted in the field (Chapter 4) using PROC NLMIXED (SAS Institute Inc. 2002-3) to estimate the *b* parameter, allowing the logistic curve to move sideways to fit different starting times within the thermal time range of field data. The goodness-of-fit was tested by calculating the Chi-square statistics (χ^2 and χ^2_{red}), root mean square deviation (RMSD) and Nash-Sutcliffe Model Efficiency coefficients (E) for each species.

7.2.2.4 Visual curing assessments

Visual assessments of curing collected by the Fire Prevention Officer of the Naracoorte Lucindale Council on behalf of the Country Fire Service in the 2009-10 and 2010-11 fire seasons were available. These were a general assessment of curing in the Avenue, Frances, Wrattonbully and Callendale districts, which represented the north-west, north-east, south-east and south-west corners of the overall council district.

The visual curing assessments were not representative of a single species or grass growth type, so logistic curves of annual ryegrass and phalaris were each fitted to the visual curing data, to determine which growth type gave the better fit. Thermal time was accrued from the initial record in each fire season, so the *b* parameter was recalculated, to allow the curve to fit the thermal time measurement period.

Chi-square statistics (χ^2 and χ^2_{red}), root mean square deviation (RMSD) and Nash-Sutcliffe Model Efficiency coefficients (E) for each district were calculated to estimate goodness-of-fit.

7.3 Results

7.3.1 Bayesian model

The mean of the posterior leaf length estimates from the Bayesian model was plotted with observed leaf data collected in the glasshouse, against thermal time for each leaf of each plant of each species (see Appendix G). An example of these plots for each species is shown in Figure 7.5. The plots show posterior predicted curves calculated for the species with observed data from individual plants. These plots showed that the model visually matched the length of each leaf with thermal time, particularly in the first several leaves produced, even though these were species-level, rather than plant level, fits. The model visually matched wheat and phalaris better than it did annual ryegrass and wallaby grass.

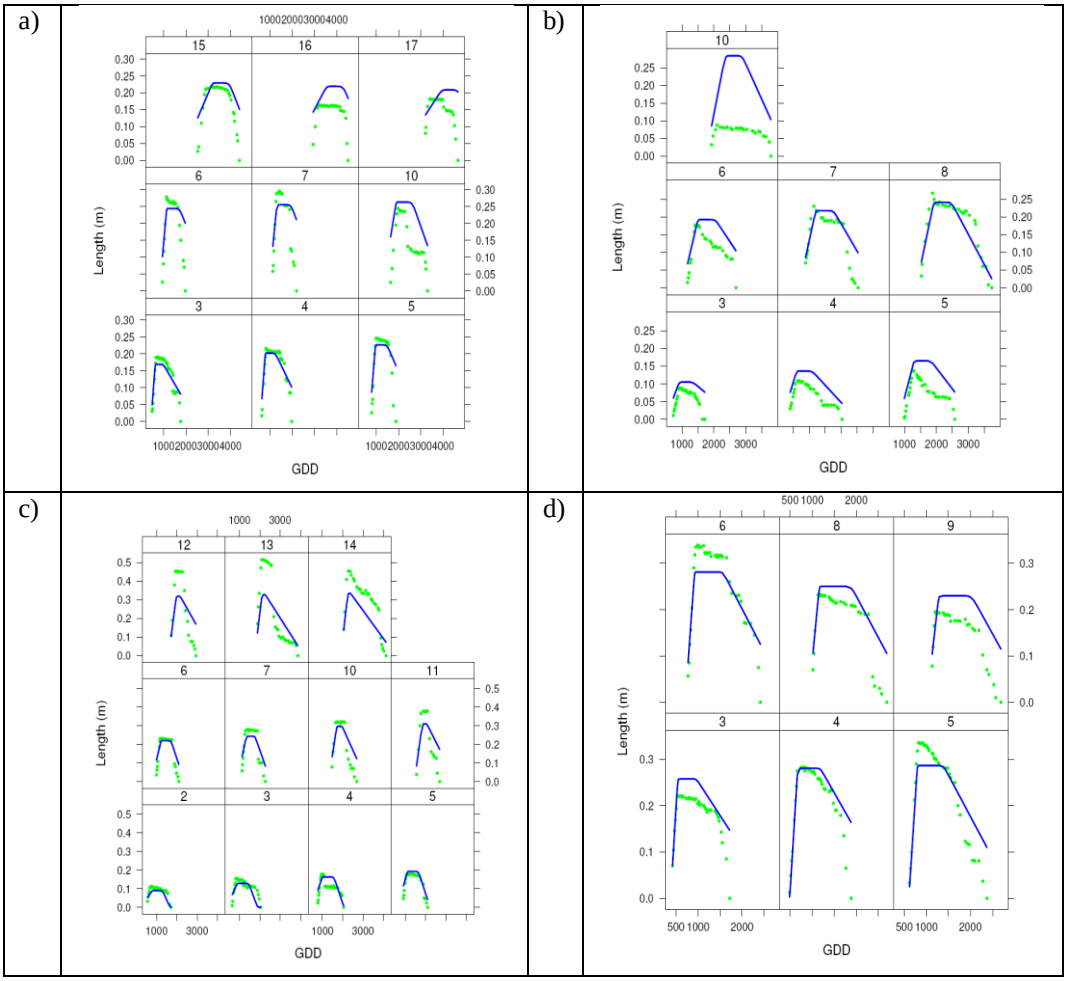

Figure 7.5. Examples of the plots of fitted curves from the Bayesian leaf length model over thermal time fitted to observed lengths of individual leaves (dots) (numbered on horizontal axis above curves) of single plants for each species: a) annual ryegrass; b) wallaby grass; c) phalaris; d) wheat.

The general shape of leaf length accumulation in many cases followed the schematic shown in Figure 7.1 and Figure 7.3. However, the individual plots of leaves in Appendix G, and Figure 7.5 show that some leaves deviated from this form. In fact, there were a variety of observed growth profiles. The variations in leaf growth profiles are categorized by shape (Figure 7.6), in which the profiles are assigned the labels a), b), …, f).

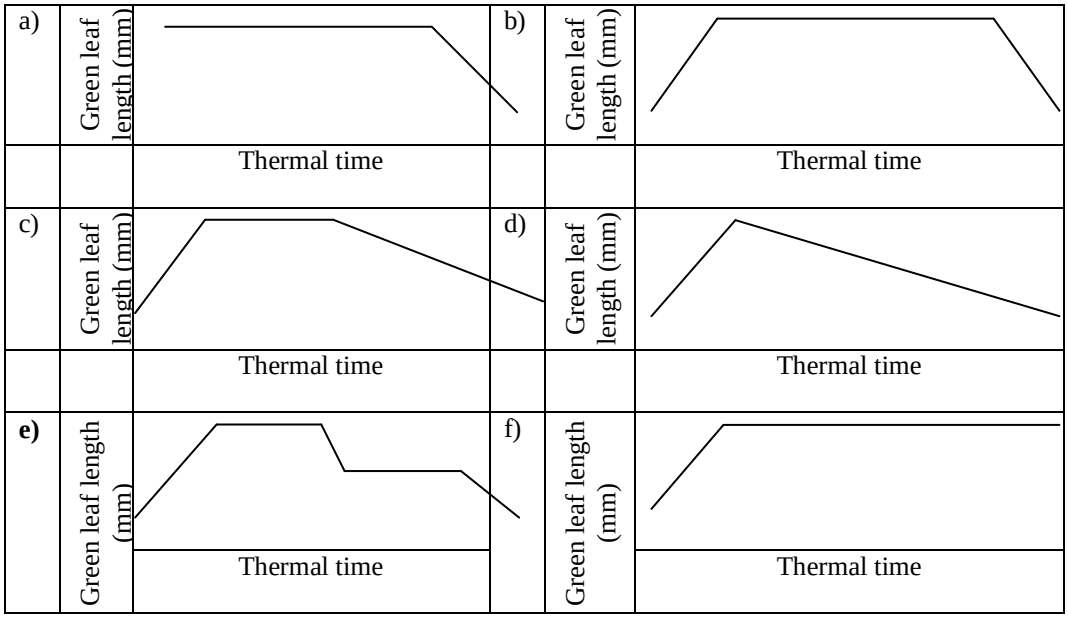

Figure 7.6. Profile of leaf length accumulation observations: a) no incline; b) slope of incline and decline are similar, with an obvious plateau; c) a short plateau before a long decline; d) senescence begins as soon as maximum length is reached, without an obvious plateau, but rather a continual decline; e) two obvious plateaux; f) plateau phase not ended.

Leaf length accumulation profiles that lacked ascents (Figure 7.6.a) all suffered from interval censorship (refer Chapter 2, section 2.10) and were removed from the analysis of frequency of leaf length patterns. Typically, these were first, second or flag leaves. They tended to be short, so that an extended interval between observations could lead to the incline being missed. An incline and decline of similar for a similar period of thermal time (Figure 7.6.b) was the most common profile (36%). 26% of leaves had a shorter period of maturity before the senescent decline (Figure 7.6.c) while 12% of leaves began to senesce almost as soon as the leaf was mature (Figure 7.6.d). 22% appeared to effectively halt the senescence process and had a second plateau of stable green length (Figure 7.6.e). Four percent of leaves which had not entered senescence prior to the cessation of measurements remained in a plateau phase (Figure 7.6.f).

Species ($F_{3,390}$=2.73, P=0.0440) and leaf position ($F_{24,390}$=4.43, P<0.0001) both had significant effects on the frequency of leaf length patterns. There were insufficient data to prove the significant effects of the maximum number of tillers

produced by the plant or an interaction between the species and leaf position at the five percent significance level.

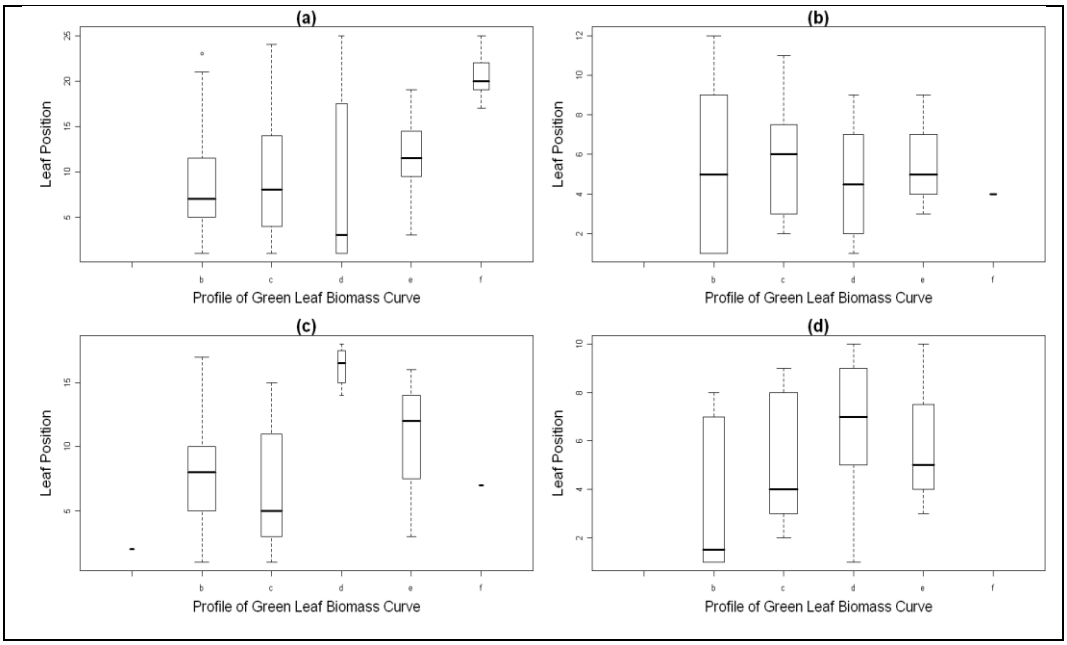

Figure 7.7. Leaf position observed for different leaf length accumulation profiles (corresponding to the caption in Figure 7.6): a) annual ryegrass; b) wallaby grass; c) phalaris; d) wheat. Upper, internal and lower bounds of each box correspond to 75th, 50th and 25th percentiles respectively. Upper and lower whiskers extend the upper and lower quartiles by 1.5 times the interquartile distance, to identify outliers beyond whiskers, which are indicated by open circles. Width of boxes is proportional to the square-roots of the number of observations in the groups.

Leaf position was plotted for each profile within each species (Figure 7.7). The most common profile (Figure 7.6.b) (labelled "b" on the x axes of Figure 7.7) occurred in all wheat and wallaby grass leaves, but only in lower leaves of phalaris and annual ryegrass. The long slow decline (Figure 7.6.d) (labelled "d" on the x axes of Figure 7.7) was found in leaves of lower positions of wallaby grass, and upper positions for phalaris and wheat, but was common for all leaf positions of annual ryegrass. The short plateau (Figure 7.6.c) (labelled "c" on the x axes of Figure 7.7) occurred in the mid-range of leaves for wheat and wallaby grass, and the lower to mid-range of phalaris and annual ryegrass. The double-plateau (Figure 7.6.e) (labelled "e" on the x axes of Figure 7.7) occurred at the

mid- to upper range of leaves in wheat, wallaby grass and phalaris, and mid-way through leaf production in annual ryegrass.

Accumulated green leaf length was derived from the mean of posterior distributions from the Bayesian model for each species and was plotted against thermal time. Green leaf length differed both in the rate and total amount of accumulation (Figure 7.8).

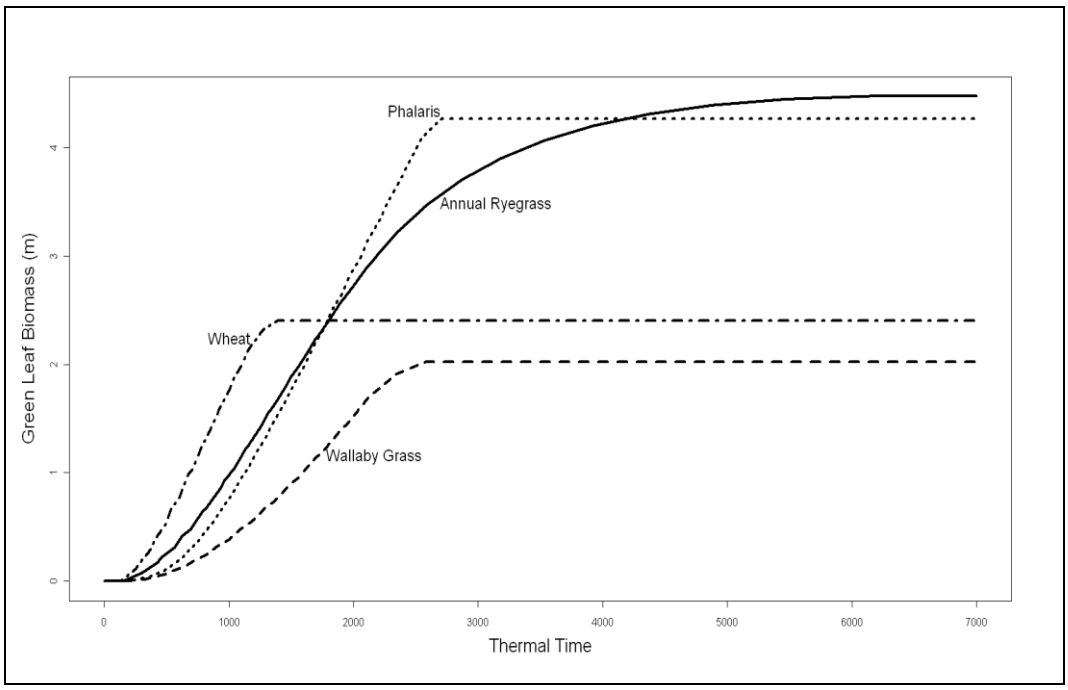

Figure 7.8. Green leaf length (calculated from posterior means) accumulated over thermal time for each species.

The graph of percentage dead matter derived from the mean of posterior distributions from the Bayesian model for each species is shown in Figure 7.9. The pattern of curing in wheat and wallaby grass was similar and had a faster rate than the other species, although wheat commenced about 1000 thermal time units before wallaby grass. In contrast, phalaris and annual ryegrass took considerably longer to cure completely, even though senescence began at a similar thermal time to that of wheat and wallaby grass.

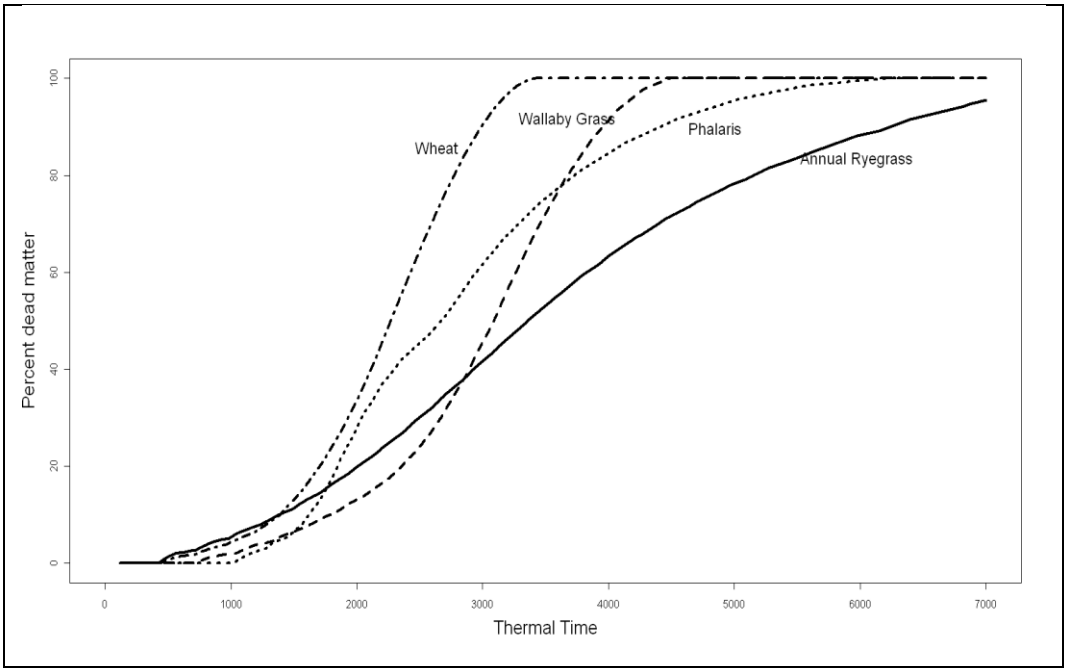

Figure 7.9. Percentage dead matter (calculated from posterior means) accumulated over thermal time for each species.

7.3.2 Validation of the Bayesian model

7.3.2.1 Leaf curing assessed in the glasshouse

The curing rates predicted by the Bayesian model were plotted against observations of leaf curing (from Chapter 4) for the four species in Figure 7.10. The Nash-Sutcliffe Model Efficiency coefficients suggested that the Bayesian curing models represented the observed data well in all species (Table 7.2). The model predictions for phalaris and wheat were within 10% of the leaf curing observations, while those for wallaby grass and annual ryegrass were slightly worse. χ^2_{red} estimates suggested that the model for phalaris best matched the observations, while the models for both wheat and wallaby grass may have been over fitted and the model for annual ryegrass did not fully represent the data. This is also reflected in the probability generated by the χ^2 calculation. The difference between the Bayesian curing model and the leaf curing observations was not

significant in wallaby grass and wheat, while it was significant in annual ryegrass and approached significance in phalaris (Table 7.2). Two plants which were omitted from the Bayesian model for annual ryegrass were represented in the observations of leaf curing. These were amongst four plants which cured completely before the cessation of the experiment. The remainder did not reach 100% curing, and hence had the effect of slowing and extending the Bayesian curve relative to the leaf curing observations.

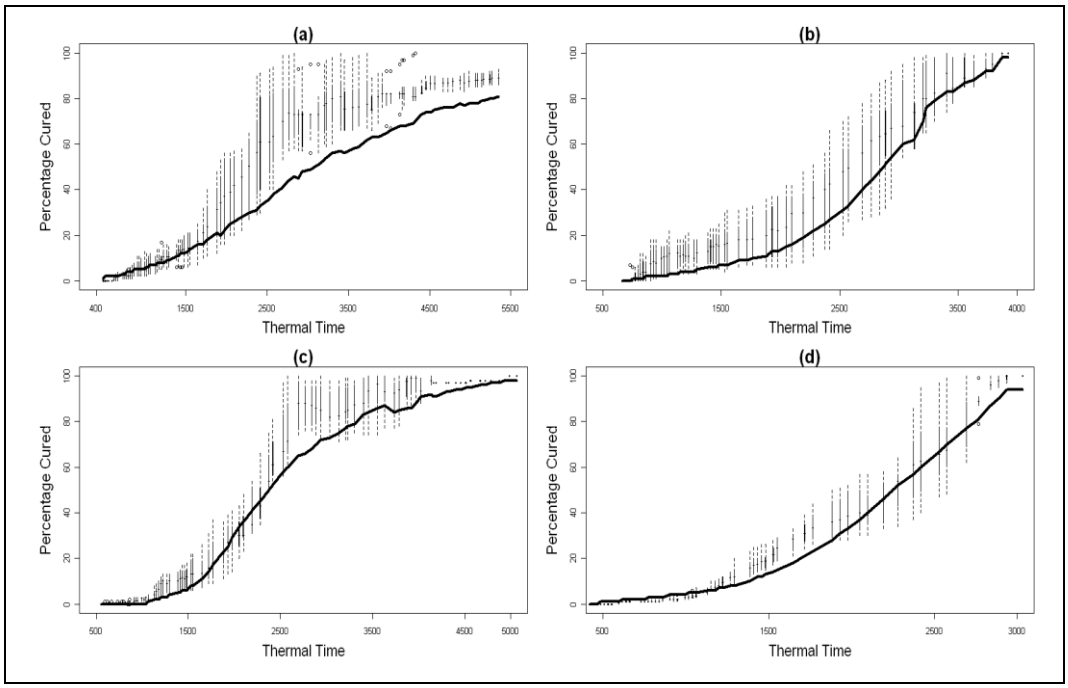

Figure 7.10. Observed leaf curing (boxplot) and modelled (line) percentage dead matter predicted by Bayesian model with thermal time (gdd (T_{base}=0°C)): a) annual ryegrass; b) wallaby grass; c) phalaris; d) wheat. The upper and lower bounds of the solid lines correspond to 75th and 25th percentiles respectively. Dotted lines forming upper and lower whiskers extend the upper and lower quartiles by 1.5 times the interquartile distance, to identify outliers beyond the whiskers, which are indicated by open circles.

Table 7.2. Chi square statistics, RMSD and Nash-Sutcliffe Model Efficiency Coefficient (E) for each species from curing values from Bayesian model fitted to leaf curing observations of glasshouse-grown plants.

Species	χ^2 statistic	χ^2_{red} statistic	prob	RMSD (%)	n	E
Annual ryegrass	χ^2 (616)=3760.14	χ^2_{red} (616)=6.14	0	16.14	618	0.79
Wallaby grass	χ^2 (456)=305.95	χ^2_{red} (456)=0.68	1	13.07	458	0.82
Phalaris	χ^2 (500)=580.75	χ^2_{red} (500)=1.17	0.00506	9.57	502	0.93
Wheat	χ^2 (452)=47.54	χ^2_{red} (452)=0.11	1	7.35	454	0.93

7.3.2.2 Fit of the logistic curve to Bayesian curing values

A logistic curve was fitted to the curing values from the Bayesian model (Figure 7.11) against thermal time to allow the shape of the Bayesian model outputs to be tested against field data. This was justified by the extremely high agreement between the logistic curves and the Bayesian curing outputs in terms of Nash-Sutcliffe Model Efficiency coefficients (Table 7.3). The logistic curve values were within 5% of the Bayesian curing values in all species. Parameters for the logistic curves are given in Appendix E, Table E-1.

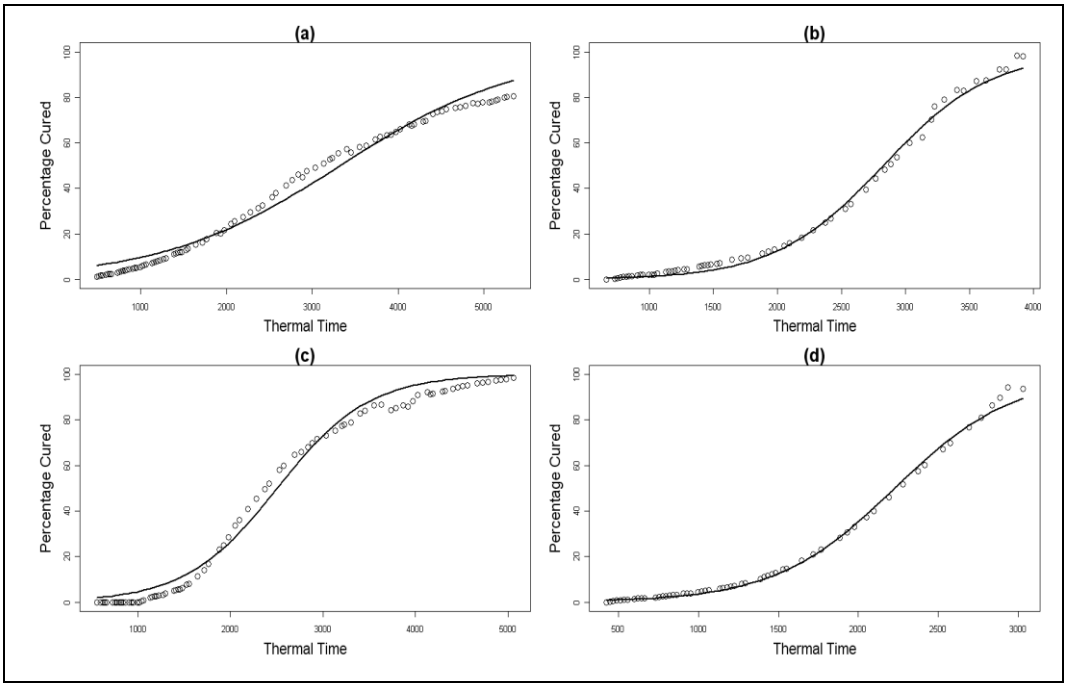

Figure 7.11. Logistic model (line) fitted against posterior predicted curing values from the Bayesian model (circles) over thermal time (gdd (T_{base}=0°C)): a) annual ryegrass; b) wallaby grass; c) phalaris; d) wheat.

Table 7.3. Chi square statistics, RMSD and Nash-Sutcliffe Model Efficiency Coefficient (E) for each species from curing values from logistic curve based on the Bayesian model fitted to curing values from the Bayesian model.

Species	χ^2 statistic	χ^2_{red} statistic	prob	RMSD (%)	n	E
Annual ryegrass	χ^2 (90)=1.81	χ^2_{red} (90)=0.020	1.00	4.02	92	0.981
Wallaby grass	χ^2 (59)=0.29	χ^2_{red} (59)=0.005	1.00	2.21	61	0.995
Phalaris	χ^2 (81)=0.94	χ^2_{red} (81)=0.012	1.00	4.24	83	0.989
Wheat	χ^2 (57)=0.18	χ^2_{red} (57)=0.003	1.00	1.57	59	0.997

7.3.2.3 Field observations of leaf curing

The Bayesian-derived logistic curve was fitted to the leaf curing observations measured (refer Chapter 4, section 4.2.2) on plants in the field (Figure 7.12) for each species, by keeping the slope parameter fixed and allowing the curve to slide horizontally with thermal time. Estimates for the *b* parameter are given in Appendix E, Table E-2. The logistic curves for wallaby grass, phalaris and wheat fitted the field-measured leaf curing observations with similar accuracy to each other, and were slightly better than that of annual ryegrass (Table 7.4). RMSD values suggested that the curves for the former species predicted curing within 20% of the observed values, while curing values of the annual ryegrass curve varied from the observed values by up to 26%.

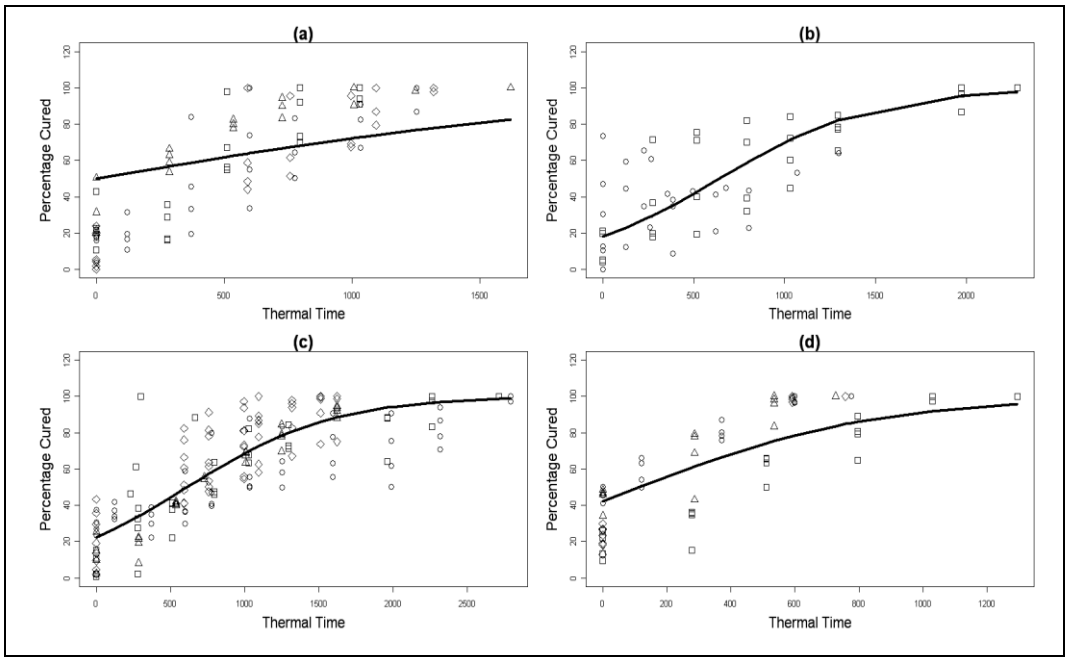

Figure 7.12. Logistic curve based on the Bayesian model fitted against field leaf curing observations with thermal time (gdd (T_{base}=0°C)): a) annual ryegrass; b) wallaby grass; c) phalaris; d) wheat. Levy Rod curing percentage (points): ○) northern site 1; △) northern site 2; □) southern site (2008); ◇) southern site (2010).

Table 7.4. Chi square statistics, RMSD and Nash-Sutcliffe Model Efficiency Coefficient (E) for each species from curing values from logistic curve based on the Bayesian model fitted to leaf curing observations in field grown plants.

Species	χ^2 statistic	χ^2_{red} statistic	prob	RMSD (%)	n	E
Annual ryegrass	χ^2 (88)=55.08	χ^2_{red} (88)=0.63	0.99	26.17	90	0.38
Wallaby grass	χ^2 (53)=25.70	χ^2_{red} (53)=0.49	0.99	19.52	55	0.52
Phalaris	χ^2 (155)=48.78	χ^2_{red} (155)=0.31	1.00	15.53	157	0.69
Wheat	χ^2 (72)=24.05	χ^2_{red} (72)=0.33	1.00	17.62	74	0.67

7.3.2.4 Levy Rod curing assessments

The Bayesian-derived logistic curves were not significantly different from the curing values (Table 7.5) from Levy Rod assessments conducted at field sites for the non-native species (Figure 7.13). The logistic curve representing the wheat Bayesian model fitted the data best, giving the lowest variation in predicted curing values compared to the observed. The logistic curve for wallaby grass, however, did not fit the Levy Rod assessments well and gave the greatest variation in curing values compared to the observed data. Parameters for the logistic models were the same as those outlined in Appendix E, Table E-2.

Table 7.5. Chi square statistics, RMSD and Nash-Sutcliffe Model Efficiency Coefficient (E) for each species from curing values from logistic curve based on the Bayesian model fitted to Levy Rod curing assessments.

Species	χ^2 statistic	χ^2_{red} statistic	prob	RMSD (%)	n	E
Annual ryegrass	χ^2 (29)=19.27	χ^2_{red} (29)=0.66	0.91	16.83	31	0.36
Wallaby grass	χ^2 (17)=47.31	χ^2_{red} (17)=2.78	0.0001	23.25	19	-1.63
Phalaris	χ^2 (28)=20.73	χ^2_{red} (28)=0.74	0.84	20.34	30	0.29
Wheat	χ^2 (26)=10.56	χ^2_{red} (26)=0.41	0.99	11.44	28	0.61

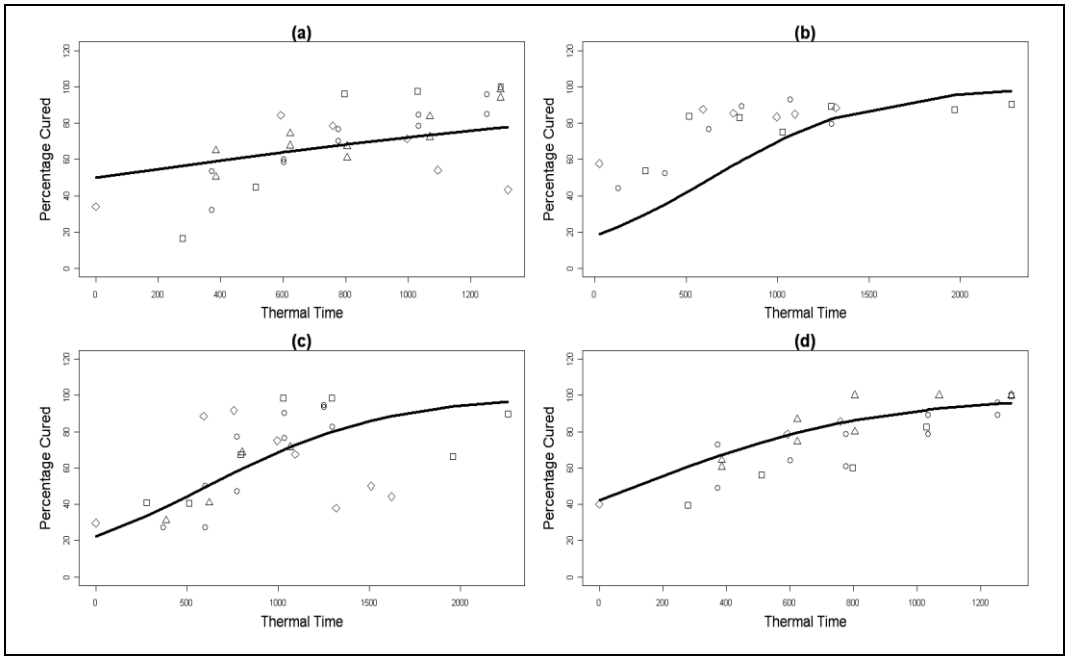

Figure 7.13. Logistic curve based on the Bayesian model plotted against Levy Rod curing observations with thermal time (gdd (T_{base}=0°C)): a) annual ryegrass; b) wallaby grass; c) phalaris; d) wheat. Levy Rod curing percentage (points): ○) northern site 1; △) northern site 2; □) southern site (2008); ◇) southern site (2010).

7.3.2.5 Visual curing assessments

The Bayesian-derived logistic curve from phalaris provided a better fit to the visual curing assessments (Figure 7.14) than did annual ryegrass (data not shown), which was not considered further. The logistic curve based on phalaris Bayesian curing values had high Nash-Sutcliffe Model Efficiency coefficients which suggested that the predictions from the curve were well matched to the visual data (Table 7.6). RMSD values indicated that the Bayesian curing predictions for phalaris were within 10% of visual curing values. The parameters used to fit the logistic curves to the visual curing data are given in Appendix E, Table E-3.

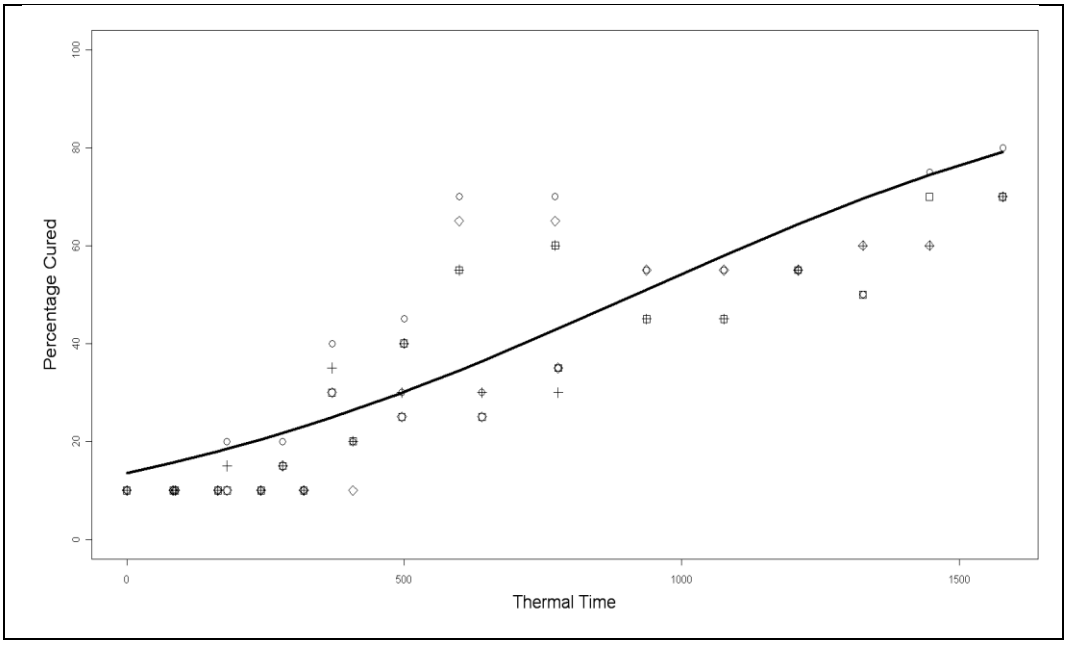

Figure 7.14. Logistic curve based on the Bayesian model for phalaris (line) fitted against visual curing observations from four sub-districts of the Naracoorte Lucindale Council over thermal time (gdd (T_{base}=0°C) in the 2009-2010 and 2010-2011 fire seasons: ○) Frances; +) Avenue; □) Callendale; ◇) Wrattonbully.

Table 7.6. Chi square statistics, RMSD and Nash-Sutcliffe Model Efficiency Coefficient (E) for phalaris curing values from the logistic curve based on the Bayesian model fitted visual curing assessments from four sites within the Naracoorte Lucindale District Council in the 2009-2010 and 2010-2011 fire seasons.

Site	χ^2 statistic	χ^2_{red} statistic	prob	RMSD (%)	n	E
Avenue	χ^2 (21)=5.48	χ^2_{red} (21)=0.26	0.99	10.08	23	0.75
Callendale	χ^2 (21)=5.42	χ^2_{red} (21)=0.26	0.99	10.28	23	0.75
Frances	χ^2 (21)=6.11	χ^2_{red} (21)=0.29	0.99	12.39	23	0.72
Wrattonbully	χ^2 (21)=5.85	χ^2_{red} (21)=0.28	0.99	11.58	23	0.73

7.4 Discussion

The Bayesian model clearly demonstrated that the curing percentage could be predicted from thermal time, both under controlled environment glasshouse conditions and in the field, in four grasses with differing growth habits. The Bayesian model was superior to the other standalone model developed in Chapter 4.

7.4.1 Bayesian model development

7.4.1.1 Accumulation of green leaf length

The Bayesian model predicted the relative rates of accumulation and ceiling limits of production of length leaf in four species with different growth habits, on the basis of thermal time since sowing (Figure 7.8). Wheat accumulated leaf length most quickly, while the perennial native wallaby grass was the slowest. Interestingly, there was no visible difference between the rates of accumulation in the two pasture species, annual ryegrass and phalaris, regardless of growth habit, at least until some 2000 thermal time units after sowing. Leaves at high leaf insertion positions became progressively shorter in annual ryegrass and longer in phalaris respectively (refer Figure 5.2). The gradual slowing of the rate of accumulation may have been caused by the short upper leaves in annual ryegrass, but the continued production of leaves in annual ryegrass allowed the accumulation to extend well beyond the other species, in the glasshouse environment at least.

7.4.1.2 Representation of curing with thermal time

The Bayesian model differed between species in relation to the pattern of curing with thermal time (Figure 7.9) and while the shape was similar between wheat and wallaby grass, it differed in timing. Although biomass production, growth habit and selection pressure are very different in wheat and wallaby grass, they each produced a statistically similar number of leaves (Table 5.7) of similar length (Figure 5.2). However, the Bayesian models fitted the leaf curing observations of these species grown in the glasshouse (Figure 7.10).

The Bayesian models for both phalaris and annual ryegrass were similar to each other in shape, particularly after 60% curing had been reached (Figure 7.9), but also differed in rate and timing before that point. Phalaris and annual ryegrass produced statistically different mean numbers of leaves to each other (Table 5.7), and the maximum leaf length produced by the model for annual ryegrass was 100 mm less than that of phalaris (Figure 5.2).

Both leaf number and leaf length appeared to drive the rate of curing in the Bayesian model. In wheat and wallaby grass, with leaves of similar number and length, curing occurred at similar rates, albeit that the exponential part of curing was delayed in wallaby grass, presumably due to the slower accumulation of leaves in the first place. In phalaris, increased leaf production, relative to wheat and wallaby grass, led to a slower curing rate. Annual ryegrass had greater leaf production again, causing curing to begin earlier than in phalaris. Initially, due to shorter leaf lengths, curing rate in annual ryegrass was slower, before it increased to a rate similar to that of phalaris.

7.4.2 Performance of the Bayesian model against leaf curing observed in the glasshouse

The semi-empirical approach of the Bayesian model is informed by, and responsive to, all the component processes of leaf growth, leading up to, and including leaf senescence (Chapter 5), in order to predict curing percentage. The prior means supplied information to the leaf parameters in the model, but each parameter was updated by data and informed the values of subsequent parameters and their posterior means. This has been used to calculate curing percentage over thermal time. The leaf curing measurements described in Chapter 4 provided a simple method of obtaining an assessment of curing over time. It was conducted

on the same set of plants from which the Bayesian model was calculated. The leaf curing observations were used to validate the performance of the Bayesian model.

The Bayesian model had high accuracy in predicting leaf curing in plants grown in the glasshouse (Table 7.2). This may be partly due to both the Bayesian model and the leaf curing measurements having been taken from the same plants grown under the same conditions. However, its success also indicates that the component algorithms in the Bayesian model do, in fact, contribute to an end-point of valid curing assessment in each of the four grass species.

The agreement between curing values from the Bayesian model and leaf curing observations was within 10% for phalaris and wheat, and slightly higher for wallaby grass and annual ryegrass (Table 7.2). These are either lower than, or comparable to, the variation recorded in field assessment methods (Anderson *et al.* 2011).

The Bayesian model performed worst against the leaf curing observations for annual ryegrass. Phalaris and annual ryegrass both had extended growth under glasshouse conditions which might be considered atypical particularly for the annual species. Half the annual ryegrass plants had not completely died and therefore had not reached 100% leaf curing by the end of the measurement period. Two plants and a number of upper leaves of annual ryegrass were removed from the dataset for the Bayesian model, and this may be responsible for the discrepancy between curing from the two sources. Inclusion of alternative leaf profiles (Figure 7.6) in future iterations of the Bayesian model may also improve the fit against leaf curing observations.

7.4.3 Performance of the logistic curve against field curing observations

The logistic curve was an appropriate choice for describing the posterior predictions of the Bayesian model, as it captured the Bayesian model output almost perfectly (Figure 7.11 and Table 7.3).

The logistic curves provided curing estimates within 20% of the leaf curing observations in the field for all species except annual ryegrass (Table 7.4). This is slightly higher than reported between destructive and Levy Rod curing values in the field (Anderson *et al.* 2011), but in part this reflects the level of variation in leaf curing observed in the field.

Cultivar and species differences existed between the Bayesian models and the field sites, although the non-native field sites were either monocultures, or at least dominated by the species of interest. This may have assisted the fit of the Bayesian-derived curves to Levy Rod assessments at those field sites, being best for wheat, with low variation in curing between the two methods (Table 7.5). The lack of fit between the wallaby grass logistic curve and Levy Rod assessments in native pastures may have been due to greater species diversity, and to the lower reliability of the Levy Rod method in native grasslands (Anderson *et al.* 2011).

Although visual assessment of curing has its problems (Cheney *et al.* 1998; Anderson *et al.* 2011; Newnham *et al.* 2011), it is still widely used by fire agencies (Watts 2008). The logistic curve for phalaris matched the visually assessed curing records of the Naracoorte Lucindale Council in two fire seasons (Table 7.6). The variation in curing between the two sources was well within the range reported between visual and destructive methods in the field (Anderson *et al.* 2011).

The Bayesian-derived logistic curves appeared to be superior to the Leaf Curing Model (Chapter 4) in estimating curing and were the only method that provided equivalent curing assessments to the field-developed Levy Rod technique in the introduced grass species tested (Table 7.7). While similar results between curing estimates from Levy Rod assessment and DST simulation were reported in Chapter 3, the statistical tests used there were not able to establish significant differences, rather than definitively proving similarity between the methods.

Table 7.7. Agreement between curing predictions of stand-alone Models and various curing assessment methods in different species.

	Annual ryegrass	**Wallaby grass**	**Phalaris**	**Wheat**
Leaf Curing Model and Levy Rod	Yes	No	Yes	No
Leaf Curing Model and DST	Yes	Yes	Variable	No
Bayesian-derived logistic curve and leaf curing observations	Yes	Yes	Yes	Yes
Bayesian-derived logistic curve and Levy Rod	Yes	No	Yes	Yes
Bayesian-derived logistic curve and visual curing assessment	Poorer than phalaris	Not tested	Yes	Not tested

7.4.4 Application of the Bayesian model in the field

The logistic curve based on the Bayesian curing values was successfully applied in retrospect to three sets of field curing data (leaf curing, Levy Rod and visual assessment) with slightly different thermal time ranges. This suggested that the logistic curve could be applied to other field situations, with an adjustment made to the thermal time parameter of the equation. In order to fit the Bayesian model, however, rather than the logistic curve as a proxy, the appropriate time at which to implement the Bayesian model would need to be determined.

The Bayesian model was derived from data in which thermal time accumulation began at seeding of the plants. This could be approximated by beginning accumulation at around the start of the growing season; either from the

first germination events or opening rains signifying the break in the season in Mediterranean environments. However, this may not be appropriate in areas where rainfall distribution was not winter dominant. However, the application of the Bayesian-derived logistic curve to field data which was not calculated on the same thermal time scale, suggested that the Bayesian model may be able to accommodate variation in the beginning of thermal time accumulation.

Once implemented, the Bayesian model will predict curing over a thermal time series. To convert this to calendar time, the likely accumulation of thermal time over the course of the winter, spring and summer seasons can also be determined by means of probabilities generated by tools such as GrassGro™. If it is known, for instance, that 70% curing is reached at around 3500 gdd in a native pasture, then GrassGro™ could be used to calculate the probability of accumulating that thermal time at various calendar dates in different regions.

The 50-70% curing range provides suitable curing conditions to conduct prescribed burns. The logistic curves generally underestimated this portion of the curve, compared to the Levy Rod assessments conducted in the field, except in wheat. The size of the RMSD between the Bayesian-derived logistic curves is also too high to allow fire agencies to confidently predict the ideal curing conditions to conduct burns safely. Underestimation of curing may result in suitable conditions for safe prescribed burns being overlooked.

7.4.5 Potential improvements in the Bayesian model

The Bayesian model appears to be an improvement on the Leaf Curing Model, but there are aspects which could be further refined. The Bayesian model defined curing under ideal glasshouse conditions, and may guide the assessment of curing in seasons with extended growth conditions. The logistic curve was a static

representation of the Bayesian model, suited to plants which exhibited extended growth but unable to display a resumption of growth after a period of curing. The ability of the Bayesian model to capture earlier leaf processes should allow it to respond to the greening-up events, such as occurred in the field in 2008 and 2010 and were captured with both the Levy Rod and leaf curing methods. The Bayesian model assumes that the nature of the response to thermal time is invariant. It would be possible include sub-models responsive to external events, to inform the α and β parameters (Equation 7.1) shown diagrammatically in Figure 7.4. This may allow the model to respond to events such as heavy rainfall or soil moisture increases late in the season.

In addition, the effect of external events would require modification to the growth model at the leaf level. For instance, if LAR were to increase, then the model LAR function could be changed to incorporate a greening-up event by inclusion of a function to delay LAR, such as $D(l;q) = \alpha(l-q)\exp(-\beta(l-q))$, where "$q$" is a quantity subtracted from the leaf index. The effect would be to move the plant back to an earlier growth stage. The same approach could be used with other component functions in the model, once the effects of events such as greening-up had been determined with glasshouse experimentation. The effect on leaf turnover rates in existing leaves would also need to be elucidated. The accumulation of green leaf biomass and curing would be calculated as before. A series of predicted curing curves could then be fitted; one without a greening-up event and others with greening-up events staged at a range thermal times (e.g. gdd=1000, gdd=2000, etc.). Logistic curves could be fitted to each as before, starting with the curve without a greening-up event, and switching to an

appropriately timed curve if a greening-up event occurs. Calibration to other field conditions may also be necessary.

Accumulation of leaf length, as reported here, referred to the main tiller, rather than the whole plant or sward. This provided information about what was happening at one point in space. In itself, this is not a limitation, as other models such as those included in GrassGro™ are point-based models, which extrapolate results to paddock scale. However, a further refinement of this work could be to incorporate a tiller function into the Bayesian model and then model the leaves of each tiller.

7.4.5.1 Representation of curing in individual leaves

There is an inevitable element of subjectivity in the categorization of the profile of green leaf accumulation; however the range of these categories does indicate that green leaf accumulation may not be entirely straightforward. The current model assumed a profile as described in Figure 7.1, and approximated this profile when a deviation was encountered. Future iterations of the Bayesian model which better represent the shape of the plateau may improve the fit of the model.

The almost symmetrical pattern in Figure 7.6.b might be considered “normal”, and it is possible that the senescent decline is caused by age of the leaf. Deviations from this pattern, particularly the onset of senescence either immediately (Figure 7.6.c) or soon after maturity (Figure 7.6.d), represent an early recycling of leaves. This may be caused by shading from other tillers on the same plant, or signals from other tillers producing new leaves. In this study, the effect of tiller numbers and hence shading as a cause of this early recycling could not be established.

The two-plateaux shape (Figure 7.6.e) is peculiar in that this would presumably extend the photosynthetic capability of the leaf. This may be due to

dynamics between tillers over the whole plant. In the event of the death of some minor tillers, the removal of sinks for retranslocated nutrients may interrupt the progression of senescence and allow the continuation of limited photosynthesis within the leaf. However, it may be that the deviations from the most common profile are primarily due to the extended production of leaves in the glasshouse, particularly for annual ryegrass and phalaris.

An advantage of the Bayesian modelling approach is that it should be able to be applied to different grass ecosystems without having to re-estimate model parameters. Species of the same growth types may have similar parameters, and indeed the generally successful application of the Bayesian-derived logistic curve to different cultivars and species in the field reported here, suggest that this may be possible. The reduced success in fitting wallaby grass to native grass field situations, however, points to the difficulty that may be experienced in natural ecosystems composed of numerous species. However, if this was more a failure of the Levy Rod assessment technique, then it could be possible to model components of a grass ecosystem individually and then sum curing, taking the grassland composition into account.

8 Discussion

The aim of this thesis was to test if the development of stand-alone plant growth models, informed by a detailed understanding of the relationships between leaf growth rates, would provide greater accuracy in the assessment of grass curing than the currently available plant growth models.

A number of approaches of increasing complexity were used to predict rates of grass curing. Estimations using commercial DST were compared to traditional field curing assessments in Chapter 3. A simple model of leaf curing based on linear leaf death was developed in Chapter 4, and then the relative importance of leaf turnover characteristics in models was explored in Chapter 5. The effects of water stress on LSR and leaf length were determined in Chapter 6. It was found that these components of leaf turnover did not estimate grass curing rates directly, but could be subsequently incorporated into a Bayesian model which predicted the accumulation of green leaf length, and curing percentage with thermal time as presented in Chapter 7.

8.1 Decision Support Tools to model curing

The results in Chapter 3 showed that the DST produced curing estimates similar to those from the Levy Rod assessments. However, the curing predictions for the same pasture type differed between the DST which had implications for using these tools to produce meaningful curing predictions. In the case of native pastures, it was even difficult to adequately assess the performance of DST curing estimates, given that the Levy Rod benchmark was least reliable in these grasslands (Anderson *et al.* 2011).

Three major differences between the DST in their ability to accurately estimate curing were highlighted in Chapter 3. Each incorporated different leaf senescence and death algorithms, which were generally simplified, with little differentiation between annual and perennial plants. The ability to simulate farming and grazing management practices, and therefore regional or landscape situations, differed widely between each DST. Finally, the range of grass species available for modelling in each DST also differed.

A single DST which incorporated multiple species and the greatest landscape management flexibility would be desirable as a tool for predicting curing, but this should be a secondary consideration to ensuring that the algorithms in the DST accurately predicted curing under the range of real life land management options. To date, there are no algorithms incorporated into DST to account for how different grass management practices affect curing. This theme is developed further in section 8.7.

To encourage adoption of DST, fire agencies would need to see this technology as a beneficial part of their core business in assessing curing. This is unlikely for several reasons. Curing assessment is currently a widely dispersed function, undertaken by a large number of volunteers or non-fire service staff (Garvey 2008; Miller 2008). Visual assessment remains the common method of curing assessment, despite its limitations and recent recommendations that it be replaced with the Levy Rod method (Anderson *et al.* 2011). Adoption of DST technology would require assessors to be trained in a number of different DST to begin to estimate curing in grass-dominated landscapes. The scale of this training component would be quite onerous if adopted at the volunteer level, and might be better suited to establishment of specialist roles for operating staff within fire

organisations. These staff would need to have at least some of the necessary knowledge to gather inputs and validate outputs of DST simulation. Finally, DST technology is unlikely to be adopted widely by fire agencies while confidence in curing outputs remains questionable.

8.2 The Leaf Curing Model

The Leaf Curing Model was simple to calculate but parameterisation of new species would be a time-consuming process because leaves need to be monitored over the life cycle of the plant. After adjustment for the differing starts of thermal time, the Leaf Curing Model was successfully applied to field data (Chapter 4, sections 4.3.3.1 and 4.3.3.2) in annual ryegrass and phalaris. It is encouraging that the validation of the Leaf Curing Model was successful in different cultivars of these species. It may also be possible to fit Leaf Curing Models to other species with similar growth habits, given that validation of the wheat and wallaby grass Leaf Curing Models was conducted in mixed species.

The Leaf Curing Model is a stand-alone model developed to assess if the relationship between accumulation of cured leaf matter and thermal time in species in the glasshouse could be extrapolated to field situations. Estimates from the Leaf Curing Models were more variable than those of the Levy Rod method (Chapter 4, section 4.3.3.2), but the following suggestions might improve its practical application in the field. The Leaf Curing Model was developed for individual species of differing growth habits, and application to grasslands with multiple grasses and other species would require further consideration. It may not be adequate to simply add outcomes of the different species models together, as competition between species in the field could alter the overall progress of curing in the sward. The Leaf Curing Model was based on an assumption of

irreversibility of curing so it does not respond to "greening-up" situations. Development of a mechanism by which the percentage cured could be reduced or thermal time delayed in the event of a rainfall event could also improve the fit of the Leaf Curing Model to field data.

8.3 Characterisation of leaf turnover

Leaf turnover is dependent on a number of genetic and environmental factors. Aspects of early leaf turnover have received some attention in the literature (Table 1.2 and Table 1.3); however, there is a lack of detailed information on leaf turnover for the entire life cycle of the plant. Limited information is available on leaf turnover dynamics for annual and native species common in southern Australian grass dominated landscapes and for the rate of leaf senescence, generally. This simply reflects the economic importance and previous investment in research on perennial pasture and annual crop species within the agricultural sector. However, this knowledge is vital for a complete understanding of grass curing in the Australian environment (Chapter 1, section 1.2.2 and 1.2.3) (Parrott 1964; McArthur 1966). Also, the variable expression of leaf turnover rates reported, particularly in terms of calendar time (e.g. Peacock 1975b; Sambo 1983; Kemp and Guobin 1992; Marriott *et al.* 1999), mass measures (e.g. Robson 1973; Bircham and Hodgson 1983; Grant *et al.* 1983; Hepp *et al.* 1996) and measurement intervals (e.g. Thomas and Norris 1979; Grant *et al.* 1983; Chapman *et al.* 1984) make it difficult to use the existing information to develop a model to estimate grass curing. Frequent measurements of four grasses of varying growth types (Chapter 5) have enabled a comprehensive study of leaf rates, with a high level of accuracy not generally available from other studies (Baker *et al.* 1986).

Interpretation of the changes in individual leaf growth rates with leaf position was simple, as leaf growth rates were expressed in terms of thermal time, and because photoperiod and temperature were relatively constant throughout the glasshouse trial. Models common to the four species were able to explain the majority of leaf turnover rates. Where models were fitted to individual species to provide a better fit, the form of the modelled curves remained similar (Table 5.7).

The interaction of leaf turnover rates in a coordinated manner manifests itself in the accumulation of green leaf material, and subsequently, in the onset and accumulation of cured plant material. Differences in the regulation of leaf turnover between the species may not be identified when data are limited in experiments of short duration (e.g.Wilson 1976; Calviere and Duru 1995; Duru and Ducrocq 2000a; b).

Future characterisation of leaf turnover rates in other grass species could potentially be developed rapidly by the knowledge that these differences in the coordination of leaf turnover appear to be due to genetic selection of grasses occupying slightly different environmental and production niches rather than differences of perenniality *per se*. In nutrient-poor environments, increased LLS and nutrient recycling via LSR are means of maximizing use of limited nutrients (Berendse *et al.* 1999). Of the species investigated here (Chapter 5, section 5.3), wheat has been genetically selected for growth under relatively nutrient-rich conditions, and had the shortest LLS and a slow LSR. In contrast, wallaby grass is adapted to Australian soils which are generally nutrient-poor, and has been subject to the least assisted genetic selection, and had a relatively long LLS but a slow LSR. The introduced pasture species had intermediate LLS and faster LSR, reflecting the genetic selection of these species in environments with nutrient

levels that exceed those of the indigenous Australian soils, but are generally less than those under which crop production is maintained.

When LER exceeds LSR, green material will accumulate, but once senescence is greater than elongation then cured material will accumulate at a faster rate. Duru and Ducrocq (2000a) showed that the rate of accumulation of senesced leaf on the tiller increased throughout the growth period until it equalled or exceeded LER by the end of the growth period. Although their finding supported the maintenance of leaf turnover equilibrium, it did not describe the differences in senescence rate between individual leaves as demonstrated in this study. This study appears to be the first to fully describe the intricacies of all facets of leaf turnover that were required to subsequently develop a Bayesian model which presented the progression of curing as a consequence of these differing leaf turnover rates. The Bayesian model is an alternative to the mechanistic approach of McMaster *et al.* (1991), the limitations of which were discussed in Chapter 5, section 5.1.

Measurements in this study focused on the leaves on the main stem. It may be necessary to establish the appropriate plant and tiller density from field surveys to account for the artificial level of competition created by the pot environment on which these results are based. It might be expected that LAR is similar for leaves on different tillers (Longnecker *et al.* 1993), but species with slow LAR would take longer to accumulate the necessary thermal time to produce many tillers (McMaster *et al.* 1991). Tiller appearance rate could be parameterized and modeled as a function of LAR. This would allow the results from this study to be extrapolated over the sward, using a compound model involving multiples leaves on multiple plants.

As individual components, these models of leaf turnover characteristics could not be used directly by fire agencies. However, they do provide the building blocks for a Bayesian model of curing (Chapter 7). They may also potentially improve modelling of leaf turnover in general, and curing in particular, if incorporated into the continuous improvement of existing DST (e.g. McCown *et al.* 1996; Keating *et al.* 2003; Moore *et al.* 2007; Moore *et al.* 2010).

8.4 The relationship between LSR and leaf length with leaf position under water stress

Compared to well-watered conditions, LSR increased with increasing water stress, but due to adaptation, the plant's ability to find more water, and relief of water stress (Turner and Begg 1978), the effect of water stress on LSR was less pronounced in the field. However, the shape of the relationship between leaf position and LSR under water stress remained similar to that of non-stressed plants (Figure 6.9), until the imposition of water stress late in the spring in the non-native species. This suggests that genetic or hormonal triggers associated with plant age and/or reproductive development may cause the increase of LSR with the onset of relatively common environmental conditions of late spring water stress (Munne-Bosch and Alegre 2004). The increase in LSR would ensure that recycling of resources contained in the leaf is maximized, ensuring the opportunity to successfully reproduce and complete the life cycle (Munne-Bosch and Alegre 2004) or initiate summer dormancy (Hoen 1968). Conversely, if water stress occurs too early in plant development, the plant is less able to increase LSR to maximize resource recycling.

The relationship between leaf position and LSR remained strong in wallaby grass regardless of the timing of stress. This suggests that the native grass may be genetically adapted to its environment to be resistant to water stress.

The shape of the relationship between leaf position and leaf length was relatively constant except occasionally with terminal stress in late spring and in wallaby grass (Figure 6.10). Differences between leaf length in the glasshouse and field may have been due to factors such as species, cultivar and tiller selection, as well as the nature of the water stress (terminal compared to gradual).

The results from Chapter 6 highlight the role for controlled environment studies to examine underlying mechanisms controlling leaf development and turnover in order to develop better models. Plant response to water stress may differ with the duration and magnitude of the stress (Munne-Bosch and Alegre 2004). This work does not cover all possible combinations of water stress, but it provides some insight on the effects of terminal water stress on leaf senescence and length. Plant responses to water stress imposed in the glasshouse were different to that of field-grown plants. The combined stress encountered by field-grown plants appeared to be less severe than the water stress developed in the glasshouse environment. Models of LSR from field-grown plants were most similar to models developed from well-watered control plants, suggesting that the latter model may be suitable for extrapolation into field conditions at least during periods of reproductive activity and plant maturation when above average rainfall occurs. Results may be different in drier years, as the summer when measurements were taken had above average rainfall. The later that water stress events occur in spring, however, the greater the effect on the LSR. The implications of this for modelling include that leaf turnover rates may need to be

altered (increased) with time into spring, and the length of time that the water stress is not relieved. Similar experimentation to that conducted here may capture the increase in LSR on a time or phenology-based scale, with sufficient accuracy to pragmatically adjust the LSR model. A more detailed understanding of this phenomenon may require biochemical and molecular biology techniques to capture changes in plant hormone levels and genetic functioning.

This work contributes to the understanding of the role that acute or chronic water stress conditions may play in the curing process. Further work should consider the rapid progression of curing under drought stress (water stress combined with high temperatures and solar radiation) (Munne-Bosch and Alegre 2004) that is a feature of grass-dominated landscapes in southern Australia.

8.5 The Bayesian model

The Bayesian model was developed from detailed leaf turnover measurements and predicted accumulation of green leaf and percentage of dead material in grasses in response to thermal time. Both predictions could be applied to the management of grassland fires, through assessment of grass fuel loads and state of curing. Bayesian models take considerable time to run, which may render their use impractical in some planned burn situations. Pre-prepared logistic curves for different grass types might be used to emulate the results of the Bayesian model with a shorter response time, especially where curing is proceeding in a predictable fashion. Testing of a logistic curve representing the curing percentage predictions from the Bayesian model indicated that the Bayesian model is able to predict curing to around 10% of visual curing estimates (Table 7.6) and 20% of Levy Rod curing estimates (Table 7.5). The logistic curves fitted to the Levy Rod assessments for non-native species were best for wheat, with low variation in

curing between the two methods (Table 7.5). The lack of fit between the wallaby grass logistic curve and Levy Rod assessments in native pastures may have been due to difficulty distinguishing between the numerous species in the field, and to the lower reliability of the Levy Rod method in native grasslands (Anderson *et al.* 2011). Anderson *et al.* (2011) compared destructive sampling to visual and Levy Rod curing assessments (Table 8.1). In that study RMSD values were lower for the Levy Rod method and higher for the visual method (Anderson *et al.* 2011) compared to the RMSD values recorded when the Bayesian model was compared to these alternative field methods in this study. The Bayesian model may require some refinement to improve its rating against the Levy Rod method, before it could be considered superior to the recommended Levy Rod method. Future work should compare the Bayesian model to curing estimates from destructive sampling, as well as the Levy Rod technique to fully test the accuracy of the model.

Table 8.1. Comparison of RMSD values from the Bayesian model and destructive sampling from Anderson *et al.* (2011)

	Destructive	**Bayesian**
Visual	19.5	~10
Levy	12.5	~20

Refinements suggested in the thesis may improve the ability of the Bayesian model to predict curing in environments which do not receive winter-dominant rainfall, or where grasslands "green-up" due to unseasonal rainfall events.

When compared to estimates of curing from field techniques, the Bayesian model provided more reliable curing estimates than did the DST tested and unlike any single DST, were able to provide curing estimates for the range of grass growth types explored here.

Taking actual leaf shape into account such as the tapering of leaf tips in grass leaves, rather than assuming uniform linearity would also improve the model, and

would be necessary for species (such as legumes or broadleaf plants) which do not have a linear leaf arrangement. Other leaf types could be modeled using a leaf position index approach if the pattern of leaf appearance is predictable and can be modelled and the leaves have a uniform shape which increases in a uniform manner. Accounting for changes in leaf width and thickness along the length of the grass leaf may provide further small refinements to the model.

Another area in which the Bayesian model could be improved is by including the correlations between the leaf turnover rates (Appendix F, Table F-1). The rates (e.g. LER, LSR, etc.) are assumed to be independent of each other but are all functions of leaf position, which can result in correlated posteriors. Incorporating known correlations between the leaf rates through the use of multivariate priors would link the leaf rate variables like LER and LSR, so that if one increased then the other would also change appropriately, resulting in improved prediction capacity.

8.6 Approaches to parameterising new species

This thesis reported the parameterisation of four grass species of differing growth types (Chapter 5), in the process of developing a Bayesian model of curing for each. While each of these species can be considered common, they certainly do not represent all grass species present in temperate Australian grass-dominated landscapes. The curing predictions from the Bayesian model may be of use to fire agencies in situations limited to monocultural swards of these particular species. To extend the ability of the Bayesian model to predict curing in grass-dominated landscapes containing species other than these four grasses, it will be necessary to parameterise the Bayesian model for additional species. Two possible approaches

are: 1) to exploit the similarities of growth types between species, and 2) to assess relationships between growth rates within species.

8.6.1 Similarities between growth types

The nature of the relationships between leaf turnover characteristics and leaf position could provide a starting point for the development of parameters in new species. The parameters presented here could be altered to represent leaf traits in different species, for instance, with longer or shorter leaves, longer or shorter life spans, faster or slower emergence, elongation, and senescence. By re-sampling the posterior distributions of all parameters in the Bayesian model (which would retain the relationships and correlations between them) and also incorporating inflated variances, predicted outcomes would be obtained that automatically included uncertainty. Combining different permutations of leaf rates in the Bayesian model could provide a wide and quantifiable range of green leaf accumulation and percentage dead curves.

Validation of the Bayesian models developed from glasshouse-grown plants was carried out on different cultivars, and in some cases, different species, in the field. This may be an unorthodox approach to model validation, but it was a practical compromise to address the lack of resources at hand. However, the success of the Bayesian model validation suggested that the parameters from the underlying leaf turnover models might be applied to similar growth types. This could allow the leaf turnover rates of the measured species to be used in other cultivars of the same species. For instance, parameters for Holdfast phalaris established in the glasshouse might be used as input parameters to define new prior distributions for new phalaris cultivars. The fit of the wheat Bayesian model to both wheat and barley in the field may have been the result of similar

development rates between the particular cultivars grown. Typically, the number of varieties sown in new pastures or crops is limited. Therefore it may be possible to parameterize monocultures or mixed grass swards either with the parameters already collected, or by conducting similar sets of measurements in new species. The leaf turnover rates described here could also be used as prior distributions for future Bayesian models.

Native or naturalized pastures generally contain a larger number of species, with greater variability within species, due to absence of artificial selection pressure, than newly-sown crops or pastures (Kemp and Dowling 1991; Tilman and Downing 1994). Whether these can be parameterized successfully with generic leaf turnover values is likely to be more problematic given the genetic diversity, especially where native species form a substantial part of the grassland. The application of a glasshouse-derived wallaby grass Bayesian model to native pastures was the least successful, and this may be due in part to the large number of species present in field sites and their genetic diversity. Wallaby grass may not be representative of the wider range of native species, in terms of nutrient value, palatability and leaf tensile strength (Henry *et al.* 1997; 2000; Coleman and Henry 2002). If other species have tougher, less palatable leaves which resist grazing or decomposition, they will retain leaves which would allow the curing rate to remain higher for longer.

8.6.2 Parameterising within a season

The measurement of leaf turnover on the entire cohort of leaves was a relatively time-consuming activity, rendering alternative means of generating parameters for new species desirable. The proportion of senescent leaves present on a plant is determined by the growth processes (appearance, elongation, leaf life

span) (Calviere and Duru 1995; McMaster *et al.* 2003) and environmental conditions (Vine 1983) that precede the senescence of individual leaves. It should therefore be possible to predict senescence rate with knowledge of earlier expressed rates, such as leaf appearance and elongation rates and leaf life span (Vine 1983; Lemaire and Agnusdei 2000). This would shorten the measurement period, and if conducted in the glasshouse under controlled lighting, then conceivably leaf turnover rates could be collected at any time of year. Alternatively it may be possible to collect leaf turnover measurements in the field where early expressed rates would coincide with the period of reduced fire danger in southern Australia.

A brief analysis of the relationships between leaf measurements collected early in the plant growth cycle and subsequent senescence rates (Daily *et al.* 2010) was conducted. Pearson correlations (Appendix F, Table F-1) indicated that LLS and LSR were both significantly correlated with LER across all species combined, and these correlations were also significant in all individual species. These consistent trends across all these grasses suggested that prediction of the onset and rate of senescence should be possible in both pure stands and mixed species swards.

The rate at which individual leaves senesced has been shown to be related to the rate at which those particular leaves appeared, rather than to the current LAR (Vine 1983; Lemaire and Agnusdei 2000). However, LAR was not consistently related to LER, LLS or LSR (Appendix F, Table F-1). This may have been due to LAR data not being available on the earliest leaves since observations commenced on randomly chosen plants, once the 3-leaf stage was reached to avoid the possible confounding effect of selecting the earliest germinating plants

as observation plants. Other studies, however, reported LAR on only the earliest leaves (Duru and Ducrocq 2000a) or frequently changed plants on which LAR was reported (Kemp and Guobin 1992) and hence may have overlooked the true relationship between LAR and other traits in the full range of leaves.

Estimation of curing rates should be possible if the commencement and duration of senescence of each leaf is known. Estimation of LLS is necessary to determine the onset of senescence. Previous studies have used LLS to predict the number or proportion of senescent leaves (Vine 1983; Calviere and Duru 1995; Lemaire and Agnusdei 2000). Daily *et al*. (2010) reported that LER and LLS were significantly negatively correlated (Appendix F, Table F-1) and as LER increased, LLS decreased (Figure 8.1). Differences in the slope suggested that the relationship may be different for annual and perennial species, but similar between species with annual or perennial growth habits (Appendix F, Table F-3). Equations for the models are shown in Appendix F, Table F-2. Further work to validate the relationship between LER and LLS is required to confidently extend this across all or most common grass species. It may be that only the slowest elongating leaves have longer life spans (Figure 8.1), and that no discernible relationship exists when LER values exceed 0.5 mm/gdd, particularly for wheat (Figure 8.1.d). Further analysis may be warranted to test if the relationship between LER and LLS is different for cohorts of leaves with different rates of leaf elongation.

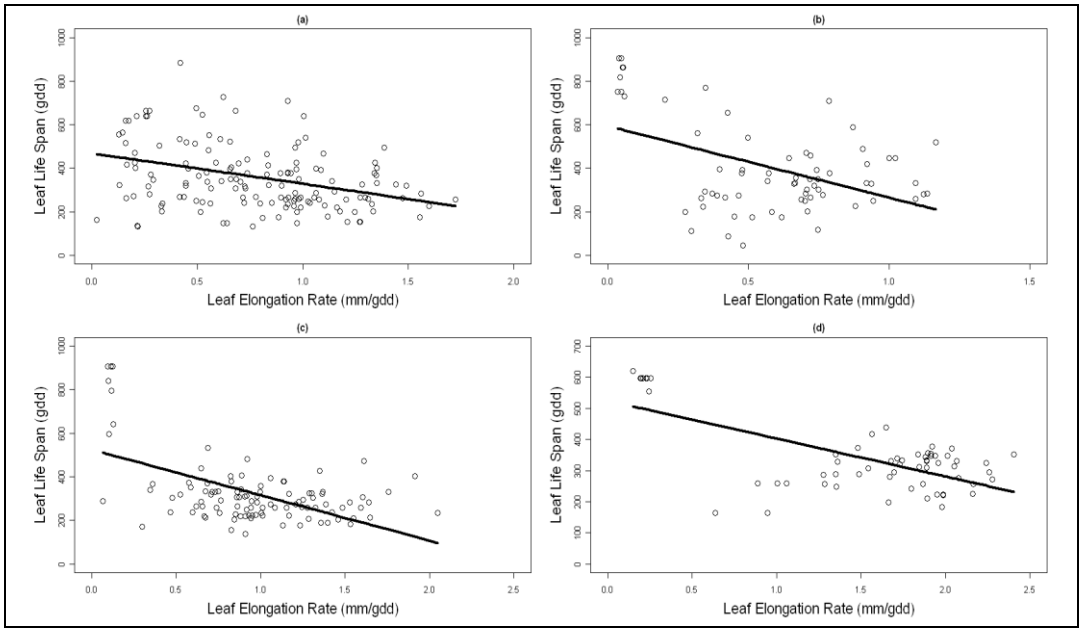

Figure 8.1. Observations (open circles) and model (line) of the relationship between LLS (gdd) and LER (mm/gdd (T_{base} = 0°C)) for four species: a) annual ryegrass; b) wallaby grass; c) phalaris; d) wheat.

Knowledge of LSR is necessary to define the duration of curing in leaves. The significant positive correlation between LER and LSR (Appendix F, Table F-1), may allow LSR to be determined from LER measured early in the growing season. LSR increased with LER in a similar fashion in the non-cereal species; however, the relationship was significantly weaker in wheat (Figure 8.2) (Appendix F, Table F-3). Equations for the model are given in Appendix F, Table F-4. Pasture species with annual and perennial growth habits showed a similar relationship, so measurement of LER may allow the subsequent LSR to be established in grasslands composed of a range of pasture species. However, it may not be possible to determine LSR from LER in cereals, given the apparent lack of relationship between these two characteristics in wheat. The relationship between these traits may have been uncoupled with intensive selection in cereals to ensure completion of the reproductive phase and subsequent ripening and maturity of grain, regardless of conditions experienced earlier in the plant's life, or the LER expressed.

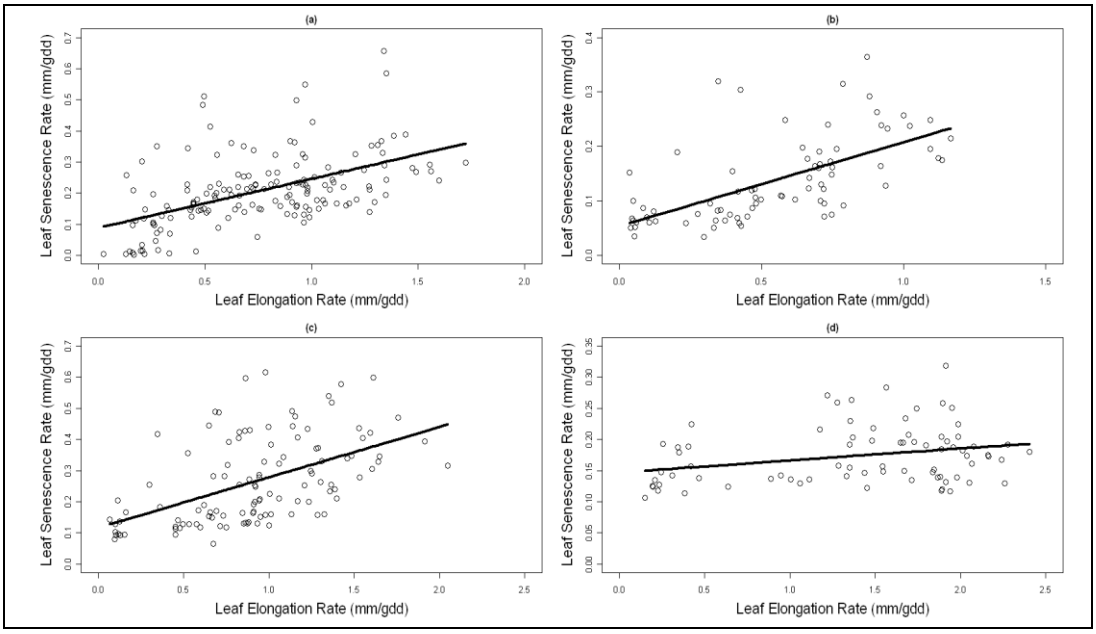

Figure 8.2. Observations (open circles) and model (line) of the relationship between LSR (mm/gdd (T_{base} = 0ºC)) and LER (mm/gdd (T_{base} = 0ºC)) for four species: a) annual ryegrass; b) wallaby grass; c) phalaris; d) wheat.

Identifying if the relationships between LER and LLS and LSR hold for a cohort of early leaves would be a refinement of the work of Daily *et al.* (2010) which might reduce the time required to conduct measurement on new species or cultivars to further accelerate parameterization. While the most accurate way to parameterise LSR and LLS in new species would appear to be achieved through direct measurement of leaf growth and death rates in the species of interest, as shown in Chapter 5, both LLS and LSR could be predicted from LER, which was measured earlier in the growing season. Only two species of each growth habit were investigated (Daily *et al.* 2010), so further work is necessary to test if the relationship between LER and both LLS and LSR remains valid across more grasses. If so, then the existing algorithms may be a suitable substitute or provide a starting point from which to determine the values for other species of a similar growth habit. The potential to indirectly parameterise new species through the collection of LER data early in the growing season would provide far more timely

advice to fire agencies than would be possible from waiting to directly measure LLS and then death.

8.7 Can models assist in the manipulation of curing?

One use of curing assessments is to plan for the safe use of fire in prescribed burns with the aim of fuel reduction. Fuel reduction aims to modify the behaviour of resultant fires (Fernandes and Botelho 2003), but manipulation of curing could help to achieve the same outcome. Curing is usually an ongoing process, so identifying the transient period in which prescribed burns might be conducted safely is of interest to fire agencies. Prescribed burns in pine forests in the US have been used to create "fuel mosaics" where fire breaks act to isolate and contain unplanned fires (Fernandes and Botelho 2003). Manipulation of curing could provide a similar though short-term effect in grass-dominated landscapes; a fire brake (slowing down) rather than fire break (stopping it outright). Manipulation of curing might entail either increasing or decreasing the rapidity with which grass-dominated landscapes cure. Earlier curing would bring forward the window of opportunity in which grass-dominated landscapes are in an optimum curing range in which to conduct prescribed burns in fire season. This strategy would increase opportunities for prescribed burns as this period would coincide with milder and therefore safer weather conditions. It may also be possible to extend the duration of curing to increase the window of opportunity for prescribed burning. However this strategy would run the risk of coinciding with more dangerous fire weather in Mediterranean environments, at least.

Field-based experimentation on the effects of management practices such as rolling (Rowell and Cheney 1979), irrigation, slashing, mowing, grazing, and herbicide application, on curing would be necessary to enhance plant growth

models to explore the effects of various grass management techniques on curing. Resultant algorithms or derivatives could be incorporated into existing DST to improve the ability of those DST to test the effects of management on curing, or the Bayesian Model could be expanded to include these management inputs with the post-simulation economic analysis of such practices subsequently conducted.

8.8 Curing in native grasses

Although the four grass species had similar leaf turnover rates in the glasshouse under optimal conditions (Chapter 5), there is some evidence that the leaf processes that influence curing in native grasses may be different to those operating in introduced species under water stress conditions and in the field (Chapter 6). It cannot be solely due to any inherent difference between spear grass and wallaby grass in the field, however, because wallaby grass performed quite differently to the introduced grasses when placed under terminal water stress in the glasshouse.

Curing was generally higher at the beginning of the measurement periods and increased more quickly in native pastures compared to the introduced grasses in the South Australian field sites. The high initial curing values registered in the field were not captured in either the leaf curing model or the Bayesian model. The SA field sites dominated by native species had a greater build up of dry residues from year to year, which were captured as higher Levy Rod curing estimates. The dead leaves did not seem to break down as quickly as those of introduced grasses; therefore these pastures did not resume the following winter-spring season with 0% curing status. This could be in response to a lack of grazing and trampling due to lower stocking rates than on the introduced pastures, as well as differences in palatability and soil fertility. Crop stubbles at Bool Lagoon in SA were also not

grazed but did not appear to reduce Levy Rod curing assessments in the new growth as markedly as in the native pastures. Stubbles might be subject to faster breakdown due to lower plant densities, and greater production of green material than that of native pastures. The intrinsic shear strength of senescent grass leaves is higher than that of vegetative leaves (Henry *et al.* 2000), which also suggests that breakdown of residues is retarded by senescence. There are also genetic differences in leaf shear strength between species (Henry *et al.* 1997; 2000), which may affect the rate of breakdown by soil decomposer populations (Coleman and Henry 2002). Certainly the generally lower palatability and nutritional value of native grasses to grazing animals would suggest that this may be the case.

The Levy Rod results recorded here and by Anderson *et al.* (2011) suggest that curing in native grasslands proceeds differently to that in introduced or naturalised pastures and crops. The relationship between curing and fuel moisture content does not appear to have been tested in C_3 native grasses (cf. Cheney *et al.* 1993; Anderson *et al.* 2005). Differences between annual and perennial introduced species were noted by McArthur (1966), and slight differences between a number of annual introduced species were discounted by Parrott and Donald (1970b).

8.9 Conclusion

This study set out to investigate and improve the assessment of grass curing through the use of plant growth models. Agricultural DST incorporating the current state of knowledge on leaf turnover were not able to produce reliable curing estimates, in part because much of the research on the senescence stage of leaf development has not been suitable to model (Chapter 1, section 1.2.3.6). A

Leaf Curing Model based on the proportion of cured leaf material over time was similarly not suitable for estimating curing in the field because it lacked responsiveness to plant leaf development and assumed irreversibility of curing.

Three major achievements have been reported in this thesis. Firstly, the most comprehensive study of leaf turnover rates over the entire lifecycle of the plant has been reported for four grass species with different growth habits including an Australian native grass, for which relatively little information has previously been published.

Secondly, a great deal more knowledge has been contributed on the nature of LSR, under both ideal conditions and those in which terminal water stress is imposed. This knowledge gap was identified in the review of the literature (Chapter 1). Along with the leaf turnover algorithms, this knowledge could be used to modify the plant growth models in current DST to improve estimation of curing, which may improve the applicability of DST to fire management goals.

Thirdly, the success of the leaf turnover algorithms described here was manifested in the development of a Bayesian model to predict curing in the field. A number of recommendations have been suggested regarding potential improvements to the Bayesian model, which would be necessary before this tool, or its outputs, would be suitable for application in fire management.

This work has demonstrated that the concept of grass curing is more complex than the widely accepted view conceived by Parrott and Donald (1970b) (Figure 1.3). Species differences and environmental effects need to be accounted for if curing is to be accurately assessed. This work has advanced the knowledge and understanding of curing in grasses and has provided detailed algorithms and models to continue the advancement of grassland curing estimation and prediction.

It can be applied in other temperate climates where grassfires are problematic such as New Zealand, South Africa, and parts of the Americas and southern Europe. This thesis established that stand-alone models, in the form of a Bayesian model, developed with a detailed understanding of the relationships between leaf growth rates, would provide a higher level of accuracy of grass curing than the pasture growth models currently incorporated into commonly-available DST. Parameterisation of additional species and investigation of the effects of common grass management techniques on curing rates will be necessary to allow widespread application of plant growth models for curing estimation. Fire agencies may need to consider funding this additional work as well as development of a delivery platform, either through an existing DST or a stand-alone Bayesian-based model, and associated training programs appropriate for use within their organisations.

9 References

Agnusdei M, Assuero SG, Fernandez Grecco RC, Cordero JJ, Burghi VH (2007) Influence of sward condition on leaf tissue turnover in tall fescue and tall wheat grass swards under continuous grazing. *Grass and Forage Science* **62**, 55-65.

Aguado I, Chuvieco E, Boren R, Nieto H (2007) Estimation of dead fuel moisture content from meteorological data in Mediterranean areas. Applications in fire danger assessment. *International Journal of Wildland Fire* **16**, 390-397.

Akaike H (1974) A New Look at the Statistical Model Identification. *IEEE Transaction on Automatic Control.* **AC-19**, 716–723.

Anderson HE (1970) Forest fire ignitability. *Fire Technology* **6**, 312-319.

Anderson HE (1990) Moisture diffusivity and response time in fine forest fuels. *Canadian Journal of Forest Research* **20**, 315-325.

Anderson S (2007) pers. comm.

Anderson S, Anderson W, Hines F, Fountain A (2005) Determination of field sampling methods for the assessment of curing levels in grasslands. Ensis / Bushfire CRC.

Anderson S, Botha E (2007) Linking field observations with remote sensing to determine grassland fire hazard. In 'Joint AFAC / Bushfire CRC Conference 2007'. Hobart, Tasmania.

Anderson S, Pearce HG (2003) Improved methods for the assessment of grassland curing. In '3rd International Wildland Fire Conference'.

Anderson SAJ, Anderson WR, Hollis JJ, Botha EJ (2011) A simple method for field-based grassland curing assessment. *International Journal of Wildland Fire* **20**, 804-814.

Anonymous (2008a) CSIRO Grassland fire spread meter. http://www.csiro.au/products/GrassFireSpreadMeter.html, accessed on 28/4/2011.

Anonymous (2008b) Evergraze national brochure. http://www.evergraze.com.au/_literature_41081/EverGraze_National_Brochure, accessed on 15/5/2008.

Anonymous (2008c) Grassland fire danger meter. http://www/csiro.au/products/Grass-Fire-Danger-Meter.html, accessed on 28/4/2011.

Anonymous (2009) APSIM 7.0 Release notes. http://www.apsim.info/Wiki/public/Upload/Versions/v70/Apsim70%20Release%20Notes.htm, accessed on 16/6/2011.

Anonymous (2010) GrassGro Help File. (CSIRO Plant Industry).

Anonymous (2011a) The APSIM-Wheat Module (Wheat). http://www.apsim.info/Wiki/Wheat.ashx, accessed on 30/5/2008.

Anonymous (2011b) Cross-validation (statistics). http://en.wikipedia.org/wiki/Cross-validation_(statistics) accessed on 20/10/2010.

Anonymous (2011c) GRAZPLAN Pasture Model - 10. Death and litterfall. Grazplan - CSIRO Plant Industry.

Anonymous (2011d) Outlier. https://secure.wikimedia.org/wikipedia/en/wiki/Outlier, accessed on 21/10/2011.

Anonymous (2012a) Harvest and vehicle movement bans. http://www.fesa.wa.gov.au/safetyinformation/fire/bushfire/pages/ruralandfarmfire.aspx#harvestvehiclemovementbans, accessed on 20/1/2012.

Anonymous (2012b) Operating farming machinery, equipment and vehicles. http://www.cfa.vic.gov.au/firesafety/farming/machinery.htm, accessed on 20/01/2012.

Ansquer P, Al Haj Khaled R, Cruz P, Theau J-P, Therond O, Duru M (2009) Characterizing and predicting plant phenology in species-rich grasslands. *Grass and Forage Science* **64**, 57-70.

Australian Bureau of Agricultural Resource Economics and Sciences (2003) Integrated Vegetation Cover. http://adl.brs.gov.au/mapserv/intveg/index.html, accessed on 25/3/2009.

Baker CK, Gallagher JN, Monteith JL (1980) Daylength change and leaf appearance in winter wheat. *Plant, Cell and Environment* **3**, 285-287.

Baker JT, Pinter PJ, Reginato RJ, Kanemasu ET (1986) Effects of temperature on leaf appearance in spring and winter wheat cultivars. *Agronomy Journal* **78**, 605-613.

Barber JR (1990) Monitoring the curing of grassland fire fuels in Victoria, Australia with sensors in satellites and aircraft. Country Fire Authority, Victoria.

Baxter GJ, Woodward SJR (1999) Estimating grassland curing using soil moisture indicators and a pasture quality model. In 'Australian Bushfire 99 Conference'. Albury, NSW pp. 33-38.

Beal SL, Sheiner LB (1982) Estimating population kinetics. *CRC Critical Reviews in Biomedical Engineering* **8**, 195-222.

Beal SL, Sheiner LB (1988) Heteroscedastic nonlinear regression. *Technometrics* **30**, 327-338.

Begg JE (1980) Morphological adaptations of leaves to water stress. In 'Adaptation of plants to water and high temperature stress.' (Eds NC Turner, PJ Kramer) pp. 33-42. (John Wiley and Sons: New York, U.S.A.).

Bellotti WD (2001) The role of forages in sustainable cropping systems of southern Australia. In '19th International Grasslands Congress'. Brazil.

Berendse F, de Kroon H, Braakhekke WG (1999) Acquisition, use, and loss of nutrients. In 'Handbook of functional plant ecology.' (Eds FI Pugnaire, F Valladeres) pp. 315-345. (Marcel Dekker Inc.: New York, U.S.A.).

Bircham JS, Hodgson J (1983) The influence of sward conditions on rates of herbage growth and senescence in mixed swards under continuous stocking management. *Grass and Forage Science* **38**, 323-331.

Bradstock RA, Gill AM, Kenny BJ, Scott J (1998) Bushfire risk at the urban interface estimated from historical weather records: consequences for the use of prescribed fire in the Sydney region of south-eastern Australia. *Journal of Environmental Management* **52**, 259-271.

Bresnehan SJ, Pyrke A (1998) 'Dry forest fuels in south-east Tasmania.' (Parks and Wildlife Service Tasmania, Forestry Tasmania, Tasmania Fire Service, Hobart City Council.).

Brougham RW (1960) The relationship between the critical leaf area, total chlorophyll content, and maximum growth-rate of some pasture and crop plants. *Annals of Botany* **24**, 463-474.

Buchanan-Wollaston V, Morris K (2000) Senescence and cell death in *Brassica napus* and *Arabidopsis*. In 'Programmed cell death in animals and plants.' (Eds JA Bryant, SG Hughes, JM Garland) pp. 163-174. (BIOS Scientific Publishers Ltd: Oxford, UK).

Bureau of Meteorology (2009) Silo: Meteorology for the Land. http://www.bom.gov.au/silo/, accessed on 30/7/2009.

Bureau of Rural Sciences (after CSIRO) (1991) Digital Atlas of Australian Soils http://www.brs.gov.au/data/datasets, accessed

Callaghan D (2010) pers. comm. (Ed. HG Daily)Naracoorte, S.A.).

Calviere I, Duru M (1995) Leaf appearance and senescence patterns of some pasture species. *Grass and Forage Science* **50**, 447-451.

Campbell GS, Norman JM (1998) 'An introduction to environmental biophysics.' (Springer: New York, USA).

Cao W, Moss DN (1989) Temperature and daylength interaction on phyllochron in wheat and barley. *Crop Science* **29**, 1046-1048.

Carrere P, Louault F, Soussana JF (1997) Tissue turnover within grass-clover mixed swards grazed by sheep. Methodology for calculating growth, senescence and intake fluxes. *Journal of Applied Ecology* **34**, 333-348.

Carter ED, Cochrane MJ (1992) Using the levy point quadrat to assess botanical composition of dairy pastures in the Adelaide Hills. In 'Looking back, planning ahead. Proceedings of the 6th Australian Agronomy Conference.' (Eds KJ Hutchinson, PJ Vickery) p. 534. (The Australian Society of Agronomy: Armidale, NSW).

Carter O, Murphy AM, Cheal D (2003) Natural temperate grassland. Arthur Rylah Institute for Environmental Research, Department of Natural Resources and Environment (Victoria).

Cary GJ, Flannigan MD, Keane RE, Bradstock RA, Davies ID, Lenihan JM, Li C, Logan KA, Parsons RA (2009) Relative importance of fuel management, ignition management and weather for area burned: evidence from five landscape-fire-succession models. *International Journal of Wildland Fire* **18**, 147-156.

Catchpole EA, Catchpole WR, Viney NR, McCaw WL, Marsden-Smedley JB (2001) Estimating fuel response time and predicting fuel moisture content from field data. *International Journal of Wildland Fire* **10**, 215-222.

Catchpole WR (2002) Fire properties and burn patterns in heterogeneous landscapes. In 'Flammable Australia - the fire regimes and biodiversity of a continent.' (Eds RA Bradstock, JE Williams, AM Gill) pp. 49-75. (Cambridge University Press: Cambridge, UK).

Cayley JWD, Bird PR, Chin JF (1980) Death and decay rates of perennial pasture as affected by season. In 'Animal Production in Australia: Proceedings of the 13th biennial conference of the Australian Society of Animal Production.' p. 469.

Chandler C, Cheney P, Thomas P, Trabaud L, Williams D (1983) 'Fire in forestry. Vol. 1. Forest fire behavior and effects.' (John Wiley and Sons, Inc.: New York, USA.).

Chapman DF, Clark DA, Land CA, Dymock N (1983) Leaf and tiller growth of *Lolium perenne* and *Agrostis* spp. and leaf appearance rates of *Trifolium repens* in set-stocked and rotationally grazed hill pastures. *New Zealand Journal of Agricultural Research* **26**, 159-168.

Chapman DF, Clark DA, Land CA, Dymock N (1984) Leaf and tiller or stolon death of *Lolium perenne*, *Agrostis* spp., and *Trifolium repens* in set-stocked and rotationally grazed hill pastures. *New Zealand Journal of Agricultural Research* **27**, 303-312.

Cheney NP (1981) Fire behaviour. In 'Fire and the Australian Biota'. (Eds AM Gill, RH Groves, IR Noble) pp. 151-175. (Australian Academy of Science: Canberra).

Cheney NP, Gould JS (1995a) Fire growth in grassland fuels. *International Journal of Wildland Fire* **5**, 237-247.

Cheney NP, Gould JS (1995b) Separating fire spread prediction and fire danger rating. *CALMScience Supplement* **4**, 3-8.

Cheney NP, Gould JS, Catchpole WR (1993) The influence of fuel, weather and fire shape variables on fire-spread in grasslands. *International Journal of Wildland Fire* **3**, 31-44.

Cheney NP, Gould JS, Catchpole WR (1998) Prediction of fire spread in grasslands. *International Journal of Wildland Fire* **8**, 1-13.

Cheney P, Sullivan A (2008) 'Grassfires: fuel, weather and fire behaviour.' (CSIRO Publishing: Melbourne, Victoria).

Chladil M, Nunez M (1995) Assessing grassland moisture and biomass in Tasmania - the application of remote-sensing and empirical-models for a cloudy environment. *International Journal of Wildland Fire* **5**, 165-171.

Chuvieco E, Cocero D, Riano D, Martin P, Martinez-Vega J, de la Riva J, Perez F (2004) Combining NDVI and surface temperature for the estimation of live fuel moisture content in forest fire danger rating. *Remote Sensing of Environment* **92**, 322-331.

Coleman JR, Sullivan AL (1996) A real-time computer application for the prediction of fire spread across the Australian landscape. *Simulation* **67**, 230-240.

Coleman SW, Henry DA (2002) Nutritive value of herbage. In 'Sheep Nutrition.' (Eds M Freer, H Dove) pp. 1-26. (CSIRO Publishing: Melbourne, Vic).

Council of Heads of Australasian Herbaria Inc (2011) Australia's Virtual Herbarium. http://www.chah.gov.au/avh/index.jsp, accessed on 6/10/2011.

Culvenor RA (1993) Effect of cutting during reproductive development on the regrowth and regenerative capacity of the perennial grass, *Phalaris aquatica* L., in a controlled environment. *Annals of Botany* **72**, 559-568.

Cutforth HW, Jame YW, Jefferson PG (1992) Effect of temperature, vernalization and water stress on phyllochron and final main-stem leaf number of HY320 and Neepawa spring wheats. *Canadian Journal of Plant Science* **72**, 1141-1151.

Daily H, Lane P, Lisson S, Bridle K, Anderson S, Corkrey R (2010) Developing grass curing algorithms for decision support tools. In '"Food Security from Sustainable Agriculture". Proceedings of 15th Agronomy Conference, 15-18

November 2010.' (Eds H Dove, RA Culvenor). (Australian Society of Agronomy: Lincoln, New Zealand).

Dale JE (1982) 'The growth of leaves.' (Edward Arnold Publishers: London, UK).

Dale JE (1988) The control of leaf expansion. *Annual Review of Plant Physiology and Plant Molecular Biology* **39**, 267-295.

Daniel TC, Ferguson IS (1989) Integrating research on hazards in fire-prone forest environments: overview. In 'Integrating research on hazards in fire-prone environments. Proceedings of the US-Australia workshop.' Melbourne, Victoria. (Eds TC Daniel, IS Ferguson) pp. 1-4. (US Man and the Biosphere Program, Washington, DC).

Davidson HR, Campbell CA (1983) The effect of temperature, moisture and nitrogen on the rate of development of spring wheat as measured by degree days. *Canadian Journal of Plant Science* **63**, 833-846.

Dawson M, Hurst E, Pratt J (1991) South Australia's fire climatology. In 'Conference on Agricultural Meteorology - Extended Abstracts'. University of Melbourne pp. 264-268. (National Committee on Agrometeorology).

Dear BS, Sandral GA, Wilson BCD (2006) Tolerance of perennial pasture grass seedlings to pre- and post-emergent grass herbicides. *Australian Journal of Experimental Agriculture* **46**, 637-644.

Dilley AC, Millie S, O'Brien DM, Edwards M (2004) The relation between Normalized Difference Vegetation Index and vegetation moisture content at three grassland locations in Victoria, Australia. *International Journal of Remote Sensing* **25**, 3913-3930.

Dimitrakopoulos AP, Bemmerzouk AM (2003) Predicting live herbaceous moisture content from a seasonal drought index. *International Journal of Biometeorology* **47**, 73-79.

Dimitrakopoulos AP, Mitsopoulos ID, Gatoulas K (2010) Assessing ignition probability and moisture of extinction in a Mediterranean grass fuel. *International Journal of Wildland Fire* **19**, 29-34.

Dimitrakopoulos AP, Papaioannou KK (2001) Flammability assessment of Mediterranean forest fuels. *Fire Technology* **37**, 143-152.

Duru M, Ducrocq H (2000a) Growth and senescence of the successive grass leaves on a tiller. Ontogenic development and the effect of temperature. *Annals of Botany* **85**, 635-643.

Duru M, Ducrocq H (2000b) Growth and senescence of the successive leaves on a cocksfoot tiller. Effect of nitrogen and cutting regime. *Annals of Botany* **85**, 645-653.

Duru M, Ducrocq H, Fabre C, Feuillerac E (2002) Modeling net herbage accumulation of an orchardgrass sward. *Agronomy Journal* **94**, 1244-1256.

Evers JB, Vos J, Fournier C, Andrieu B, Chelle M, Struik PC (2005) Towards a generic architectural model of tillering in Gramineae, as exemplified by spring wheat (*Triticum aestivum*). *New Phytologist* **166**, 801-812.

Faber-Langendoen D, Josse C (2010) World grasslands and biodiversity patterns. Arlington, Virginia, U.S.A.

Feller U (1979) Effect of changed source/sink relations on proteolytic activities and on nitrogen mobilization in field-grown wheat (*Triticum aestivum* L.). *Plant and Cell Physiology* **20**, 1577-1583.

Feller U, Fischer A (1994) Nitrogen metabolism in senescing leaves. *Critical Reviews in Plant Sciences* **13**, 241-273.

Fernandes PM, Botelho HS (2003) A review of prescribed burning effectiveness in fire hazard reduction. *International Journal of Wildland Fire* **12**, 117-128.

Fischer RA, Hagan RM (1965) Plant water relations, irrigation management and crop yield. *Experimental Agriculture* **1**, 161-177.

Fischer RA, Kohn GD (1966) The relationship of grain yield to vegetative growth and post-flowering leaf area in the wheat crop under conditions of limited soil moisture. *Australian Journal of Agricultural Research* **17**, 281-295.

Flannigan MD, Krawchuk MA, de Groot WJ, Wotton BM, Gowman LM (2009) Implications of changing climate for global wildland fires. *International Journal of Wildland Fire* **18**, 483-507.

Flavelle M (2002) Kimberley grasslands field curing guide. Kimberley Regional Fire Management Project, Broome, WA.

Frame J (1992) 'Improved grassland management.' (Farming Press: Ipswich, UK).

Frank AB, Bauer A (1995) Phyllochron differences in wheat, barley, and forage grasses. *Crop Science* **35**, 19-23.

Frank AB, Berdahl JD, Barker RE (1995) Morphological development and water use in clonal lines of four forage grasses. *Crop Science* **25**, 339-344.

Friend MA, Robertson S, Masters D, Avery A (2007) Evergraze - a project to achieve profit and environmental outcomes in the Australian grazing industries. *Journal of Animal and Feed Sciences* **16**, 70-75.

Frith GJT, Dalling MJ (1980) The role of peptide hydrolases in leaf senescence. In 'Senescence in plants.' (Ed. KV Thimann) pp. 117-130. (CRC Press: Boca Raton, Florida, USA).

Gallagher JN (1979) Field studies of cereal leaf growth. I. Initiation and expansion in relation to temperature and ontogeny. *Journal of Experimental Botany* **30**, 625-636.

Garvey M (1989) Report on field sampling program -1987/1988 and 1988/1989 - to provide database for satellite-based fuel moisture mapping project. Country Fire Authority, Victoria.

Garvey M (2008) pers. comm.

Garvey M, Millie S (1999) 'Grassland Curing Guide.' (Country Fire Authority: Melbourne).

Gelman A, Carlin JB, Stern HS, Rubin DB (2004) 'Bayesian data analysis - Second edition.' (Chapman & Hall / CRC: Boca Raton, Florida, U.S.A.).

Gill AM (2008) pers. comm.

Gill AM, Bradstock RA (1994) The prescribed burning debate in temperate Australian forests: towards a resolution. In 'Proceedings of the 2nd International Conference on Forest Fire Research' pp. 703-712. (Viegas, D.X.: Coimbra, Portugal).

Gill AM, Christian KR, Moore PHR, Forrester RI (1987) Bushfire incidence, fire hazard and fuel reduction burning. *Australian Journal of Ecology* **12**, 299-306.

Gill AM, King KJ, Moore AD (2010) Australian grassland fire danger using inputs from the GRAZPLAN grassland simulation model. *International Journal of Wildland Fire* **19**, 338-345.

Gill AM, Moore PHR, Donnelly JR, Moore AD (1989) Fire hazard assessment of farms and forests near Canberra, ACT, Australia. In 'Integrating research on hazards in fire-prone environments. Proceedings of the US-Australia workshop.' (Eds TC Daniel, IS Ferguson) pp. 53-57. (US Man and the biosphere program: Melbourne, Vic.).

Gill M (1999) Fire danger, grass curing and fuel management. http://www.firebreak.com.au/resletter15.html, accessed on 17/01/2012.

Grant SA, Barthram GT, Torvell L, King J, Smith HK (1983) Sward management, lamina turnover and tiller population density in continuously stocked *Lolium perenne*-dominated swards. *Grass and Forage Science* **38**, 333-344.

Hall AE (2001) 'Crop responses to environment.' (CRC Press LLC.: Boca Raton, U.S.A.).

Hatton TJ, Viney NR (1988) Modelling fine, dead, surface fuel moisture. In 'Conference on bushfire modelling and fire danger rating systems'. Canberra, ACT. (Eds NP Cheney, AM Gill) pp. 119-125. (CSIRO Division of Forestry).

Haun JR (1973) Visual quantification of wheat development. *Agronomy Journal* **65**, 116-119.

Henry DA, Simpson RJ, Macmillan RH (1997) Intrinsic shear strength of leaves of pasture grasses and legumes. *Australian Journal of Agricultural Research* **48**, 667-674.

Henry DA, Simpson RJ, Macmillan RH (2000) Seasonal changes and effect of temperature and leaf moisture content on intrinsic shear strength of leaves of pasture grasses. *Australian Journal of Agricultural Research* **51**, 823-831.

Hepp C, Milne JA, Illius AW, Robertson E (1996) The effect of summer management of perennial ryegrass-dominant swards on plant and animal responses in the autumn when grazed by sheep. 1. Tissue turnover and sward structure. *Grass and Forage Science* **51**, 250-259.

Higgins A, Whitten S, Slijepcevic A, Fogarty L, Laredo L (2011) An optimisation modelling approach to seasonal resource allocation for planned burning. *International Journal of Wildland Fire* **20**, 175-183.

Higgins SI, Bond WJ, Trollope WSW, Williams RJ (2008) Physically motivated empirical models for the spread and intensity of grass fires. *International Journal of Wildland Fire* **17**, 595-601.

Hignett CT (1975) Cereal - A cereal crop water balance model. In 'Notes on soil techniques 1975'. (CSIRO Division of Soils, Australia).

Hodgkinson KC, Quinn JA (1976) Adaptive variability in the growth of *Danthonia caespitosa* Gaud. populations at different temperatures. *Australian Journal of Botany* **24**, 381-396.

Hoen K (1968) Summer dormancy in *Phalaris tuberosa* L. *Australian Journal of Agricultural Research* **19**, 227-239.

Hsiao TC (1982) The soil-plant-atmosphere continuum in relation to drought and crop production. In 'Drought resistance in crops with emphasis on rice.' pp. 39-52. (International Rice Research Institute: Los Banos, Philippines.).

Hsiao TC, O'Toole JC, Yambao EB, Turner NC (1984) Influence of osmotic adjustment on leaf rolling and tissue death in rice (*Oryza sativa* L.). *Plant Physiology* **75**, 338-341.

Humphries EC, Wheeler AW (1963) The physiology of leaf growth. *Annual Review of Plant Physiology* **14**, 385-410.

Hutchinson KJ (1992) The grazing resource. In 'Proceedings of the 6th Australian Society of Agronomy Conference, Armidale, NSW.' pp. 54-60.

Islam MA, Dowling PM, Milham PJ, Campbell LC, Jacobs BC, Garden DL (2006) Ranking acidity tolerance and growth potential of *Austrodanthonia* accessions. *Grassland Science* **52**, 127-132.

Johnson I (1997) Climate and pasture production. In 'Pasture production and management.' (Eds JV Lovett, JM Scott) pp. 17-32. (Inkata Press: Melbourne).

Johnson I (2008) Pasture growth. http://www.imj.com.au/consultancy/wfsat/Pasture.pdf, accessed on 7/4/2011.

Johnson I (2011) Documentation. http://www.imj.com.au/consultancy/wfsat/wfsat.html, accessed on 7/4/2011.

Johnson IR, Lodge GM, White RE (2003) The Sustainable Grazing Systems Pasture Model: description, philosophy and application to the SGS National Experiment. *Australian Journal of Experimental Agriculture* **43**, 711-728.

Jones MB, Leafe EL, Stiles W (1980a) Water stress in field-grown perennial ryegrass. I. Its effect on growth, canopy photosynthesis and transpiration. *Annals of Applied Biology* **96**, 87-101.

Jones MB, Leafe EL, Stiles W (1980b) Water stress in field-grown perennial ryegrass. II. Its effect on leaf water status, stomatal resistance and leaf morphology. *Annals of Applied Biology* **96**, 103-110.

Keating BA, Carberry PS, Hammer GL, Probert ME, Robertson MJ, Holzworth D, Huth NI, Hargreaves JNG, Meinke H, Hochman Z, McLean G, Verburg K, Snow V, Dimes JP, Silburn M, Wang E, Brown S, Bristow KL, Asseng S, Chapman S, McCown RL, Freebairn DM, Smith CJ (2003) An overview of APSIM, a model designed for farming systems simulation. *European Journal of Agronomy* **18**, 267-288.

Kemp DR, Culvenor RA (1994) Improving the grazing and drought tolerance of temperate perennial grasses. *New Zealand Journal of Agricultural Research* **37**, 365-378.

Kemp DR, Dowling PM (1991) Species distribution within improved pastures over central NSW in relation to rainfall and altitude. *Australian Journal of Agricultural Research* **42**, 647-659.

Kemp DR, Dowling PM (2000) Towards sustainable temperate perennial pastures. *Australian Journal of Experimental Agriculture* **40**, 125-132.

Kemp DR, Guobin L (1992) Winter temperatures and reproductive development affect the productivity and growth components of white clover and phalaris growing in a mixed pasture. *Australian Journal of Agricultural Research* **43**, 673-683.

Kenward MG, Roger JH (1997) Small sample inference for fixed effects from restricted maximum likelihood. *Biometrics* **53**, 983-997.

King KJ, Cary GJ, Bradstock RA, Chapman J, Pyrke A, Marsden-Smedley JB (2006) Simulation of prescribed burning strategies in south-west Tasmania, Australia: effects on unplanned fires, fire regimes, and ecological management values. *International Journal of Wildland Fire* **15**, 527-540.

Kirby EJM (1995) Factors affecting rate of leaf emergence in barley and wheat. *Crop Science* **35**, 11-19.

Kirby EJM, Appleyard M, Fellowes G (1985) Effect of sowing date and variety on main shoot leaf emergence and number of leaves of barley and wheat. *Agronomie* **5**, 117-126.

Kirby EJM, Perry MW (1987) Leaf emergence rates of wheat in a Mediterranean environment. *Australian Journal of Agricultural Research* **38**, 455-464.

Klepper B, Rickman RW, Peterson CM (1982) Quantitative characterization of vegetative development in small cereal grains. *Agronomy Journal* **74**, 789-792.

Kloot PM (1983) The genus *Lolium* in Australia. *Australian Journal of Botany* **31**, 421-435.

Kuroyanagi T, Paulsen GM (1988) Mediation of high-temperature injury by roots and shoots during reproductive growth of wheat. *Plant, Cell and Environment* **11**, 517-523.

Langer RHM (1979) 'How grasses grow.' (Edward Arnold Publishers: London).

Langer RHM, Ampong A (1970) A study of New Zealand wheats. III. Effects of soil moisture stress at different stages of development. *New Zealand Journal of Agricultural Research* **13**, 869-877.

Large EC (1954) Growth stages in cereals. Illustration of the Feekes scale. *Plant pathology* **3**, 128-129.

Lemaire G, Agnusdei M (2000) Leaf tissue turnover and efficiency of herbage utilization. In 'Grazing Ecophysiology and Grazing Ecology'. (Eds G Lemaire, J Hodgson, A de Moraes, P.C.deF., Carvalho, C Nabinger) pp. 265-287. (CABI Publishing: Oxford, UK).

Lemaire G, Chapman D (1996) Tissue flows in grazed plant communities. In 'The Ecology and Management of Grazing Systems.' (Eds J Hodgson, AW Illius) pp. 3-36. (CAB International: Oxford, UK).

Lemaire G, Da Silva SC, Agnusdei M, Wade M, Hodgson J (2009) Interactions between leaf lifespan and defoliation frequency in temperate and tropical pastures: a review. *Grass and Forage Science* **64**, 341-353.

Leonard S, Kirkpatrick J, Marsden-Smedley J (2010) Variation in the effects of vertebrate grazing on fire potential between grassland structural types. *Journal of Applied Ecology* **47**, 876-883.

Levy EB, Madden EA (1933) The point method of pasture analysis. *New Zealand Journal of Agricultural Research* **46**, 267-279.

Littell RC, Milliken GA, Stroup WW, Wolfinger RD, Schabenberger O (2006) 'SAS for mixed models.' (SAS Institute Inc.: Cary, N.C., U.S.A.).

Lodge GM, Scott JM, King KL, Hutchinson KJ (1998) A review of sustainable pasture production issues in temperate native and improved pastures. In "'Animal Production in Australia" - Proceedings of the Australian Society of Animal Production.' pp. 79-89.

Longnecker N, Kirby EJM, Robson A (1993) Leaf emergence, tiller growth, and apical development of nitrogen-deficient spring wheat. *Crop Science* **33**, 154-160.

Lopez-Castaneda C, Richards RA (1994) Variation in temperate cereals in rainfed environments. I. Grain yield, biomass and agronomic characteristics. *Field Crops Research* **37**, 51-62.

Ludlow MM (1975) Effect of water stress on the decline of leaf net photosynthesis with age. In 'Environmental and biological control of photosynthesis.' (Ed. R Marcelle) pp. 123-134. (Dr W Junk b.v.: The Hague, Netherlands).

Luke RH, McArthur AG (1978) 'Bushfires in Australia.' (Australian Government Publishing Service: Canberra, ACT).

Mandahar CL, Garg ID (1975) Effect of ear removal on sugars and chlorophylls of barley leaves. *Photosynthetica* **9**, 407-409.

Marriott CA, Barthram GT, Bolton GR (1999) Seasonal dynamics of leaf extension and losses to senescence and herbivory in extensively managed sown ryegrass-white clover swards. *Journal of Agricultural Science* **132**, 77-89.

Marsden-Smedley JB, Catchpole WR (1995a) Fire behaviour modelling in Tasmanian Buttongrass Moorlands. I. Fuel characteristics. *International Journal of Wildland Fire* **5**, 203-214.

Marsden-Smedley JB, Catchpole WR (1995b) Fire behaviour modelling in Tasmanian Buttongrass Moorlands. II. Fire behaviour. *International Journal of Wildland Fire* **5**, 215-228.

Martin D, Grant I, Jones S, Anderson S (2007) Spatial techniques for grassland curing across Australia and New Zealand. In 'Joint AFAC / Bushfire CRC Conference'. Hobart, Tasmania.

Martin DN (2009) Development of satellite vegetation indices to assess grassland curing across Australia and New Zealand. PhD., RMIT University.

Mason WK, Kay G (2000) Temperate Pasture Sustainability Key Program: an overview. *Australian Journal of Experimental Agriculture* **40**, 121-123.

Matthews S (2010) Effect of drying temperature on fuel moisture content measurements. *International Journal of Wildland Fire* **19**, 800-802.

Mazzanti A, Lemaire G (1994) Effect of nitrogen fertilization on herbage production of tall fescue swards continuously grazed by sheep. 2. Consumption and efficiency of herbage utilization. *Grass and Forage Science* **49**, 352-359.

Mazzanti A, Lemaire G, Gastal F (1994) The effect of nitrogen fertilization upon the herbage production of tall fescue swards continuously grazed with sheep. 1. Herbage growth dynamics. *Grass and Forage Science* **49**, 111-120.

McArthur AG (1958) The preparation and use of fire danger tables. In 'Proceedings of the Fire Weather Conference.' Melbourne, Vic p. 18. (Bureau of Meteorology).

McArthur AG (1966) Weather and grassland fire behaviour. Forest Research Institute, Forestry and Timber Bureau. Leaflet 100, Canberra, ACT.

McArthur AG (1967) Fire behaviour in Eucalypt forests. Forest Research Institute, Forestry and Timber Bureau. Leaflet 107, Canberra, ACT.

McCarthy MM (1989) The management of land in fire-prone environments: a summary of strategies. In 'Integrating research on hazards in fire-prone environments. Proceedings of the US - Australia Workshop.' Melbourne, Victoria. (Eds TC Daniel, IS Ferguson) pp. 13-21. (US Man and the Biosphere Program, Washington, DC).

McCown RL, Hammer GL, Hargreaves JNG, Holzworth DP, Freebairn DM (1996) APSIM: a novel software system for model development, model testing and simulation in agricultural systems research. *Agricultural Systems* **50**, 255-271.

McMaster GS (1997) Phenology, development, and growth of the wheat (*Triticum aestivum* L.) shoot apex: A review. *Advances in Agronomy* **59**, 63-118.

McMaster GS (2005) Phytomers, phyllochrons, phenology and temperate cereal development. *Journal of Agricultural Science* **143**, 137-150.

McMaster GS, Klepper B, Rickman RW, Wilhelm WW, Willis WO (1991) Simulation of shoot vegetative development and growth of unstressed winter wheat. *Ecological Modelling* **53**, 189-204.

McMaster GS, Wilhelm WW (1995) Accuracy of equations predicting the phyllochron of wheat. *Crop Science* **35**, 30-36.

McMaster GS, Wilhelm WW (1997) Growing degree-days: one equation, two interpretations. *Agricultural and Forest Meteorology* **87**, 291-300.

McMaster GS, Wilhelm WW, Palic DB, Porter JR, Jamieson PD (2003) Spring wheat leaf appearance and temperature: Extending the paradigm? *Annals of Botany* **91**, 697-705.

Miller L (2008) pers. comm.

Millie S (1999) The accuracy of methods used to predict grassland curing. Honours, Deakin University.

Mitchell M (2008) Native grasses - how they stack up. In 'Survive, adapt, prosper. Proceedings of the 49th Annual Conference of the Grassland Society of Southern Australia Inc.' Bairnsdale, Vic. pp. 11-17. (Grassland Society of Southern Australia Inc.).

Moore AD (2010) pers. comm.

Moore AD, Alcock DJ, Pope LC, Powells JI (2010) Validating the GRAZPLAN pasture model for native grasslands of the Monaro region. In "'Food Security from Sustainable Agriculture". Proceedings of 15th Agronomy Conference 2010, 15-18 November 2010.' (Eds H Dove, RA Culvenor). (Australian Society of Agronomy: Lincoln, New Zealand).

Moore AD, Donnelly JR, Freer M (1997) GRAZPLAN: Decision support systems for Australian grazing enterprises. III Pasture growth and soil moisture submodels and the GrassGro DSS. *Agricultural Systems* **55**, 535-582.

Moore AD, Holzworth DP, Herrmann NI, Huth NI, Robertson MJ (2007) The Common Modelling Protocol: A hierarchical framework for simulation of agricultural and environmental systems. *Agricultural Systems* **95**, 37-48.

Moore KJ, Moser LE (1995) Quantifying developmental morphology of perennial grasses. *Crop Science* **35**, 37-43.

Moore KJ, Moser LE, Vogel KP, Waller SS, Johnson BE, Pedersen JF (1991) Describing and quantifying growth stages of perennial forage grasses. *Agronomy Journal* **83**, 1073-1077.

Morley FHW, Bennett D, McKinney GT (1969) The effect of intensity of rotational grazing with breeding ewes on phalaris-subterranean clover pasture. *Australian Journal of Experimental Agriculture and Animal Husbandry* **9**, 74-84.

Munne-Bosch S, Alegre L (2004) Die and let live: leaf senescence contributes to plant survival under drought stress. *Functional Plant Biology* **31**, 203-216.

Munro C, Frakes I, Thackway R (2007) What burns when? Distribution of non-forest bushfires across Australia.

http://affashop.gov.au/PdfFiles/what_burns_when_final.pdf, accessed on 27/5/2008.

Murphy BP, Russell-Smith J (2010) Fire severity in a northern Australian savanna landscape: the importance of time since previous fire. *International Journal of Wildland Fire* **19**, 46-51.

Murty KS, Ramakrishnaya G (1982) Shoot characteristics of rice for drought resistance. In 'Drought resistance in crops with emphasis on rice.' pp. 145-152. (International Rice Research Institute: Los Banos, Phillipines).

Nash JE, Sutcliffe V (1970) River flow forecasting through conceptual models part 1. A discussion of principles. *Journal of Hydrology* **10**, 282-290.

Newnham GJ, Grant IF, Martin DN, Anderson SAJ (2010) Improved methods for assessment and prediction of grassland curing. Satellite based curing methods and mapping. Final Report: Project A1.4. Bushfire Cooperative Research Centre.

Newnham GJ, Verbesselt J, Grant IF, Anderson SAJ (2011) Relative Greenness Index for assessing curing of grassland fuel. *Remote Sensing of Environment* **115**, 1456-1463.

Nooden LD (1988) The phenomena of senescence and aging. In 'Senescence and aging in plants'. (Eds LD Nooden, AC Leopold) pp. 1-50. (Academic Press Inc: San Diego, USA).

Nooden LD (2004) Introduction. In 'Plant cell death processes.' (Ed. LD Nooden) pp. 1-18. (Elsevier Science: San Diego, USA).

Nooden LD, Guiamet JJ, John I (2004) Whole plant senescence. In 'Plant cell death processes.' (Ed. LD Nooden) pp. 227-224. (Elsevier Science: San Diego, USA).

Ong CK (1978) The physiology of tiller death in grasses. 1. The influence of tiller age, size and position. *Journal of the British Grassland Society* **33**, 197-203.

Onofri A, Carbonell EA, Piepho H-P, Mortimer AM, Cousens RD (2010) Current statistical issues in *Weed Research. Weed Research* **50**, 5-24.

Otto S, Masin R, Chiste G, Zanin G (2007) Modelling the correlation between plant phenology and weed emergence for improving weed control. *Weed Research* **47**, 488-498.

Owen MJ, Walsh MJ, Llewellyn RS, Powles SN (2007) Widespread occurrence of multiple herbicide resistance in Western Australian annual ryegrass (*Lolium rigidum*) populations. *Australian Journal of Agricultural Research* **58**, 711-718.

Packham D, Bally J, Clark T, Knight I, Krusel N, Tapper N (1995) The orchestra grows! Two new fire models. *CALMScience Supplement* **4**, 9-16.

Parrott RT (1964) The growth, senescence and ignitability of annual pastures. Masters, University of Adelaide.

Parrott RT, Donald CM (1970a) Growth and ignitability of annual pastures in a Mediterranean environment. 1. Effect of length of season and of defoliation on the growth, water content and desiccation of annual pastures. *Australian Journal of Experimental Agriculture and Animal Husbandry* **10**, 67-75.

Parrott RT, Donald CM (1970b) Growth and ignitability of annual pastures in a Mediterranean environment. 2. Ignitability of swards of various annual species. *Australian Journal of Experimental Agriculture and Animal Husbandry* **10**, 76-83.

Parsons AJ, Harvey A, Woledge J (1991) Plant-animal interactions in a continuously grazed mixture. I. Differences in the physiology of leaf expansion and fate of leaves of grass and clover. *Journal of Applied Ecology* **28**, 619-634.

Pastor E, Zarate L, Planas E, Arnaldos J (2003) Mathematical models and calculation systems for the study of wildland fire behaviour. *Progress in Energy and Combustion Science* **29**, 139-153.

Patterson TG, Brun WA (1980) Influence of sink removal in the senescence pattern of wheat. *Crop Science* **20**, 19-23.

Peacock JM (1975a) Temperature and leaf growth in *Lolium perenne*. 1. The thermal microclimate: its measurement and relation to crop growth. *Journal of Applied Ecology* **12**, 99-113.

Peacock JM (1975b) Temperature and leaf growth in Lolium perenne. III. Factors affecting seasonal differences. *Journal of Applied Ecology* **12**, 685-697.

Peacock JM (1976) Temperature and leaf growth in four grass species. *Journal of Applied Ecology* **13**, 225-232.

Pearson R (2011) Boxplots and Beyond – Part I. http://www.r-bloggers.com/boxplots-and-beyond-part-i/, accessed on 20/10/2011.

Peoples MB, Dalling MJ (1988) The interplay between proteolysis and amino acid metabolism during senescence and nitrogen reallocation. In 'Senescence and aging in plants'. (Eds LD Nooden, AC Leopold) pp. 181-217. (Academic Press, Inc: San Diego, USA).

Perestrello de Vasconcelos MJ (1995) Integration of remote sensing and geographic information systems for fire risk managment. In 'Remote sensing and GIS applications to forest fire management.' University of Alcala de Henares, Spain. (Ed. E Chuvieco) pp. 129-147. (European Association of Remote Sensing Laboratories).

Perry MW, Siddique KHM, Wallace JF (1987) Predicting phenological development for Australian wheats. *Australian Journal of Agricultural Research* **38**, 809-819.

Pinheiro JC, Bates DM (1995) Approximations to the log-likelihood function in the nonlinear mixed-effects model. *Journal of Computational and Graphical Statistics.* **4**, 12-35.

Pompe A, Vines RG (1966) The influence of moisture on the combustion of leaves. *Australian Forestry* **30**, 231-241.

Pook EW, Gill AM (1993) Variation in live and dead fine fuel moisture in *Pinus radiata* plantations of the Australian Capital Territory. *International Journal of Wildland Fire* **3**, 155-168.

Porter JR, Gawith M (1999) Temperatures and the growth and development of wheat: a review. *European Journal of Agronomy* **10**, 23-36.

Price OF, Bradstock RA (2011) Quantifying the influence of fuel age and weather on the annual extent of unplanned fires in the Sydney region of Australia. *International Journal of Wildland Fire* **20**, 142-151.

Prober SM, Thiele KR, Lunt ID (2007) Fire frequency regulates tussock grass composition, structure and resilience in endangered temperate woodlands. *Austral Ecology* **32**, 808-824.

Purvis I (1995) 2a. Identifying superior animals. In 'Breeding Merinos for the 21st Century - proceedings of a workshop at CSIRO Division of Animal Production, Prospect, NSW.' pp. 16-19.

Pyne SJ, Andrews PL, Laven RD (1996) 'Introduction to wildland fire.' (John Wiley and Sons, Inc.: New York, USA).

Quinn GP, Keough MJ (2002) 'Experimental design and data analysis for biologists.' (Cambridge University Press: Cambridge, UK).

Ratkowsky DA (1990) 'Handbook of nonlinear regression models.' (Marcel Dekker Inc.: New York, USA.).

Rawson HM, Zajac M (1993) Effects of higher temperatures, photoperiod and seed vernalisation on development in two spring wheats. *Australian Journal of Plant Physiology* **20**, 211-222.

Rickman RW, Klepper BL (1995) The phyllochron: Where do we go in the future? *Crop Science* **35**, 44-49.

Robertson D (1985) Interrelationships between kangaroos, fire and vegetation dynamics at Gellibrand Hill Park, Victoria., University of Melbourne.

Robertson M, Carberry P (2010) The evolving role of crop modelling in agronomy research. In "'Food Security from Sustainable Agriculture" Proceedings of 15th Australian Agronomy Conference 2010'. (Ed. H Dove). (Australian Society of Agronomy Lincoln, New Zealand.).

Robson MJ (1972) The effect of temperature on the growth of S.170 tall fescue (*Festuca arundinacea*). I. Constant temperature. *Journal of Applied Ecology* **9**, 643-653.

Robson MJ (1973) The growth and development of simulated swards of perennial ryegrass. I. Leaf growth and dry weight change as related to the ceiling yield of a seedling sward. *Annals of Botany* **37**, 487-500.

Rowell MN, Cheney NP (1979) Firebreak preparation in tropical areas by rolling and burning. *Australian Forestry* **42**, 8-12.

Sambo EY (1983) Comparative growth of the Australian temperate pasture grasses: *Phalaris tuberosa* L., *Dactylis glomerata* L. and *Festuca arundinacea* Schreb. *New Phytologist* **93**, 89-104.

Sanford P, Cullen BR, Dowling PM, Chapman DF, Garden DL, Lodge GM, Andrew MH, Quigley PE, Murphy SR, King WM, Johnston WH, Kemp DR (2003) SGS Pasture Theme: effect of climate, soil factors and management on pasture production and stability across the high rainfall zone of southern Australia. *Australian Journal of Experimental Agriculture* **43**, 945-959.

SAS Institute Inc. (2002-3) SAS 9.1.3 for Windows. (Cary, North Carolina, U.S.A.).

Schroder PM, Cayley JWD, Patterson AP, Quigley PE, Saul GR (1992) Achieving the potential of the pasture resource in south-west Victoria. In 'Proceedings of the 6th Australian Agronomy Conference'. Armidale, NSW. (Eds KJ Hutchinson, PJ Vickery) pp. 154-156. (Australian Society of Agronomy, Parkville, Vic).

Schulze E-D, Robichaux RH, Grace J, Rundel PW, Ehleringer JR (1987) Plant water balance. *Bioscience* **37**, 30-37.

Scott JM, Hutchinson KJ, King KJ, Chen W, McLeod M, Blair GJ, White A, Wilkinson D, Lefroy RDB, Cresswell H, Daniel H, Harris C, MacLeod DA, Blair N, Chamberlain G (2000) Quantifying the sustainability of grazed pastures on the Northern Tablelands of New South Wales. *Australian Journal of Experimental Agriculture* **40**, 257-265.

Silsbury JH (1964) Tiller dynamics, growth, and persistency of *Lolium perenne* L. and of *Lolium rigidum* Gaud. *Australian Journal of Agricultural Research* **15**, 9-20.

Simon U, Park BH (1983) A descriptive scheme for stages of development in perennial forage grasses. In 'Proceedings of the 14th International Grassland Congress'. Lexington, Kentucky, USA. (Eds JA Smith, VW Hays). (Westview Press).

Sinha SK (1987) Drought resistance in crop plants: A critical physiological and biochemical assessment. In 'Drought tolerance in winter cereals.' (Eds JP Srivastava, E Porceddu, E Acevedo, S Varma) pp. 349-364. (John Wiley and Sons: Chichester, UK).

Slafer GA, Rawson HM (1995) Photoperiod x temperature interactions in contrasting wheat genotypes: Time to heading and final leaf number. *Field Crops Research* **44**, 73-83.

Slafer GA, Rawson HM (1997) Phyllochron in wheat as affected by photoperiod under two temperature regimes. *Australian Journal of Plant Physiology* **24**, 151-158.

Stocks BJ, Lawson BD, Alexander ME, Van Wagner CE, McAlpine RS, Lynham TJ, Dube DE (1988) The Canadian system of forest fire danger rating. In 'Conference on Bushfire Modelling and Fire Danger Rating Systems - Proceedings'. Canberra, ACT. (Eds NP Cheney, AM Gill) pp. 9-18. (CSIRO Division of Forestry, Australia).

Stocks BJ, Lawson BD, Alexander ME, Van Wagner CE, McAlpine RS, Lynham TJ, Dube DE (1989) Canadian forest fire danger rating system: an overview. *The Forestry Chronicle* **65**, 258-265.

Streck NA, Weiss A, Xue Q, Baenziger PS (2003) Incorporating a chronology response into the prediction of leaf appearance rate in winter wheat. *Annals of Botany* **92**, 181-190.

Tainton NM (1974) Effects of different grazing rotations on pasture production. *Journal of British Grassland Society* **29**, 191-202.

Thomas H (1980) Terminology and definitions in studies of grassland plants. *Grass and Forage Science* **35**, 13-23.

Thomas H, Donnison I (2000) Back from the brink: plant senescence and its reversibility. In 'Programmed cell death in animals and plants.' (Eds JA Bryant, SG Hughes, JM Garland) pp. 149-162. (BIOS Scientific Publishers Ltd.: Oxford, UK.).

Thomas H, Norris IB (1977) The growth responses of *Lolium perenne* to weather during winter and spring at various altitudes in mid-Wales. *Journal of Applied Ecology* **14**, 949-964.

Thomas H, Norris IB (1979) Winter growth of contrasting ryegrass varieties at two altitudes in mid-Wales. *Journal of Applied Ecology* **16**, 553-565.

Thomas H, Sadras VO (2001) The capture and gratuitous disposal of resources by plants. *Functional Ecology* **15**, 3-12.

Thomas H, Smart CM (1993) Crops that stay green. *Annals of Applied Biology* **123**, 193-219.

Tilman D, Downing JA (1994) Biodiversity and stability in grasslands. *Nature* **367**, 363-365.

Trevitt ACF (1988) Weather parameters and fuel moisture content: standards for fire model inputs. In 'Conference on bushfire modelling and fire danger rating systems'. Canberra ACT. (Eds NP Cheney, AM Gill) pp. 157-166. (CSIRO Division of Forestry).

Tunstall B (1988) Live fuel water content. In 'Conference on bushfire modelling and fire danger rating systems.' Canberra, ACT. (Eds NP Cheney, AM Gill) pp. 127-136. (CSIRO Division of Forestry).

Turner NC (1982) The role of shoot characteristics in drought resistance of crop plants. In 'Drought resistance in crops with emphasis on rice.' pp. 115-134. (International Rice Research Institute: Los Banos, Philippines.).

Turner NC, Begg JE (1978) Responses of pasture plants to water deficits. In 'Plant relations in pastures.' (Ed. JR Wilson) pp. 50-66. (CSIRO: Melbourne, Victoria).

Turner NC, O'Toole JC, Cruz RT, Yambao EB, Ahmad S, Namuco OS, Dingkuhn M (1986) Responses of seven diverse rice cultivars to water deficits. II. Osmotic adjustment, leaf elasticity, leaf extension, leaf death, stomatal conductance and photosynthesis. *Field Crops Research* **13**, 273-286.

Valentine I, Matthew C (1999) Plant growth, development and yield. In 'New Zealand Pasture and Crop Science'. (Eds J White, J Hodgson) pp. 11-27. (Oxford University Press: Auckland, NZ).

Van Herwaarden AF, Richards RA, Farquhar GD, Angus JF (1998) 'Haying-off', the negative grain yield response of dryland wheat to nitrogen fertiliser. III. The influence of water deficit and heat shock. *Australian Journal of Agricultural Research* **49**, 1095-1110.

Viegas DX, Pinol J, Viegas MT, Ogaya R (2001) Estimating live fine fuels moisture content using meteorologically-based indices. *International Journal of Wildland Fire* **10**, 223-240.

Vine DA (1983) Sward structure changes within a perennial ryegrass sward: leaf appearance and death. *Grass and Forage Science* **38**, 231-242.

Viney NR (1991) A review of fine fuel moisture modelling. *International Journal of Wildland Fire* **1**, 215-234.

Virgona J, Hildebrand S (2007) Biodiversity and sown pastures: what you sow is not what you get. In 'From the ground up: Grassland Society of Southern Australia Inc. 48th Annual Conference Proceedings.' Murray Bridge, South Australia pp. 33-39. (Grassland Society of Southern Australia Inc).

Virgona J, Mitchell M, Ridley A (2002) Native pastures - research and development directions with respect to the mitigation of dryland salinity. In '2002 Fenner Conference on the Environment' pp. 223-234.

Wade MH (1979) Leaf and tiller dynamics in grazed swards. M. Phil., University of Reading.

Wallace LL, McNaughton SJ, Coughenour MB (1985) Effects of clipping and four levels of nitrogen on the gas exchange, growth, and production of two east African graminoids. *American Journal of Botany* **72**, 222-230.

Waters CM (2007) A genecological study of the Australian native grass *Austrodanthonia caespitosa* (Gaudich.) H.P. Linder and four other related species. PhD., Charles Sturt University.

Watson MA, Lu Y (2004) Annual shoot senescence in perennials. In 'Plant cell death processes'. (Ed. LD Nooden) pp. 259-269. (Elsevier Science: San Diego, USA).

Watts M (2008) pers. comm.

Weber RO (1991) Modelling fire spread through fuel beds. *Progress in Energy and Combustion Science* **17**, 67-82.

White RE, Christy BP, Ridley AM, Okom AE, Murphy SR, Johnston WH, Michalk DL, Sanford P, McCaskill MR, Johnson IR, Garden DL, Hall DJM, Andrew MH (2003) SGS Water Theme: influence of soil, pasture type and management on water use in grazing systems across the high rainfall zone of southern Australia. *Australian Journal of Experimental Agriculture* **43**, 907-926.

White RH, Zipperer WC (2010) Testing and classification of individual plants for fire behviour: plant selection for the wildland-urban interface. *International Journal of Wildland Fire* **19**, 213-227.

Wilhelm WW, McMaster GS (1995) Importance of the phyllochron in studying development and growth in grasses. *Crop Science* **35**, 1-3.

Wilman D, Mares Martins VM (1977) Senescence and death of herbage during periods of regrowth in ryegrass and red and white clover, and the effect of applied nitrogen. *Journal of Applied Ecology* **14**, 615-620.

Wilson GU (1958) Some problems of estimating and predicting moisture content of forest and grass fuels. In 'Proceedings of the fire weather conference'. Melbourne, Vic. (Bureau of Meteorology).

Wilson JR (1976) Variation of leaf characteristics with level of insertion on a grass tiller. I. Development rate, chemical composition and dry matter digestibility. *Australian Journal of Agricultural Research* **27**, 343-354.

Woodward SJR (1998) Quantifying different causes of leaf and tiller death in grazed perennial ryegrass swards. *New Zealand Journal of Agricultural Research* **41**, 149-159.

Xue Q, Weiss A, Baenziger PS (2004) Predicting leaf appearance in field-grown winter wheat: evaluating linear and non-linear models. *Ecological Modelling* **175**, 261-270.

Zadoks JC, Chang TT, Konzak CF (1974) A decimal code for the growth stage of cereals. *Weed Research* **14**, 415-421.

Table of Appendix Tables

Appendix A.

Table A-1. Ingredients for a 3-bin mix of the Coco-Peat potting mix – supplied by Paul Ingham, SARDI.

Ingredient	Amount
Waikerie sand	300 l
Coco-Peat blocks	9 blocks
Water	150 l
Dolomite Lime	0.54kg
Ag Lime	1.8kg
Hydrated Lime	0.4kg
Gypsum	0.54kg
Superphosphate	0.54kg
Iron sulphate	1.35kg
Iron chelate	0.09kg
Micromax	0.54kg
Calcium nitrate	1.35kg
Mini Osmocote	5.4kg

Table A-2. Abbreviated inventory of recent and current grassland research sites in southern Australia.

Name and location	**Grassland type and major species**	**Pasture and curing measurements**	**Animal, soil or management information; timing and authors of study; measurements collected**
Red Gum Plains Sustainable Stocking Rate and Pasture Management Trial, Emu Park, Fernbank, East Gippsland, Vic	Annual, perennial	Green herbage mass, composition, plants/m^2, no specific curing data	Sheep Liveweight (LW) and condition score (CS). Commenced 13/07/2007. Grasslands Society of Southern Australia – East Gippsland Branch
Mid North Grasslands working group, Clare, SA	Native - *Austrodanthonia, Austrostipa*	Pasture composition, herbage mass, no specific curing data	Stocking rate (SR), LW, Study ran from 2000-2005. www.nativegrass.org.au
Pastures from Space, SE SA and Western District, Vic		Green mass, no specific curing data	Commenced spring 2007, ongoing. www.pasturesfromspace.csiro.au
Tas FACE, Pontville, Tas	Native - *Austrodanthonia, Themeda*	Germination, establishment, survival, no specific curing data	No animal data, commenced 2002, ongoing. www.utas.edu.au/docs/plant_science/ps/ps/face.html
Steve Leonard and Jamie Kirkpatrick fire and grazing interactions project			(Leonard *et al.* 2010)
Limekiln, Ross, Tas	Native - *Themeda, Austrodanthonia*	Spp. Cover and height, curing data	Spp., numbers, Study ran from Aug 05-Feb 07
Stockers Bottom, Ross, Tas	Native - *Themeda, Austrodanthonia*	Spp. Cover and height, curing data	Spp., numbers, Study ran from Aug 05-Feb 07
Staghorn, Ross, Tas	Native - *Themeda, Austrodanthonia*	Spp. Cover and height, curing data	Spp., numbers, Study ran from Aug 05-Feb 07
London Lakes, Bronte Park, Tas	Native - *Austrodanthonia*	Spp. Cover and height, curing data	Spp., numbers, Study ran from Sept 05-March 07
Paradise Plains NE highlands, Tas	Native - *Poa*	Spp. Cover and height, curing data	Spp., numbers, Study ran from Sept 05-March 07
Vale of Belvoir, NW Tas	Native - *Poa*	Spp. Cover and height, curing data	Spp., numbers, Study ran from Sept 05-March 07
Land Water and Wool Project			lwa.gov.au/land-water-and-wool/theme/8

Northern Tablelands, NSW	native, sown - *Microlaena, Poa tussock, Bothriochloa*	Pasture composition , no specific curing data	SR, wool yield Study ran from 15/3 -3/5/2004
Evergraze Projects			www.evergraze.com.au
Albany, WA	summer active perennials - lucerne, tall fescue, kikuyu, chicory, panic	Food on offer (FOO), ground cover %, % green	SR, wool yield, LW, Commenced February 2006
Hamilton, Vic	Perennial - lucerne, tall fescue, perennial ryegrass, chicory, kikuyu, Italian ryegrass		Commenced Autumn 2006
Chiltern, NE Vic	Perennial natives & introduced annuals - *Austrodantho nia, Microlaena*		
Holbrook, NSW	Perennial natives & introduced annuals - *Austrodantho nia, Microlaena, Bothriochloa,* phalaris		
Wagga Wagga, southern slopes, NSW	Perennial - lucerne, tall fescue, phalaris		
Orange, central slopes, NSW	Perennial natives - *Austrodantho nia, Microlaena, Bothriochloa*	pasture composition , production, no specific curing data	SR, wool yield, LW
Tamworth, northern slopes, NSW	Native & introduced perennials		
South Australia	Perennial – Lucerne etc		
Midlands, Tas	Perennial - spanish cocksfoot		
Grain and Graze projects			www.grainandgraze.com.au
Maranoa-Balonne, QLD	Introduced perennial and		

	native, crop - mitchell grass, bluegrass, panic,buffel, lucerne		
Border Rivers, NSW/QLD	Native & improved, crop lucerne,		
Central West, Lachlan, NSW	Perennial & natives, crop		
Glenelg/Coranga mite, Vic	Perennials & natives, crop		
Murrumbidgee, NSW	Crop, pasture		
Mallee, SA, Vic, NSW	Annual pastures, crop		
Avon, WA	Annual pastures, crop		
Eyre Peninsula, SA	Annual pastures, crop		
Northern agricultural, WA	Annual, perennial, crop		
Historical sites			
Kybybolite, SA	Annual pasture - Annual ryegrass, subclover	pasture mass, growth rate (GR) %green	SR, wool yield, LW 1970-1974. (Brown 1977a; b)
Hamilton, Vic	Perennial, annual - Perennial ryegrass, annual ryegrass, phalaris, subclover	pasture mass, GR	SR, wool yield, LW, 1965-1991. (Birrell and Thompson 2006)
Armidale, NSW	Perennial - phalaris, white clover	pasture mass, GR	SR, wool yield, LW, 1960s. (Hamilton *et al.* 1973)
Armidale, NSW			Cicerone Project 2000s. www.cicerone.org.au
Kojonup, WA	Annual - brome, subclover	pasture mass, GR	SR, wool yield, LW (Lloyd Davies and Greenwood 1972)
Turretfield, SA	Annual - Annual ryegrass, subclover		Mid 1990s. (Ru *et al.* 1997)
Rutherglen, Vic	Annual - barley grass, brome, annual ryegrass, subclover		late 1990s. (Grey *et al.* 2001)

Table A-3. Selection criteria for choosing field sites for data collection for model validation.

Essential	Desirable
What is the grass system e.g. native / annual / perennial pasture, crop, hay? - Can we cover a number of different systems?	Is it already known to modellers? (GrassGro™ or APSIM groups) (eg Hamilton Pastoral and Veterinary Institute, Kybybolite Research Station, Ginninderra Research Station etc)
Is it included on the land use mapping tool - How much of Australia (or temperate southern Australia) does that broad class represent?	Is there historical information and data available? (eg Hamilton Pastoral and Veterinary Institute, Kybybolite Research Station Waite Campus continuous cropping experiment, Roseworthy Paddock South 3 GRDC experiment)
Is the grassland type being monitored elsewhere? - Are the data available to Bushfire CRC (BCRC) or to me?	If historical data available, is there current access?
Can a number of geographic regions be covered? e.g. winter rainfall, uniform rainfall	Is weather data that represents the site available? - If not, what is the distance to a known weather station?
Is the geographic region being monitored elsewhere? Are the data available to BCRC/me?	
How important is that grassland or region to the fire agencies?	
Is "collaboration" available? - site information, experimentation permission	
Can the site be modeled with existing DST, species parameters, suitable weather & soil info etc?	
What parameters/ field data have been collected?	
Cost of field data collection - distance from Adelaide?	
Cost and availability of alternative field collectors?	

Table A-4. Details of sampling frequency to assess curing at field sites. Penwortham and Black Springs were agronomy demonstration sites, and destructive sampling was not possible. Wet weather restricted destructive sampling opportunities at Struan, Bool Lagoon and Kybybolite in 2008-9, due to potential interference with fuel moisture calculation. Destructive sampling was not conducted during 2010-11 because sampling commenced late in the spring season, and access to drying ovens was limited. Sampling at Majura and Tidbinbilla was conducted by the Bushfire CRC.

Field site	Species and sampling duration	Assessment method	Number of samples
Penwortham	Barley 30/9/2008-26/11/2008	Levy Rod	10
		Visual	10
		Destructive	-
	Annual ryegrass 30/9/2008-26/11/2008	Levy Rod	10
		Visual	10
		Destructive	-
	Phalaris 30/9/2008-26/11/2008	Levy Rod	10
		Visual	10
		Destructive	-
Black Springs	Barley 30/9/2008-26/11/2008	Levy Rod	10
		Visual	10
		Destructive	-
	Annual ryegrass 30/9/2008-26/11/2008	Levy Rod	10
		Visual	10
		Destructive	-
	Phalaris 30/9/2008-26/11/2008	Levy Rod	5
		Visual	5
		Destructive	-
Farrell Flat	Spear grass 9/9/2008-26/11/2008	Levy Rod	6
		Visual	6
		Destructive	5
Bool Lagoon	Wheat 3/10/2008-8/12/2008	Levy Rod	5
		Visual	5
		Destructive	2
	Barley 18/10/2010-3/12/2010	Levy Rod	3
		Visual	3
		Destructive	-
Struan	Annual ryegrass 3/10/2008-8/12/2008	Levy Rod	5
		Visual	5
		Destructive	1
	Annual ryegrass 18/10/2010-4/1/2011	Levy Rod	6
		Visual	6
		Destructive	-
	Phalaris 3/10/2008-29/1/2009	Levy Rod	7
		Visual	7
		Destructive	2
	Phalaris 18/10/2010-19/1/2011	Levy Rod	8
		Visual	8
		Destructive	-
Kybybolite	Spear grass 3/10/2008-29/1/2009	Levy Rod	7
		Visual	7
		Destructive	2
	Kangaroo grass 18/10/2010-4/1/2011	Levy Rod	6
		Visual	6

		Destructive	-
Majura	Native 16/8/2005-21/1/2008	Levy Rod	21
		Visual	21
		Destructive	8
Tidbinbilla	Native 20/12/2005-15/1/2008	Levy Rod	28
		Visual	19
		Destructive	5

Appendix B.

Table B-1. Coefficients (standard errors and significance values are given in brackets) for non-linear models of leaf curing over thermal time (gdd) for annual ryegrass, phalaris and wheat grown in the glasshouse, with the general form $\%cured = a/\left((b/1000) + e^{-(c(gdd/1000))}\right)$**. Refer Chapter 4, section 4.3.1.**

Species	*a*	*b*	*c*
Annual ryegrass	0.5339 (s.e.=0.07426, t_2=7.19, *P*=0.0188)	5.9949 (s.e.= 0.7681, t_2=7.80, *P*=0.0160)	2.3434 (s.e.=0.1364, t_2=17.18, *P*=0.0034)
Phalaris	0.1746 (s.e.=0.02845, t_2=6.14, *P*=0.0255)	1.6285 (s.e.=0.2121, t_2=7.68, *P*=0.0165)	2.7877 (s.e.=0.08583, t_2=32.48, *P*=0.0009)
Wheat	0.9874 (s.e.=0.1528, t_2=6.46, *P*=0.0231)	6.3713 (s.e.=0.4521, t_2=14.09, *P*=0.0050)	1.9856 (s.e.=0.1296, t_2=15.33, *P*=0.0042)

Table B-2. Coefficients (standard errors and significance values are given in brackets) for non-linear model of leaf curing over thermal time (gdd) for wallaby grass grown in the glasshouse, with the general form $\%cured = a + \left(b(gdd/1000)^2\right)$**. Refer Chapter 4, section 4.3.1.**

a	*b*
-1.2317 (s.e.=3.6049, $F_{1,3.2}$=-0.34, *P*=0.7538)	7.4406 (s.e.=0.1018, $F_{1,453}$=5346.6, *P*<0.0001)

Table B-3. Coefficients used to adjust thermal time in the leaf curing models to fit field thermal time frames, where adjusted thermal time $= (gdd + R)$**. Refer Chapter 4, section 4.3.2.1.**

Species	*R*
Annual ryegrass	1.9482 (s.e.=0.04717, t_{90}=41.31, *P*<0.0001)
Wallaby grass	5.9288 (s.e.=0.4028, t_{55}=14.72, *P*<0.0001)
Phalaris	1.5994 (s.e.=0.02982, t_{157}=53.64, *P*<0.0001)
Wheat	2.0102 (s.e.=0.02852, t_{74}=70.48, *P*<0.0001)

Appendix C.

Table C-1. Coefficients (standard errors and significance values in brackets) for LSR (mm/gdd (T_{base} = 0ºC)) in each species with a model of the general form $LSR = 1/(a + b\ell + c\ell^2)$ where ℓ is leaf position. Refer Chapter 5, section 5.3.1.

Species	*a*	*b*	*c*
Annual ryegrass	8.144 (s.e.=0.759, t_1=10.73, *P*=0.0592)	-0.8549 (s.e.=0.125, t_1=-6.83, *P*=0.0925)	0.0381 (s.e.=0.00559, t_1=6.81, *P*=0.0928)
Wallaby grass	21.68 (s.e.=3.125, t_1=6.94, *P*=0.0912)	-4.230 (s.e.=0.853, t_1=-4.96, *P*=0.1267)	0.2656 (s.e.=0.0589, t_1=4.51, *P*=0.1387)
Phalaris	9.383 (s.e.=1.191, t_1=7.88, *P*=0.0804)	-1.181 (s.e.=0.229, t_1=-5.15, *P*=0.1221)	0.05075 (s.e.=0.0112, t_1=4.54, *P*=0.1380)
Wheat	8.765 (s.e.=0.623, t_1=14.06, *P*=0.0452)	-1.593 (s.e.=0.203, t_1=-7.84, *P*=0.0808)	0.1536 (s.e.=0.0189, t_1=8.15, *P*=0.0778)

Table C-2. Coefficients for leaf length (mm) in each species with a model of the general form $LL = 1/(a + b\ell + c\ell^2)$ where ℓ is leaf position. Standard errors were not available due to the use of bootstrapping sampling procedure. Refer Chapter 5, section 5.3.2.

Species	*a*	*b*	*c*
Annual ryegrass	0.00854	-0.000734	0.000033
Wallaby grass	0.02497	-0.006194	0.00044
Phalaris	0.1536	-0.002575	0.000135
Wheat	0.01005	-0.002476	0.000216

Table C-3. Coefficients (standard errors and significance values in brackets) for LER (mm/gdd (T_{base} = 0ºC)) in each species with a model of the general form $LER = \frac{1}{a + (aR \times REPRODUCTIVE) + (aM \times MATURE) + b\ell + c\ell^2}$; where ℓ is leaf position, and REPRODUCTIVE and MATURE are variables referred to in Chapter 5, section 5.3.3.

Species	*a*	*aR*	*aM*	*b*	*c*
Annual ryegrass	1.9482 (s.e.=0.125, t_{13}=15.65, *P*<0.0001)	n/a	n/a	-0.2755 (s.e.=0.028, t_{13}=-9.84, *P*<0.0001)	0.0171 (s.e.=0.000169, t_{13}=10.10, *P*<0.0001)
Wallaby grass	6.425 (s.e.=0.496, t_{13}=12.96, *P*<0.0001)	-2.072 (s.e.=0.613, t_{13}=-3.38, *P*=0.0049)	2.289 (s.e.=0.575, t_{13}=3.98, *P*=0.0016)	-1.486 (s.e.=0.127, t_{13}=-11.75, *P*<0.0001)	0.1035 (s.e.=0.00946, t_{13}=10.95, *P*<0.0001)
Phalaris	2.513 (s.e.=0.162, t_{13}=15.50, *P*<0.0001)	-0.8269 (s.e.=0.134, t_{13}=-6.18, *P*<0.0001)	0.4457 (s.e.=0.120, t_{13}=3.70, *P*=0.0027)	-0.4199 (s.e.=0.037, t_{13}=-11.32, *P*<0.0001)	0.02512 (s.e.=0.00226, t_{13}=11.10, *P*<0.0001)
Wheat	2.179 (s.e.=0.177, t_{13}=12.34, *P*<0.0001)	-0.244 (s.e.=0.0645, t_{13}=-3.79, *P*=0.0023)	0.1768 (s.e.=0.0461, t_{13}=3.83, *P*=0.0021)	-0.4963 (s.e.=0.0551, t_{13}=-9.01, *P*<0.0001)	0.03798 (s.e.=0.00462, t_{13}=8.22, *P*<0.0001)

Table C-4. Coefficients (standard errors and significance values in brackets) for LLS (gdd (T_{base} = 0ºC)) with a model of the general form $LLS = a + b\ell + c\ell^2 + d\ell^3$, where ℓ is leaf position. Coefficients for annual ryegrass and phalaris are relative to wheat. For wallaby grass, $LLS = a + b\ell + c\ell^2$, where a=-261.1 (s.e.=112.1, $t_{55.3}$=-2.33, *P*=0.0235), b=165.3 (s.e.=33.24, $t_{55.38}$=4.97, *P*<0.0001) and c=-10.11 (s.e.=2.47, $t_{55.9}$=-4.09, *P*=0.0001). Refer Chapter 5, section 5.3.4.

Species	*a*	*b*	*c*	*d*
Annual ryegrass	-1448 (s.e.=703.1, t_{279}=-2.06, *P*=0.0404)	595 (s.e.=328.5, t_{279}=1.81, *P*=0.0712)	-81.06 (s.e.=0.4894, t_{279}=-1.663, *P*=0.0988)	3.76 (s.e.=2.336, t_{280}=1.61, *P*=0.1085)
Phalaris	-962.1 (s.e.=706.2, t_{279}=-1.36, *P*=0.1742)	439.7 (s.e.=329.9, t_{279}=1.33, *P*=0.1837)	-67.5 (s.e.=49.08, t_{279}=-1.38, *P*=0.1701)	3.391 (s.e.=2.339, t_{280}=1.45, *P*=0.1483)
Wheat	1405 (s.e.=699.1, t_{279}=2.01, *P*=0.0455)	-505.3 (s.e.=327.9, t_{279}=-1.54, *P*=0.1244)	75.13 (s.e.=48.91, t_{279}=1.54, *P*=0.1256)	-3.639 (s.e.=2.3351, t_{280}=-1.56, *P*=0.1203)

Table C-5. Coefficients (standard errors and significance values in brackets) for LAR (leaves/gdd (T_{base} = 0ºC)) per day degrees), with a model of the general form $LAR = a + b\ell$, where ℓ is leaf position. Coefficients for annual ryegrass, wallaby grass and phalaris are relative to wheat. Refer Chapter 5, section 5.3.5.

Species	*a*	*b*
Annual ryegrass	0.003178 (s.e.=0.00139, t_{282}=2.28, *P*=0.0233)	-0.00067 (s.e.=0.000166, t_{307}=-4.03, *P*<0.0001)
Wallaby grass	0.00386 (s.e.=0.00169, t_{292}=2.29, *P*=0.0227)	-0.00088 (s.e.=0.000213, t_{310}=-4.12, *P*<0.0001)
Phalaris	0.006636 (s.e.=0.00146, t_{276}=4.55, *P*<0.0001)	-0.00092 (s.e.=0.000172, t_{308}=-5.36, *P*<0.0001)
Wheat	0.004494 (s.e.=0.00130, t_{305}=3.47, *P*=0.0006)	0.000542 (s.e.=0.000164, t_{307}=3.31, *P*=0.0010)

Appendix D.

Table D-1. Coefficients (standard errors and significance values in brackets) for LSR (mm/gdd (T_{base} = 0°C)) in each species grown in the field with a model of the general form $LSR = e^{(a+b\ell+c\ell^2)}$ where ℓ is leaf position. Coefficients for annual ryegrass, cereal and phalaris are relative to spear grass. Refer Chapter 6, section 6.3.1.

Species	*a*	*b*	*c*
Annual ryegrass	-1.4851 (s.e.=0.695, t_{237}=-2.14, *P*=0.0337)	2.0460 (s.e.=0.387, t_{229}=5.29, *P*<0.0001)	-0.2809 (s.e.=0.054, t_{229}=-5.18, *P*<0.0001)
Spear grass	-0.5004 (s.e.=0.556, t_{241}=-0.90, *P*=0.3691)	-1.4696 (s.e.=0.336, t_{229}=-4.37, *P*<0.0001)	0.2051 (s.e.=0.049, t_{232}=4.15, *P*<0.0001)
Phalaris	-2.4848 (s.e.=0.601, t_{224}=-4.13, *P*<0.0001)	1.9294 (s.e.=0.344, t_{233}=5.61, *P*<0.0001)	-0.2509 (s.e.=0.050, t_{232}=-5.03, *P*<0.0001)
Cereal	-3.2534 (s.e.=0.750, t_{249}=-4.34, *P*<0.0001)	2.4540 (s.e.=0.39, t_{230}=6.29, *P*<0.0001)	-0.2932 (s.e.=0.053, t_{231}=-5.53, *P*<0.0001)

Table D-2. Coefficients (standard errors and significance values in brackets) for LSR (mm/gdd (T_{base} = 0°C) for each species grown in the glasshouse under terminal water stress in early spring with a model of the general form $LSR = 1/(a + b\ell + c\ell^2)$ where ℓ is leaf position. Refer Chapter 6, section 6.3.1.

Species	*a*	*b*	*c*
Annual ryegrass	2.0724 (s.e.=0.935, t_1=2.22, *P*=0.0364)	-0.2788 (s.e.=0.357, t_1=-0.78, *P*=0.4427)	0.0319 (s.e.=0.032, t_1=0.99, *P*=0.3303)
Wallaby grass	15.2592 (s.e.=2.403, t_1=6.35, *P*<0.0001)	-3.3999 (s.e.=0.647, t_1=-5.26, *P*<0.0001)	0.2126 (s.e.=0.043, t_1=4.91, *P*<0.0001)
Phalaris	1.3572 (s.e.=0.432, t_1=3.14, *P*=0.0035)	-0.1393 (s.e.=0.134, t_1=-1.04, *P*=0.3057)	0.00942 (s.e.=0.010, t_1=0.97, *P*=0.3397)
Wheat	2.6562 (s.e.=0.613, t_1=4.33, *P*=0.0002)	-0.6733 (s.e.=0.213, t_1=-3.17, *P*=0.0036)	0.0571 (s.e.=0.018, t_1=3.15, *P*=0.0038)

Table D-3. Coefficients (standard errors and significance values in brackets) for LSR (mm/gdd (T_{base} = 0°C) for each species grown in the glasshouse under terminal water stress in mid-spring with a model of the general form $LSR = 1/(a + b\ell + c\ell^2)$ where ℓ is leaf position. Refer Chapter 6, section 6.3.1.

Species	*a*	*b*	*c*
Annual ryegrass	-0.1422 (s.e.=0.125, t_1=-1.15, *P*=0.2641)	0.4177 (s.e.=0.131, t_1=3.20, *P*=0.0048)	-0.0316 (s.e.=0.021, t_1=-1.54, *P*=0.1403)
Wallaby grass	7.0897 (s.e.=1.995, t_1=3.55, *P*=0.0016)	-1.8305 (s.e.=0.696, t_1=-2.63, *P*=0.0147)	0.1531 (s.e.=0.060, t_1=2.57, *P*=0.0169)
Phalaris	1.0084 (s.e.=0.319, t_1=3.16, *P*=0.0037)	-0.2093 (s.e.=0.115, t_1=-1.82, *P*=0.0799)	0.0221 (s.e.=0.010, t_1=2.22, *P*=0.0348)
Wheat	0.0242 (s.e.=0.504, t_1=0.05, *P*=0.9624)	0.3487 (s.e.=0.307, t_1=1.14, *P*=0.2744)	-0.0217 (s.e.=0.041, t_1=-0.53, *P*=0.6021)

Table D-4. Coefficients (standard errors and significance values in brackets) for LSR (mm/gdd (T_{base} = 0°C) for each species grown in the glasshouse under terminal water stress in late spring with a model of the general form $LSR = 1/(a + b\ell + c\ell^2)$ where ℓ is leaf position. Refer Chapter 6, section 6.3.1.

Species	*a*	*b*	*c*
Annual ryegrass	0.8477 (s.e.=0.635, t_1=1.34, *P*=0.2003)	-0.0960 (s.e.=0.350, t_1=-0.27, *P*=0.7873)	0.0346 (s.e.=0.044, t_1=0.78, *P*=0.4478)
Wallaby grass	1.9293 (s.e.=1.156, t_1=1.67, *P*=0.1136)	-0.7939 (s.e.=0.783, t_1=-1.01, *P*=0.3250)	0.1453 (s.e.=0.128, t_1=1.14, *P*=0.2704)
Phalaris	0.1923 (s.e.=0.159, t_1=1.21, *P*=0.2365)	0.1165 (s.e.=0.055, t_1=2.12, *P*=0.0431)	-0.00365 (s.e.=0.004, t_1=-1.04, *P*=0.3080)

Table D-5. Coefficients (standard errors and significance values in brackets) for leaf length (mm) in each species grown in the field with a model of the general form $LL = e^{(a+b\ell+c\ell^2)}$ where ℓ is leaf position. Coefficients for annual ryegrass and cereal are relative to phalaris. No solution was evident for spear grass. Refer Chapter 6, section 0.

Species	*a*	*b*	*c*
Annual ryegrass	0.3209 (s.e.=0.277, $t_{83.5}$=1.16, *P*=0.2506)	0.1762 (s.e.=0.108, t_{208}=1.62, *P*=0.1058)	-0.03530 (s.e.=0.014, t_{122}=-2.49, *P*=0.0142)
Phalaris	3.5472 (s.e.=0.166, $t_{61.5}$=21.32, *P*<0.0001)	0.5831 (s.e.=0.049, t_{121}=11.87, *P*<0.0001)	-0.05448 (s.e.=0.006, $t_{36.5}$=-8.93, *P*<0.0001)
Cereal	1.1160 (s.e.=0.265, $t_{80.7}$=4.22, *P*<0.0001)	-0.2582 (s.e.=0.093, t_{211}=-2.78, *P*=0.0060)	0.01876 (s.e.=0.011, $t_{83.1}$=1.65, *P*=0.1032)

Table D-6. Coefficients (standard errors and significance values in brackets) for leaf length (mm) for each species grown in the glasshouse under terminal water stress in early spring with a model of the general form $LL = 10/(a + b\ell + c\ell^2)$ where ℓ is leaf position. Refer Chapter 6, section 0.

Species	*a*	*b*	*c*
Annual ryegrass	-0.1706 (s.e.=0.032, t_{34}=5.41, *P*<0.0001)	-0.04534 (s.e.=0.010, t_{34}=-4.38, *P*=0.0001)	0.003660 (s.e.=0.001, t_{34}=4.37, *P*=0.0001)
Wallaby grass	0.2751 (s.e.=0.038, t_{37}=7.29, *P*<0.0001)	-0.07280 (s.e.=0.011, t_{37}=-6.50, *P*<0.0001)	0.005354 (s.e.=0.001, t_{37}=6.46, *P*<0.0001)
Phalaris	0.1224 (s.e.=0.011, t_{42}=11.21, *P*<0.0001)	-0.02586 (s.e.=0.003, t_{42}=-8.93, *P*<0.0001)	0.001646 (s.e.=0.0002, t_{42}=8.61, *P*<0.0001)
Wheat	0.08941 (s.e.=0.007, t_{36}=12.64, *P*<0.0001)	-0.01993 (s.e.=0.003, t_{36}=-7.86, *P*<0.0001)	0.001633 (s.e.=0.0002, t_{36}=7.30, *P*<0.0001)

Table D-7. Coefficients (standard errors and significance values in brackets) for leaf length (mm) for each species grown in the glasshouse under terminal water stress in mid-spring with a model of the general form $LL = 10/(a + b\ell + c\ell^2)$ where ℓ is leaf position. Refer Chapter 6, section 0.

Species	*a*	*b*	*c*
Annual ryegrass	0.05768 (s.e.=0.012, *t26*=4.96, *P*<0.0001)	-0.01304 (s.e.=0.006, t_{26}=-2.10, *P*=0.0456)	0.001641 (s.e.=0.001, t_{26}=2.10, *P*=0.0458)
Wallaby grass	0.2043 (s.e.=0.021, t_{32}=9.66, *P*<0.0001)	-0.06657 (s.e.=0.008, t_{32}=-8.49, *P*<0.0001)	0.006216 (s.e.=0.001, t_{32}=8.57, *P*<0.0001)
Phalaris	0.06513 (s.e.=0.007, t_{43}=9.60, *P*<0.0001)	-0.01484 (s.e.=0.002, t_{43}=-6.95, *P*<0.0001)	0.001185 (s.e.=0.0002, t_{43}=7.19, *P*<0.0001)
Wheat	0.05510 (s.e.=0.011, t_{24}=5.25, *P*<0.0001)	-0.00960 (s.e.=0.007, t_{24}=-1.45, *P*=0.1593)	0.001499 (s.e.=0.001, t_{24}=1.60, *P*=0.1230)

Table D-8. Coefficients (standard errors and significance values in brackets) for leaf length (mm) for each species grown in the glasshouse under terminal water stress in late spring with a model of the general form $LL = 10/(a + b\ell + c\ell^2)$ where ℓ is leaf position. Refer Chapter 6, section 0.

Species	*a*	*b*	*c*
Annual ryegrass	0.05031 (s.e.=0.12, t_{26}=4.30, *P*=0.0002)	-0.00828 (s.e.=0.007, t_{26}=-1.21, *P*=0.2354)	0.001526 (s.e.=0.001, t_{26}=1.70, *P*=0.1002)
Wallaby grass	0.04977 (s.e.=0.015, t_{22}=3.32, *P*=0.0031)	-0.01595 (s.e.=0.011, t_{22}=-1.49, *P*=0.1508)	0.003091 (s.e.=0.002, t_{22}=1.72, *P*=0.1002)
Phalaris	0.03968 (s.e.=0.006, t_{48}=6.70, *P*<0.0001)	-0.00403 (s.e.=0.002, t_{48}=-2.47, *P*=0.0171)	0.000278 (s.e.=0.0001, t_{48}=2.55, *P*=0.0139)
Wheat	0.02993 (s.e.=0.003, t_{17}=11.56, *P*<0.0001)	0.000423 (s.e.=0.002, t_{17}=0.18, *P*=0.8590)	0.000669 (s.e.=0.0005, t_{17}=1.49, *P*=0.1551)

Appendix E.

Table E-1. Parameters for logistic models based on the Bayesian model curing values over thermal time (gdd) for four grass species, with the general form; $\%cured = 100/\left(1+e^{(-c(gdd-b))}\right)$**. Refer Chapter 7, section 7.3.2.2.**

Species	***b***	***c***
Annual ryegrass	3322.9	0.000959
Wallaby grass	2825.6	0.00235
Phalaris	2504.5	0.00202
Wheat	2227.1	0.00267

Table E-2. Coefficients used to adjust the logistic curve derived from Bayesian model curing values (Table E-1) to fit thermal time in the field leaf curing observations, with the general form; $\%cured = 100/\left(1+e^{(-c(gdd-b))}\right)$**. The *c* parameter remains the same as in Table E-1. Refer Chapter 7, section 7.3.2.3**

Species	***b***
Annual ryegrass	1.0118
Wallaby grass	643.24
Phalaris	613.65
Wheat	115.58

Table E-3. Coefficients used to adjust thermal time in the logistic curves derived from Bayesian model curing values (Table E-1) to fit visual curing assessments, after adjusting the thermal time (gdd) range, for the Naracoorte-Lucindale Council district in 2009-2010 and 2010-2011 fire seasons, with the general form; $\%cured = 100/\left(1+e^{(-c(gdd-b))}\right)$**. The *c* parameter remains the same as in Table E-1. Refer Chapter 7, section 7.3.2.4.**

Species	***b***
Annual ryegrass	1060.78
Phalaris	916.43

Appendix F.

Table F-1. Pearson correlations and probability values between leaf rates in all and individual species with significant result indicated in bold. Refer Chapter 8, section 8.6.2.

Leaf rates tested	Combined	Annual ryegrass	Wallaby grass	Phalaris	Wheat
LAR and LER	**0.42** ***P* <0.0001**	**0.35** ***P* <0.0001**	0.03 *P* =0.86	**0.33** ***P* =0.0018**	-0.15 *P*=0.31
LAR and LLS	0.01 *P* =0.88	**0.24** ***P* =0.0058**	0.02 *P* =0.90	-0.06 *P* =0.57	-0.01 *P* =0.94
LAR and LSR	0.06 *P* =0.27	**0.27** ***P* =0.0017**	-0.09 *P* =0.51	-0.21 *P* =0.0555	**-0.60** ***P* <0.0001**
LER and LLS	**-0.41** ***P* <0.0001**	**-0.35** ***P* <0.0001**	**-0.46** ***P* <0.0001**	**-0.53** ***P* <0.0001**	**-0.65** ***P* <0.0001**
LER and LSR	**0.37** ***P* <0.0001**	**0.50** ***P* <0.0001**	**0.62** ***P* <0.0001**	**0.52** ***P* <0.0001**	**0.26** ***P* =0.0213**
LLS and LSR	-0.02 *P* =0.77	**0.20** ***P* =0.0149**	0.07 *P* =0.55	-0.13 *P* =0.19	-0.17 *P* =0.18

Table F-2. Coefficients (standard errors and significance values in brackets) relating LER (mm/gdd (T_{base} = 0ºC)) to LLS (gdd (T_{base} = 0ºC)) in each species with a model of the general form $LLS = a + (b \times LER)$. Coefficients for annual ryegrass, wallaby grass and phalaris are relative to wheat. Refer Chapter 8, section 8.6.2.

Species	*a*	*b*
Annual ryegrass	-55.97 (s.e.=57.68, t_{243}=-0.97, *P*=0.3328)	-17.92 (s.e.=41.52, t_{367}=-0.43, *P*=0.6664)
Wallaby grass	69.76 (s.e.=63.66, t_{276}=1.10, *P*=0.2741)	-207.44 (s.e.=64.09, t_{374}=-3.24, *P*=0.0013)
Phalaris	-0.1304 (s.e.=61.32, t_{270}=0.00, *P*=0.9983)	-86.99 (s.e.=43.20, t_{366}=-2.01, *P*=0.0448)
Wheat	524.29 (s.e.=49.24, t_{323}=10.65, *P*<0.0001)	-121.72 (s.e.=28.40, t_{353}=-4.29, *P*<0.0001)

Table F-3. Species differences in model slope. Statistically significant differences are indicated by different letters. Refer Chapter 8, section 8.6.2.

Species	LLS	LSR
Wheat	A	A
Annual ryegrass	A, B	B
Phalaris	B, C	B
Wallaby grass	C	B

Table F-4. Coefficients (standard errors and significance values in brackets) relating LER (mm/gdd (T_{base} = 0ºC)) to LSR (mm/gdd (T_{base} = 0ºC)) in each species with a model of the general form $LSR = a + bLER$. Coefficients for annual ryegrass, wallaby grass and phalaris are relative to wheat. Refer Chapter 8, section 8.6.2.

Species	*a*	*b*
Annual ryegrass	-0.05897 (s.e.=0.03, t_{223}=-1.89, *P*=0.0601)	0.1386 (s.e.=0.02, t_{412}=5.61, *P*<0.0001)
Wallaby grass	-0.09347 (s.e.=0.03, t_{263}=-2.76, *P*=0.0062)	0.1353 (s.e.=0.04, t_{417}=3.63, *P*=0.0003)
Phalaris	-0.0307 (s.e.=0.03, t_{255}=-0.92, *P*=0.3579)	0.1428 (s.e.=0.03, t_{413}=5.63, *P*<0.0001)
Wheat	0.1470 (s.e.=0.03, t_{305}=5.80, *P*<0.0001)	0.01922 (s.e.=0.02, t_{397}=1.23, *P*=0.2182)

Appendix G.

Bayesian curing model

Ross Corkrey

September 15, 2011

Contents

List of Figures

1 Changes

2 Introduction

This is how I see the model structure, data required, and assumptions, etc.

3 Bayesian modelling

The Bayesian approach [Gelman et al., 2000] allows all data and parameters to be simultaneously considered which allows for the proper propagation of uncertainty throughout the model. Additionally, the Bayesian approach allows the calculation of the probability of any number of hypotheses, based on the posterior distribution, whereas the classical approach of multiple hypothesis testing is more complex. Since the 1990s, applications have expanded due to an increase in computational capacity that has made more practical the complex mathematical calculations required, principally through the introduction of Markov Chain Monte Carlo (MCMC) methods[Gilks et al., 1998]. Consequently, the use of Bayesian statistics in a variety of areas has become more common in recent years.

Whereas classical statistics assumes parameters in models are fixed quantities, Bayesian statistics assumes them to be uncertain and represent that uncertainty by the use of probability distributions known as prior distributions. In a

Bayesian analysis there are two components that are supplied, the prior distribution and the likelihood derived from the data, and an outcome, the posterior probability distribution of all parameters in the model. The posterior distribution can be reported by means of summary statistics or other calculations.

4 Model structure

I define the following symbols. [Not sure I use all these?]

l: leaf id, taking values $1, 2, \ldots$;
m: leaf length (m);
t: an analogue of time (gdd);
n: eventual number of leaves on a plant;
j: species, (ARG, wallaby grass, phalaris, wheat);
k: ID code for a plant;
r: ID code for a pot;
E: leaf elongation rate;
L: final leaf length;
S: length of leaf that is dead;
P: time when a leaf starts to die;
X: leaf senescence rate;
D: time to leaf appearance;
B: length;
Y: percentage dead;
a: time at which the leaf starts to grow;
f: time at which the leaf stops growing;
w: time at which the leaf start dying;
z: time at which the leaf has zero length.

I construct a series of constitutive models that each control a rate or limit related to leaf growth. The models are used in an ensemble of models to describe leaf growth.

After considerable experimentation I abandoned polynomials and inverse polynomials to describe the parameters since they resulted in a very unstable model. This was mainly because an inverse polynomial can go negative if not constrained and the constraints would be tricky to apply. In addition, the inverse of a quantity can have considerable range with only small changes in the quantity.

Instead I adopted the function shown in equation 1 in which there are two parameters. I show the function in Figure 1 for $\alpha = 1$ and $\beta = 0.1$. It consists of an ascending line whose slope is controlled mostly by α, reaches a peak at $l = 1/\beta$ and then subtends to zero at $l = \infty$.

$$y(l) = \alpha l \exp(-\beta l) \tag{1}$$

4.1 The model for one leaf

We need a parameter for the rate a leaf, l, elongates, E; another for the length at which it stops growing, L; for how long it stays the final length, P; and for

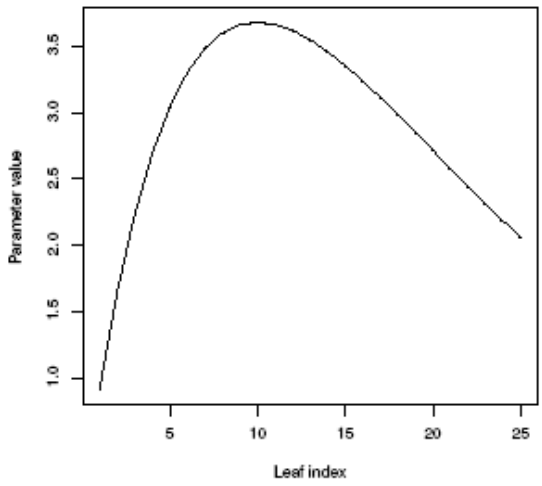

Figure 1: Plot of equation 1.

4

the senescence rate, X which is maintained until the leaf is of length 0. The leaf also appears at time, D, and this is another parameter.

The models for E, L, and P are given by equation 1. The model for X is given by equation 1 multiplied by -1, as shown in equation 2 . The D is described later.

$$y(l) = -\alpha l \exp(-\beta l) \tag{2}$$

I combine these models to describe the evolution of a single leaf from the time at which it appears as shown in equation 3. This is illustrated in figure 2.

$$m_{l,t} = \begin{cases} Et & 0 \leq t < f \\ L & f \leq t < P \\ L - X(t-P) & P \leq t < \frac{(L+XP)}{X} \\ 0 & \frac{(L+XP)}{X} \leq t \end{cases} \tag{3}$$

in which $f = L/E$.

Note that fitting this model requires that there be data for the ascending, plateau, and descending portions. The model stability was improved by removing cases where these portions are not observed. Details of omitted data are given in the appendix.

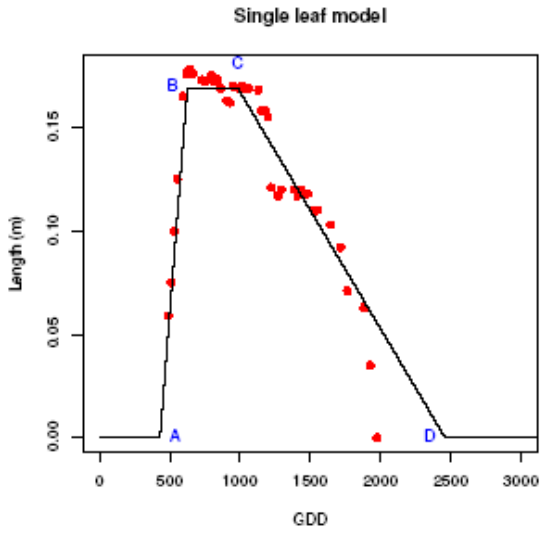

Figure 2: Model for the growth and death of a single leaf. The leaf length, measured in meters, increases from zero (A) at rate of E until it reaches L (B). It keeps the same length until it begins to die back (C) at rate X until it reaches zero (D). Points labeled are: (A) $t = D$, (B) $t = (L/E) + D$, (C) $t = P + D + L/E$, (D) $t = -[L - X * (P + D + L/E)]/X$.

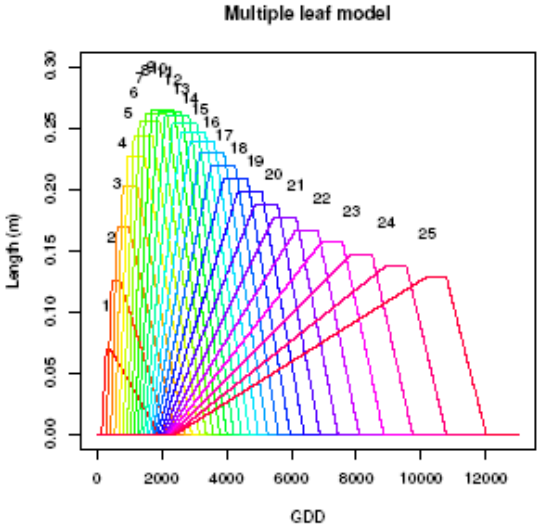

Figure 3: Model for a series of 25 leaves. Leaves are numbered sequentially. Colours are used to assist in distinguishing curves for each leaf.

4.2 The model for multiple leaves

We additionally model the GDD (D) at which a leaf appears using equation 1. I use the estimated D to modify equation 3 as shown in equation 4. This is the function used in the model. I show the growth and senescence of multiple leaves in figure 3.

$$m_{l,t} = \begin{cases} 0 & t < D \\ E(t-D) & D \leq t < D+f \\ L & D+f \leq t < D+P \\ L - X(t-D-P) & D+P \leq \frac{L+X(D+P)}{X} < t \\ 0 & \frac{L+X(D+P)}{X} \leq t \end{cases} \quad (4)$$

4.3 The model for multiple plants

The value of a parameter such as E is calculated according to equation 1 using the leaf index. Therefore all we need are the parameters of equation 1 and we can then calculate E for any leaf. This is also the case for L, P, X, and D. Since we have 5 models, each with two parameters, α and β, there are $2 \times 5 = 10$ parameters. I refer to these parameters as, for example, α_D and β_X.

Since this is a Bayesian model[1] I assign prior probability distributions to the 10 parameters described above. I adopt hierarchical priors as described below; namely: α_E, β_E, α_L, β_L, α_P, β_P, α_X, β_X, α_D, β_D. I adopt a Gaussian distribution for each with a mean and a precision (reciprocal variance) so that $\alpha_E \sim \mathrm{N}(\mu_E, \tau_E)$, $\beta_E \sim \mathrm{N}(\nu_E, \varsigma_E)$, ... $\alpha_D \sim \mathrm{N}(\mu_D, \tau_D)$, $\beta_D \sim \mathrm{N}(\nu_D, \varsigma_D)$. Each prior parameter has its own mean and precision. For example, for the E priors we have μ_E and ν_E, which are the means for α_E and β_E, respectively, and τ_E and ς_E are their respective precisions. I illustrate this in the Appendix Figure B.1.

Each species has it own distinct set of means and precisions. I show their prior means in Table 1. There are obtained during exploratory analysis by fitting equation 1 to the data. The use of the means in Table 1 assists in model convergence.

Table 1: Prior means for the model parameters by species.

	ARG	wallaby	phalaris	wheat
μ_E	0.0005	0.0002	0.0003	0.0007
ν_E	0.1579	0.1019	0.1103	0.1779
μ_L	0.0489	0.0256	0.0355	0.1082
ν_L	0.0915	0.0359	0.0432	0.1950
μ_P	0.3555	0.4898	0.4278	0.4708
ν_P	0.0302	0.0477	0.0545	0.0585
μ_X	0.0002	0.0000	0.0002	0.0002
ν_X	0.1399	0.0272	0.1242	0.1410
μ_D	0.1561	0.2215	0.1547	0.1360
ν_D	-0.0055	0.0135	-0.0027	0.0083

The precisions for the parameters also need definition. In all cases these are assigned vague Gamma distributions. A vague distribution has a large variance and so does not influence the outcome greatly. For example, I use $\tau_E \sim \Gamma(0.001, 0.001)$ and $\varsigma_E \sim \Gamma(0.001, 0.001)$. Since these are vague they allow the priors to be uninformative.

After assigning priors, the full joint distribution can be determined as the product of the likelihood with the associated prior distributions. The resulting posterior is complex and high-dimensional and so inference is obtained in the form of posterior means and variances obtained via MCMC simulation. We chose to use an implementation in which each parameter is updated in turn using adaptive Metropolis Hastings updates [Roberts and Rosenthal, 2009]. All simulation software is written in FORTRAN 95. The model is run for 1 000 000

[1] I actually attempted a more complex alternative model in which I fitted each plant separately so that each has its own set of parameters but it didn't do very much better than this one.

iterations and a 50% burn-in is used. Sensitivity studies and standard diagnostic techniques are used [Brooks and Roberts, 1998] to assess model validity.

5 Results

5.1 Plant level fits

Below I show the fitted curves by leaf, plant and species in Figures 4–33. Note that the figures show the observed data from the plants but the fitted curves correspond to the species. For example, Figure 4 shows the fitted curves for plant 3 for each of its leaves. Similarly, Figure 5 shows the fitted curves for plant 4 for each of its leaves. The fitted curve for leaf 3 in Figure 4 is the same fitted curve as shown in Figure 5 for its leaf 3. They only appear different due to scaling differences.

In some cases, not all of the fitted curve is shown since only the part that overlaps the observed data is plotted. For example, the curve for leaf 17 in Figure 6 appears as a straight line. This is because the curve has been chopped off to the right.

Since these are species fits and not plant level fits it is not expected that the curves will for all plants equally well. Rather it is intended that they will fit most plants adequately well. If this experiment were repeated I'd suggest more plants but fewer leaves per plant.

The lower leaves fit satisfactorily for leaves up to number 7 but less well for later leaves. This is because the later leaves are more variable between plants. Wheat seems to fit better for later leaves, however.

I note that in many cases the observed data do not simply rise to a plateau where they remain for a period, before descending. Instead, the plateau appears to have a slope of its own; e.g. the observed data for leaf 5 in Figure 14. Second, some leaves have two plateaus; e.g. the observed data for leaf 4 in Figure 30. Neither of these behaviours are accommodated in the model.

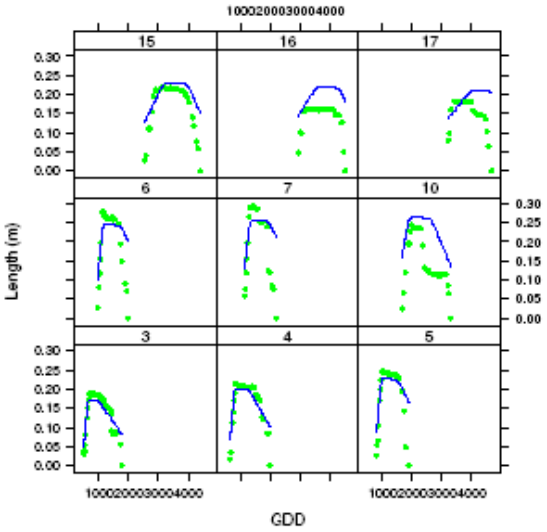

Figure 4: Fitted model for leaves for species ARG, plant 3.

10

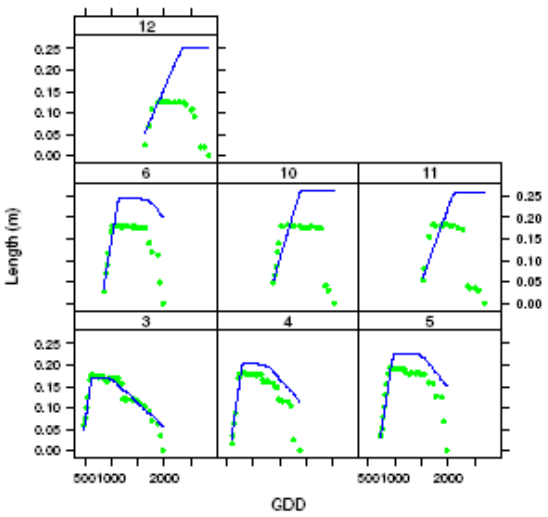

Figure 5: Fitted model for leaves for species ARG, plant 4.

11

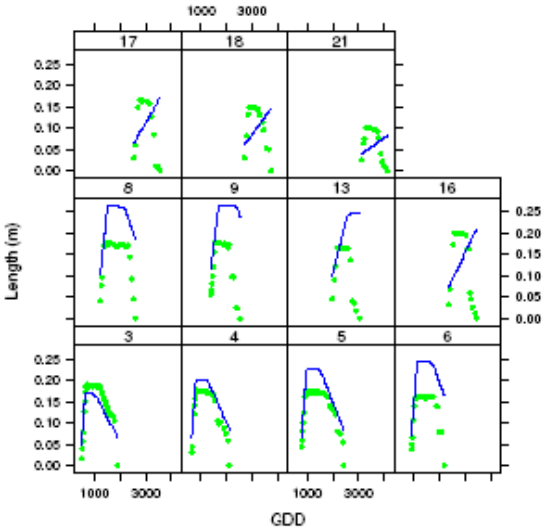

Figure 6: Fitted model for leaves for species ARG, plant 7.

12

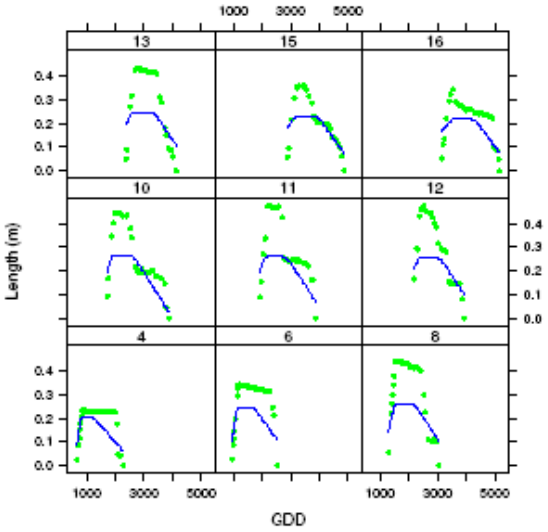

Figure 7: Fitted model for leaves for species ARG, plant 8.

13

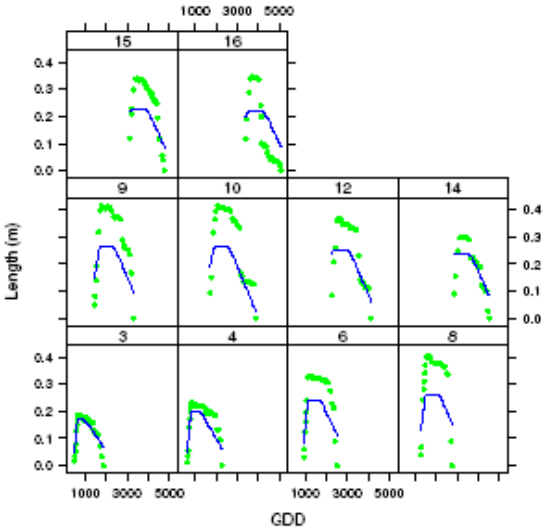

Figure 8: Fitted model for leaves for species ARG, plant 11.

14

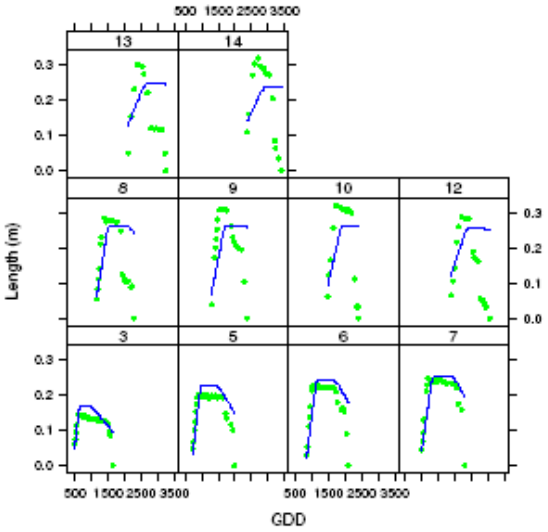

Figure 9: Fitted model for leaves for species ARG, plant 12.

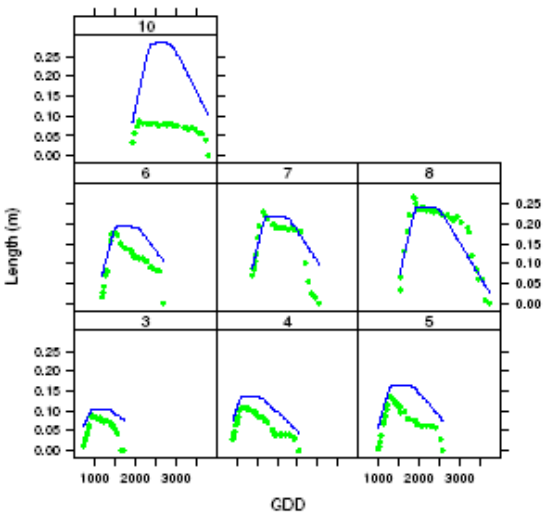

Figure 10: Fitted model for leaves for species wallaby grass, plant 1.

16

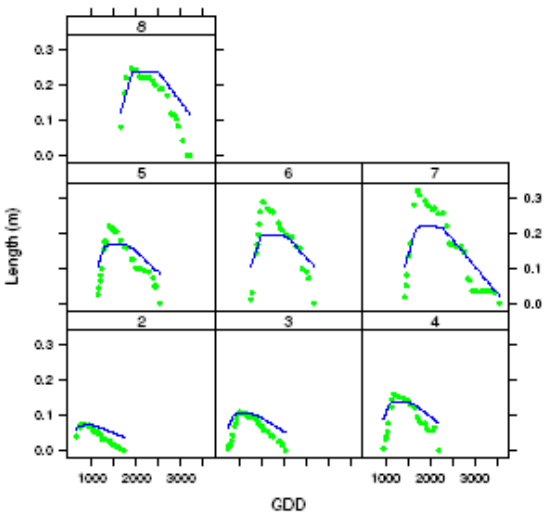

Figure 11: Fitted model for leaves for species wallaby grass, plant 2.

17

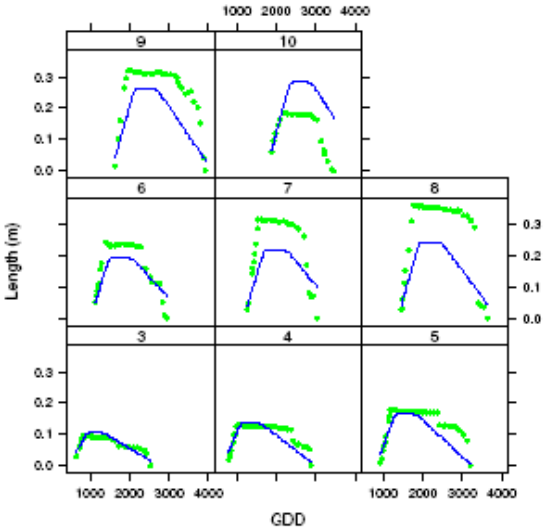

Figure 12: Fitted model for leaves for species wallaby grass, plant 9.

18

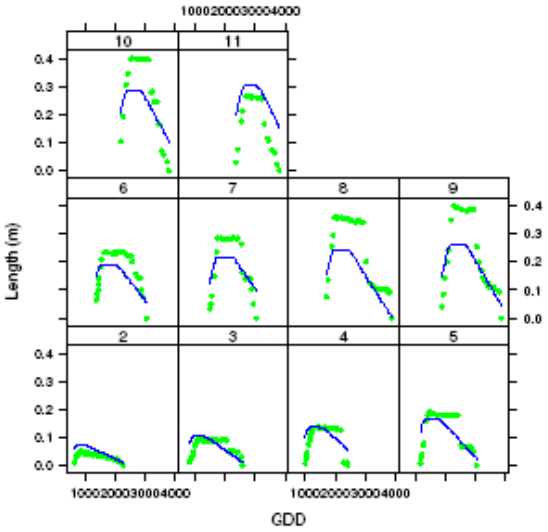

Figure 13: Fitted model for leaves for species wallaby grass, plant 10.

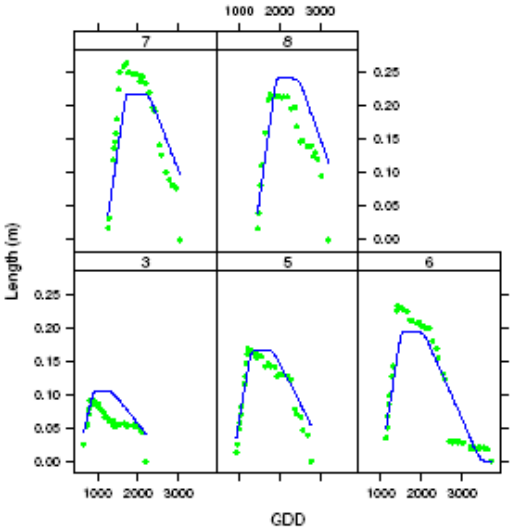

Figure 14: Fitted model for leaves for species wallaby grass, plant 21.

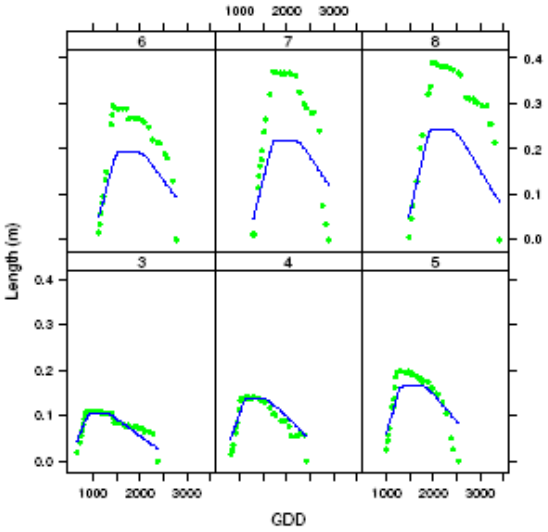

Figure 15: Fitted model for leaves for species wallaby grass, plant 22.

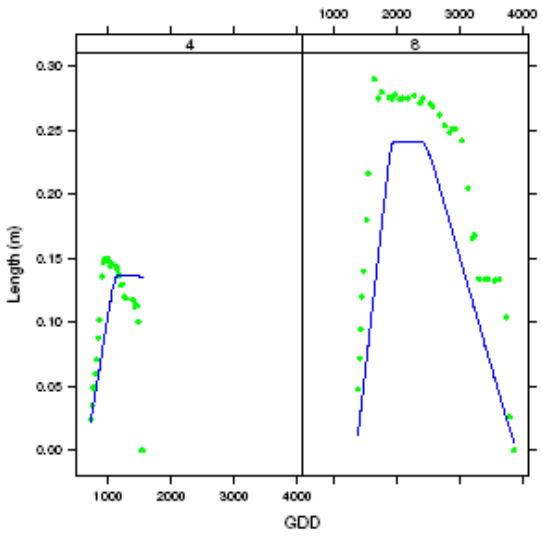

Figure 16: Fitted model for leaves for species wallaby grass, plant 23.

22

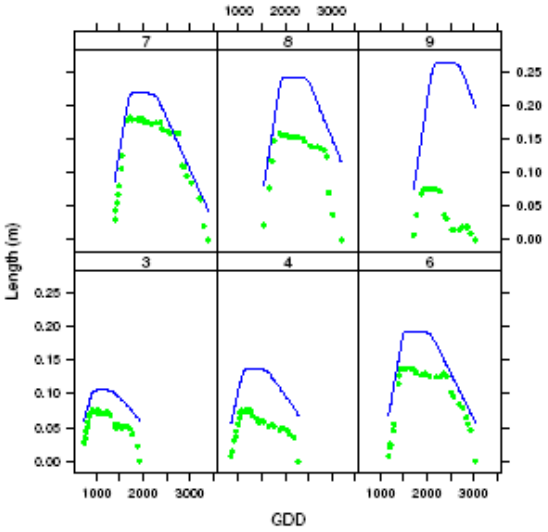

Figure 17: Fitted model for leaves for species wallaby grass, plant 24.

23

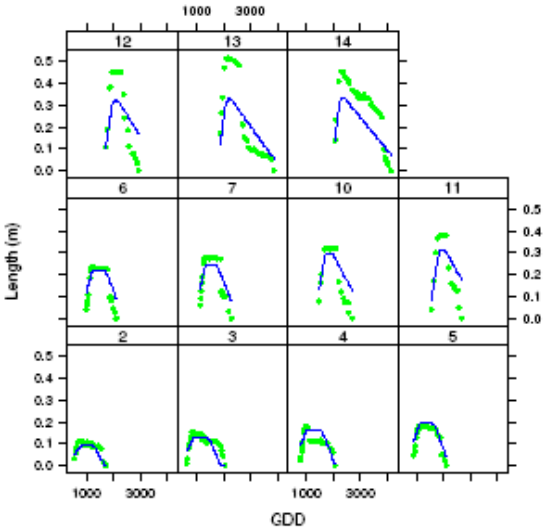

Figure 18: Fitted model for leaves for species phalaris, plant 13.

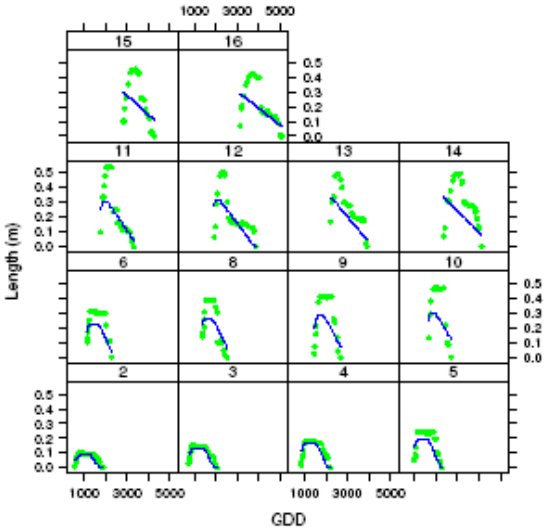

Figure 19: Fitted model for leaves for species phalaris, plant 14.

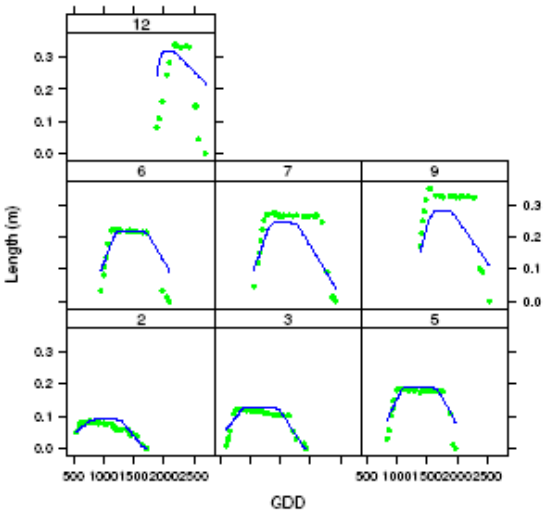

Figure 20: Fitted model for leaves for species phalaris, plant 19.

26

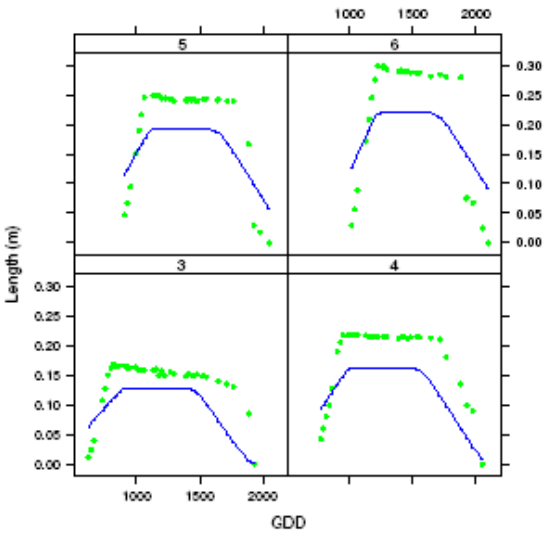

Figure 21: Fitted model for leaves for species phalaris, plant 20.

27

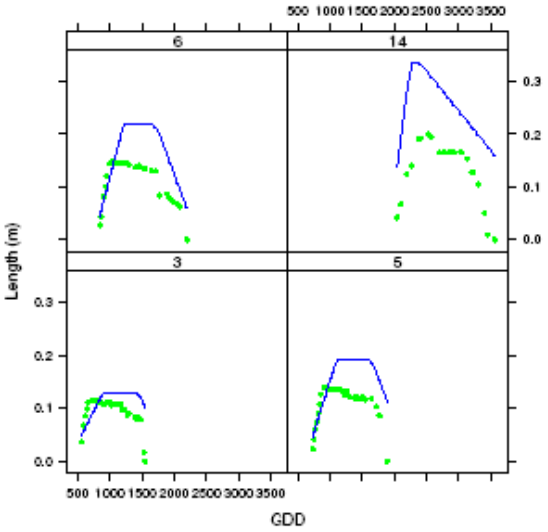

Figure 22: Fitted model for leaves for species phalaris, plant 27.

28

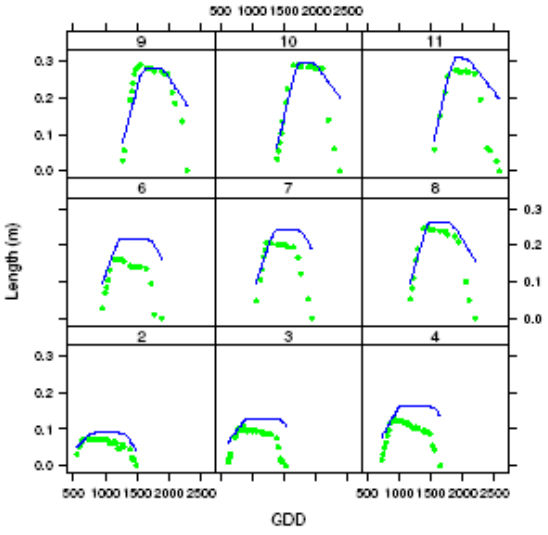

Figure 23: Fitted model for leaves for species phalaris, plant 28.

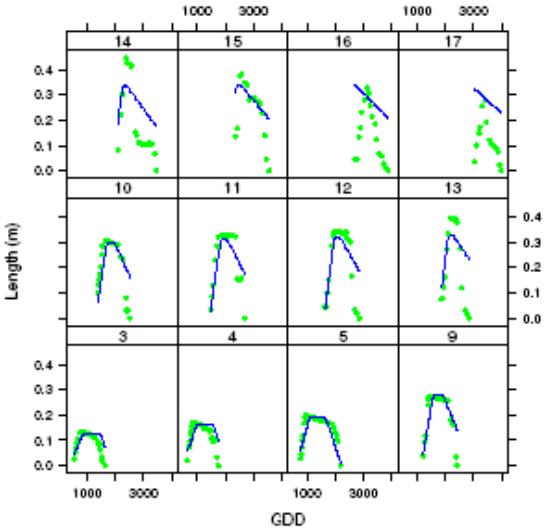

Figure 24: Fitted model for leaves for species phalaris, plant 29.

30

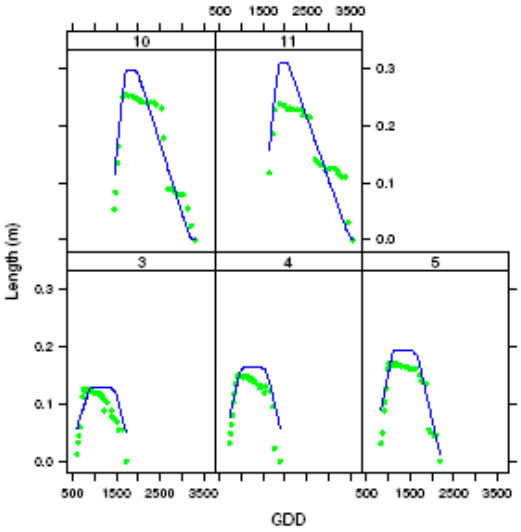

Figure 25: Fitted model for leaves for species phalaris, plant 30.

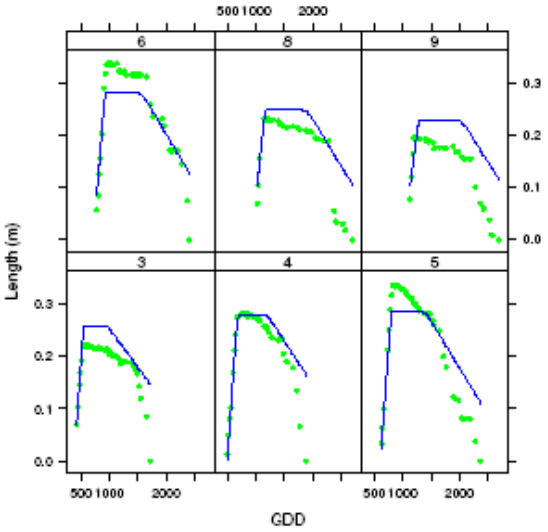

Figure 26: Fitted model for leaves for species wheat, plant 5.

32

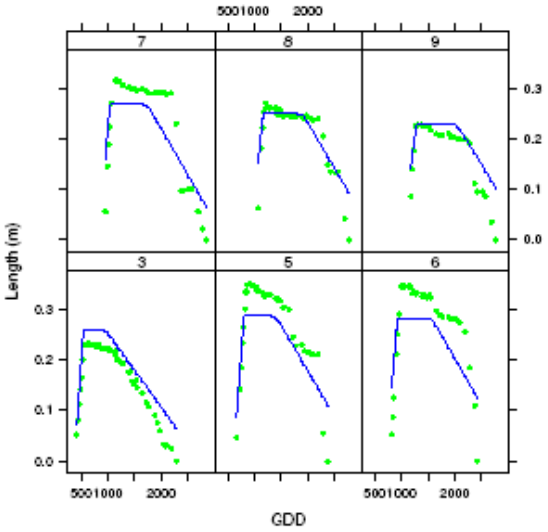

Figure 27: Fitted model for leaves for species wheat, plant 6.

33

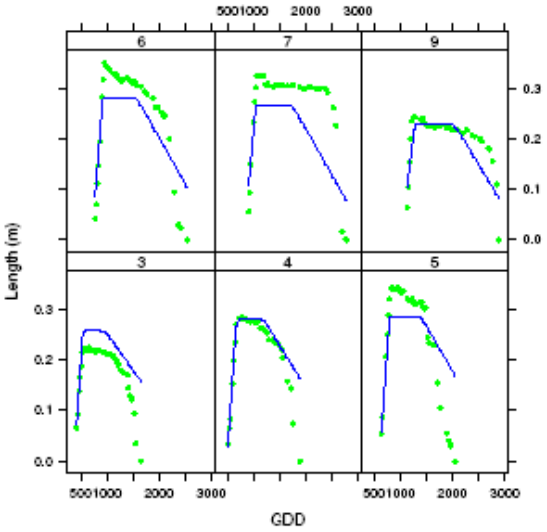

Figure 28: Fitted model for leaves for species wheat, plant 15.

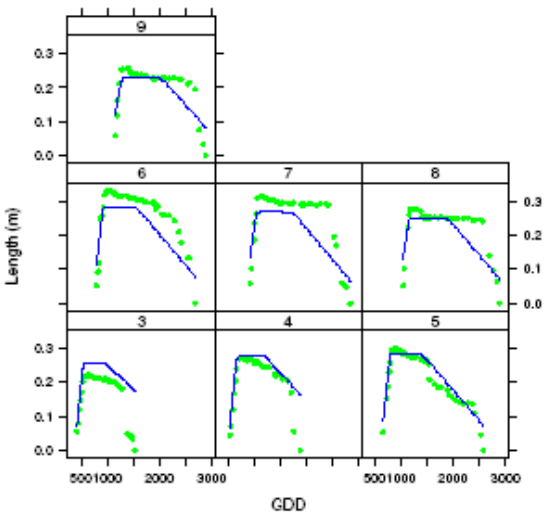

Figure 29: Fitted model for leaves for species wheat, plant 16.

35

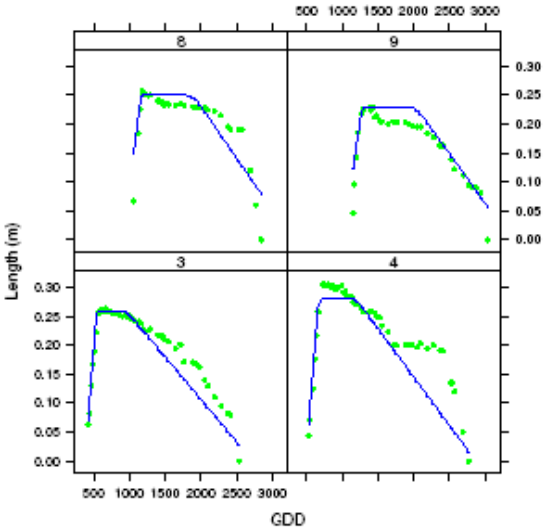

Figure 30: Fitted model for leaves for species wheat, plant 17.

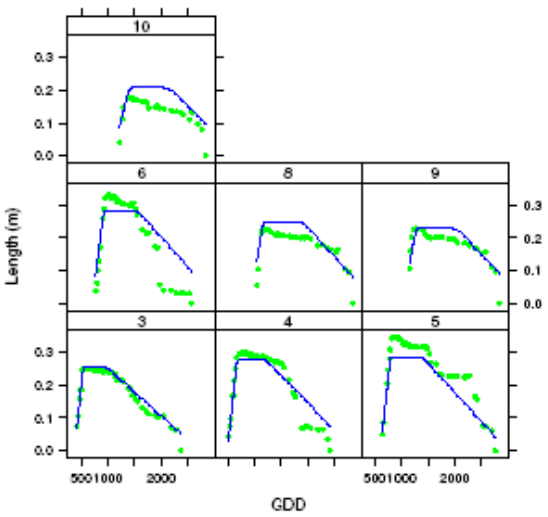

Figure 31: Fitted model for leaves for species wheat, plant 18.

37

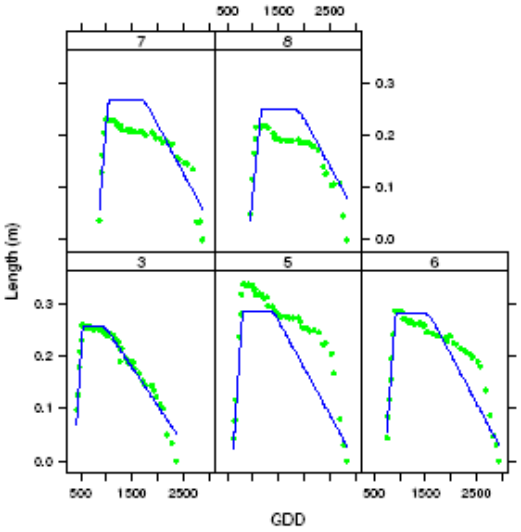

Figure 32: Fitted model for leaves for species wheat, plant 25.

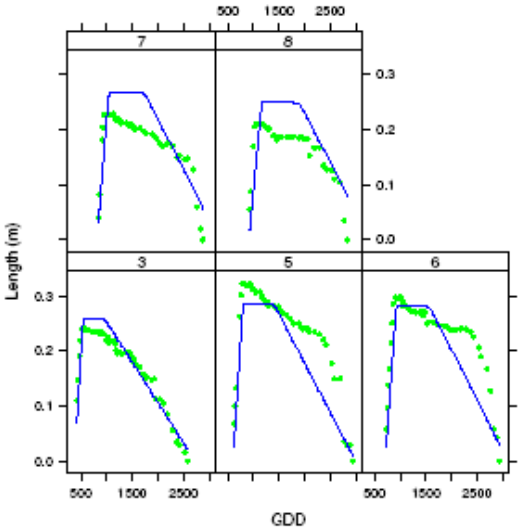

Figure 33: Fitted model for leaves for species wheat, plant 26.

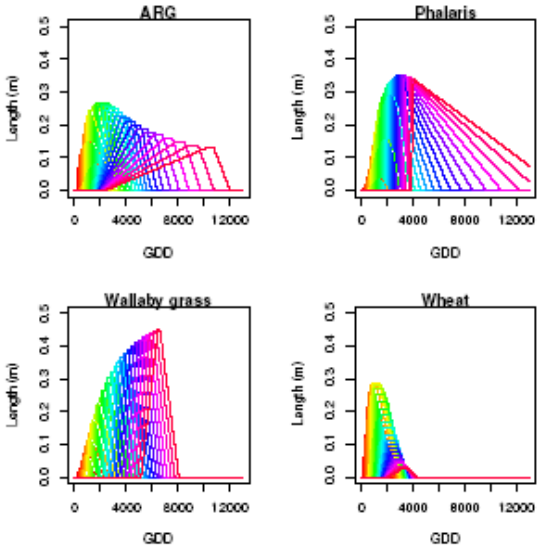

Figure 34: Predicted curves for all species for a series of leaves.

5.2 Species level fits

I show in Figures 34 the predicted curves for all species for leaves up to number 25. Leaf number 25 is beyond that observed for some species and so may not be reasonable. This may have some impact further below.

5.3 Posterior estimates

Summary statistics (means and 95% credible interval limits) for the posterior estimates are shown in Table 2. A 95% credible interval contains the parameter with 95% probability. These can be used in the construction of further models.

Table 2: Posterior means for the model parameters by species.

	ARG	lo.ARG	up.ARG	wallaby	lo.wallaby	up.wallaby	phalaris	lo.phalaris	up.phalaris	wheat	lo.wheat	up.wheat
α_E	0.0007	0.0005	0.0008	0.0001	0.0001	0.0002	0.0001	0.0001	0.0001	0.0013	0.0008	0.0017
β_E	0.2764	0.2565	0.2943	0.0824	0.0120	0.1474	0.0144	-0.0187	0.0466	0.2874	0.2220	0.3570
α_L	0.0781	0.0742	0.0831	0.0385	0.0352	0.0425	0.0502	0.0473	0.0529	0.1576	0.1493	0.1661
β_L	0.1088	0.1035	0.1144	0.0305	0.0161	0.0426	0.0525	0.0471	0.0588	0.2021	0.1936	0.2111
α_P	148.7208	84.8119	201.2875	215.3512	128.6494	325.7213	436.0913	320.1188	583.1166	183.3843	132.9801	233.4616
β_P	0.0733	40.6306	104.9447	0.1403	83.1948	206.1870	0.2816	234.4702	330.3971	0.0896	46.6121	129.6354
α_X	0.0001	0.0000	0.0001	0.0000	0.0000	0.0000	0.0002	0.0001	0.0003	0.0001	0.0001	0.0001
β_X	0.1008	0.0701	0.1301	0.0335	-0.0106	0.0835	0.2029	0.1712	0.2349	0.1572	0.1215	0.1950
α_D	151.7630	139.4056	162.9849	156.8979	127.4777	193.1380	116.1245	104.2114	126.9270	132.6214	121.9237	142.7210
β_D	0.0186	8.2581	26.5523	-0.0107	-32.1706	20.6562	-0.0113	-20.0783	-3.6595	0.0192	5.7345	32.3815

5.4 Derived quantities

Given the fitted model a number of quantities can be derived.

Length: The biomass for a single leaf is proportional to the maximum leaf length reached at any particular time. The biomass for a plant is the sum of the biomasses of all leaves that have appeared. I refer to this as 'length' below since this is a lineal quantity; i.e. metres. This can be expressed

$$B_j = \sum_{i=1}^{i=n_j} \int_{t=a_{j,i}}^{t=P_{j,1}} L_{t,i}$$

Percent dead matter: For a single leaf this is the percentage of the leaf that is dead. For a plant it is the percentage of the plant length that is dead. This can be expressed:

$$Y_j = \frac{1}{B_j} \sum_{i=1}^{i=n_j} \int_{t=a_{j,i}}^{t=P_{j,1}} S_{j,t,i}$$

In Figure 35 I show the predicted length versus GDD assuming all species grew 25 leaves. Since this probably isn't realistic, as noted earlier, I show in Figure 36 the predicted length versus GDD assuming all species grew as many leaves as were actually observed. I also show in Figure 37 the predicted length versus GDD assuming all species grew as many leaves as were actually observed.

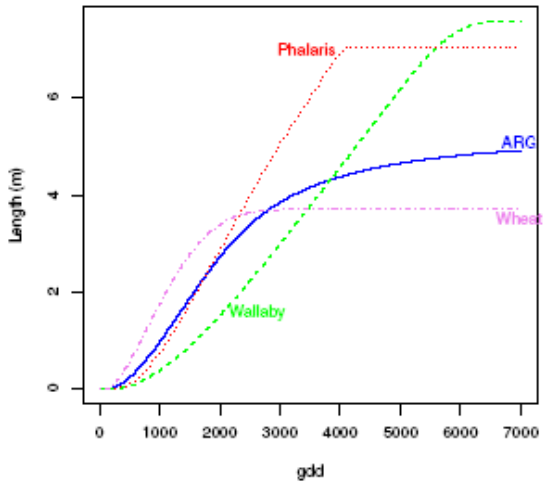

Figure 35: Length versus gdd for the leaf sequence 1 ... 25.

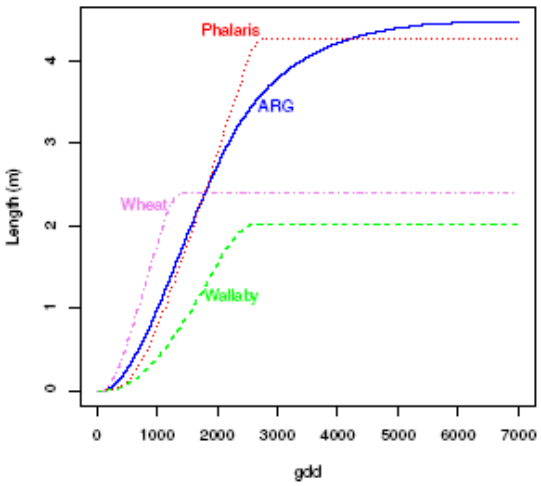

Figure 36: Length versus gdd for the leaf sequences to the maximum number observed per species. This was 21 leaves for ARG, 11 leaves for Wallaby grass, 17 leaves for Phalaris, and 10 leaves for wheat.

45

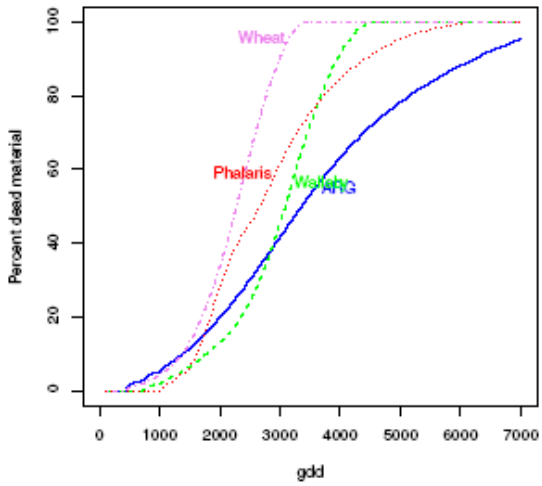

Figure 37: Percentage dead matter for the leaf sequences to the maximum number observed per species. This was 21 leaves for ARG, 11 leaves for Wallaby grass, 17 leaves for Phalaris, and 10 leaves for wheat.

A Data

I collapse the pot and plant ID codes in the data to form a unique code to represent each plant. The plant codes by species, pot and plant ID code are shown in table 3.

Table 3: Plant codes by pot and plant ID.

	1	2
1	1	2
2	3	4
3	5	6
4	7	8
5	9	10
6	11	12
7	13	14
8	15	16
9	17	18
10	19	20
11	21	22
12	23	24
13	25	26
14	27	28
15	29	30

I removed a number of leaves where there were insufficient observations on the growth phase and senescent phase. I tabulate these cases below.

Table 4: Removed cases.

	spp	plant.id	leaf.id
1	4	1	1
2	4	1	2
3	4	1	7
4	4	1	10
5	4	2	1
6	4	2	2
7	4	2	4
8	4	2	10
9	4	1	8
10	4	1	5
11	4	1	6
12	4	2	7
13	4	1	4
14	4	1	9
15	4	2	9
16	3	1	1
17	3	1	8
18	3	1	9
19	3	1	15
20	3	1	16
21	3	1	17

22	3	2	1
23	3	2	7
24	3	2	17
25	3	1	4
26	3	1	10
27	3	1	11
28	3	1	13
29	3	2	2
30	3	2	8
31	3	2	9
32	3	2	10
33	3	2	11
34	3	2	12
35	3	1	2
36	3	1	7
37	3	1	12
38	3	2	5
39	3	2	13
40	3	2	14
41	3	2	15
42	3	1	6
43	3	1	18
44	3	2	6
45	2	1	1
46	2	1	2
47	2	1	9
48	2	2	1
49	2	2	9
50	2	2	12
51	2	1	4
52	2	2	2
53	2	2	10
54	2	1	3
55	2	1	5
56	2	1	6
57	2	1	7
58	2	2	5
59	1	1	1
60	1	1	2
61	1	1	8
62	1	1	9
63	1	1	11
64	1	1	12
65	1	1	13
66	1	1	14
67	1	1	18
68	1	1	19
69	1	1	20
70	1	1	21
71	1	1	22
72	1	1	23
73	1	1	24
74	1	1	25
75	1	2	1

48

76	1	2	2
77	1	2	7
78	1	2	9
79	1	1	7
80	1	1	10
81	1	1	15
82	1	2	3
83	1	2	5
84	1	2	14
85	1	2	17
86	1	2	18
87	1	2	19
88	1	2	20
89	1	2	21
90	1	2	22
91	1	1	5
92	1	1	17
93	1	2	4
94	1	2	11

B Directed Acyclic Diagram (DAG)

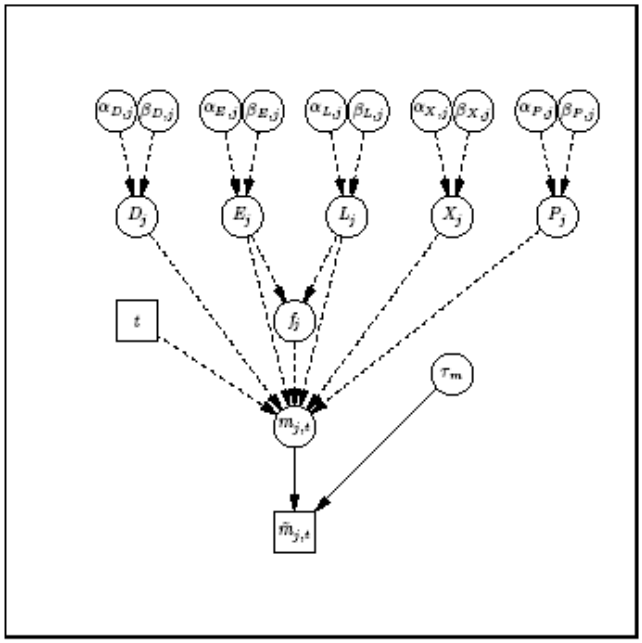

Figure B.1: Directed acyclic graph for history for species j and time t. Stochastic relationships are indicated by solid edges, deterministic relationships by dotted lines, observed data by square symbols, and unobserved parameters by round symbols.

50

References

Stephen P. Brooks and Gareth O. Roberts. Convergence assessment techniques for Markov chain Monte Carlo. *Stat. Comput.*, 8:319–335, 1998. ISSN 0960-3174.

Andrew Gelman, John B. Carlin, Hal S. Stern, and Donald B. Rubin. *Bayesian data analysis*. Chapman & Hall/CRC, London, 2000.

W.R. Gilks, S. Richardson, and D.J. Spiegelhalter. *Markov chain Monte Carlo in practice*. Chapman & Hall/CRC, 1998.

Gareth O. Roberts and Jeffrey S. Rosenthal. Examples of adaptive MCMC. *Journal of Computational and Graphical Statistics*, 18(2):349–367, June 2009. ISSN 1061-8600. URL `http://probability.ca/jeff/research.html`.